Functional importance of the APP/APLP protein family at the cellular and network level in the mouse central nervous system

Von der Fakultät für Lebenswissenschaften
der Technischen Universität Carolo-Wilhelmina zu Braunschweig
zur Erlangung des Grades einer
Doktorin der Naturwissenschaften
(Dr. rer. nat.)
genehmigte
D i s s e r t a t i o n

von Susann Ludewig
aus Dresden

1. Referent: Prof. Dr. Martin Korte
2. Referent: Prof. Dr. Reinhard Köster
eingereicht am: 15.05.2017
mündliche Prüfung (Disputation) am: 05.04.2018

Druckjahr 2018

Vorveröffentlichungen der Dissertation

Teilergebnisse aus dieser Arbeit wurden mit Genehmigung der Fakultät für Lebenswissenschaften, vertreten durch den Mentor der Arbeit, in folgenden Beiträgen vorab veröffentlicht:

Publikationen

Strecker P, **Ludewig S**, Rust M, Mundinger TA, Gorlich A, Krachan EG, Mehrfeld C, Herz J, Korte M, Guenette SY, Kins S (2016) FE65 and FE65L1 share common synaptic functions and genetically interact with the APP family in neuromuscular junction formation. Scientific reports 6:25652.

Fol R, Braudeau J, **Ludewig S**, Abel T, Weyer SW, Roederer JP, Brod F, Audrain M, Bemelmans AP, Buchholz CJ, Korte M, Cartier N, Muller UC (2016) Viral gene transfer of APPsalpha rescues synaptic failure in an Alzheimer's disease mouse model. Acta neuropathologica 131:247-266.

Ludewig S, Korte M (2017) Novel Insights into the Physiological Function of the APP (Gene) Family and Its Proteolytic Fragments in Synaptic Plasticity. Frontiers in Molecular Neuroscience 9.

Schilling S, Mehr A, **Ludewig S**, Stephan J, Zimmermann M, August A, Strecker P, Korte M, Koo EH, Muller U, Kins S, Eggert S (2017) APLP1 is a synaptic cell adhesion molecule, supporting maintenance of dendritic spines and basal synaptic transmission. The Journal of neuroscience: the official journal of the Society for Neuroscience.

Tagungsbeiträge

S. Ludewig, U. Herrmann, M. Hick, U. Müller, S. Guénette, S. Kins and M. Korte*. The APP interacting protein family Fe65 reveals a crucial role for synaptic function and plasticity.* (Poster) The 2nd RMN2 Biennial Meeting, Oberwesel, Germany, 2014, June 25 - 27, 2014.

S. Ludewig, U. Herrmann, M. Hick, U. Müller, S. Guénette, S. Kins and M. Korte*. The APP interacting protein family Fe65 reveals a crucial role for synaptic function and plasticity.* (Poster) The 11th Göttingen Meeting of the German Neuroscience Society, Germany, March 18 - 21, 2015.

S. Ludewig*, R. Fol*, J. Bradeau, T. Abel, S. Weyer, J. Roederer, M. Audrian, A. Bemelmanns, C. Buchholz,N. Cartier*, U. Müller*, M. Korte. *APPsα rescues impaired synaptic plasticity, spine density and behavior in an aged AD mouse model.* (Poster and Flash Talk) EMBO|EMBL Symposium Mechanisms of Neurodegeneration, Germany, 14 - 17 June 2015. (*equal contribution)

S. Ludewig, U. Herrmann, M. Hick, U. Müller and M. Korte. *An electrophysiological study to uncover the physiological role of the Amyloid Precursor Protein (APP) Family.* (Poster) The 10th FENS Forum of European Neuroscience, Copenhagen, Denmark, July 02 - 06, 2016.

“If the human brain were so simple that we could understand it, we would be so simple that we couldn’t.”

-Emerson M. Pugh-

Für meine Liebsten!

Table of Contents

Abstract 1

Zusammenfassung 2

1 Introduction 3

1.1 Alzheimer´s Disease 3

1.2 Synaptic Plasticity 4

1.2.1. The Hippocampus 5

1.2.2 Long-Term Potentiation and Long-Term Depression 7

1.2.3 Temporal Phases of LTP 9

1.2.4 Synaptic Plasticity in Alzheimer's Disease 10

1.3 The Amyloid Precursor Protein Family 11

1.3.1 Amyloid Precursor Protein Processing 12

1.3.2 Physiological Functions of the APP Family and their Proteolytic Fragments in the Brain 14

1.4 Scope of the Study 18

2 Material and Methods 19

2.1 Mouse strains 19

2.1.1 Constitutive APLP1-Knockout 19

2.1.2 Conditional Double or Triple Knockout of APP Protein Family Members 20

2.1.3 AD Model Mice - APPswe/PS1ΔE9 Transgenics 20

2.1.4 Fe65 and Fe65L1 Single and Double Knockouts 21

2.2 Electrophysiology 21

2.2.1 Artificial Cerebral Spinal Fluid (ACSF) 21

2.2.2 Preparation of Acute Hippocampal Slices 22

2.2.3 Extracellular Field Recordings 22

2.2.4 Stimulation Protocols 24

2.2.5 Pharmaca and Peptides 25

2.2.6 Electrophysiology - Data Analysis 26

2.3 Dendrite and Spine Analysis Following Golgi Cox Staining 26

2.4 Primary Hippocampal Dissociated Neuronal Cultures 27

2.4.1 Media and Solutions 27

2.4.2 Preparation of Poly-L-Lysine -Coated Coverslips 27

2.4.3 Preparation of Primary Embryonic Hippocampal Cultures 28

2.5 Ratiometric Calcium Imaging 28
2.5.1 Media, Solutions, Pharmaca and Viruses 28
2.5.2 Fura-2-AM Ca^{2+} Imaging Experiments 29
2.5.3 AAV-constructs and Transduction of Primary Cultures 30
2.5.4 Transfection of Primary Hippocampal Neurons 30
2.6 Immunhistochemistry 31
2.6.1 Solutions and Antibodies 31
2.6.2 Immunhistochemical Staining of Acute Slices 31
2.7 Statistical analysis 32
3 Results 33
3.1 The APP Homolog APLP1 Supports Basal Synaptic Transmission 33
3.1.1 Young APLP1 Knockout Mice 33
3.1.2 Aged APLP1 Knockout Mice 34
3.1.3 APLP1 KO: Age-Dependent Comparison of Basal Synaptic Transmission 36
3.2 Conditional APP Triple Knockout Mice 37
3.3 The Role of the Fe65 Protein Family as Downstream Actors of APP 38
3.4 Acute Inhibition of the APP α-Secretase ADAM-10 41
3.5 Viral Gene Transfer of Extracellular Liberated APP Domains and Their Dose-Dependent Effects on Synaptic Plasticity in APP/APLP2 Deficient Mice 42
3.5.1 High Amounts of APPsα Modulate LTP Negatively 43
3.5.2 Viral Driven APPsα Expression Rescues LTP and Impaired PPF in NexCre cDKO Mice 46
3.5.3 APPsβ Has No Modulatory Role on Synaptic Plasticity in NexCre cDKO Mice 47
3.6 AVV-driven Expression of APPsα and APPsβ in APP/PS1ΔE9 tg Mice and Their Effects on Synaptic Plasticity and Spine Density 49
3.6.1 AVV-driven Expression of APPsα Rescues Synaptic Plasticity and Spine density in APP/PS1ΔE9 tg mice 49
3.6.2 APPsβ Has No Modulatory Role on Synaptic Plasticity and Spine Density in APP/PS1ΔE9 tg Mice 53
3.6.3 Effect of AAV-driven APPsβ Expression in Wild-type Littermates 55
3.7 Disturbed Ca^{2+} Homeostasis in Primary Dissociated Hippocampal Cultures of NexCre cDKO Mice 57
3.7.1 Disturbed ER Activity in NexCre cDKO Mice Contributes to Impaired cLTP 60
3.7.2 Unaltered Ca^{2+} Signal Frequency in NexCre cDKO Mice 63
3.7.3 Spontaneous Ca^{2+} Dynamics in NexCre cDKO Cultures 65

3.7.4 External Ca^{2+} Modulates Spontaneous Ca^{2+} Frequency 68
3.7.5 APPsα Expression Rescues Spine Density in NexCre cDKO Cultures 70
3.8 The 16 Amino Acid Difference Between APPsα and APPsβ and Its Effect on Synaptic Plasticity 71
3.8.1 Influence of the α7-nAChR in Aβ1-16 Mediated Signaling in Synaptic Plasticity 72
3.8.2 Co-application of Aβ1-16 and α-Bungarotoxin During Recordings of Synaptic Plasticity in NexCre cDKO Mice 74
3.8.3 Efficacy of Aβ1-16 in Comparison to APPsα to Rescue Impaired LTP in NexCre cDKO Mice 76
4 Discussion 78
4.1 APLP1 Deficiency Causes Age-Dependent Impairments in Basal Synaptic Transmission 79
4.2 The APP Protein Family Is Essential During Brain Development and Adult Brain Function 80
4.3 The Fe65 Protein Family Interaction with APP/APLPs Is Essential for Synaptic Plasticity 81
4.4 Acute Inhibition of α-Secretase Activity Does Not Influence Synaptic Plasticity 83
4.5 APPsα But Not APPsβ Is the Functional Domain Supporting Synaptic Plasticity 84
4.5.1 APPsα, But Not APPsβ, Rescues the Synaptic Failure in an Alzheimer´s Disease Mouse Model 86
4.6 The APP Family is Essential for Intact Ca^{2+} Homeostasis 89
4.6.1 Alterations in ER Ca^{2+} Stores Contribute to Impaired cLTP in NexCre cDKO Mice 90
4.6.2 Evidence for Altered SOCC-Activity in NexCre cDKO Cultures 92
4.7 The 16 Amino Acid Difference between APPsα and APPsβ Mediates the Neurotrophic Peptide Functions 93
4.8 Conclusion and Outlook 96
5 References 98
6 List of Abbreviations 117
Danksagung 119

Abstract

Alzheimer´s disease (AD) is a neurodegenerative disorder with aging as most significant risk factor. AD is the most common form of dementia, being responsible for 60 to 80% of the cases. The number of diagnosed patients per year is growing rapidly and intense research focuses on the development of effective therapeutics as well as on ways to prevent the disease. While it is well known that accumulation of the neurotoxic amyloid β (Aβ) peptide, a cleavage product of the amyloid precursor protein (APP), is the key event of the disease, the physiological role of the APP protein family is still not fully understood. To develop potential therapeutic approaches it is essential to elucidate the physiological role of the APP protein family and their secreted peptides. It is necessary to understand how APP/APLPs modulate synaptic function as also a shift in the balance between APPsα and APPsß ectodomains might cause AD.

Investigation of gene targeted mice allowed me to examine the physiological function of APP family proteins and their cleavage fragments in synaptic transmission and activity-dependent synaptic plasticity in the hippocampus, the highly plastic brain region severely affected within AD. I could show that the so far less attended APP homolog APLP1 has an age-dependent role in supporting basal synaptic transmission at the hippocampal CA3-CA1 synapse. Moreover, the generation of a conditional APP triple knockout mouse model allowed me to study synaptic plasticity in surviving adult mice and revealed an important role for all three family members during brain development. Besides investigating the APP proteins in full-length, the role of their functional domains was addressed. My studies indicated that the Fe65 protein family is an important downstream actor of APP as the link between the adapter family and APP is essential to modulate synaptic function by intracellular signaling. The detailed analysis of the α-secretase cleavage product of APP, APPsα, supported the reports of its neurotrophic properties. I could show that the stable, viral driven expression of APPsα in APP/APLP2 deficient mice as well as in a mouse model of AD restored LTP deficits presumably by acting at presynaptic terminals. In contrast, the 16 amino acid shorter APP fragment APPsβ seems not to be involved in processes of synaptic plasticity. The analysis of dendritic spine density revealed a pivotal role for APPsα ameliorating spine density in AD mice and APP/APLP2 deficient cultures, while APPsβ was again ineffective. Elucidating the role of the 16 amino acids differentiating APPsα and APPsß, revealed that it is the domain carrying the functional neuroprotective properties of APPsα. Pharmacological experiments performed to provide a potential targeted receptor further yielded that the α7-nAChR receptor might be involved in synaptic signaling.

The key messenger in processes of activity-dependent synaptic plasticity is calcium (Ca^{2+}) and several studies indicate that the Ca^{2+} homeostasis is severely affected in AD patients. Investigation of Ca^{2+} dynamics in primary hippocampal cultures of APP/APLP2 deficient mice underscored a deficit in chemical LTP induction and Ca^{2+} homeostasis, which was rescued by the viral transduction of cultures with APPsα. Moreover, I observed a dysregulation of endomplasmatic reticulum Ca^{2+} handling and store-operated Ca^{2+} channel (SOCC) activity in APP/APLP2 deficient cultures consistent to results found in the literature for AD mice, emphasizing that APP family members are important regulators of Ca^{2+} dynamics in the brain. Moreover, these results highlight the neurotrophic role of APPsα and strengthen its potential as therapeutic agent for AD.

Zusammenfassung

Die Alzheimerkrankheit (AK) ist eine neurodegenerative Erkrankung bei der das Alter einen der höchsten Risikofaktoren bildet. Die AK ist mit 60 bis 80% der Demenzerkrankungen die häufigste Demenzform. Die Zahl der diagnostizierten Patienten steigt pro Jahr stark an, sodass intensive Forschung darauf fokussiert ist, effektive Behandlungsmöglichkeiten zu entwickeln und ebenso versucht Wege zu finden, die Krankheit zu verhindern. Während das Schlüsselereignis, der ansteigende Gehalt des neurotoxischen amyloidogenen Aß-Peptides als Spaltproduktes des amyloidogenen Vorläuferproteins (APP) bekannt ist, bleibt die physiologische Rolle der APP-Proteinfamilie nur hinreichend geklärt. Um jedoch potenzielle Therapiemöglichkeiten zu entwickeln, ist es essentiell die physiologische Rolle der APP-Proteinfamilie und ihrer sekretorischen Peptide zu verstehen. Ebenso wichtig ist es die Bedeutung von APP/APLPs hinsichtlich der Funktion von Synapsen zu klären, da auch ein Ungleichgewicht in deren Ektodomänen APPsα und APPsß die AK verursachen kann.

Die Untersuchung von transgenen Mäusen ermöglichte es die physiologische Funktion der APP-Proteinfamilie sowie ihrer Spaltprodukte im Hinblick auf synaptische Transmission und aktivitätsabhängige Plastizität im Hippokampus zu erforschen, der plastischen Hirnregion, die in der AK stark betroffen ist. Ich konnte zeigen, dass das solang wenig betrachtete APP Homolog APLP1 eine altersabhängige Rolle einnimmt, die darin besteht die basale synaptische Transmission zwischen den hippokampalen CA3-CA1 Synapsen zu unterstützen. Weiterhin ergab die Analyse eines adulten, lebensfähigen konditionalen Dreifach-*Knockouts* von APP hinsichtlich synaptischer Plastizität, dass alle drei Familienmitglieder eine wichtige Rolle in der Gehirnentwicklung einnehmen. Neben der Untersuchung der APP-Proteine in voller Länge, wurde die Rolle der funktionellen Domänen erforscht. Die Untersuchung ergab, dass die Fe65 Proteinfamilie einen wichtigen *Downstream*-Akteur von APP bildet, da der Link zwischen der Adapterfamilie und APP essentiell für die Modulation der synaptischen Funktion über intrazelluläre Signalwege ist. Die detaillierte Analyse des α-Sekretase Spaltproduktes von APP, APPsα, spiegelte die Forschungsergebnisse zu seinen neurotrophen Eigenschaften wider. Die stabile, virus-vermittelte Expression von APPsα in APP/APLP2-defizienten Mäusen und in einem AK-Mausmodell behob vorhandene LTP-Defizite, mutmaßlich über die Aktivität an Präsynapsen. Im Gegensatz dazu zeigte sich, dass das 16 Aminosäuren (AS) kürzere APPsß-Peptid die Prozesse von synaptischer Plastizität nicht moduliert. Die morphologische Analyse der *Spine*-Dichte erwies, dass nur APPsα die Anzahl an *Spine*s in AK-Mäusen sowie APP/APLP2-defizienten Kulturen verbessert, während APPsß keinen Einfluss hatte. Die Untersuchung der 16 AS, die APPsα und APPsβ differenzieren, ergab, dass sie die neuroprotektiven Eigenschaften von APPsα enthalten. Pharmakologische Experimente bezüglich eines Zielrezeptors zeigten, dass der α7-nAChR in der synaptischen Transmission beteiligt sein könnte.

Das Schlüsselmolekül für Prozesse der synaptischen Plastizität ist Calcium (Ca^{2+}) und Studien belegen, dass die Ca^{2+} Homöostase in der AK stark gestört ist. Untersuchungen bezüglich der Ca^{2+} Dynamik an primären hippokampalen Kulturen APP/APLP2-defizienter Mäuse ergaben Defizite in der Induktion der chemischen LTP sowie in der Ca^{2+} Homöostase, die jedoch durch die Transduktion der Zellen mit APPsα wiederhergestellt werden konnten. Weiterhin wurde eine Fehlregulation von Ca^{2+} im endoplasmatischen Retikulum und der *store-operated* Ca^{2+}-Kanalaktivität in APP/APLP2-defizienten Kulturen beobachtet, wie sie in der Literatur für AK-Mäuse beschrieben ist. Dies hebt die Rolle der APP-Familienmitglieder als wichtige Regulatoren der Ca^{2+} Dynamik im Gehirn hervor. Weiterhin betonen diese Ergebnisse die neurotrophe Funktion von APPsα und stärken sein Potential als Medikament für die AK.

1 Introduction

"Today, someone in the country develops Alzheimer's disease every 66 seconds. By 2050, one new case of Alzheimer's is expected to develop every 33 seconds, resulting in nearly 1 million new cases per year." (Alzheimer's, 2016)

"Alzheimer's disease: the silver tsunami of the 21st century" (Sarkar et al., 2016)

These are only two examples out of many headlines or facts, one is reading more and more often in the news. It is projected that by the year 2050 more than 100 million people across the world will be battling with Alzheimer´s disease - a quite exploding development. In the last eleven years, the number of adults suffering from the disease increased from almost 26 million to more than 36 million (Figure 1.1A). And even more alarming is the expected increase within the next 33 years to more than 100 million (Alzheimer's, 2016). The rise in patients is restricted to a so called aging population as the National Institute of Health diagnosed patients after the age of 65 with women having a higher estimated risk to develop Alzheimer´s than men (Seshadri et al., 2006)(Figure 1.1B).

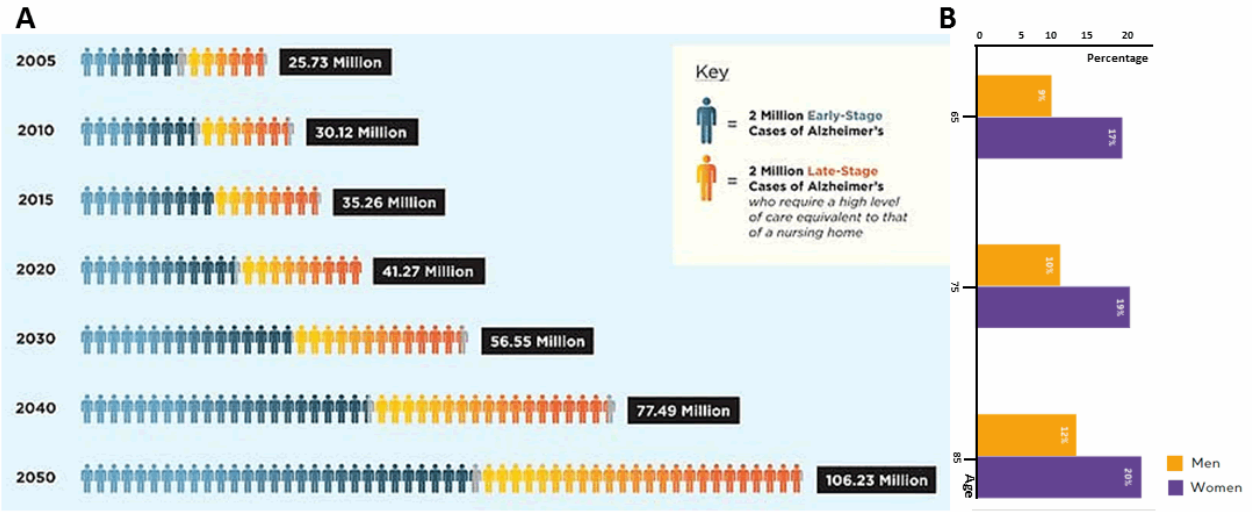

Figure 1.1: (A) Worldwide projections of Alzheimer´s prevalence. The numbers of cases in millions for the years 2005 to 2050 are shown, differentiated by the stage of disease (early or late stage). (Adapted from Medicalexpress.com, Report by Carla Denly, January 6, 2016) **(B)** Estimated lifetime risk for Alzheimer´s disease by age and sex created from data of the Framingham study. (Adapted from Alzheimer´s, 2016)

1.1 Alzheimer´s Disease

In 1906 Alois Alzheimer documented the first case of Alzheimer´s disease (AD). His patient Auguste Deter displayed the typical symptoms of sporadic AD including disorientation, depression and progressive memory decline. AD is the most common cause of dementia and accounts for estimated 60 to 80 percent of the cases. Patients suffering from this disease display difficulties in remembering recent conversations, events or names and often also show apathy and depression as early clinical symptoms.

Symptoms occurring at later stages include impaired communication, disorientation, confusion, poor judgement, behavioral changes and in the end difficulties in speaking, swallowing as well as walking (Alzheimer's, 2016). The pathological hallmarks of AD, seen and described already in 1907 by Alois Alzheimer, are the progressive extracellular accumulation of the amyloid-β (Aβ) protein fragment in so called amyloid plaques (or senile plaques) and the formation of intracellular neurofibrillary tangles (NFTs). NFT deposits are fibrillar aggregates of the microtubule associated binding protein tau which exhibits hyperphosporylation as well as oxidative modifications (Selkoe, 2002). Plaques and NFTs are mainly observed in brain regions that are involved in learning and memory processes as well as in emotional behaviors like the entorhinal cortex, the hippocampus, the basal forebrain and the amygdala. Within these brain regions, the number of synapses representing the contact sites between neurons is reduced and neurites in proximity to plaques are often damaged. This degeneration finally leads to shrinkage of affected brain areas with neurons exhibiting increased oxidative damage, impaired energy metabolism and altered calcium homeostasis (Mattson, 2004). Aβ plaques and NFTs built the major hallmarks of AD, while additionally genetic, molecular, epidemiological and immunological alterations are proposed to contribute to the disease (Heneka and O'Banion, 2007, Povova et al., 2012, Heneka et al., 2014). The greatest risk factors for sporadic AD are older age (Hebert et al., 2013), having several familiar AD cases (Fratiglioni et al., 1993, Lautenschlager et al., 1996) and being carrier of the APOE-e4 gene (Farrer et al., 1997, El Haj et al., 2016). Currently two hypotheses exist that describe the origin of the disease. In the familial form of AD (FAD), mutations in presinilin-1 and 2 (PS1 and PS2) as well as mutations in the amyloid precursor protein (APP) cause the disease and lead to an increased production of Aβ or changes in the ratio of Aβ42 and Aβ40 (Selkoe and Hardy, 2016). In contrast to the inherited forms of AD, a failure in Aβ clearance mechanisms is the primary cause of non-dominant disease forms resulting in gradually rising Aβ levels in the brain. In both cases of the amyloid cascade hypothesis, the accumulation and oligomerization of Aβ42 is observed in limbic and association cortices and subtle effects of Aβ oligomers on synaptic efficacy are noticed. The following gradual deposition of Aβ42 oligomers in diffuse plaques activates microglia and astrocytes, the supportive cells of the brain (Purves et al., 2001) and attendant inflammatory responses. Later stages of the cascade are characterized by alterations in neuronal ionic homeostasis and the appearance of oxidative injury. Moreover impairments in kinase and phosphatase activities lead to tangle formation within neurons. Overall these alterations result in a widespread neuronal and synaptic dysfunction accompanied by selective neuronal loss associated to neurotransmitter deficits (Selkoe and Hardy, 2016). Synaptic dysfunction is represented by impairments of synaptic plasticity as intact synaptic structure and function are fundamental for synaptic encoding forming stable memories (Mayford et al., 2012, Korte and Schmitz, 2016).

1.2 Synaptic Plasticity

It is by now widely believed and accepted that neurons in mammalian brain regions, relevant for learning and memory, are highly plastic. In this regard, plasticity means that activity patterns generated by sensory organs modulate neuronal function as well as their structure. Activity-dependent synaptic plasticity that alters the efficacy of synaptic transmission (functional plasticity) and modifies the structure and number of synaptic connections (structural plasticity) are essential for processes of learning and memory (Korte and Schmitz, 2016). Neuronal plasticity builds the foundation for learning and memory while additionally neuronal networks need to be adjusted. In 1949 already the psychologist

Donald Hebb postulated how neurons adapt to patterns of activity by forming engrams during learning and memory (Morris, 1999):

"When an axon of cell A is near enough to excite a cell B and repeatedly or persistently takes part in firing it, some growth process or metabolic change takes place in one or both cells such that A's efficiency, as one of the cells firing B, is increased ''.

"….any two cells or systems of cells that are repeatedly active at the same time will tend to become 'associated', so that activity in one facilitates activity in the other ''. (Donald Hebb, 1949)

In 1973 Timothy Bliss and Terje Lømo experimentally verified the Hebb´s postulate. They observed that high electrical frequency stimulation of the hippocampal perforant path projecting to granule cell synapses resulted in long-lasting strengthening of synaptic connections (Bliss and Lomo, 1973), a phenomenon nowadays termed long-term-potentiation (LTP, see chapter 1.2.1 and 1.2.2). LTP was first described in the hippocampus which is also today one of the most studied brain regions in mammals in regard to activity-dependent synaptic plasticity.

1.2.1. The Hippocampus

The hippocampus with its bulb-like shape, protruding into the lateral ventricles is an evolutionary old bilateral structure of the cerebral cortex (Andersen et al., 2006). It is essential for the formation of spatial, contextual and episodic memory and moreover for the recall of consolidated memory (O'Keefe and Nadel, 1978, Eichenbaum, 2004). The hippocampus integrates incoming sensory and spatial information from the entorhinal cortex into context-specific representations, so that short-term memory is transferred into long-term memory. Especially the formation of declarative memory, involving facts about ourselves and our surrounding world, is an essential feature of the hippocampus (Korte and Schmitz, 2016). This is furthermore supported by hippocampal lesion studies like the one of the well-known case of the epileptic patient H.M. 60 years ago. The hippocampus of H.M. was bilaterally removed during a surgery resulting in a permanent anterograde and partial retrograde amnesia (Scoville and Milner, 1957). H.M. displayed an intact short-term and working memory and was able to retrieve very old memories, while the acquisition of new declarative memories was impossible. The fact that the hippocampus is further essential for spatial memory formation was also shown by Mumby and colleagues in 1999 using hippocampal lesioning of rodent hippocampi. Rats with hippocampal lesions that were trained in the Morris water-maze task were no longer able to form a spatial map to locate the platform as exit of the maze (Mumby et al., 1999). Both studies further indicate that the hippocampus is an attractive region to study neurological disorders like epilepsy or Alzheimer´s disease (AD), because pathological processes are observed within that brain area and novel therapeutics can be tested.

The hippocampus has a unique and highly organized structure making it a suitable model for investigations in mammals. It is organized in a lamellar way and comprises the dentate gyrus (DG) and the ammon's horn (CA, lat. *cornu ammonis*). Related cortical subregions are the entorhinal cortex (EC), the subicular complex, the pre- and parasubiculum forming together with the CA and the DG the hippocampal formation (HF). The ammon´s horn is further divided into three subdivisions: CA1, CA2 and CA3 with distinct neuronal populations of excitatory connected cells forming a trisynaptic circuit (see

Figure 1.2A, B). Information enters the hippocampus from the EC which itself is connected to various cortical areas. The EC projects unidirectional via the perforant path to the principal cells of the DG. The axons of DG granule cells give rise to axons called mossy fibers that connect DG granule cells with pyramidal neurons of the hippocampal CA3 area. The axons of pyramidal cells of CA3 in turn build the major input to CA1 neurons by the Schaffer collateral pathway. The CA1 neurons of the hippocampus project to the subiculum and moreover to the EC, while the subiculum itself projects to the pre- and parasubiculum, but predominantly to the EC. Thereby, CA1 and the subiculum close the hippocampal information processing loop starting in the superficial layers of the EC and ending into its deep layers (Andersen et al., 2006). The CA2 area, a very small region of the hippocampus, receives its input from DG neurons and innervates CA1 neurons (Kohara et al., 2014). Beside the 95% excitatory hippocampal neurons in all subregions also inhibitory cells exist, mediating feedback and feed-forward inhibition and thus shape the rhythm of activity. Interneurons are inter-connected and display oscillations with variable frequencies to ensure the synchronization of the hippocampal network (Buzsaki, 2002).

The unique hippocampal architecture with axons projecting in-line with pyramidal neurons (see Figure 1.2C) makes it a suitable model to investigate synaptic plasticity not only *in vivo*, but also *in vitro* as transversal slice preparations keep neuronal projections mostly intact (Korte and Schmitz, 2016). In this dissertation I recorded basal synaptic transmission as well as activity-dependent alterations between synapses of area CA3 and CA1 that were connected by the Schaffer collateral pathway in murine slice preparations.

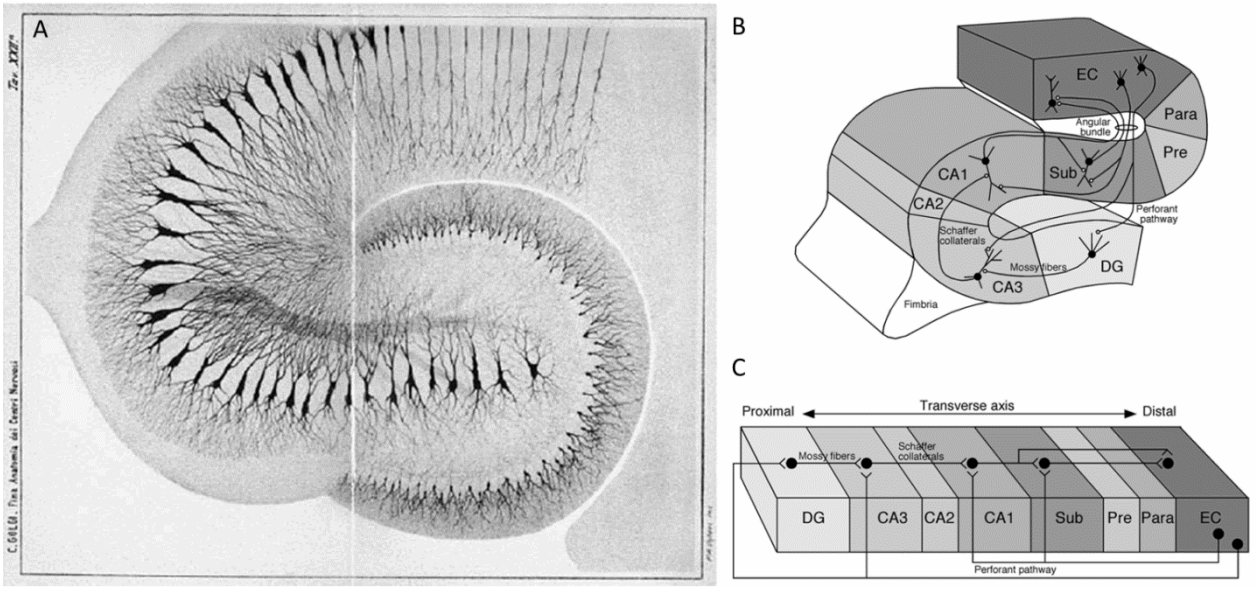

Figure 1.2: The hippocampal formation. (A) Section of a rabbit hippocampus stained with the original Golgi method (1886) showing the cell population in their different layers (Golgi et al., 2001). **(B)** Neurons in layer II of the entorhinal cortex (EC) project to the dentate gyrus (DG) and the CA3 field of the hippocampus via the perforant pathway. Neurons in layer III of EC innervate cells of the CA1 field of the hippocampus and the subiculum (Sub) via the perforant and alvear pathways. The granule cells of the DG project to the CA3 field of the hippocampus via mossy fiber projections. Pyramidal neurons in the CA3 field of the hippocampus project to CA1 via Schaffer collaterals. Pyramidal cells in CA1 innervate neurons of the subiculum. Both, CA1 and the subiculum project back to the deep layers of the EC. **(C)** Projections along the transverse axis of the hippocampal formation where the DG is located proximally and the EC distally (adapted from *The Hippocampus Book*).

1.2.2 Long-Term Potentiation and Long-Term Depression

The fascinating capacity of the mammalian brain to be plastic allows it to modify synaptic strength among connected neurons upon activity patterns generated by experiences (Citri and Malenka, 2007, Abrahamsson et al., 2016) initially described by D. Hebb (1949). Activity either enhances or depresses synaptic transmission at excitatory synapses on timescales ranging from milliseconds to hours or even days. Distinct stimuli alter synaptic efficacy, thus high-frequency stimulation (200 ms to 5 s at 10 to 200 HZ) results in an persistent increase in synaptic strength lasting for at least one hour called long-term potentiation (LTP) (Bliss and Lomo, 1973, Zucker and Regehr, 2002), while low-frequency stimulation produces synaptic weakening named long-term depression (LTD) (Ho et al., 2011, Luscher and Malenka, 2012). The underlying mechanisms of LTP and LTD are not uniform as they depend on the circuit in which they occur. For example, LTP at mossy fiber-CA3 synapses is independent from the N-methyl-D-aspartate receptor (NMDA-R) while synapses of the perforant path-DG pathway or the Schaffer collateral-CA1 pathway are NMDA-R dependent (Lynch, 2004, Luscher and Malenka, 2012, Volianskis et al., 2015). The most intensively studied and well described form is the NMDA-R-dependent LTP (and LTD) at CA3-CA1 synapses in the hippocampus and in the focus of this thesis.

The NMDA-R is a ligand-gated ion channel with glutamate as agonist and glycine as well as D-serine as co-agonists (Henneberger et al., 2013) being permeable for sodium (Na^+) and calcium (Ca^{2+}). Under resting membrane conditions NMDA-R function is prevented due to a magnesium block hindering the channel pore to open for Na^+ and Ca^{2+} (see Figure 1.3A). Hence, basal synaptic transmission is mainly mediated by α-amino-3-hydroxy-5-methyl-4-isoxazole propionic acid receptors (AMPA-R) allowing Na^+ and potassium (K^+) influx in response to glutamate binding (Citri and Malenka, 2007). Following postsynaptic depolarization the Mg^{2+} block is released from the NMDA-R and when simultaneously glutamate binds, the receptor gets permeable for Na^+ and Ca^{2+} (Herron et al., 1986). Due to the characteristic that the NMDA-R is only conductive when pre- and postsynapse are active at the same time he functions as a coincidence detector. This defines moreover one of the three key properties of LTP (Bliss and Collingridge, 1993):

1) Input specificity meaning that only activated synapses release glutamate at the presynaptic site and that only postsynapses that receive the neurotransmitter get stimulated and not adjacent inactive ones.
2) Cooperativity confining LTP to a critical number of synapses that are coincidently active and
3) Associativity representing the capacity to potentiate a weak input (a small number of synapses) when it is activated in association with a strong input (a larger number of synapses).

The key characteristics of NMDA-R dependent LTP and LTD are to require active connections between synapses, the presynaptic terminals and postsynaptic dendritic spines. Spines are small membrane protrusions that consist of a bulbous head and a thinner neck connecting the spine to the dendritic shaft (Ho et al., 2011). Interestingly, the spine head size and spine volume correlate with synaptic strength (Kirov and Harris, 1999, Holtmaat and Svoboda, 2009), implying that spines with large heads contain more receptors for neurotransmitter and reflect a greater synaptic strength (see Figure 1.3B). As spines serve as single compartmentalized signaling units, they build the active postsynaptic part of the synapse changing in number and shape during synaptic plasticity (Engert and Bonhoeffer, 1999). While during LTP, AMPA-Rs are inserted into the membrane to support synaptic strengthening, they are internalized in processes of LTD (Figure 1.3B). Prolonged low frequency stimulation induces only a moderate increase in postsynaptic Ca^{2+} levels whereas contrary high frequency stimulation strongly increases the amount of Ca^{2+} in the postsynapse. Low Ca^{2+} levels result in the activation of phosphatases, e.g. calcineurin or

protein phosphatase PP1, which in turn increases the endocytosis of AMPA-R at extrasynaptic sites. Tetanic stimulation increases cytosolic Ca^{2+} levels in the postsynapse and leads to the activation of protein kinases, e.g. calcium/calmodulin-dependent kinase II (CaMKII), enhancing AMPA-R exocytosis and mediate the fusion of recycling endosomes by Rab11a as well as AMPA-R stabilization within the post-synaptic density (PSD) (Citri and Malenka, 2007, Korte and Schmitz, 2016) (Figure 1.3B).

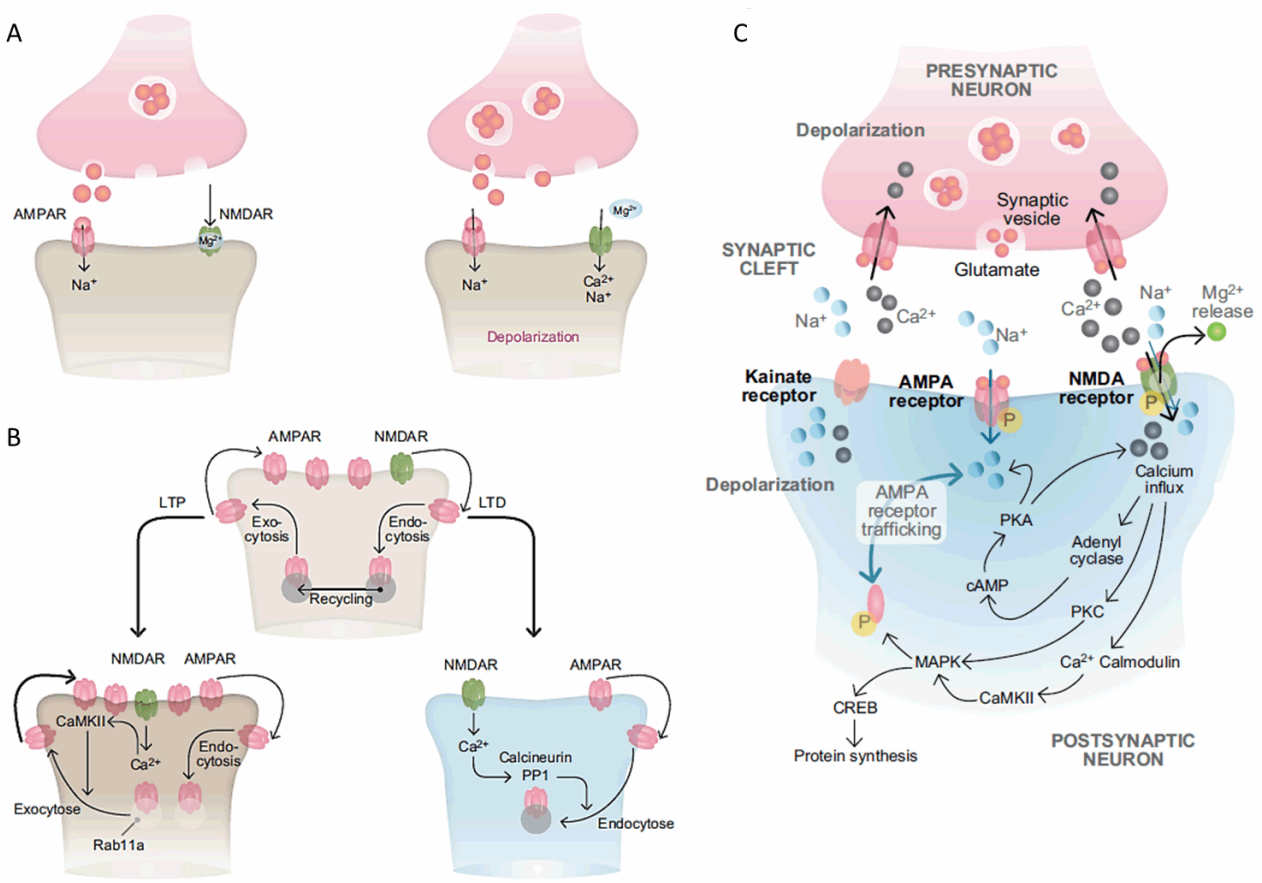

Figure 1.3: Cellular processes at resting membrane conditions and following synaptic plasticity. (A) Schematic synaptic transmission at excitatory synapses. *Left:* During basal synaptic transmission presynaptically released glutamate binds to AMPA-Rs and NMDA-Rs, but results only in activation of AMPA-R mediating Na^+ influx while the NMDA-R is blocked by Mg^{2+}. *Right:* Depolarization of the postsynaptic cell released the Mg^{2+} block of the NMDA-R channel allowing Na^+ and Ca^{2+} to enter the spine. **(B)** Schematic AMPA-R trafficking during LTP and LTD. *Top:* Under resting membrane conditions, AMPA-R cycle between the postsynaptic membrane and intracellular compartments by lateral movement of receptors into endocytic zones. AMPA-R containing early endosomes were transferred to recycling endosomes and returned to the plasma membrane by exocytosis. They move again laterally into the synapse and are there retained. *Bottom left:* LTP induction leads to enhanced AMPA-R exocytosis. Inserted AMPA-R are stabilized at the synapse through a Ca^{2+}-driven process involving the CamKII, while fusion of recycling endosomes is mediated by Rab11a. *Bottom right:* LTD induction results in enhanced AMPA-R endocytosis at extrasynaptic sites in a Ca^{2+}-dependent process including the protein phosphatase PP1 or calcineurin. Endocytosed AMPA-Rs are retained within the cell or degraded. **(C)** Action potential driven pre- and postsynaptic signaling. The arrival of an action potential at the presynaptic terminal induces a Ca^{2+} influx via voltage-gated Ca^{2+} channels triggering the fusion of synaptic vesicles and the exocytosis of glutamate. The neurotransmitter binds and thus activates kainite receptors and AMPA-R at the postsynapse mediating the influx of Na^+ into the cell. The initiated depolarization released the Mg^{2+} block from the NMDA-R allowing additional Ca^{2+} to enter the cell. Increase in cytosolic Ca^{2+} levels activates Ca^{2+}-dependent enzymes like CamKII, protein-kinase C (PKA) and adenyl cyclase facilitating AMPA-R trafficking by phosphorylation of specific receptor subunits (adapted from Korte and Schmitz, 2016).

At resting membrane conditions AMPA-Rs provide most of the inward currents generating an excitatory postsynaptic response (EPSP), while NMDA-Rs are strong voltage dependent and are blocked by Mg^{2+}. When an action potential reaches the presynaptic terminal of a neuron, voltage-gated Ca^{2+} channels (VGCCs) are activated and allow the influx of Ca^{2+} (Figure 1.3C). This in turn triggers the fusion of synaptic vesicles filled with neurotransmitter with the presynaptic membrane and the exocytosis of glutamate (at excitatory synapses). Following diffusion of glutamate through the synaptic cleft it binds and thus activates in first instance kainite receptors and AMPA-Rs expressed on the postsynaptic membrane. The two channels allow Na^{+} to enter the cell which in turn depolarizes the postsynapse and results in the dissociation of the Mg^{2+} block from the NMDA-Rs allowing additional Ca^{2+} to enter the cell. The influx of Ca^{2+} via NMDA-Rs activates Ca^{2+}-dependent enzymes like CamKII, protein-kinase C (PKA) and adenyl cyclase facilitating AMPA-R trafficking by phosphorylation of specific receptor subunits. There is strong evidence that the activation of CamKII is the key component to trigger the molecular machinery of LTP. Supportive for the essential role of CamKII is the prevention of LTP induction in knock-out mice lacking a critical CamKII subunit (Silva et al., 1992) or in knock-in mice in which the endogenous CamKII was replaced by a from that lacks the autophosphorylation site (Giese et al., 1998). Following LTP induction the CamKII gets autophosphorylated and initiates downstream signaling cascades including the synthesis of new proteins (Fukunaga et al., 1995, Barria et al., 1997). However, the early phase of LTP (E-LTP), lasting from one to three hours is independent of protein synthesis, while maintained LTP lasting longer than three hours is dependent on altered gene expression and referred to as late LTP (L-LTP) (Bliss and Collingridge, 1993, Kandel, 2001, Korte and Schmitz, 2016). Comparably to L-LTP also the long-lasting maintenance of LTD (L-LTD) is dependent on *de novo* protein synthesis (Manahan-Vaughan et al., 2000, Sajikumar et al., 2005). Furthermore, the expression of long-lasting LTP or LTD is dependent on the type of stimulation; so that only repetitive or tetanic stimulation of synapses with prolonged (~200 ms to 5 s) trains of stimulation applied at high frequencies induce long-lasting changes in synaptic efficacy. In contrast, short bursts of activity result in plasticity lasting only for several milliseconds to minutes and are called mechanism of short-term synaptic plasticity (Zucker and Regehr, 2002, Citri and Malenka, 2007).

1.2.3 Temporal Phases of LTP

Excitatory synapses of the mammalian brain express different forms of synaptic plasticity that can be differentiated by their varying temporal phases. Short-term plasticity (STP) elicits changes in synaptic strength lasting from milliseconds to minutes and is believed to be important for short-term adaptations to sensory inputs as well as transient changes in behavior and for a short-lasting form of memory (Citri and Malenka, 2007). Following short burst of activity, Ca^{2+} accumulates transiently in the presynaptic terminal and causes changes in the probability of neurotransmitter release due to the modification of biochemical processes that mediate synaptic vesicle exocytosis (Zucker and Regehr, 2002). Thus, STP is a presynaptic phenomenon and can be investigated easily by applying two stimuli within a short interval. The response of the second stimulus to the first one can thereby either be enhanced (Paired-Pulse-Facilitation, PPF) or depressed (Paired-Pulse-Depression, PPD) depending on the length of the inter-stimulus interval delivered (ISI) (Katz and Miledi, 1968). At ISIs less than 20 ms PPD is observed caused by the inactivation of voltage-dependent Na^{+} or Ca^{2+} channels as well as by the transient depletion of the ready releasable pool (RRP) of synaptic vesicles at the presynaptic membrane. At ISIs longer than 20 ms and up to 500 ms PPF is detected due to residual Ca^{2+} left from the first action potential in the

presynaptic terminal increasing the release of synaptic vesicles to the second stimulus (Zucker and Regehr, 2002, Kaeser and Regehr, 2017). Similar to PPF, additional mechanisms might be involved in the facilitation like the activation of protein kinases modulating the activity of phophoproteins expressed in the presynapse (Citri and Malenka, 2007, Regehr, 2012). Importantly, the same synapse can display PPF or PPD depending on its recent history of activation and modulation. Synapses with a very high probability of neurotransmitter release will show a depression to the second stimulus applied, while synapses with a low probability of neurotransmitter release exhibit a facilitation in transmitter release to the second pulse (Dobrunz et al., 1997, Dobrunz and Stevens, 1997). PPF thereby defines a form of presynaptic Ca^{2+}-dependent STP reflecting the probability of neurotransmitter release with reduced ratios representing an increased probability of vesicle release (Briggs et al., 2017). Moreover, the presynaptic vesicle release probability is inversely associated with the post-tetanic potentiation (PTP) magnitude and the paired pulse ratio (Zucker and Regehr, 2002, Brager et al., 2003).
High frequent stimulation induces long-lasting forms of STP named augmentation which lasts five to ten seconds and PTP with a time course of several seconds to minutes (Citri and Malenka, 2007). Augmentation and PTP describe both an enhancement of neurotransmitter release and are caused by an increase in the probability of synaptic vesicle release in response to stimuli leading to a buildup of higher Ca^{2+} concentrations as well as biochemical alterations of proteins in the presynaptic terminal (Zengel and Magleby, 1982, Zucker and Regehr, 2002). PTP characterizes furthermore the initial induction phase of LTP that is followed by STP being the phase of LTP lasting for up to one hour. The time-course of early LTP (E-LTP) is detectable for less than a few hours, while the late component of LTP (L-LTP) lasts from several hours *in vitro* to up to weeks or months *in vivo* (Citri and Malenka, 2007, Reymann and Frey, 2007). STP is an essential feature of synapses as it enables them to influence the information processing and thus STP can be seen to act as filter between synapses. Early and late LTP and LTD are seen as cellular correlates for learning and memory and to understand their mechanisms plays an important role with regard to neurodegenerative disorders like epilepsy, Parkinson's and Alzheimer's disease.

1.2.4 Synaptic Plasticity in Alzheimer's Disease

It is by now commonly accepted that Alzheimer´s disease (AD) is caused by a synaptic failure. Indeed, it begins with subtle alterations in the efficacy of synaptic transmission (Selkoe, 2002). These alterations are not caused by the pathological hallmarks of the disease, Aβ plaques and neurofibrillary tangles (see chapter 1.1), but by the amyloid peptide Aβ that accumulates during the disease progression to form Aβ plaques (Selkoe, 2008, Parihar and Brewer, 2010). Aβ is a natural proteolytic product that is extracellularly released following sequential amyloidogenic cleavage of the amyloid precursor protein (APP, see chapter 1.3.1). Different Aβ peptides are generated upon the initial endopeptidase cleavage of APP due to multiple carboxypeptidase cleavages that each remove three to four C-terminal amino acids (Okochi et al., 2013, Fernandez et al., 2014). In this regard, Aβ42, Aβ43 and longer Aβ peptides were shown to be more hydrophobic and to highly self-aggregate (Kim et al., 2007). Aβ is found in the brain and the cerebrospinal fluid (CSF) of humans and animals (Haass et al., 1992). At picomolar concentrations and in its monomeric form, Aβ plays an important physiological role. Aβ was shown to modulate presynaptic vesicle release and therefore proven to be essential for processes of synaptic plasticity (Abramov et al., 2009, Wang et al., 2012) as LTP was enhanced upon exogenous Aβ42 administration (Puzzo et al., 2008). Nevertheless, when Aβ42 reaches nanomolar concentrations neurotoxic effects are observable. Subneurotoxic concentrations of Aβ peptides (Aβ42, Aβ40 or Aβ25-

35) exogenously applied on hippocampal slices inhibited LTP induction at the medial perforant path to DG cells and at the Schaffer collateral CA1 pathway without altering basal synaptic transmission (Chen et al., 2000, Chen et al., 2002, Zhao et al., 2004). Supporting results were gained in the *in vivo* study of Walsh and colleagues (2002), where injection of secreted Aβ into the hippocampal CA1 region prevented stable LTP induction. In that study it was further shown, that only soluble Aβ oligomers but not monomeric Aβ or Aβ fibrils cause the LTP deficit (Walsh et al., 2002). Furthermore Aβ42 alters the counterpart of LTP, LTD. An *in vivo* injection of Aβ42 was shown to facilitate LTD and reversal LTD in the CA1 region of the hippocampus (Kim et al., 2001). Aβ mediated alterations of synaptic plasticity occur at both sites of the synapse. It was shown that Aβ co-localizes with the postsynaptic density marker PSD95 (Lacor et al., 2004) and augments NMDA-R currents in the DG of acute hippocampal slices without affecting AMPA-R currents (Wu et al., 1995). Moreover, synthetic Aβ42 peptides as well as naturally secreted Aβ from APP/PS1 transgenic mice (AD mouse model: mice express the human APP gene carrying the Swedish double mutation (K595N/M596L)) promoted the endocytosis of NMDA-R from the postsynaptic surface depressing the NMDA-R current in wildtype cortical neurons (Snyder et al., 2005). Also reduced expression of AMPA-R on the cell surface was noted in neurons that overexpress wildtype APP or the APP Swedish double mutation as well as in neurons where exogenously Aβ42 peptides were applied (Almeida et al., 2005, Hsieh et al., 2006). Aβ mediated alterations within the postsynapse suggest that it alters Ca^{2+}-dependent signaling pathways that usually support synaptic plasticity like the exocytosis of AMPA-R or the phosphorylation of AMPA-R subunits which were affected in the presence of nanomalor Aβ (Hsieh et al., 2006, Minano-Molina et al., 2011). The amyloid peptide was moreover shown to influence presynaptic function as Aβ42 oligomers directly inhibited presynaptic P/Q type Ca^{2+} channels and decreased the synaptic vesicle release (Nimmrich et al., 2008). *In vitro* studies in which synthetic Aβ was applied on cultured hippocampal neurons revealed downregulation of dynamin, a protein that is essential for synaptic vesicle endocytosis and additional interrupted synaptic vesicle recycling (Kelly et al., 2005, Kelly and Ferreira, 2007). Kelly and colleagues further reported that decreased levels of dynamin depend on NMDA-R mediated Ca^{2+} influx and the activation of the intracellular cysteine protease calpain by Ca^{2+}, supporting the presence of retrograde signaling from the post- to the presynapse (Kelly et al., 2005, Kelly and Ferreira, 2006). As Ca^{2+} is an essential mediator of basal synaptic transmission it is therefore not surprising that synaptic dysfunction and altered Ca^{2+} homeostasis are key pathologies of Alzheimer´s disease (Agostini and Fasolato, 2016). Besides Aβ, sequential cleavage of APP releases a variety of functional domains that might additionally contribute to the disease, possibly by their reduced generation or by modified gene expression (Nhan et al., 2015). The investigation of the physiological function of the APP family and its proteolytic products is still poorly understood and in the focus of this thesis.

1.3 The Amyloid Precursor Protein Family

The amyloid precursor protein (APP) is a type I integral membrane protein involved in the pathogenesis of Alzheimer´s disease (AD). The APP gene is localized on chromosome 21 in humans and its expression gives rise to three major isoforms: APP695, APP751 and APP770 that all have a molecular weight of around 170 kDa and are generated via alternative splicing (Robakis et al., 1987, Barthet et al., 2012). The APP695 isoform is primarily found in neurons, especially in excitatory neurons as well as in GABAergic interneurons, while the two longer APP versions are expressed in other tissues and cell types (Wang et

al., 2014, Hick et al., 2015, Nhan et al., 2015, Del Turco et al., 2016). The mammal APP is part of a larger gene family including two homologs, the amyloid precursor-like protein 1 and 2 (APLP1 and APLP2). The APP/APLPs share a common structure comprised of a large extracellular domain containing the conserved regions E1 and E2, while the cytoplasmic region is relatively short. Importantly, the AD associated Aβ domain, is expressed only in APP but not in its homologs. The complete X-ray structure of APP is not solved by now, but for some independently folded subdomains structural information is available. The E1 domain of APP695 is subdivided into the heparin-binding/growth factor-like domain (GFLD) and the so-called copper-binding domain (CuBD), while APP751 and APP770 moreover contain one or two differentially spliced exons encoding for the Kunitz-like protease inhibitor domain (KPI) and a short Ox-2 antigen domain (Rossjohn et al., 1999, Dahms et al., 2010). The second conserved region, the E2 domain, contains the RERMS motif which is implicated in trophic functions and moreover another heparin binding domain (Ninomiya et al., 1993, Roch et al., 1993). These individual domains enable the APP isoforms to interact with a variety of proteins or receptors like Alcadein (Araki et al., 2003), F-spondin (Ho and Sudhof, 2004), Reelin (Hoe et al., 2009), LRP1 via the adapter Fe65 (Pietrzik et al., 2004), sorL1/LR11 (Schmidt et al., 2007), Nogo-66 receptor (Park et al., 2006) and Notch2 (Chen et al., 2006a). Additionally, the E1 domain was demonstrated to be crucial for the homo- and heterodimerization of APP family members (Soba et al., 2005). The APP structure and function is moreover modulated by posttranslational modifications like N- and O-glycosilation and sialyation (Dawkins and Small, 2014) which might further influence the proteins function. The expression of APP mRNA arises early in embryonic development (E7.5) and is found during adulthood dependent on the isoform throughout the body nervous system (brain, spinal cord, retina), immune system (thymus, spleen), muscle (smooth, cardiac, and skeletal), kidney, lung, pancreas, prostate gland, and thyroid gland (Wasco et al., 1993, Liu et al., 2008, Aydin et al., 2012). Interestingly, the APP and APLP2 proteins are found at particularly high levels in the brain where their expression patterns largely overlap in pyramidal neurons of the cortex and hippocampus (Lorent et al., 1995). *In vitro* studies revealed APP expression in astrocytes and microglia that is increased following brain injury (LeBlanc et al., 1997, Rohan de Silva et al., 1997). A more recent study reported that APP expression is restricted to neurons and cannot be found in major glial cells like astrocytes or microglia under basal as well as neuroinflammatory conditions (Guo et al., 2012a) due to the fact that utilized antibodies were not specific. The APP homolog APLP1 shows in contrast to APP and APLP2 nervous system specific expression (Lorent et al., 1995, Thinakaran and Koo, 2008, Klevanski et al., 2014). The intracellular domain of APP family members contains the highly conserved YENPTY motif which was shown to promote clathrin mediated endocytosis, modulate Aβ generation, interfere with Ca^{2+} homeostasis and interact with multiple kinases and adapter proteins (Leissring et al., 2000, Ring et al., 2007, Jacobsen and Iverfeldt, 2009). Although APP/APLP structure is well studied, the precise cellular functions of the APP family proteins remain elusive. Several studies tried to assess putative functions of the protein family during development and in the adult nervous system (Jacobsen and Iverfeldt, 2009). Certainly, one of the most intriguing discoveries in this respect is the involvement of APP and its cleavage products in processes of synaptic plasticity (Korte et al., 2012).

1.3.1 Amyloid Precursor Protein Processing

APP family members undergo very complex processing, whereupon secretase activities a variety of biological active fragments are generated. Depending on their site of release, extra- and/or intracellularly, they might have functions as signaling molecules or initiate signaling cascades by binding

to different types of receptors. Proteolytic processing of APP is depicted in Figure 1.4 and was shown to be similar among APP family members except for the release of Aβ as this coding sequence is absent in the APP homologs (Eggert et al., 2004, Walsh et al., 2007). The current view allows differentiation between three different processing pathways initiated by the α-, β- or -η-secretase. In the non-amyloidogenic pathway the α-secretase, in neurons and brain the α-disintegrin and metalloproteinase (mainly ADAM-10), cuts within the Aβ domain liberating the large APPsα ectodomain and a membrane-anchored C-terminal fragment α (CTFα) (Kuhn et al., 2010). The latter is further cut by the γ-secretase releasing the p3 fragment extracellularly and the remaining APP intracellular domain (AICD) into the cytoplasm. The amyloidogenic processing of APP by the β-secretase BACE-1 (β-site APP cleaving enzyme) yields the APPsβ ectodomain and the membrane-tethered CTFβ, afterwards the activity of the γ-secretase generates the AICD peptide along with Aβ (Vassar et al., 1999). In contrast to the α- and β-secretase, the γ-secretase is composed of a large protein complex including presinilin 1 and 2 (PSEN1 and PSEN2) building the catalytic core unit, while additionally the presinilin enhancer (Pen-2) as well as the anterior pharynx-defective 1 (APH-1) and nicastrin are involved (Tomita, 2014). Recently Willem et al. (2015) identified a η-secretase cleavage site in the extracellular domain of APP releasing a short extracellular APPsη ectodomain. Subsequent processing of the remaining membrane anchored CTFη by the α- or β-secretase generates two new peptides, Aη-α and Aη-β (Willem et al., 2015). Importantly, APP processing is not restricted to the plasma membrane, but was also shown to occur within synaptic vesicles (Del Prete et al., 2014). In the healthy organism APP is cleaved in 90% of cases in the non-amyloidogenic pathway and thus precludes the secretion of Aβ.

In vivo studies have shown that secreted APP fragments have a half-life time of four to five hours in the adult moue brain while full-length APP reveals a much lower half-life-time with only one hour (Morales-Corraliza et al., 2009). APP family proteins are present in somatodendritic as well as axonal compartments of neurons. In axons they are enriched at active zones (Lassek et al., 2013). In conclusion, Aβ can be released both, from dendrites and axons (DeBoer et al., 2014). APP family proteins are enriched in intracellular compartments, mainly the golgi apparatus and the trans-golgi-network (TGN), and only a small proportion is embedded in the membrane (Thinakaran and Koo, 2008). Is APP not cleaved while being embedded in the membrane, it is reinternalized into endosomes so that the amount of surface APP is defined by secretory trafficking, internalization and the efficiency of secretase processing (Jiang et al., 2014). APP family members reveal different levels of cell surface expression with APLP1 being the most abundant (Kaden et al., 2009), indicating that APP family members might have individual functions in the brain.

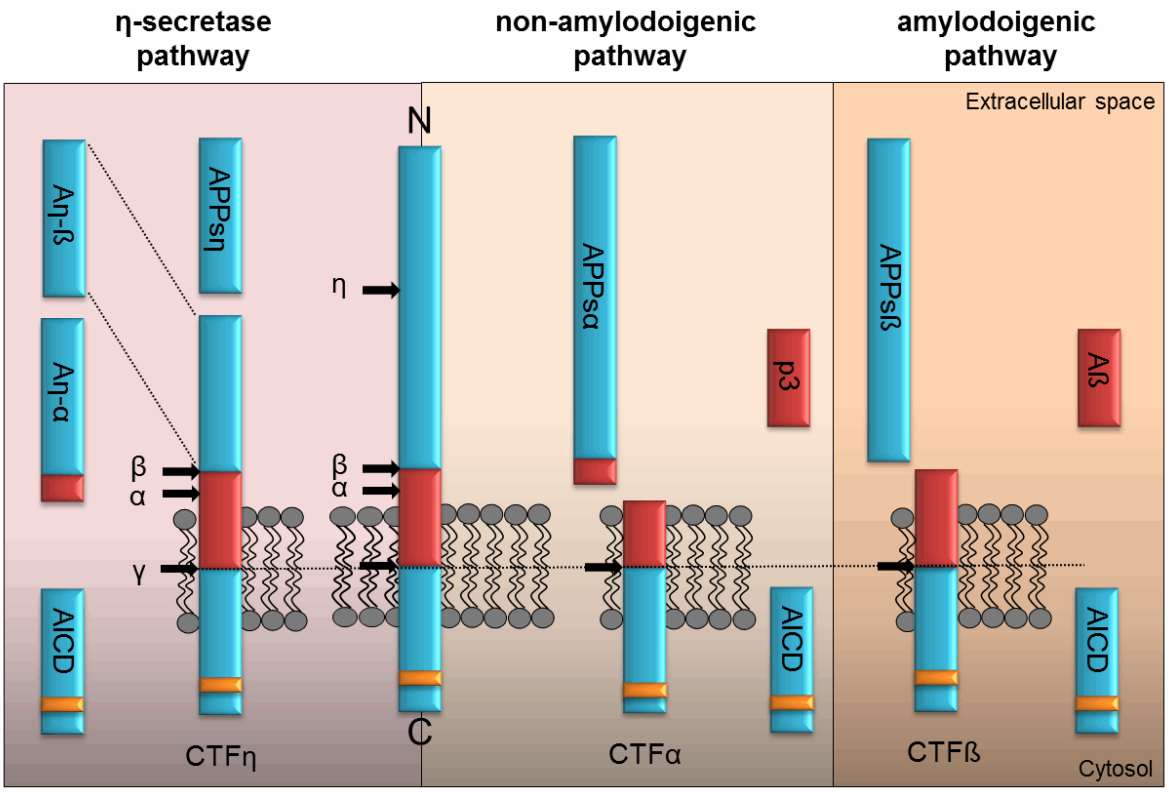

Figure 1.4: Proteolytic processing of APP. Full-length APP can be processed by α-, β-, η-, and γ-secretases in three different pathways. The left panel illustrates the η-secretase processing of APP. Initially η-secretase cleavage releases the soluble APPsη, while CTFη remains embedded in the membrane. It is further processed by α- or β-secretase at the extracellular side generating An-α or An-β. Shedding of CTFη within the transmembrane domain by γ-secretase yields the APP intracellular domain (AICD) containing the highly conserved interaction motif (YENPTY, yellow box) or the short extracellular peptides Aβ seen in the amyloidogenic or p3 within the non-amyloidogenic pathway. The non-amyloidogenic pathway depicted in the middle is driven by the α-secretase liberating APPsα in the extracellular space. Subsequently processing of membrane tethered CTFα by γ-secretase generates the p3 peptide and cytoplasmic AICD. The right panel illustrates APP processing in the amyloidogenic pathway by β-secretase resulting initially in the release of the APPsβ ectodomain. Following γ-secretase shedding of the membrane tethered CTFβ the Aβ peptide is secreted along with AICD in the cytoplasm. (Ludewig and Korte, 2017)

1.3.2 Physiological Functions of the APP Family and their Proteolytic Fragments in the Brain

The physiological role of APP family proteins and their proteolytic products is well-focused in the research as APP/APLPs are multifaceted proteins involved in the regulation of biological processes including transcription as well as synaptic function. Depending on their structure and expression they act as cell surface receptor-like proteins or as ligands initiating downstream signaling starting at the cell surface or via their secreted domains.

When APP/APLPs are present at the plasma membrane they were shown to form homo- and heterotypic *cis* interactions and have been proposed to mediate cell–cell interactions in *trans* (Soba et al., 2005, Kaden et al., 2009, Baumkotter et al., 2012, Mayer et al., 2016). APP family mediated synaptic adhesion is thereby not only crucial to build and maintain synaptic contacts, but also to regulate synaptic plasticity. Highest expression levels at the membrane were observed for APLP1 suggesting that it might be the family member with the upmost potential to mediate cell contacts (Kaden et al., 2009). Recently, the study of Mayer et al. (2016) identified APP and APLP2 to exhibit basal adhesive properties while APLP1 mediated neuronal adhesion is dynamic and regulated by zinc. Importantly, enhanced *trans* or *cis* interaction of APPs or APLPs is accompanied by a reduction of ectodomain shedding of the APP/APLP

proteins (Stahl et al., 2014, Mayer et al., 2016) and might therefore interfere with the ability to modulate synaptic function.

1.3.2.1 Functions of Full-Length APP Family Members

Information about APP/APLPs *in vivo* function is gained by mouse mutants ranging from single (KO) to double (DKO) and even triple knockouts (TKO) as well as from conditional and knock-in (KI) mouse lines.

APP-KO: The constitutive APP-KO is well-studied and revealed reductions in brain and body weight, grip strength and increased susceptibility to epileptic seizures (Steinbach et al., 1998). Quite interesting are the age-dependent alterations in synaptic plasticity, mainly LTP, which were found only in aged (9 to 12 months), but not in younger animals. Adult APP-KOs revealed normal basal synaptic transmission properties and short-term synaptic plasticity (STP) which was in line with the intact behavioral learning and neuronal morphology, while in aged mice behavior and spine number were significantly impaired (Seabrook et al., 1999, Ring et al., 2007, Lee et al., 2010, Tyan et al., 2012). These results indicate that the loss of APP does not impair synaptic plasticity and other biological functions in the adult organism and thereby APLP2 and maybe APLP1 are considered to perform redundant functions, but fail to compensate for APP deficiency with age.

APLP2-KO: The function of APLP2 in synaptic plasticity has also been addressed in detail since this protein shares the highest degree of sequence homology with APP within the gene family. Furthermore, the spatial and temporal expression pattern of APLP2 is highly reminiscent to that of APP (Wasco et al., 1993). In contrast to APP-KO mice, young and aged APLP2 single KOs behave like wildtype mice. They display no impairments in LTP, STP, PPF or basal synaptic transmission (Weyer et al., 2011, Midthune et al., 2012, Weyer et al., 2014). These observations go in line with normal learning and memory performances in cognitive tasks like the Morris-Water-Maze (MWM) or the passive avoidance test (Heber et al., 2000, Guo et al., 2012b). The functional effects are consistent with investigations of dendritic spine numbers of excitatory neurons. Whereas the spine density assessed *in vivo* was affected in aged APP-KO animals, it was unaltered in APLP2-KO mice as well as in organotypic hippocampal cultures (OHCs) of APLP2-KOs *in vitro* (Lee et al., 2010, Midthune et al., 2012, Weyer et al., 2014). It seems likely that endogenous APP is able to compensate for the genetic ablation of APLP2 with age, while vice versa APLP2 is incapable to compensate the loss of APP in aged animals. This implicates that APP has either different or dominant neuronal functions compared to APLP2.

APLP1-KO: The APLP1 family protein was not studied in similar detail maybe due to the fact that APLP1 has a different expression pattern than APP and APLP2. APLP1 shows restricted expression to the brain (Lorent et al., 1995, Thinakaran and Koo, 2008, Klevanski et al., 2014), but might therefore has a unique neuronal role and be of particular importance for synaptic plasticity. However, Heber et al. (2000) described only minor (if any) distinct phenotypes of APLP1-KO with unaltered cognitive behavior. *In vivo* analysis at the perforant path-granule cell synapse (PP-DG) in young adult APLP1-KO mice (16 to 20 weeks old) revealed unaltered STP and LTP, while enhanced excitatory transmission has been observed (Vnencak et al., 2015). The authors argued that maybe a larger number of perforant path synapses or an increased synaptic strength in APLP1-deficient mice may cause this enhancement, but final clarification is missing. Furthermore the paired-pulse-inhibition (PPD) paradigm of the population spike pointed towards decreased GABAergic network inhibition in APLP1-KOs, an effect observed also for other APP-KO models.

APP/APLP2-DKO: The high content of APP and APLP2 especially in pyramidal cells of the cortex and hippocampus (Lorent et al., 1995) and their localization at synaptic sites (Lassek et al., 2013) suggest a role in synaptic transmission and synaptic plasticity. Addressing the function of these redundantly expressed proteins by a combined KO is unfeasible as APP and APLP2 DKO mice die perinatally (von Koch et al., 1997, Heber et al., 2000) indicating an indispensable role for both proteins during development. The lethal phenotype of these DKO mice is most likely due to important functions of APP and APLP2 at the neuromuscular junction (NMJ) (Wang et al., 2005, Weyer et al., 2011). Neuromuscular transmission is severely impaired due to a reduced amount of synaptic vesicles and their impaired release. While the Knock-In of APPsα in the APP/APLP2-DKO mouse (APPsα-DM) rescued the lethal phenotype it resulted in muscular weakness and severe alterations in NMJ morphology (Ring et al., 2007). Elucidating the CNS specific role of APP and APLP2 was achieved by a conditional approach used by Hick and colleagues (2015) leaving the PNS unaffected. Crossing of $APP^{flox/flox}$ on an APLP2 null background to NexCre-deleter mice generated viable double mutants (cDKO). In these mice the depletion of APP is initiated from embryonic stage 11.5 onwards in excitatory neurons of the forebrain, while APLP2 is constitutively not expressed allowing the investigation of neurodevelopmental effects. Young adult mice revealed a pronounced deficit in LTP induction and maintenance as well as impairments in PPF. Alterations during the initial phase of LTP, the so-called post-tetanic potentiation (PTP) and also STP provided a hint towards an impaired presynaptic function. In contrast, the functionality of the postsynapse remained unaffected as basal synaptic transmission was unaltered. Impairments in hippocampal LTP were further reflected in impaired hippocampus-dependent learning and memory tasks with deficits in the Morris water maze and in radial maze performance. Moreover, the quantitative analysis of adult hippocampal CA1 neurons yielded pronounced reductions in total neurite length, dendritic branching, reduced spine density and reduced spine head volume (Hick et al., 2015). Another study using young conventional APP/APLP2 deficient mice (surviving escape mutants) described increased PPF and synaptic frequency facilitation (FF) (Fanutza et al., 2015), supporting the assumption that APP and APLP2 are involved in presynaptic function.

The combined KO of APLP2 with one of the other APP family member is embryonic lethal due to severe neuromuscular deficits (Heber et al., 2000, Klevanski et al., 2014). Strikingly, APP/APLP1-DKOs are viable and thus indicating that APLP2 serves unique functions when APP or APLP1 are missing. This moreover indicates that APP family members conduct redundant functions when they are regionally co-expressed.

1.3.2.2 Role of APP Proteolytic Fragments

The before mentioned impairments in physiological function might be caused either by deletion of APP/APLPs in full-length or because their proteolytic active fragments are absent. A large body of evidence points to APPsα as the neurotrophic domain within the APP family. Several studies implicated an important function of APPsα in synaptic plasticity as that extracellular APP domain facilitates LTP induction in hippocampal slices (Ishida et al., 1997) and was moreover shown to enhance memory in mice, rats and chicken (Roch et al., 1993, Meziane et al., 1998, Mileusnic et al., 2000, Mileusnic et al., 2004). APPsα acts on a rapid time-scale shown by the rescue of the LTP deficit described by Hick and colleagues (2015) in APP/APLP2 cDKO mice through the acute application of the recombinant peptide *in vitro*. These results confirmed previous observations by Taylor et al. (2008) reporting that intrahippocampal infusion of recAPPsα in the dentate gyrus (DG) of anesthetized rats enhances LTP recorded at the PP-DG pathway *in vivo*. Moreover, a recent study showed that recAPPsα is able to rescue

age-dependent LTP deficits *in vitro* (Moreno et al., 2015). APPsα is further essential for spine density regulation and dynamics highlighted by the exogenous application of the extracellular domain (Tyan et al., 2012) or by the Knock-In of APPsα rescuing the spine phenotype in APP deficient mice (Weyer et al., 2011, Weyer et al., 2014). In-line with the results following exogenous application of APPsα are the opposite effects observed after α-secretase inhibition leading to a reduction in APPsα production. The conditional KO of the major α-secretase ADAM-10 resulted in strongly impaired LTP and altered STP (Prox et al., 2013) and is consistent with the observations gained in studies using conventional α-secretase inhibitors in OHCs (Weyer et al., 2011) or *in vivo* (Taylor et al., 2008). It is by now not clear how APPsα mediates the rescue in activity-dependent synaptic plasticity and which receptor might be activated. Overall there is good evidence for a prominent role of APPsα directly at the synapse, in particular by influencing NMDA-R function and synaptodendritic protein synthesis (Taylor et al., 2008, Claasen et al., 2009). In contrast, for APPsβ being only 16 amino acids shorter than APPsα, no modulatory role with regard to synaptic plasticity (Taylor et al., 2008, Hick et al., 2015), neuroprotection (Li et al., 2010, Chasseigneaux et al., 2011), synaptic protein synthesis (Claasen et al., 2009) or spine morphology and density (Tyan et al., 2012) has been attributed. Interestingly, the newly identified η-secretase leads to the production of two small peptides Aη-α and Aη-β which have like APPsα and APPsβ differential roles in synaptic plasticity (see Figure 1.4, (Willem et al., 2015)). While both peptides had no influence on baseline synaptic transmission, hippocampal LTP was severely impaired by Aη-α but not by Aη-β administration *in vitro*. The structural difference between the two molecules is a C-terminal elongation of the Aη-α peptide by 16 additional amino acids, the same 16 amino acids that are also present at the C-terminus of the APPsα fragment, but not APPsβ. This short peptide sequence contains a predicted neuroprotective domain and a heparin binding site (Furukawa et al., 1996) and might lead to differential conformations enabling the peptides to activate different receptors. While APPsα and Aη-α share an overlapping sequence, they modulate LTP in an opposite way with Aη-α inhibiting LTP and neuronal activity as demonstrated by Ca^{2+} imaging experiments *in vivo* (Willem et al., 2015). That present results indicate that clearly more work is needed to investigate the underlying mechanism at the synapse mediated by the proteolytic domains of APP.

Several studies indicate that also the APP intracellular domain (AICD) has essential roles at synaptic sites. APPΔCT15-DMs, mice that lack the last 15 amino acids of APP including the highly conserved YENPTY motif on an APLP2 deficient background, reveal impaired induction and maintenance of LTP paralleled by severely altered hippocampus-dependent behavior. These mice have altered postsynaptic properties and a trend toward defective protein-synthesis dependent late-LTP which is presumably caused be abolished YENPTY interactions (Klevanski et al., 2014). For instance, APP interaction partners like Dab1, Shc, Grb, and Mint/X11 proteins mediate not only clathrin-mediated endocytosis of APP, but are also involved in the translocation of APP to the cell-surface (Aydin et al., 2012, van der Kant and Goldstein, 2015). Of particular importance might be the interaction with the adapter protein family Fe65. Interestingly Fe65/Fe65L1 double deficient mice show a similar phenotype of cortical dysplasia as APP triple KO animals (Guenette et al., 2006). The Fe65 proteins co-localize with APP in the endoplasmatic reticulum (ER) and Golgi apparatus and facilitate the translocation of the precursor protein to the cell surface (Sabo et al., 1999). In addition, these proteins also regulate the shuttling of a multimeric complex of AICD/Fe65/Tip60 into the nucleus to regulate gene transcription (Cao and Sudhof, 2001). The link between APP and Fe65 seems to be essential and the modulatory role regarding synaptic function should therefore be further elucidated.

1.4 Scope of the Study

AD is a neurodegenerative disorder with a quite dramatic development in numbers of diagnosed patients per year. Beside the cortex, the hippocampus is one of the first brain regions being affected by impaired synaptic function progressively resulting in cell death and causing cognitive deficits in humans. Today, it is widely accepted that the major cause of the disease is the Aβ-fragment. It accumulates in the brain upon increased processing of APP within the amyloidogenic pathway. Early stages of the disease are characterized by oligomeric Aβ which later on accumulates to Aβ plaques and are accompanied by inflammatory processes. But might it not also be the other way around that decreased levels of proteolytic APP products generated in the healthy organism within the non-amyloidogenic pathway lead to synaptic dysfunction? To develop potential therapeutic targets it is essential to understand first of all the physiological role of the APP protein family and their secreted peptides and how they modulate synaptic function. To this extent I investigated different gene-targeted mice to elucidate the role of APP/APLPs and their functional domains in processes of activity-dependent synaptic plasticity. I examined the age-dependent deletion of APLP1, the APP homolog which has been less attended in the research so far, as well as the role of the Fe65 protein family as downstream actors of APP, because several previous studies supposed an essential link between the adapter family and APP modulating synaptic function by intracellular signaling. Moreover, the generation of a conditional APP triple KO allowed me to study synaptic plasticity in surviving adult mice as the constitutive KO of APLP2 with one of the other family members is embryonic lethal. Furthermore I proved if the α-secretase cleavage product of APP, APPsα, is capable to rescue LTP deficits in APP/APLP2 deficient mice as well as in a mouse model of AD (APP/PS1ΔE9 tg) upon stable viral-driven overexpression. Within those readouts I included the analysis of APPsβ as well to monitor if the 16 amino acid shorter extracellular APP fragment might not be involved in processes of synaptic plasticity as claimed so far by the literature. Beside the functional analysis I included morphological investigations of spine density using the Golgi-Cox staining upon APPsα and APPsβ overexpression in AD mice and checked for the functional consequences resulting from the acute inhibition of the α-secretase ADAM-10 in wild-type mice. All experiments regarding synaptic plasticity were performed on acute hippocampal slices as the hippocampus is well known to be involved in learning and memory and is the brain region being affected within AD. *In vitro* recordings at the Schaffer collateral-CA1 pathway are well described and provide a suitable *in vitro* model for investigations of synaptic plasticity due to the lamellar structure of the hippocampus keeping neuronal circuits in transversal slice preparations intact. Beside the mainly electrophysiological read-outs I included Ca^{2+} imaging experiments where I chemically induced LTP in primary hippocampal cultures of APP/APLP2 deficient mice as Ca^{2+} signaling is essential for functional synaptic plasticity and was shown to be impaired in AD. Within those experiments I examined the neurotrophic properties of APPsα by AAV-driven overexpression following viral transduction of cultures. As APPsα was indeed able to rescue LTP in AD transgenics and APP deficient mice and restored moreover Ca^{2+} homeostasis in APP/APLP2 deficient cultures, while APPsβ was ineffective, I extended my experiments to study the role of the 16 amino acids differentiating both extracellular APP domains. Administration of the recombinant peptide should show if it carries the functional neuroprotective properties of APP and additional pharmacological experiments should give insights if the α7-nAChR receptor might be a potential receptor targeted. Overall, the investigations of the physiological role of APP family members performed might reveal new targets for AD treatment.

2 Material and Methods

2.1 Mouse strains

To elucidate the physiological role of the APP protein family using electrophysiological techniques, I investigated different mutant mouse strains. Beside the well-established and commercial available AD transgenic mouse model APPswe/PS1ΔE9, I examined gene-targeted mice carrying deletions of APP, APLP1 and APLP2 or APP family transgenes generated in the laboratory of Prof. Dr. Ulrike Müller, University Heidelberg. Table 2.1 provides an overview over the different mouse mutants and their genotypes as well as the age of mice analyzed in this thesis.

Table 2.1: ***Names, genotypes and age of transgenic mice.***

Name	Genotype	Age
Wildtype	C57Bl/6	2-3 months
APLP1-KO	$APLP1^{-/-}$	4-6 and 11-13 months
Littermate control	C57Bl/6	
NexCre cDKO	$NexCre^{+/T}APP^{flox/flox}APLP2^{-/-}$	5-6 months
Littermate control	$APP^{flox/flox}APLP2^{-/-}$	
APP cTKO	$NexCre^{+/T}APP^{flox/flox}APLP2^{flox/flox}APLP1^{-/-}$	3.5 months
Littermate control	$APP^{flox/flox}APLP2^{flox/flox}APLP1^{-/-}$	
APP/PS1ΔE9	APPKM670/671NL(Swedish)/PSEN1deltaE9	12-13 months
Littermate control	C57Bl/6JxC3H/HeJ	
FE65-KO	$FE65^{-/-}$	8-10 months
FE65L1-KO	$FE65L1^{-/-}$	
FE65/FE65L1-dKO	$FE65^{-/-}FE65L1^{-/-}$	
Littermate control	C57Bl/6J	

2.1.1 Constitutive APLP1-Knockout

The generation of the constitutive APLP1-knockout (KO) is described in detail in the publication of Heber (2000). It comprises the construction of a gene targeting vector that allowed the inactivation of the murine APLP1 gene by an ~8 kb genomic deletion involving the promotor, start codon and nearly 50% of the APLP1 coding region. The targeting vector was inserted into embryonic stem cells by electroporation. Heterozygous embryonic stem (ES) cells for the APLP1 gene, in which homologues recombination was successful, were transferred into foster mothers. Chimeric males were mated to C57Bl/6 females to generate heterozygous offspring that were further intercrossed to generate homozygous $APLP1^{-/-}$ mice.

2.1.2 Conditional Double or Triple Knockout of APP Protein Family Members

Any co-deletion of APLP2 with one of the other family member is embryonic lethal caused by defects in neuromuscular transmission and morphology (Heber et al., 2000; Wang et al., 2005). To circumvent postnatal lethality and to open the possibility to study the functions of the APP protein family members in synaptic plasticity, conditional null alleles for the APP and APLP2 gene have been generated. Therefore the promotor and the exon 1 of the APP or APLP2 gene were flanked by *loxP* sites in the targeting vector which was electroporated in ES cells ($APP^{flox/flox}$ or $APLP2^{flox/flox}$) (Mallm et al., 2010). By homologous recombination obtained heterozygous ES cells were implanted in foster mothers and male chimeric offspring were mate with C57/BL6 females. Heterozygous offspring were intercrossed to generate homozygous $APP^{flox/flox}$ or $APLP2^{flox/flox}$ mice. $APP^{flox/flox}$ mice were then further bred with $APLP2^{-/-}$ KO mice (Heber et al., 2000) to generate the conditional $APP^{flox/flox}$ $APLP2^{-/-}$ KO mouse model. APP triple KOs were generated by crossbreeding of $APP^{flox/flox}$ to $APLP2^{flox/flox}$ and $APLP1^{-/-}$ KO mice. These gene floxed mice built the possibility to selectively delete APP (and APLP2) at defined time points and in a tissue specific manner when crossed to Cre-transgenic deleter strains. I analyzed $APP^{flox/flox}APLP2^{-/-}$ or $APP^{flox/flox}APLP2^{flox/flox}APLP1^{-/-}$ mice that were crossed to the $NexCre^{+/T}$ strain (Goebbels et al., 2006) to receive either $NexCre^{+/T}APP^{flox/flox}APLP2^{-/-}$ or $NexCre^{+/T}APP^{flox/flox}APLP2^{flox/flox}APLP1^{-/-}$ individuals. $NexCre^{+/T}APP^{flox/flox}APLP2^{-/-}$ were crossbred with $APP^{flox/flox}APLP2^{-/-}$ to obtain 50% $NexCre^{+/T}APP^{flox/flox}APLP2^{-/-}$ (NexCre cDKO) and 50 % $APP^{flox/flox}APLP2^{-/-}$ (littermate control). To study conditional triple KOs, crossbreeding of $NexCre^{+/T}APP^{flox/flox}APLP2^{flox/flox}APLP1^{-/-}$ (NexCre cTKO) and $APP^{flox/flox}APLP2^{flox/flox}APLP1^{-/-}$ (littermate control) was done to generate respective offspring with a probability of 50 %. Nex is a gene encoding for a neuronal basic helix-loop-helix (bHLH) protein and was shown to be involved in neuronal differentiation. As Nex is expressed from E11.5 onwards in excitatory pyramidal forebrain neurons it triggers from then on constitutively the Cre-mediated APP removal.

Additionally stereotactically injected NexCre cDKO and littermate controls were investigated. Injection of AAV-viruses (either AAV-Venus, AAV-APPsα or AAV-APPsβ) was performed by M. Richter (IPMB, University Heidelberg) bilaterally into the hippocampus using 2 µl of viral preparation (10^{10} vg/hippocampus) at a rate of 0.2 µl/minute. For optimal virus spreading, two injection sites per hippocampus were used. Stereotactic AAV delivery was performed at an age of 12-15 weeks and investigation of synaptic plasticity was done 2 months later at an age of 4-5 months. In-between animals were housed in a temperature- and humidity-controlled room with a 12 h light-dark cycle and had access to food and water *ad libitum*.

2.1.3 AD Model Mice - APPswe/PS1ΔE9 Transgenics

Male APPswe/PS1ΔE9 mice (referred as APP/PS1ΔE9; Jackson Laboratories, Bar Harbor, USA) and age-matched littermate control mice (C57BL/6JxC3H/HeJ) were used for electrophysiology and spine density analysis. APP/PS1ΔE9 mice express the human APP gene carrying the Swedish double mutation (K595 N/M596L) and moreover the human PS1ΔE9 variant lacking exon 9 (Borchelt et al., 1997, Jankowsky et al., 2004). Transgenic and littermate control mice were stereotactically injected with AAV-viruses (either AAV-Venus, AAV-APPsα or AAV-APPsβ). The stereotactic surgery was performed by R. Fol and J. Braudeau (INSERM U1169 / MIRCen CEA Fontenay aux Roses 92265 France and Université Paris-Sud, 91400 Orsay, France). Viral constructs were bilaterally injected into the hippocampus using 2 µl of viral preparation (10^{10} vg/hippocampus) at a rate of 0.2 µl/minute. Two injection sites per hippocampus were

used to optimize virus spreading. Investigation of synaptic plasticity and spine density were perfromed 4-5 months after injection at an age of 12-13 months. In-between animals were housed in a temperature- and humidity-controlled room with a 12h light-dark cycle and had access to food and water *ad libitum*.

2.1.4 Fe65 and Fe65L1 Single and Double Knockouts

The generation of mice with targeted alleles for Fe65 and Fe65L1 is detailed described by Guenette et al., 2006. The Fe65 targeting vector was constructed to replace a 6.5 kb genomic sequence including a part of the C-terminus of exon 2 and intron 2 as well as a portion of the exon 3 N-terminus. The Fe65L1 targeting vector was constructed to replace 692 nucleotides of exon 4. Targeting vectors were inserted into ES cells by electroporation. Heterozygous ES cells for the Fe65 or Fe65L1 gene, in which homologues recombination was successful, were transferred into foster mothers. Chimeric males were mated to C57Bl/6J females to generate heterozygous offspring that were further intercrossed to generate homozygous $Fe65^{-/-}$ or $Fe65L1^{-/-}$ mice. $Fe65^{-/-}$ mice lack both isoforms, p97 and p60. Intercrossing of both single mutants generated $Fe65^{-/-}FEe5L1^{-/-}$ dKO animals. Proofing the absence of Fe65 and Fe65L1 proteins in targeted mutant mice by western blot analysis revealed for $Fe65^{-/-}$ and $Fe65^{-/-}Fe65L1^{-/-}$ mouse brains an upregulation of a p58 band (approximately 50 % increase) with unknown identity (Guenette et al., 2006).

2.2 Electrophysiology

2.2.1 Artificial Cerebral Spinal Fluid (ACSF)

The components of the Artificial Cerebral Spinal Fluid (ACSF) mimic the ion composition of the cerebral spinal fluid *in vivo* and provide thereby an optimal possibility to keep brain slices *ex vivo* viable. The composition of the ACSF with the respective ion concentrations used is shown in Table 2.2. All the chemicals are purchased from AppliChem (Germany). The ACSF and its physiological pH of 7.3, achieved by continuously saturation with 95 % O_2 and 5 % CO_2, provided an optimal environment for proper neuronal function. Dependent on the mouse model investigated, I used two different high Mg^{2+} ACSFs for preparing acute hippocampal slices (see Table 2.2), one that contained $CaCl_2$ and one without $CaCl_2$. As the Ca^{2+} influx and Ca^{2+}-induced Ca^{2+}-release is already elevated in aged rodents and mouse models of AD, Ca^{2+} free media was used to slow down metabolism and to minimize Ca^{2+}-dependent hypoxic and excitotoxic damage during dissection (Sajikumar et al., 2005, Gant et al., 2006, Mathis et al., 2011). The further high Mg^{2+} concentration in both ACSFs blocked the NMDA-R and prevented its pre-activation during slice preparation. The recovery of prepared slices took place in high Mg^{2+} ACSF for all experiments. The bathing media used for electrophysiological recordings differed between transgenic mice analyzed. The mutant APP/APLP mouse lines revealed a low threshold to induce long-term potentiation (LTP) so that for recording the high Mg^{2+} ACSF was used to uncover differences in synaptic plasticity without causing hyperpolarization. The opposite, meaning lowered potential to enhance synaptic strength, is reported for aged AD mouse models so that recordings were performed in low Mg^{2+} ACSF (Mathis et al., 2011).

Table 2.2: ***Composition of the ACSFs.***

substance	high Mg^{2+} ACSF [mM]	low Mg^{2+} ACSF [mM]	Ca^{2+} free-ACSF [mM]
NaCl	125	125	125
KCl	2,5	2,5	2,5
NaH_2PO_4*H_2O	1,25	1,25	1,25
$MgCl_2$*6 H_2O	1	2	2
$NaHCO_3$	26	26	26
D^+-Glucose	25	25	25
$CaCl_2$*H_2O	2	2	-

2.2.2 Preparation of Acute Hippocampal Slices

The transversal slice preparation used in this thesis is a powerful tool to investigate synaptic properties *ex vivo* as the preparation retains the cytoarchitecture and synaptic circuitry of the hippocampus intact. After a brief anesthesia with 200 µl Isofluran (Baxter Healthcare Corporation, Deerfield, USA), the mice were rapidly decapitated and the brain was removed from the scull. This procedure was done in less than 90 sec as duration of this step is crucial for neuronal cell survival. The subsequent transfer of the brain into cold (4 °C), carbogenated high Mg^{2+} ACSF for 3 minutes slowed metabolism and reduced oxidative stress. To keep the tissue in the best conditions, the following preparation procedure was performed using ice-cold ACSF as well. The removal of the cerebellum and prefrontal cortex with a razor blade was followed by the separation of both hemispheres along the intrahemispheric fissure. In each hemisphere the hippocampus was first of all removed from the striatum with two rounded spatula from the medial side. Placing the spatula underneath the fimbria allowed folding out the hippocampus and further its separation from the cortex after cutting the subiculum. In all steps of preparation care was taken to avoid any damage of the hippocampus by direct touching or stretching. After dissecting the hippocampi, their ventral end was glued onto a specimen plate leaning upright against an agar block with the dentate gyrus facing the agar. The hippocampus was sectioned into 400 µm thick transversal slices along its longitudinal axis by a vibrating microtome (VT 1200S; Leica, Nussloch, Germany) being bathed in ice-cold ACSF. The slowly, but very gentle cutting with the vibrating blade caused less neuronal damage near the slice surface. After cutting, the slices were transferred into a custom-made submerged chamber constantly perfused with carbogenated high Mg^{2+}-ACSF and were allowed to recover for at least 90 min at room temperature.

2.2.3 Extracellular Field Recordings

In vitro extracellular recordings on acute hippocampal slices were performed on two submerged setups with similar technical equipment. Glass microelectrodes were used to record electrically evoked field excitatory postsynaptic potentials (*f*EPSPs, Figure 2.2A). The recording electrodes were pulled from borosilicate glass capillaries (0.58 x 1.00 x 100 mm, Biomedical Instruments, Germany) with a Flaming/Brown Micropipette Puller (P-97, Sutter Instruments, USA) generating tips of approximately 1 to 3 MΩ resistance. Submerged slice recordings in which continuously carbogenated ACSF flows over the

entire slice at a rate of 1.5 ml/min started after a period of 1.5 to 2 h enabling the recovery of slices from the preparation procedure. Dependent on the application of recombinant peptides or inhibitors either silicon tubings (PharMed® Ismaprene, Ismatec) avoiding absorbance of substances by the tubing walls or PVC tubings (TYGONE, Ismatec) for standard recording procedures were used. The submerged recording chamber (RC-22, Warner instruments, USA) was fixed onto a vibration damped table (Spindler & Hoyer, Germany and TMC, Massachusetts, USA) and further onto an aluminum heating base (PH-1, Warner Instruments) which was connected to a thermistor measuring to achieve constant temperature being crucial for stable recordings. Additionally, both setups contained a pre-heating and by connection to an adjustable Dual Channel Heater Controller (TC-334B, Warner Instruments) a constant temperature of 22 – 24 °C (RT) for fiber volley experiments and 32 ± 0.2 °C for all other type of recordings were achieved.

The lamellar organization of the hippocampus is well preserved after transversal slice preparation keeping the majority of intra-hippocampal connections intact. In order to prevent recording of cells that might likely be injured by the slicing, glass microelectrodes filled with 3M NaCl were precisely placed in the s*tratum radiatum* of hippocampal area CA1 (Figure 2.1) to a depth of ~130 to 170 µm beyond the surface of the slice. The recording electrode was therefore fixed to an electrical micromanipulator (SM-5, Luigs and Neumann or Nano-Stepper, WSE Electronics) and moved by a motor driven remote control. The stimulation electrode, a lacquer coated, monopolar tungsten electrode (WPI, USA) with a resistance of 0.1 MΩ, was positioned into the *stratum radiatum* of CA3, stimulating the Schaffer collateral axons (Figure 2.1). Movement of the stimulation electrode was achieved with a mechanical micromanipulator (Leitz, Germany), while precise positioning of the electrodes was possible by visual control with a stereo microscope (SMZ 654, Nikon, Japan or Heerbrugg at Leica Microsystems). As the negative pole of the stimulation electrode was connected to a stimulus isolator (A360 or A365, WPI, USA) defined stimuli patterns programmed in the master pulse generator Master 8 (A.M.P.I., Israel) could be applied. Stimuli consisted of constant current rectangular pulses lasting 200 µs applied at 0.1 Hz and ranged from 20 to 40 µA for baseline stimulation. The stimulus current thereby depended on the age and mice strain analyzed as well as on the preparation quality and treatment. The negative pole of the stimulation electrode was connected to an Ag/AgCl pellet (E201, WPI, USA) serving as indifferent electrode, which

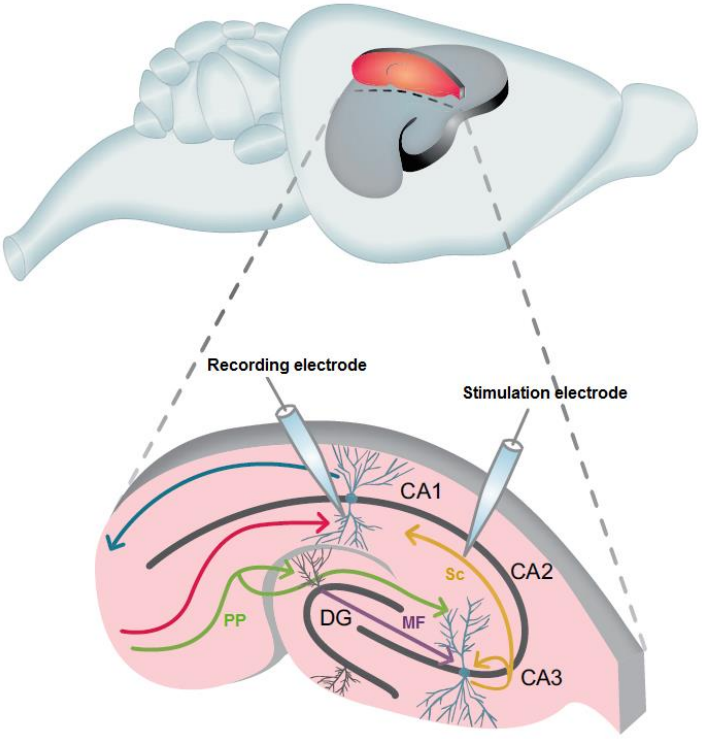

Figure 2.1: Localization of the hippocampus in the rodent brain and position of electrodes in a transversal acute slice. *Upper panel:* Position of the hippocampus inside the rodent brain and in red the transversal intersecting plane. *Lower panel:* The stimulation electrode was placed in the hippocampal CA3 region to stimulate the Schaffer collateral pathway (Sc). The recording electrode was positioned in the *stratum radiatum* of the CA1 region. Adapted from (Korte and Schmitz, 2016)

was bathed in ACSF and further connected to the amplifiers headstage (Axoclamp-2B, Axon Instruments at Molecular Devices, USA). On the headstage the recording electrode was additionally mounted either directly or indirectly by a cable. Therefore, the recording electrode was inserted before into an electrode holder (WPI, USA). Evoked *f*EPSPs were recorded in bridge mode and amplified (200 times) by the Axoclamp2B differential amplifier (Axon Instruments Molecular Devices, USA) and band-pass filtered (LHBF-48X, NPI Electronic, Germany). Another 50-60 Hz filter (Hum Bug, Quest Scientific, UK) eliminated noise that would have otherwise contaminated the recorded responses. The signal was digitized with a multi-IO card (National Instruments, USA) and stored on a personal computer for subsequent analysis with National Instruments LabView based software (DAP Version 4.751, written by M. Korte and V.Staiger) or online monitoring during recording. The signal was checked in parallel with an oscilloscope (HM507, Hameg, Germany). In all recordings the initial negative slope provided a measurement of the monosynaptic excitatory CA3-CA1 current. It corresponds directly to the activation of depolarizing synaptic currents in CA1 pyramidal neurons in response to glutamate release from Schaffer Collateral terminals. Following the acclimatization of the slice to the altered conditions in the submerged recording chamber like temperature and ion conditions of the bathing medium reflected by a stable signal size, electrophysiological recordings started. First of all, a stimulus–response curve was obtained at the beginning of each experiment to define the minimal stimulus strength generating a population spike in the *f*EPSP (Figure 2.2B). For LTP experiments stimulus intensity was adjusted to elicit a slope size resulting in 40 % of the maximal *f*EPSP slope.

2.2.4 Stimulation Protocols

All stimulus paradigms used, were programmed in the Master 8 pulse generator which triggered the application of currents with defined frequencies. Baseline synaptic transmission was investigated by input-output (IO) measurements. The IO measurements were performed either by application of defined current values (25–250 µA with 25 µA steps) at 32°C or by adjusting the stimulus intensity to certain fiber volley (FV) amplitudes (0.1–0.8 mV with 0.1 mV steps). The FV represents the presynaptic part of the *f*EPSP or in more detail the summated action potentials of the population of axons stimulated and thereby provide a direct correlation of stimulus strength and *f*EPSP response (Figure 2.2). FV recordings were performed at RT (22- 24 °C) to avoid an overlay of FV and *f*EPSP signal like it occurs at 32 °C (Figure 2.2A, C).

Short-term synaptic plasticity and presynaptic function were investigated with the Paired-Pulse-Facilitation (PPF) paradigm. PPF is the simplest form of plasticity exhibited by the most excitatory synapses in the hippocampus. It is defined as an increase in the synaptic response size to a second pulse delivered within a short interval of time following the first pulse. PPF is maximal at short interstimulus intervals (ISIs) and declines exponentially over a period of ∼500 msec. It is well established that PPF is a presynaptic phenomenon depending on the probability of neurotransmitter release (see chapter 1.2.3 (Citri and Malenka, 2007)). PPF was investigated by applying a pair of two closely spaced stimuli in different ISIs ranging from 160, 80, 40, 20 to 10 ms at 32 °C (Figure 2.2D).

To investigate long-term synaptic changes in synaptic plasticity, long-term potentiation (LTP) was induced in acute hippocampal slices. Following 20 minutes of stable baseline synaptic recordings with 40 % of maximal *f*EPSP slope at 0.1 Hz LTP was induced in the slice by applying theta-burst stimulation (TBS: 10 trains of 4 pulses at 100 Hz in an 200 ms interval, repeated 3 times). Responses are monitored continually for 60 min to access *f*EPSP strengthening and stability of the LTP. TBS is based on naturally

occurring theta firing patterns in the hippocampus and can therefore be seen to be physiological (Vertes, 2005). Following the brief period of high-frequency stimulation there is a rapidly decaying potentiation, often referred to as phase of post-tetanic potentiation (PTP). PTP generally lasts for ~1 min following a tetanus and is also thought to be due to presynaptic changes, similar to those that underlie PPF (see chapter 1.2.3 (Regehr, 2012)).

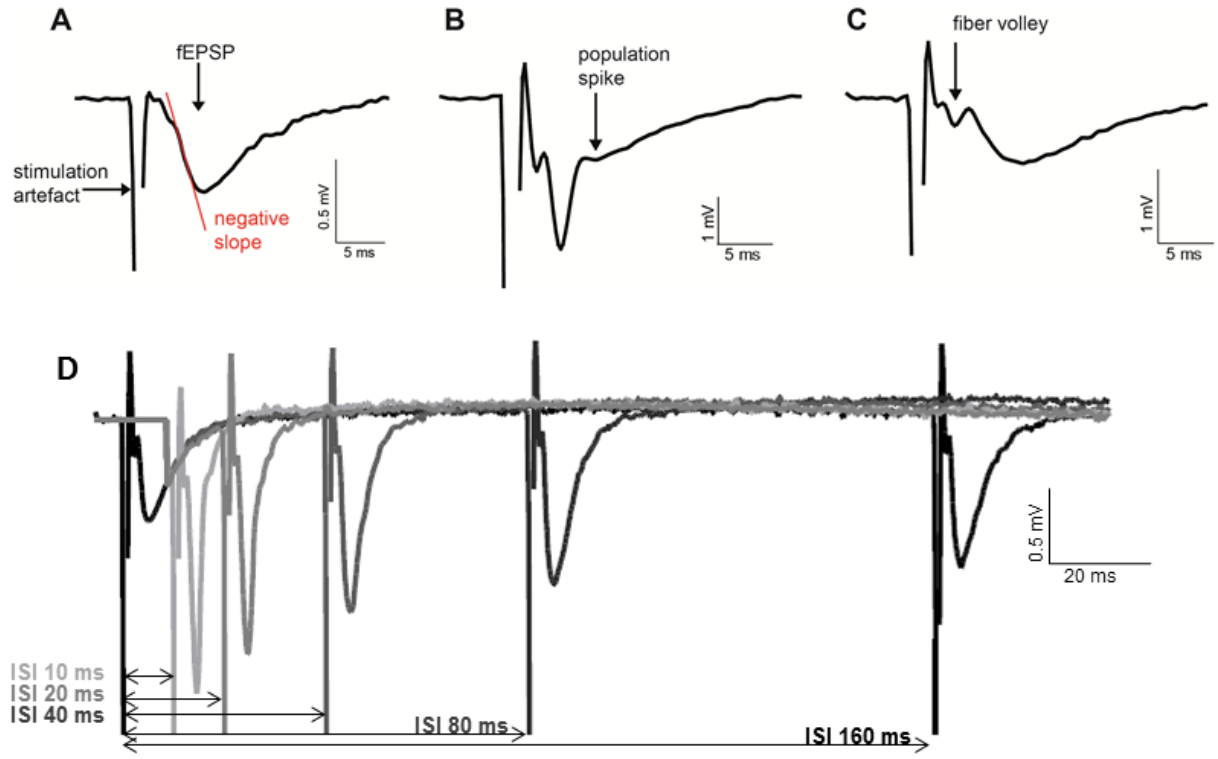

Figure 2.2: Example traces of the *f*EPSP, populations spike, fiber volley and PPF recordings from CA1 *stratum radiatum*. (A) Representative tracing of an excitatory postsynaptic field potential (*f*EPSP) with stimulation artifact. In red the negative slope is shown which was measured before and after LTP induction. **(B)** Example *f*EPSP with population spike. **(C)** Example *f*EPSP with clearly identifiable fiber volley signal at room temperature. **(D)** Representative tracing of the Paired Pulse Facilitation (PPF) paradigm. Two stimuli were applied in defined inter-stimulus intervals (ISIs) ranging from 160 to 10 ms. Second *f*EPSP signal becomes larger than the first depending on size of ISIs.

2.2.5 Pharmaca and Peptides

Despite viral overexpression of APP peptides (AAV-APPsα or AAV-APPsβ) over a long time range *in vivo*, also acute treatment with recombinant peptides applied *ex vivo* on acute slices allowed the investigation of effects on synaptic plasticity occurring on a rapid time scale. Therefore recombinant Aβ1-16 (recAβ1-16) or its scrambled version for control experiments, kindly provided by Prof. Dr. Ulrike Müller (University Heidelberg), was diluted in 30 mL high Mg^{2+} ACSF. That volume was sufficient to circulate during the entire recordings per day in a closed loop system. By using silicon tubings (PharMed® Ismaprene, Ismatec) the absorbance of peptides by the tubing walls was avoided. To further circumvent osmolarity changes in the small volume of the high Mg^{2+} ACSF caused by evaporation, moisturized carbogen was introduced in the 30 mL recording solution which was additionally covered with Parafilm® (Bemis, USA). Synthetized murine Aβ1-16, the sequence difference between APPsα and APPsβ, diluted in PBS or its scrambled version (Aβ1-16 scr) were used in a final concentration of 10 nM. The concentration was based on previous acute peptide recordings with recAPPsα (Hick et al., 2015). Before recordings,

acute hippocampal slices of APLP2-KO (littermate control) and NexCre cDKO were pre-incubated in 30 mL gently carbogenated high Mg^{2+} ACSF containing either Aβ1-16 or Aβ1-16 scr in a custom made incubation chamber covered with Parafilm® for 1 h at RT. After that, slices were transferred into the submerged recording chamber where 30 mL of high Mg^{2+} ACSF with the respective peptide circulated in a closed loop. Recordings were performed as described before. In another set of experiments, the α7-nicotininc acetylcholine receptor antagonist (α7-nAChR) α-Bungarotoxin (BTX, Merck Millipore, Germany) solved in Aqua dest. was used at a final concentration of 10 nM and either co-applied already at the step of pre-incubation together with 10 nM Aβ1-16 on acute slices or washed in 10 minutes before baseline recording started.

2.2.6 Electrophysiology - Data Analysis

Acquired raw data of recordings were analyzed with custom made programs based on National Lab View Software (ANA-DAP version 4.755 or ANA-PPF version 4.2, written by M. Korte and V. Staiger). Using those programs precise measurements of the negative *f*EPSP slopes for fiber volley, EPSP and LTP recordings were feasible by a manually defined window. For the analysis of the PPF data, the ratio of the slope of the second *f*EPSP divided by the slope of the first one was calculated, written as equation: (slope *f*EPSP2/slope *f*EPSP1)*100.

Both LabView programs generated Microsoft Excel files (Microsoft, USA) containing all single values of each *f*EPSP slope measurement. Baseline synaptic transmission properties assessed with FV, EPSP or PPF paradigms were shown as the average of three values per condition analyzed. For LTP recordings six values of *f*EPSP slopes were averaged resulting in the mean value for one minute that was plotted within the graphs. The LTP data were shown as an increase compared to baseline synaptic activity. Therefore all *f*EPSP slopes were averaged and set to 100%. The slope sizes obtained after TBS induction were normalized to baseline and calculated as following: (slope $f\text{EPSP}_{\text{minute}}$/mean slope $f\text{EPSPs}_{\text{baseline}}$)*100.

Within the analysis only experiments were included that revealed a stable baseline with not more than 10% variability or where *f*EPSP after stimulation looked physiological without displaying a large population spike or seizure-like activity.

2.3 Dendrite and Spine Analysis Following Golgi Cox Staining

For different approaches addressed within that thesis only one hemisphere served for electro-physiological recordings, while the other was used for morphological analysis using the Golgi-Cox method. Golgi staining was done using the FD Rapid GolgiStainTM Kit (FD NeuroTechnologies, Inc., USA) according to the manufacturer's instructions. After division of the two hemispheres during slice preparation for electrophysiology, one hemisphere was immersed in 2 mL mixtures of equal parts of kit solutions A and B and stored at RT for 2 weeks. Solution AB was prepared at least 24 h before first brain tissue impregnation and renewed 12 to 24 h later. After 2 weeks, brain tissues were transferred in solution C for at least 48 h and up to 7 days at 4 °C before sectioning. Solution C was renewed within the first 24 h. Coronal brain sections of 200 µm were cut with a vibrating microtome while embedded in 2% Agar in 0.1 M PB (Leica, VT1200S, Germany). Each section was mounted with Solution C on an adhesive microscope slide pre-coated with 1 % gelatin/0.1 % chromalaun and stained according to the manufacturer´s protocol with exception that AppliClear (AppliChem, Germany) was used instead of xylene. Finally, slices were cover-slipped with Permount (Fisher Scientific, Germany).

Images of hippocampal CA1 and CA3 pyramidal neurons were taken with an Axioplan 2 imaging

microscope (Zeiss, Germany) using a 63x oil objective and a z-stack thickness of 0.5 µm under reflected light. The number of spines was determined per micrometer of dendritic length (in total 100 µm) at apical compartments in midapical regions of the *stratum radiatum* (second or third order dendritic branches) and basal compartments within *stratum oriens* (>20 µm away from the soma) using ImageJ (1.48v, National Instruments of Health, USA). At minimum 4 animals per genotype and 5 neurons per animal were analyzed blinded to genotype and particular treatment. Data of Golgi-Cox staining were analyzed using GraphPad Prism (Version, 5.01) software. Spine density is expressed as mean±SEM.

2.4 Primary Hippocampal Dissociated Neuronal Cultures

2.4.1 Media and Solutions

Borate buffer, pH 8.5 Dissolve 0.31 g boric acid and 0.475 g borax in 100 mL sterile MilliQ water, adjust pH to 8.5.

Poly-L-Lysine stock solution 10 mg/mL in MilliQ water

Gey's balanced salt solution (GBSS), pH 7.4	KCl	0.37 g
	KH_2PO_4	0.03 g
	$MgCl_2 * 6H_2O$	0.21 g
	$MgSO_4 * H_2O$	0.07 g
	NaCl	8 g
	$NaHCO_3$	0.227 g
	NaH_2PO_4	0.12 g
	D-Glucose	1g
	$CaCl_2 * 2H_2O$	0.22 g
	MilliQ water	fill up to 1000 mL
Serum medium	FCS	200 µL
	DMEM (2 %)	10 mL
Medium for dissociated hippocampal cultures	Neurobasal (NB)	50 mL
	B27	1 mL
	L-Glutamin (200 mM)	125 µL
	N2 (10x)	5 mL

2.4.2 Preparation of Poly-L-Lysine -Coated Coverslips

Glass coverslips (Ø 13 mm, 1 mm thick, VWR) were incubated in 10 M NaOH for 3-5 h at 100 °C and afterwards washed 5x with MilliQ water. After sterilization at 225 °C, coverslips were coated with 0.5 mg/mL poly-L-Lysine (P2636, Sigma) in boric acid buffer at 36.5 °C for 2-3 h. Next, they were washed 5x with sterile MilliQ water, dried and stored at 4 °C.

2.4.3 Preparation of Primary Embryonic Hippocampal Cultures

Primary embryonic hippocampal cultures were prepared at embryonic day (E) 18.5. Initially, the pregnant mouse was sacrificed by cervical dislocation and all embryos were extracted from the uterus and decapitated under sterile conditions. The skull was carefully opened and the upper part of the brain, containing cortex and hippocampus, was separated from the rest of the brain tissue and quickly transferred into ice-cold GBSS/glucose solution. The dorsal parts of the brain (cerebellum and pons) were removed and the two hippocampi separated along the midline under visual control using a dissecting microscope (Stemi 2000, Zeiss, Germany). Hippocampi were dissected from the cortex and digested in 1 mL Trypsin / EDTA (Sigma) for 30 min at 36.5 °C. In order to stop digestion, the Trypsin/EDTA solution was sucked away and replaced by 1 mL serum medium. After washing with serum medium for 3 times, cells were carefully dissociated using pipets with different tip sizes. The dissociated tissue was centrifuged 5 min at 1500 rpm, the supernatant removed and the cell pellet re-suspended in 1 mL medium. Following cell counting, cells were plated at a density of 7 x 10^4 cells/well on poly-L-Lysine coated coverslips and incubated in medium at 36.5 °C, 5 % CO_2 and 99 % humidity. Medium was exchanged after 9 days *in vitro* (DIV9). Cells have been used for experiments between DIV12-16.

2.5 Ratiometric Calcium Imaging

2.5.1 Media, Solutions, Pharmaca and Viruses

1x Hank's Balanced Salt Solution (HBSS) for Imaging (3.8 mM Ca^{2+})	10 x HBSS stock solution	50 mL
	$CaCl_2$* H_2O	145 mg
	$NaHCO_3$	175 mg
	H_2O (MilliQ)	fill up to 500 mL
1x Hank's Balanced Salt Solution (HBSS) for Imaging (1.3 mM Ca^{2+})	10 x HBSS stock solution	50 mL
	$NaHCO_3$	175 mg
	H_2O (MilliQ)	fill up to 500 mL
Fura-2 AM calcium dye stock solution	Solve 50 µg Fura-2 AM (Invitrogen, Germany) in 50 µL DMSO (Roth, Germany) for a 1 mM stock solution	
Glycine stimulation medium (1 mM)	Glycine (1 M in D-PBS)	40 µL
	Strychnine (1 mM in H_2Odest.)	40 µL
	1x HBSS	40 mL
CPA medium (10 µM)	CPA (10 mM in DMSO)	40 µL
	Glycine (1 M in D-PBS)	40 µL
	Strychnine (1 mM in H_2Odest.)	40 µL
	1x HBSS	40 mL

Table 2.3: ***Pharmaca and AAV viruses used for quantitative calcium imaging.***

substance	concentration or titer	reference
glycine	1 mM	AppliChem
Cyclopiazonic acid (CPA)	10 µM	Tocris
Nifedipine	10 µM	Tocris
Strychnine hydrochloride	1 µM	Sigma
AAV9-ss-Syn-Venus-f	$1.4*10^{10}$ gc/µL	Tobias Abel (PEI, Langen) (Fol et al., 2016)
AAV9-ss-Syn-lck-Venus-HA-msAPPsα	$5,4*10^{9}$ gc/µL	
Pluronic acid	2.5 %	Sigma

2.5.2 Fura-2-AM Ca^{2+} Imaging Experiments

Fura-2-AM Ca^{2+} imaging experiments were performed with cultured DIV12 to DIV16 old hippocampal neurons. Neuronal cultures were loaded with 4 mM Fura-2-AM (Life Technologies, solved in DMSO) solved in Hank's Buffered Salt Solution (HBSS) with 2.5 % Pluronic F127 (Sigma) for 45 min at 37 °C. Following two washing steps with pre-warmed 1x HBSS, the coverslips were mounted on a perfusion chamber continuously perfused with HBSS at RT. The perfusion chamber was fixed on a moveable stage of an upright Olympus BX61WI fluorescence microscope system (Cell^M software) equipped with a 40× 0.8-N.A. objective (Olympus) and a CCD camera (VisiCam QE, Visitron Systems) with 4 x 4 binning. Visualization of Fura-2-AM calcium signals was achieved using 340 nm and 380 nm UV light while light intensity was set to 70.9 % and exposure time constantly held at 130 ms for time lapse imaging taking 500 images in a cycle time of 326 ms and 200 cycles repetition.

cLTP induction: After 20 min of adaptation to the chamber conditions, 2 images of spontaneous activity (baseline activity) were taken at an interval of 10 min (t-20, t-10). For stimulation and chemical LTP induction (cLTP) 1x HBBS containing Glycine (Gly, 1 mM) and Strychnine hydrochloride (Str, 1 µM, Sigma), blocking specifically endogenously expressed glycine receptors, were bath applied for 10 min and followed by continuously perfusion with 1x HBBS to acquire 3 additional time points upon cLTP induction (t0, t10, t40). In another set of experiments the stimulation solution (1 mM Glycine/1 µM Strychnine) contained additionally Cyclopiazoic acid (CPA, 10 µM, Tocris) to block the re-uptake of Ca^{2+} into intracellular Ca^{2+} stores.

SOCC experiments: Prior to Ca^{2+} withdrawal by a switch of HBSS perfusion solution to low Ca^{2+}-HBSS (1.3 mM), one image of spontaneous activity was taken after 20 min of adaptation to the chamber conditions (t1). Following acquisition of one Ca^{2+} signal recording after 10 min of Ca^{2+} withdrawal (t2), cells were perfused with HBSS (3.8 mM) for 5 min to re-build extracellular Ca^{2+} concentration and to investigate intracellular Ca^{2+} changes in neurons (t3). To examine endoplasmatic reticulum (ER) Ca^{2+} stores, ER stores were unloaded with 10 µM CPA perfused in low Ca^{2+}-HBSS and calcium signals monitored (t4). The calcium signals evoked by restoration of external Ca^{2+} are used to detect store-operated Ca^{2+} entry (SOCE) activity (Linde et al., 2011) being crucial for ER store Ca^{2+} re-filling (Parekh and Putney, 2005).

Images were captured at 340 and 380 nm excitation wavelengths and the mean pixel intensity for each cell was determined in the region-of-interest (ROI) using ImageJ. ROIs were set around the cell bodies of five neurons per time-point, averaged and corrected for background fluorescence. In case of AAV transduced neurons, only cells were included in the analysis that expressed the Venus fluorescent protein. Changes in intracellular Ca^{2+} concentration are represented as Ratio of (fluorescence emission intensity at 340 nm – background fluorescence emission at 340 nm)/ (fluorescence emission intensity at 380 nm – background fluorescence emission at 380 nm). The amplitude of Ca^{2+} peaks were analyzed and plotted to assess differences in Ca^{2+} dynamics upon neuronal activity between genotypes and treatments.

2.5.3 AAV-constructs and Transduction of Primary Cultures

The codon optimized (Geneart, Regensburg) mouse APPsα coding sequence (derived from Uniprot: P12023-2) was cloned under control of the synapsin promoter into the single-stranded rAAV2-based shuttle vector pAAVSynMCS-2A-Venus (Tang et al., 2009) by T. Abel (PEI, Langen, Germany). An N-terminal double HA-tag was inserted downstream of the APP signal peptide at the N-terminus of APPsα as well as the yellow fluorescent protein Venus containing at its C-Terminus a farnesylation signal (FA) for membrane anchoring (referred as AAV-syn-APPsα-Venus) allowing easy detection. The control vector (AAV-syn-Venus) encodes only for FA-Venus. All constructs were packaged into AAV9 by the MIRCen viral production platform as described previously (Berger et al., 2015, Fol et al., 2016). The concentration of the vector stocks was estimated by quantitative PCR according to the method described by (Aurnhammer et al., 2012) and expressed as viral genomes per mL of concentrated stocks (vg/mL).
AAV-syn-Venus and AAV-syn-APPsα-Venus were added to primary hippocampal cultures of NexCre cDKO or littermate control mice 6 days before imaging with a MOI of $2*10^4$.

2.5.4 Transfection of Primary Hippocampal Neurons

Primary hippocampal cultures were transfected after completion of Ca^{2+} Imaging experiments between DIV12 and DIV17 using Lipofectamine® 2000 (ThermoFisher Scientific) transfection reagent with the plasmid pmApple-N1 encoding for the red fluorescent monomeric derivative of DsRed to investigate spine density. All used amounts were calculated per well. 300 µL Neurobasal (NB) medium without supplements were pre-incubated at 37 °C, 5 % CO2 and 99 % humidity. Afterwards, 0.8 µg plasmid DNA and 2 µL Lipofectamin were each diluted in 50 µL NB medium without supplements. Following 5 min of incubation, the two solutions were combined and incubated for another 20 min at RT. The old cell culture medium was replaced by 300 µL of pre-warmed NB medium without supplements, while the old cell medium was kept in empty wells and incubated at 37 °C and 5 % CO_2. Subsequently, 100 µL transfection medium was added drop wise to each well followed by 60 minutes incubation at 37 °C and 5 % CO_2. Afterwards, the transfection medium was replaced by the old culture medium and cells were incubated for 24 h at 37 °C and 5 % CO_2 before fixation with 4 % PFA in 0.1 M PB.

2.6 Immunhistochemistry

2.6.1 Solutions and Antibodies

0.1M PB	solve 0.78 g NaH_2PO_4 3.45 g Na_2HPO_4 in 500 mL MilliQ water
4% Paraformaldehyde (in 0.1 M phosphate buffer, pH 7.4)	solve 40 g PFA in 500 mL warm dH_2O, cool down and filtrate add 500 mL of 0.2 M phosphate buffer
10x Phosphatebuffered saline (1 M PBS, pH 7.4)	solve 11.5 g $Na_2HPO \times H_2O$ 2.0 g KH_2PO_4 80.0 g NaCl 2.0 g KCl in ca. 900 mL MilliQ water adjust pH to 7.4 fill up to 1 L final volume with MilliQ water

Table 2.4: ***Primary and secondary antibodies for immunohistochemistry.***

primary or secondary antibody	species	manufacturer	dilution
anti-HA-16B12	mouse	Covance	1:500
anti-active Caspase-3	rabbit	Promega	1:250
anti-IBA1	rabbit	Synaptic Systems	1:1000
anti-rabbit-Cy3	goat	Dianova	1:500
anti-rabbit-Cy5	goat	Dianova	1:500
biotinylated anti-mouse	goat	novex life technologies	1:500
streptavidine Cy5		Life technologies	1:500
DAPI		Applichem	1:1000
ABC kit		Vectastain	1:250 for A and B

2.6.2 Immunhistochemical Staining of Acute Slices

HA-tag staining: Hippocampal acute slices were fixed overnight in 4 % PFA in 0.1 M PB, de-hydrated in 20 % sucrose in PBS and either embedded in Tissue-Tek® O.C.T. Compound, frozen at -80 °C and stored at -20 °C till sectioning or cutted directly following de-hydration into 30 µm free-floating slices using a cyro-microtome. Slices were collected and washed in 1x PBS, permeabilized with PBS-Triton-X-100 0.25 % and

then saturated in PBS-Triton-X-100 0.25 % containing 5 % normal goat serum for 1 hour at RT. Following, slices were incubated with the specific primary antibody (HA.11 Clone 16B12, Covance, 1/500 in 5 % NGS-PBS-Triton-X-100 0.25 %) overnight at 4 °C. 3 successive washes in PBS-Triton-X-100 0.25 % were followed by a secondary antibody incubation (Biotinylated anti-mouse, 1/500 in PBS-Triton-x-100 0.25 %) for 1 hour at RT. After 3 successive washes and an incubation with the standard ABC kit (Vectastain, 1/250 for A and B in PBS, 1 hour at RT) sections were rinsed with PBS-Triton-X-100 0.25 % and incubated with Streptavidine Cy5 (1/500 in 0.1 M PBS) for 1 hour at RT. Sections were stained for DAPI, transferred on Superfrost glass slides, mounted with Fluorogel with Tris buffer (Electron Microscopy Science) and cover-slipped.

IBA-1 and Caspase-3 staining: Following fixation of acute hippocampal slices in 4 % PFA in 0.1M PB overnight, they were de-hydrated in 20 % sucrose in PBS and embedded in Tissue-Tek® O.C.T. Compound for cryo-sectioning. 30 µm free-floating slices were collected and washed in 1x PBS, permeabilized with PBS-Triton-X-100 0.25 % (2x 5 min) and then saturated in PBS-Triton-X-100 0.25 % containing 10 % normal goat serum for 1 hour at RT. Slices were then incubated with the specific primary antibody (IBA-1, Synaptic systems, 1/1000 in 10 % NGS-PBS-Triton-X-100 0.25 % and active caspase-3, Promega, 1/250 in 10 % NGS-PBS-Triton-X-100 0.25 %) overnight at 4 °C. 3 successive washes in 1x PBS were followed by the secondary antibody incubation (goat anti-rabbit-Cy3 and goat anti-rabbit-Cy5, each 1/500 in PBS) for 2 hours at RT in the dark. Sections were washed 3 times with PBS (10 min each) stained for DAPI, transferred on Superfrost glass slides, mounted with Fluorogel with Tris buffer (Electron Microscopy Science) and cover-slipped.

2.7 Statistical analysis

The statistical analysis was performed using Microsoft Excel or GraphPad Prism. The data obtained between two genotypes or two different experimental conditions were compared using an unpaired two-tailed Student's *t*-test. Data including more than 2 different groups were analyzed using a One-Way ANOVA followed by a *post-hoc* Bonferroni´s or Turkey´s Multiple Comparison Test. Values of $p = 0.05$ were considered significant and plotted as follows $*p < 0.05$; $**p < 0.01$; $***p < 0.001$. All data are indicated as mean ± SEM.

3 Results

3.1 The APP Homolog APLP1 Supports Basal Synaptic Transmission

APLP1 is the protein family member showing exclusive expression in the CNS (Lorent et al., 1995, Thinakaran and Koo, 2008, Klevanski et al., 2014), while APP and APLP2 share a common ubiquitous expression pattern throughout the body. Due to its local expression, APLP1 might have individual roles within the synaptic network. Despite the generation and first characterization of the conventional APLP1-KO mouse by Heber and coworkers in 2000, the function of the homolog has been less attended in synaptic plasticity. Therefore, a detailed characterization of the conventional APLP1-KO mice at two different ages, adult (14 to 16 weeks old) and aged (11 to 12 months old), regarding their electrophysiological properties at the Schaffer collateral CA1 pathway was conducted. This analysis included measurements of basal synaptic transmission by correlating input-output strength via fiber volley size or size of the EPSP and to proof for presynaptic functionality using the PPF paradigm. Moreover, investigations to elucidate if the deletion of APLP1 itself or with age altered activity-dependent synaptic plasticity was examined by induction of LTP by TBS.

3.1.1 Young APLP1 Knockout Mice

I investigated activity-dependent synaptic plasticity on acute hippocampal slices of 14 to 16 weeks old APLP1-KO mice and their age-matched littermate controls (LM). Acute slices of APLP1-KO mice (open circles) displayed an LTP curve that is statistically indistinguishable in induction and maintenance to that of littermate controls (black circles, Figure 3.1). Unaltered activity-dependent synaptic plasticity is moreover reflected in the average potentiation levels of the last five minutes of LTP recording (Figure 3.1B). Potentiation levels of APLP1-KO mice with 141.59 ± 2.66% were not significantly different to that of littermate controls with 147.31 ± 3.79% (Student´s t-test, p= 0.23). To further test if basal synaptic transmission is intact after APLP1 deletion in young mice, I analyzed the input-output characteristics at CA3-CA1 neurons. Neuronal excitability at postsynapses was comparable at all stimulus intensities tested (25 – 250 µA, Figure 3.1C) and when I measured the *f*EPSP slopes at defined fiber volley amplitudes (0.1 – 0.8, Figure 3.1D). Knowing about intact postsynaptic function led to testing in a next step the functionality of the presynaptic part of the synapse. Therefore, I used the PPF paradigm which allows checking for intact short-term synaptic plasticity (Figure 3.1E). The resulting curve revealed no differences between the two genotypes within that paradigm. Overall, these results indicate intact activity-dependent synaptic plasticity and no alterations at the pre- or postsynapses following APLP1 deletion in young mice.

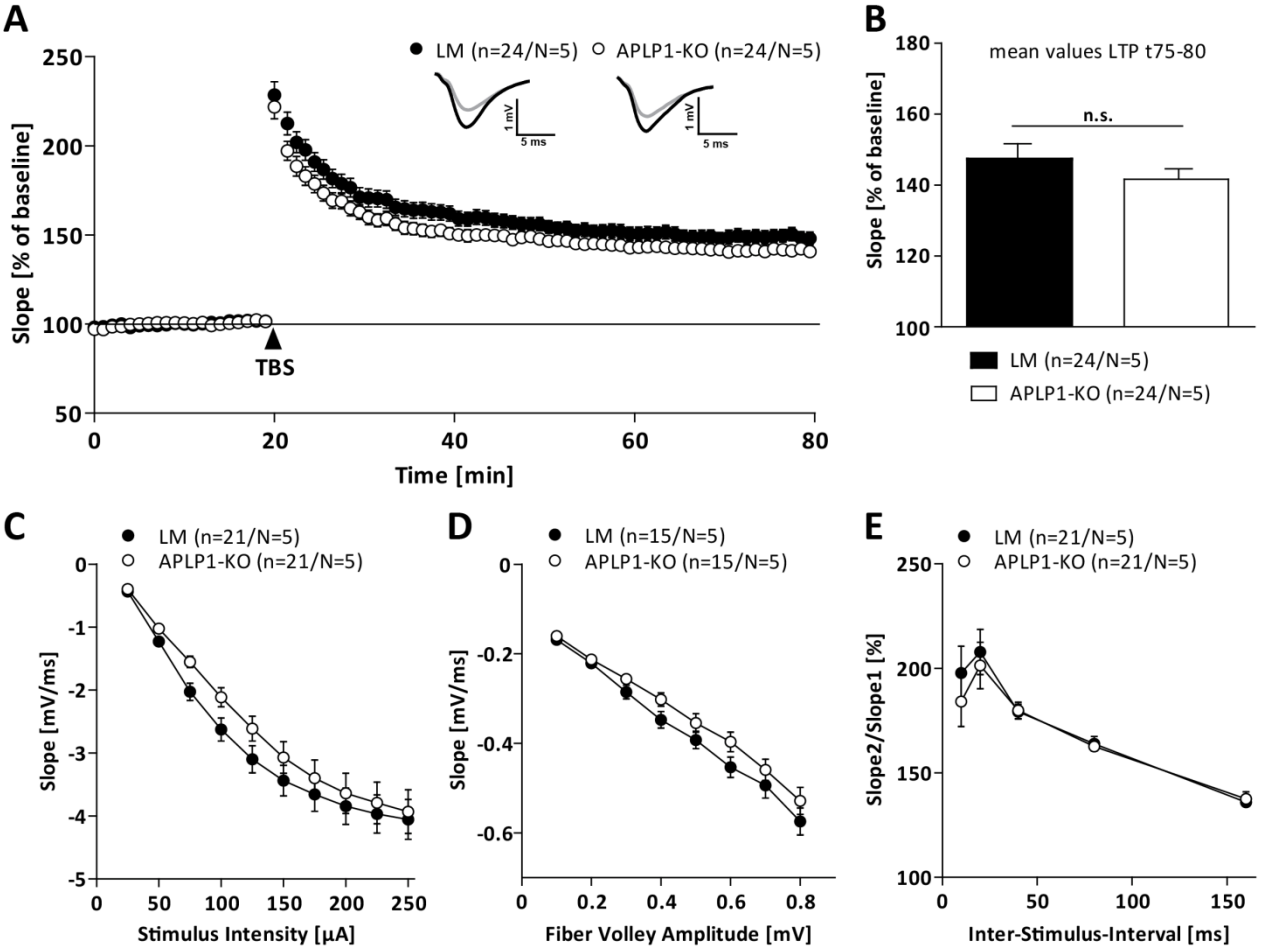

Figure 3.1: Unaltered activity-dependent synaptic plasticity in young (14 to 16 weeks old) littermate control and APLP-1 KO mice. Field excitatory postsynaptic potentials (*f*EPSPs) were recorded in CA1 region by stimulating Schaffer collateral axons of area CA3 at a frequency of 0.1 Hz of littermate control (LM, black circles) and APLP-1 KO mice (open circles). The LTP induction rate is shown as percentage % of mean baseline slope. Data points were averaged over 6 time points and error bars indicate SEM, n= number of recorded slices/N= number of animals. Data were analyzed by Student´s t-test. **(A)** After 20 min baseline recording, LTP was induced by application of Theta burst stimulation (TBS, arrowhead). Acute slices of APLP1-KO mice displayed an LTP curve that is statistical indistinguishable in induction and maintenance to that of littermate controls. Representative insets of original traces at baseline (light grey) or following stimulation (black) **(B)** Averaged potentiation levels of the last 5 minutes of LTP (55 -60 minutes after TBS) were 147.31 ± 3.79% in littermate control slices compared to 141.59 ± 2.66% in APLP1-KOs (Student´s t-test, p= 0.23). **(C)** Neuronal excitability was comparable at all stimulus intensities (25 – 250 µA) between genotypes. **(D)** Analyzing the Input-Output (IO) strength revealed no alterations between groups at any FV amplitude. **(E)** PPF was unaltered between littermates and APLP-1 KO mice.

3.1.2 Aged APLP1 Knockout Mice

As we know from the well-studied constitutive APP-KO, that alterations in synaptic plasticity or behavioral performance can be age-related, I investigated also aged APLP1-KO mice (Seabrook et al., 1999, Ring et al., 2007). Therefore, I have chosen the same age frame of 11 to 12 months when impairments in APP-KO mice became visible.

LTP induction following TBS resulted in an overall and comparable increase in synaptic strength in aged APLP1-KO (open circles) and littermate controls at the initial phase of LTP as well as in its maintenance (black circles, Figure 3.2A). Similar potentiation levels of 160.81 ± 4.29% for littermate controls versus 162.03 ± 4.42% in APLP1-KOs (Student´s t-test, p= 0.85) within the final five minutes of LTP recording indicated unaltered synaptic plasticity (Figure 3.2B). When assessing basal synaptic transmission by

correlating *f*EPSP slopes to defined stimulus intensities, APLP1-KO mice showed significantly lowered responses at stimulus intensities ranging from 100 to 250 µA (p_{100}= 0.02, p_{125}= 0.02, p_{150}= 0.01, p_{175}=0.01, p_{200}= 0.008, p_{225}= 0.006, p_{250}= 0.004, Student´s t-test, Figure 3.2C). I obtained similar results when adjusting the fiber volley amplitude to values ranging from 0.1 to 0.8 mV and measured the corresponding *f*EPSP slope (Figure 3.2.D). Again, APLP1-KOs revealed impaired excitability at amplitudes from 0.3 to 0.8 mV ($p_{0.3}$= 0.03, $p_{0.4}$= 0.01, $p_{0.5}$= 0.04, $p_{0.6}$= 0.03, $p_{0.7}$= 0.03, $p_{0.8}$= 0.04, Student´s t-test, Figure 3.2D). Both measurements performed to investigate basal synaptic transmission revealed impaired post-synaptic function in aged APLP1-KO mice in comparison to their age-matched littermate controls. With the PPF paradigm I further tested for presynaptic functionality, but found no differences in short-term synaptic plasticity or *f*EPSP responses at varying ISIs (Figure 3.2E). Based on the results reported before, I show that aged APLP1-KO mice revealed no deficits in activity-dependent short- and long-term synaptic plasticity as well as presynaptic function, while basal synaptic transmission is heavily impaired following APLP1 deletion with age.

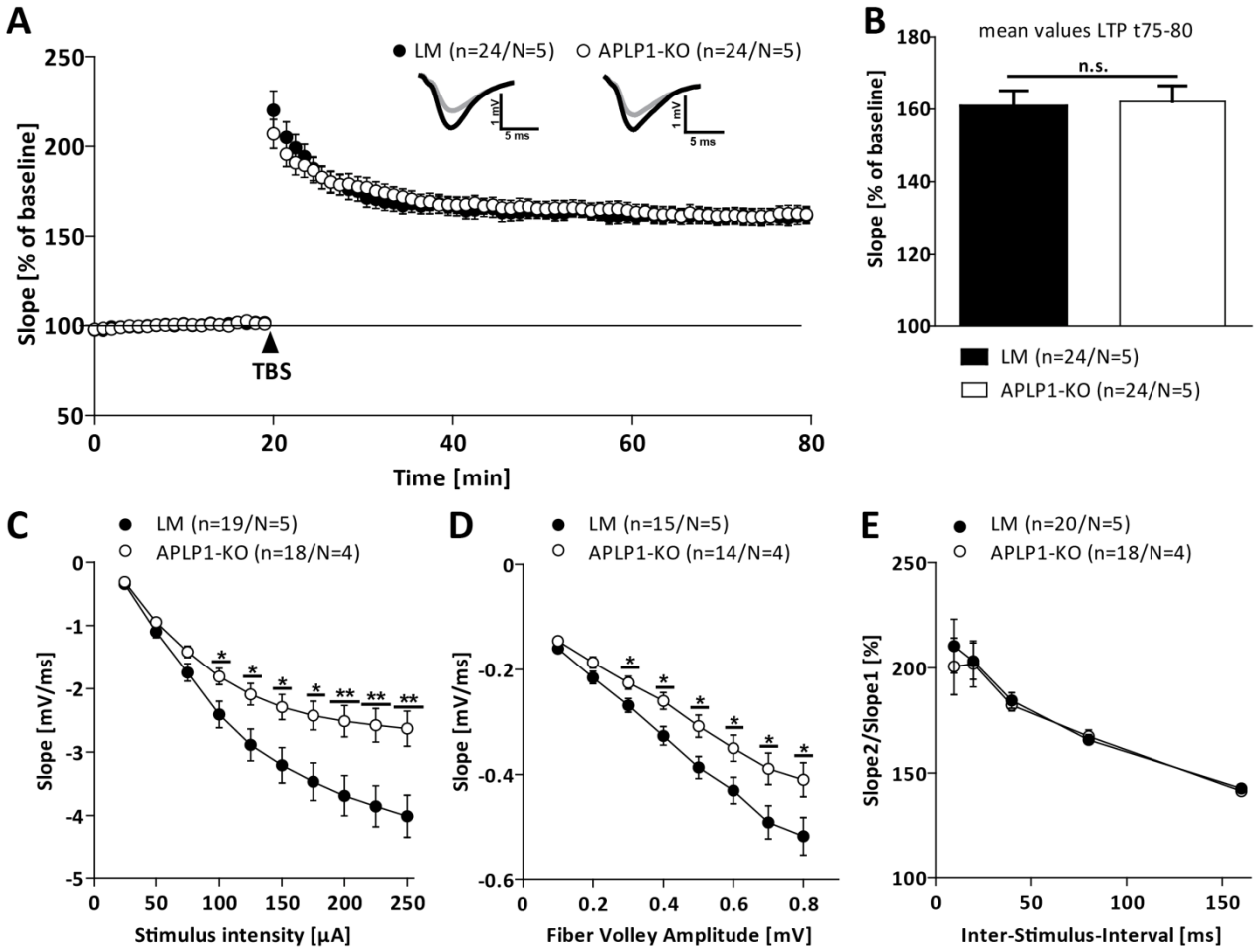

Figure 3.2: Impaired basal synaptic transmission in aged (11 to 12 months old) APLP-1 KO mice, but intact LTP. Field excitatory postsynaptic potentials (*f*EPSPs) were recorded in CA1 region by stimulating Schaffer collateral axons of area CA3 at a frequency of 0.1 Hz. The LTP induction rate is shown as percentage % of mean baseline slope. Data points were averaged over 6 time points and error bars indicate SEM, n= number of recorded slices/N= number of animals. Data were analyzed by Student´s t-test. **(A)** After 20 min baseline recording, LTP was induced by application of Theta burst stimulation (TBS, arrowhead). Acute slices of APLP1-KO (open circles) mice displayed an LTP curve that is statistical indistinguishable in induction and maintenance to that of

littermate controls (black circles). Representative insets of original traces at baseline (light grey) or following stimulation (black). **(B)** Averaged potentiation levels of the last 5 minutes of LTP (55 -60 minutes after TBS) were 160.81 ± 4.29% in littermate control slices compared to 162.03 ± 4.42% in APLP1-KOs (Student´s t-test, p= 0.85). **(C)** Neuronal excitability was significantly altered at stimulus intensities ranging from 100 µA to 250 µA in APLP1-KO acute slices (25 – 250 µA). **(D)** Analyzing Input-Output (IO) strength revealed significantly lowered output characteristics for APLP1-KO mice at FV amplitudes from 0.3 to 0.8 mV. **(E)** PPF was unaltered between genotypes.

3.1.3 APLP1 KO: Age-Dependent Comparison of Basal Synaptic Transmission

The results of young and aged APLP1-KO mice indicate that the APP homolog might have an important role in supporting basal synaptic transmission. To further prove if aging itself might have an influence on the read-out, I plotted the input-output curves for littermate controls and APLP1-KO separated by age (Figure 3.3).

Correlating stimulus intensities and *f*EPSP slopes of young and aged littermate controls (LM) (Figure 3.3A) or *f*EPSP slopes at adjusted fiber volley amplitudes (Figure 3.3C) revealed unaltered input-output characteristics with aging. In contrast, acute slices of aged APLP1-KO mice showed impaired excitability when compared to young KOs when the stimulus intensity was increased from 100 to 250 µA (p_{100}= 0.047, p_{125}= 0.02, p_{150}= 0.009, p_{175}=0.005, p_{200}= 0.004, p_{225}= 0.003, p_{250}= 0.003, Student´s t-test, Figure 3.3B). The same trend can be seen when the fiber volley amplitude was adjusted and significantly for an amplitude of 0.8 mV (p= 0.01, Student´s t-test, Figure 3.3D).

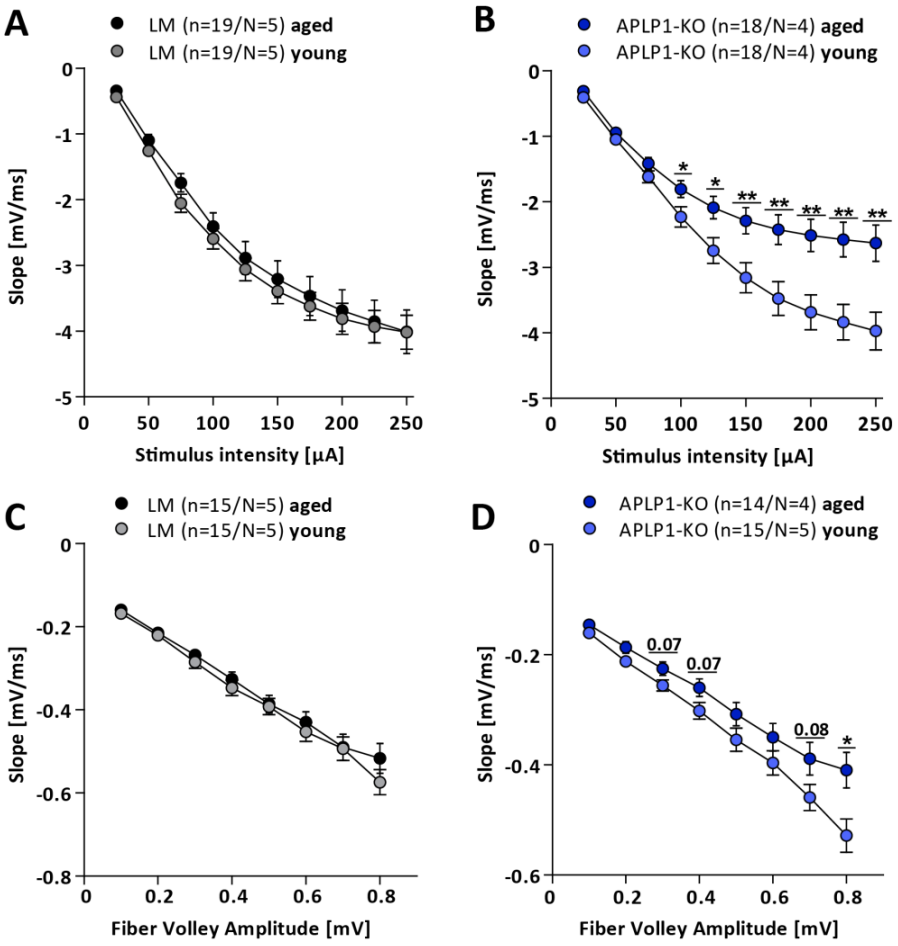

Figure 3.3: Aged APLP1-KO mice are impaired in basal synaptic transmission. **(A)** Neuronal excitability is unaltered in LM with aging. **(B)** Aged APLP1-KO reveal significantly impaired output response at stimulus intensities from 100 to 200 µA. **(C)** No alteration in input-output behavior at defined fiber volley amplitudes between young and aged LM. **(D)** By trend reduced excitability in aged APLP1-KOs at adjusted fiber volley amplitudes.

3.2 Conditional APP Triple Knockout Mice

The investigation of the APP protein family is hindered by the fact that the constitutive triple and nearly all double knockouts of APP proteins are embryonically lethal (von Koch et al., 1997, Heber et al., 2000). APP triple KO animals suffer of cortical dysplasia resembling human type 2 lissencephaly and show a partial loss of Cajal Retzius cells in the cortex at embryonic stage 18.5 (Herms et al., 2004). The generation of a conditional APP/APLP1/APLP2 knockout model (described in 2.1.2 and named APP cTKO) opened the possibility to investigate synaptic plasticity in viable mice at an age of 3.5 months. The breading of $APP^{flox/flox}APLP2^{flox/flox}APLP1^{-/-}$ mice with a NexCre-deleter line led to an APP and APLP2 ablation in excitatory neurons of the forebrain on an APLP1 deficient background starting at embryonic stage 11.5. As littermate controls (LM) I used $APP^{flox/flox}APLP2^{flox/flox}APLP1^{-/-}$ negative for the Cre-transgene which means that these are like the young APLP1-KO mice characterized in section 3.1, showing no differences in all electrophysiological read-outs used when compared to C57BL/6 mice.

To study the APP cTKO mice in activity-dependent synaptic plasticity, I recorded the enlargement of *f*EPSP slope for 60 minutes following TBS and observed a pronounced defect in induction and maintenance of LTP in acute slices of triple transgenics (Figure 3.4A). The quantification of the potentiation of the last five minutes of LTP recording (75 -80 minutes after TBS) revealed a highly significant reduction in APP cTKOs with potentiation levels of 109.42 ± 3.37% when compared to that of littermate controls: 144.98 ± 4.88% (Student´s t-test, $p= 5.72*10^{-7}$). Moreover, I investigated if the LTP deficit in APP cTKO mice might be accompanied by alterations in basal synaptic properties and tested the functionality of pre- and postsynapses. As shown in Figure 3.4C and D, illustrating the input-output characteristic of the *f*EPSP size as a function of stimulus intensity or fiber volley amplitude, APP cTKO mice are significantly impaired in their neuronal excitability. In order to further explore if short-term plasticity or presynaptic function are affected, I applied the PPF paradigm. APP cTKO yielded also here an impairment as the response at high ($p(ISI_{160ms})= 0.016$) as well as very short ($p(ISI_{10ms})= 0.047$, Student´s t-test) Inter-Stimulus-Intervals was altered in APP cTKO mice. Altogether these findings indicate that APP, APLP1 and APLP2 have an essential synaptic role during early development and adult brain function.

Figure 3.4 (next page): APP cTKO reveal a severe LTP deficit, impaired basal synaptic transmission and altered PPF. *f*EPSPs were recorded in CA1 region by stimulating Schaffer collateral axons of area CA3 at a frequency of 0.1 Hz in acute hippocampal slices of littermate control (APLP1-KO, black circles) or APP cTKO mice (open circles) at an age of 3.5 months. The LTP induction rate is shown as percentage % of mean baseline slope. Data points were averaged over 6 time points and error bars indicate SEM, n= number of recorded slices/N= number of animals. Data were analyzed by Student´s t-test. **(A)** Acute slices of APP cTKO mice revealed significantly lower levels of potentiation directly after LTP induction (TBS, arrowhead) compared to littermate controls. This impairment is maintained over the complete recording time. Representative insets of original traces at baseline (light grey) or following stimulation (black). **(B)** Averaged potentiation levels of the last 5 minutes of LTP (75 -80 minutes after TBS) were highly significant reduced in APP cTKOs compared to that of littermate controls. **(C)** Neuronal excitability was significantly impaired in APP cTKO mice at all stimulus intensities (25 – 250 µA). **(D)** Analyzing the Input-Output (IO) strength revealed strong alterations between genotypes at every FV amplitude tested. **(E)** PPF was significantly altered at the longest and shortest ISI in APP cTKO mice.

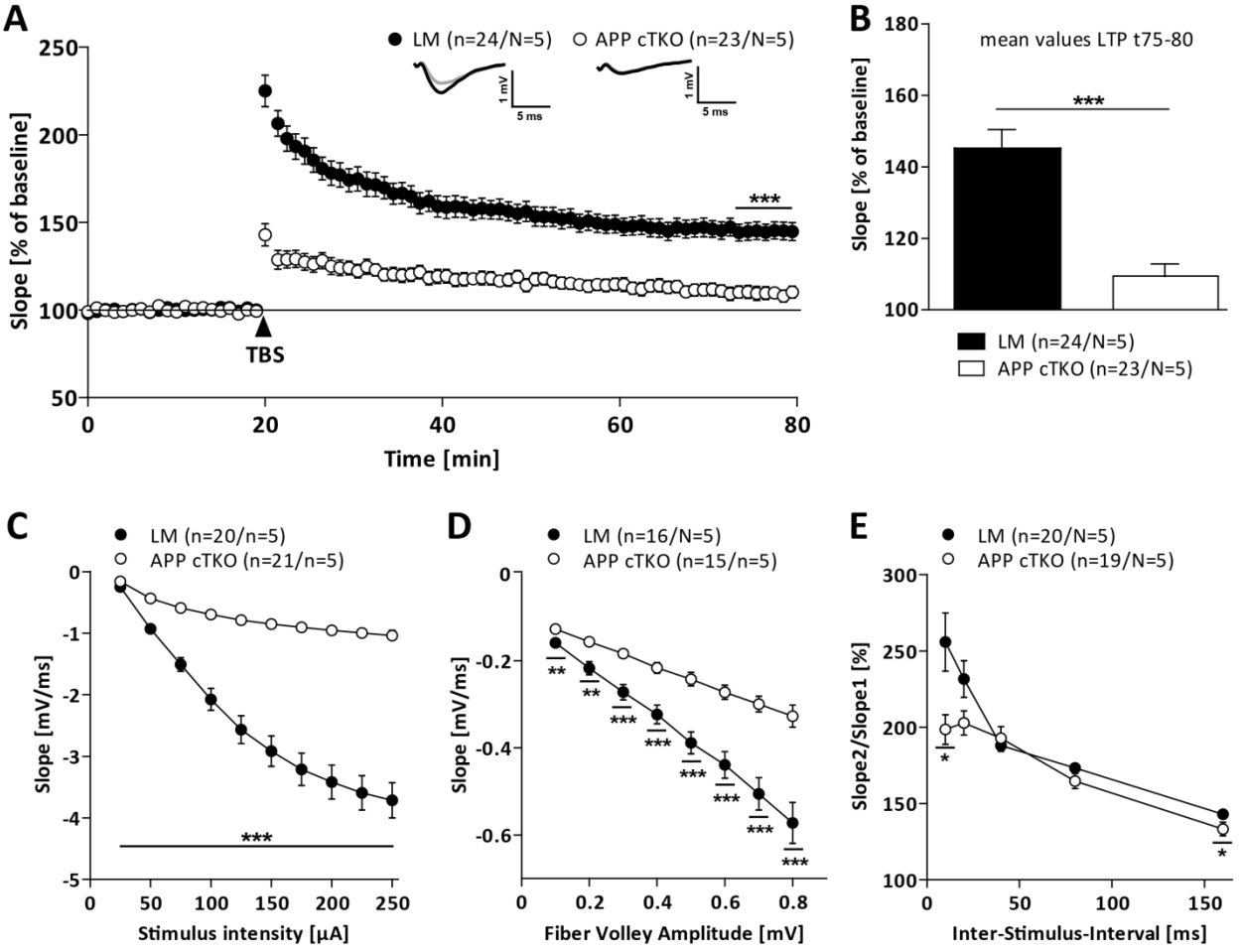

3.3 The Role of the Fe65 Protein Family as Downstream Actors of APP

The Fe65 family proteins, including Fe65 and the two like proteins Fe65L1 and Fe65L2, are scaffolding proteins interacting with the APP protein family members, lipoprotein receptors and regulators of cellular processes (Strecker et al., 2016). The biological importance of the Fe65 protein family has only been started to be understood. There are by now only two knockout models. One is the isoform specific p97Fe65-KO mouse which has only a loss of the p97 isoform of Fe65, but an upregulated expression of the truncated soluble isoform p60 (Wang et al., 2004, Guenette et al., 2006). These mice reveal deficits only in non-spatial learning tasks like the temporal dissociative passive avoidance (Wang et al., 2004) or the classical fear conditioning, while only aged mice (> 14 months) show deficits in the MWM task (Wang et al., 2009). Beside the behavioral phenotype these mice display impaired early-phase LTP elicited by a 100 Hz train recorded *in vivo* (Wang et al., 2009). The other mouse model lacks the p97 as well as the p60 isoform of Fe65 and displays muscular weakness (Suh et al., 2015). While severe neuronal positioning abnormalities were found that are quite similar to that of APP triple KO mice, Fe65-KO and Fe65L1-KO mice showed no morphological phenotype (Guenette et al., 2006). Therefore, I studied the role of each individual Fe65 family regarding its function in regulating the electrophysiological characteristics of hippocampal neurons.

Field excitatory postsynaptic potentials were recorded in the CA1 region upon stimulating Schaffer collateral axons in the CA3 at a frequency of 0.1 Hz of WT, Fe65-KO, F65L1-KO, and Fe65/Fe65L1-dKO mice (9 to 10 months of age). LTP was induced via theta burst stimulation (TBS) after 20 min of baseline stimulation and was recorded for 60 min. During these sixty minutes of LTP recording, acute slices of Fe65/Fe65L1-dKO mice exhibited lower potentiation compared to WT (p= 0.023) or Fe65L1-KO mice (p= 0.023, one-way ANOVA, Fig. 3.4A). The overall shape of potentiation after TBS application (LTP curve) of Fe65L1-KO was similar to that of WT mice (Figure 3.5A). The potentiation values of the post-tetanic (PTP, 5 min after TBS) and the stable phase of LTP were averaged for each genotype. Significantly reduced PTP was observed in Fe65/Fe65L1-dKO mice when compared to WT mice (184.34 ± 13.97% vs. 277.74 ± 29.15%, p = 0.013, one-way ANOVA, Fig. 3.5B). Fe65-KO mice also showed reduced PTP compared to WT mice, but this was not statistically significant (205.69 ± 10.52% vs. 277.74 ± 29.15%). A significant reduction in the maintenance of LTP, obtained from the mean slope of field potentials during the last 30 min of LTP recording, was observed for Fe65/Fe65L1-dKO mice in comparison to WT (137.67 ± 4.53% vs. 173.42 ± 12.98%, one-way ANOVA, p= 0.023, Fig. 3.5B). Importantly, for Fe65-KO mice, only a reduction in PTP was observed, whereas the overall LTP level 60 minutes after TBS application was only significantly affected in Fe65/Fe65L1-dKO mice, suggesting partial overlapping functions of Fe65 and Fe65L1 in synaptic plasticity. In order to further elucidate whether the LTP defect and the lower PTP observed in Fe65/Fe65L1-dKO and Fe65-KO mice, respectively, were due to altered synaptic transmission, I probed the excitability of hippocampal neurons by increasing the fiber volley (FV) amplitude (Figure 3.5C) or the stimulus intensity (Figure 3.5D). Analyzing the input-output strength of Fe65 protein family deficient mice yielded no alterations between genotypes at any FV amplitude (p> 0.1, one-way ANOVA). Although not significant, a trend towards hindered excitability was observed in Fe65/Fe65L1-dKOs. FV measurements showed for this genotype the lowest input-output curve of all, while a trend towards increased *f*EPSP responses in Fe65L1-KOs showing the highest input-output curve (Figure 3.5C) was observed. Significantly effects in neuronal excitability were seen after correlating the stimulus intensity to *f*EPSP response in Fe65/Fe65L1-dKO and Fe65L1-KO mice (Figure 3.5D). Fe65/Fe65L1-dKOs revealed significantly reduced excitability of their hippocampal neurons at stimulus intensities ranging from 50 up to 200 µA compared to Fe65L1-KO mice ($p_{50\mu A}$= 0.0004, $p_{75\mu A}$= 0.0009, $p_{100\mu A}$= 0.0011, $p_{125\mu A}$= 0.0031, $p_{150\mu A}$= 0.0088, $p_{175\mu A}$= 0.016, $p_{200\mu A}$= 0.032, one-way ANOVA). These results were a hint towards altered postsynaptic functionality in the Fe65/Fe65L1-dKO mice, an impairment that could well be responsible for the observed LTP defect. Nevertheless, acute hippocampal slices of Fe65-KO mice displayed a similar input-output curve which was comparable to that of WT controls. It should be noted, that there was just one significantly increased response of Fe65L1-KO mice at 50 µA compared to Fe65-KOs (p= 0.028, one-way ANOVA). Taken together, none of the other genotypes showed any alteration in basal synaptic transmission so that I furthermore assessed presynaptic functionality and short-term plasticity using the PPF paradigm (Figure 3.5E). The PPF analysis yielded significant alterations in the presynapse of Fe65L1-KO mice as they showed altered *f*EPSP responses in comparison to Fe65-KOs (p_{40ISI}= 0.0014, p_{80ISI}= 0.0023, p_{160ISI}= 0.00068, one-way ANOVA) and to WT mice (p_{40ISI}= 0.007, p_{80ISI}= 0.028, one-way ANOVA) at ISIs of 40, 80 and 160 ms. None of the other genotypes exhibited any significant difference in PPF values. Collectively these data point towards altered presynaptic functionality in Fe65L1-KO mice, impaired PTP in Fe65-KOs after LTP induction and a deficit in LTP induction as well as maintenance in Fe65/Fe65L1-dKOs leading to the assumption that the

Fe65 protein could be an important prerequisite of synapses in order to trigger processes of synaptic plasticity.

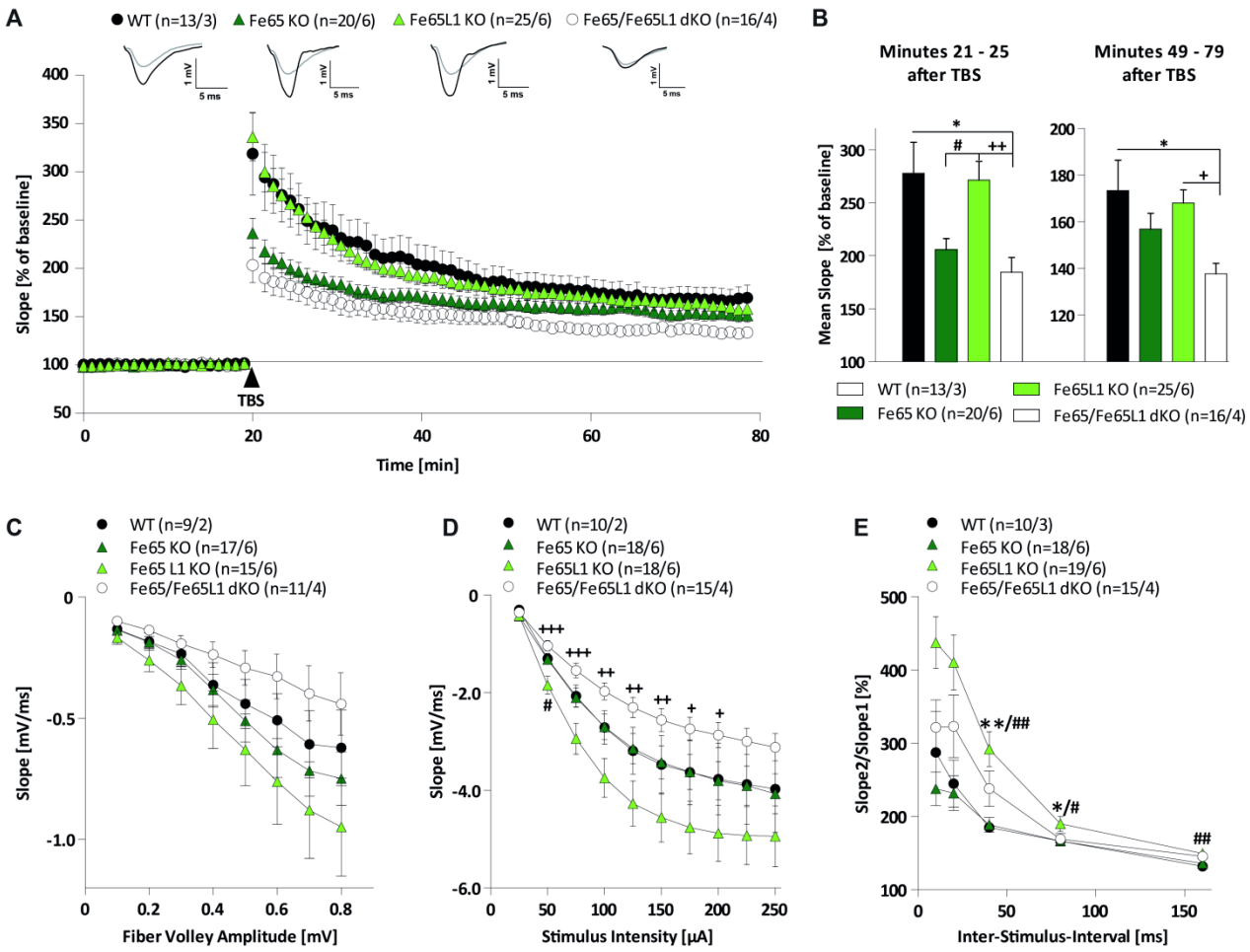

Figure 3.5: Electrophysiological recordings on hippocampal slices of Fe65 deficient and WT mice. Recording of *f*EPSPs on acute hippocampal slices of Fe65 single KO mice (dark grey triangles), Fe65L1 single KO mice (light grey triangles), Fe65/Fe65L1 double KO (dKO) mice (open circles) or wild type (WT) mice (black circles) in CA1 region by stimulating Schaffer collateral axons of CA3 at a frequency of 0.1 Hz. **(A)** LTP was induced by application of TBS after 20 min baseline stimulation (arrowhead). During sixty minutes of LTP recording, acute slices of Fe65/Fe65L1-dKO mice exhibited significant lower potentiation compared to WTs (p= 0.023) and Fe65L1-KO mice (p= 0.023). The phase of post-tetanic potentiation (5 minutes after TBS) revealed for Fe65-KO and Fe65/Fe65L1 dKO-mice significant lower levels of potentiation in comparison to Fe65L1-KO or WT mice. The LTP curve of Fe65L1-KO mice was similar to that of WT controls. The LTP induction rate is shown as percentage (%) of the mean baseline slope. Data points were averaged over 6 time points and error bars indicate SEM, n= number of recorded slices/ number of animals. Representative insets of original traces at baseline (light color) or following stimulation (black). **(B)** Averaged potentiation 5 minutes after TBS indicate significantly reduced PTP in Fe65-KO (205.69 ± 10.52%) and Fe65/Fe65L1-dKO (184.34 ± 13.97%) mice and further a significant reduction in the maintenance of LTP in Fe65/Fe65L1-dKO mice (137.67 ± 4.53%) in comparison to WT controls (173.42 ± 12.98%, p= 0.023) and Fe65L1-KOs (168.40 ± 5.67%, p= 0.023) by the mean slope of the last 30 minutes of LTP recording. **(C)** Analyzing the input-output strength of Fe65 deficient mice yielded no alterations between genotypes at any FV amplitude. **(D)** Neuronal excitability of Fe65/Fe65L1-dKOs was significantly lower at increased stimulus intensities (50 – 200 µA) compared to Fe65L1-KO mice while Fe65-KO and WTs displayed similar IO curves. **(E)** PPF yielded significant alterations in the presynapse of Fe65L1-KO mice as they showed altered PPF in comparison to Fe65-KO and WT mice at an inter-stimulus-interval (ISI) of 40, 80 and 160 ms. Data were analyzed by one-way ANOVA followed by Bonferroni´s post-hoc test. Significant (p< 0.05, *) or highly significant (p< 0.01; **) differences between Fe65-KO and Fe65L1-KO are displayed by #, between Fe65L1-KO and Fe65/Fe65L1-dKO using + and between WT and Fe65/Fe65L1-dKO by *.

3.4 Acute Inhibition of the APP α-Secretase ADAM-10

As several studies pointed to a neurotrophic action of APPsα, especially with regard to synaptic plasticity (Ring et al., 2007, Taylor et al., 2008), which might occur on a rapid time-scale (Hick et al., 2015), I performed electrophysiological recordings upon acute inhibition of the α-secretase ADAM-10. To investigate the role of the α-secretase cleavage products in activity-dependent synaptic plasticity, the production of APPsα/APLP1sα/APLP2sα was blocked using the ADAM-10 inhibitor GI254023X (Weyer et al., 2011) in C57Bl/6 mice. I recorded LTP at the Schaffer collateral-CA1 pathway and applied the inhibitor or vehicle control (DMSO) 10 minutes before TBS, while the inhibitor or vehicle control circulated continuously throughout 60 minutes of LTP recording.

First of all, the ADAM-10 inhibitor itself or DMSO had no effect on the baseline *f*EPSP slopes that were as stable as before the application of the respective compound (Figure 3.6A). Following LTP induction *f*EPSP sizes increased in both groups, but to a lesser extent in the ADAM-10 treated acute slices. The lower post-tetanic potentiation (PTP) following inhibition of the α-secretase lasted till the end of recording and resulted in potentiation levels (t85-90) of 155.37 ± 6.92% in the ADAM-10 treated slices or 169.44 ± 7.80% in DMSO controls, failing to reach statistical significance (t85-90: p= 0.20, t30-90 p= 0.13, Student´s t-test). Despite the fact that I observed no significant reduction on LTP levels, I further investigated if basal synaptic transmission or short-term synaptic plasticity were altered due to α-secretase inhibition. Therefore, I performed FV or PPF measurements 10 min after application of the ADAM-10 inhibitor or DMSO control on acute slices. As shown in Figure 3.6C input-output-behavior was unaltered following α-secretase inhibition. Analyzing presynaptic functionality revealed a significantly increased response at an inter-stimulus-interval (IS) of 80 ms, while no significant differences between treatments were observed at any other ISI. Altogether the findings showed that short-term inhibition of the α-secretase ADAM-10 had no significant effect on any synaptic transmission characteristic analyzed.

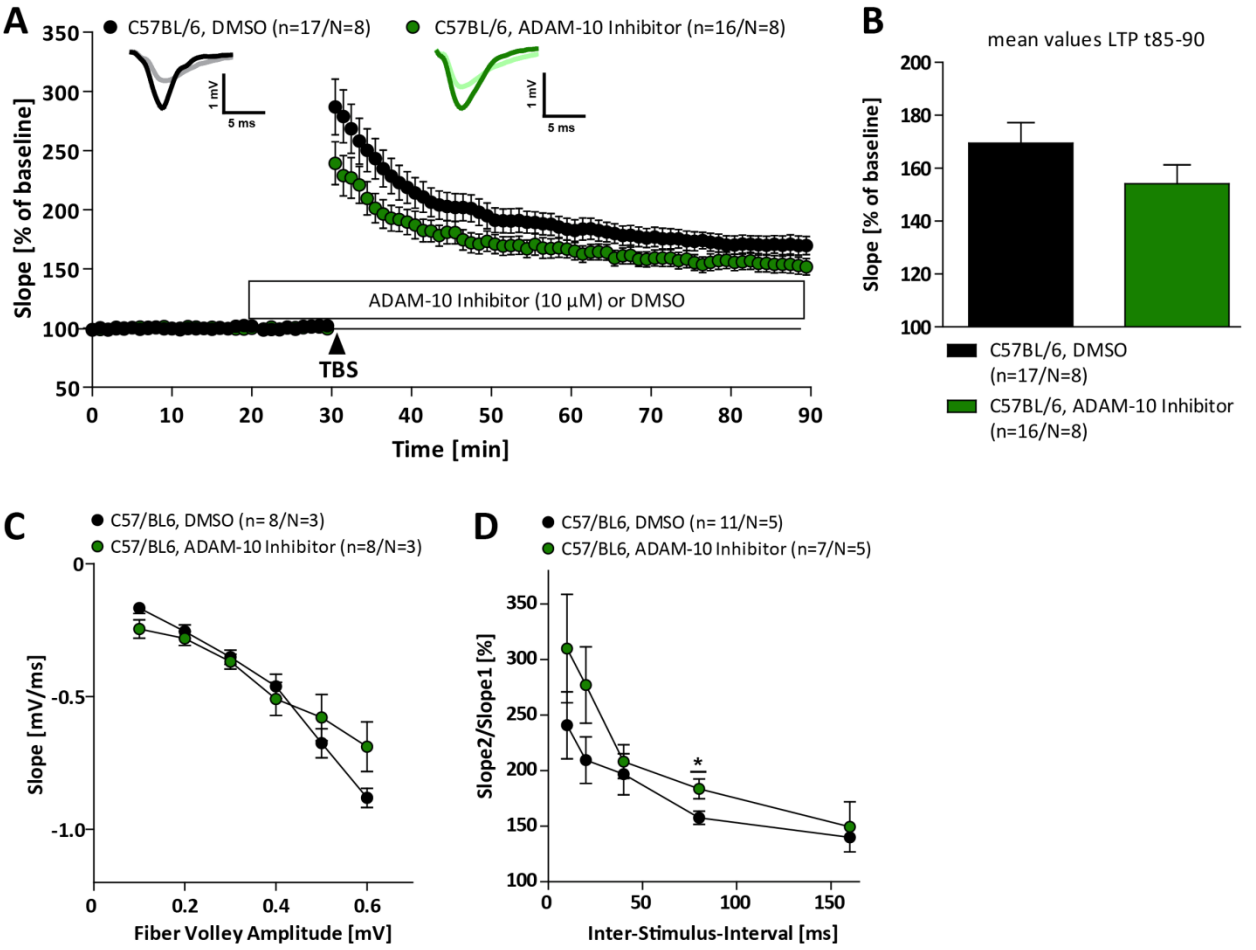

Figure 3.6: Acute inhibition of the α-secretase ADAM-10 during LTP recording at the CA3-CA1 pathway. Recording of *f*EPSPs on acute hippocampal slices 2 to 3 months old C57Bl/6 mice in CA1 region by stimulating Schaffer collateral axons of CA3 at a frequency of 0.1 Hz. **(A, B)** Either DMSO as vehicle control (black circles) or the ADAM-10 inhibitor (10 µM, green circles) were washed in 20 minutes before LTP induction by TBS (arrowhead). During sixty minutes of LTP recording DMSO or the inhibitor circulated continuously. After LTP induction *f*EPSP sizes were slightly smaller in ADAM-10 treated slices and lasted till the end of recording, resulting in not significant different potentiation levels (t85-90) of 155.37 ± 6.92% in the ADAM-10 treated slices or 169.44 ± 7.80% in DMSO controls. The LTP induction rate is shown as percentage (%) of the mean baseline slope. Data points were averaged over 6 time points and error bars indicating SEM, n= number of recorded slices/ number of animals. Representative insets of original traces at baseline (light color) or following stimulation (dark color). **(C)** Analyzing the input-output strength of inhibitor treated slices yielded no alterations at any FV amplitude compared to vehicle treated group. **(D)** PPF was significantly increased in ADAM-10 treated slices at the 80 ms ISI, while no significant differences at any other ISI could be observed.

3.5 Viral Gene Transfer of Extracellular Liberated APP Domains and Their Dose-Dependent Effects on Synaptic Plasticity in APP/APLP2 Deficient Mice

As the short-term inhibition of the α-secretase ADAM-10 had not provided convincing results, I started next another way to investigate the role of the APP cleavage products in synaptic plasticity. I used therefore, the well-characterized conditional APP/APLP2 double knockout model (cDKO) in which APLP2 is constitutively not expressed and APP via the Nex promoter selectively deleted in excitatory neurons in the hippocampus and cortex from embryonic stage 18.5 onwards. These mice reveal a strong electrophysiological phenotype with a pronounced deficit in induction and maintenance of LTP as well as altered presynaptic function (Hick et al., 2015). I could therefore prove if the viral overexpression of the

α-secretase cleavage product APPsα might be able to rescue the before mentioned alterations. First hints are thereby provided within the study of Hick et al., 2015 where the acute exogenously application of recombinant APPsα rescued the LTP deficit, while no rescue in presynaptic function was achieved.

3.5.1 High Amounts of APPsα Modulate LTP Negatively

Four weeks following viral injection with the respective virus (AAV-Venus or AAV-APPsα-Venus) with a titer of $8*10^{10}$ gc/hemisphere, NexCre cDKO or littermate controls (LM) were analyzed regarding synaptic plasticity at an age of three to four months. Recording of *f*EPSPs was performed in CA1 region by stimulating the Schaffer collateral axons of area CA3 at a frequency of 0.1 Hz only in slices showing expression of the fluorescent protein Venus in the recording areas. Induction of LTP occurred via TBS after 20 min baseline recording and was monitored for another 60 minutes (Figure 3.7A). During these sixty minutes of LTP recording acute slices of injected NexCre cDKOs revealed a significantly lower induction of LTP. In the ongoing LTP progress only APPsα injected NexCre cDKOs yielded an impairment in LTP maintenance reaching potentiation levels (t75-80) of 126.52 ± 2.73% which were significantly reduced when compared to LM controls with 148.38 ± 4.84% (p= 0.002, one-way ANOVA). Nevertheless, I was not able to detect the before described highly significant LTP defect in NexCre cDKO mice (139.39 ± 4.90%) that received the AAV-Venus control virus, which might be due to the unstable LTP curve during the maintenance of LTP in LM controls. I further assessed basal synaptic transmission properties in the injected mice and found impairments only in NexCre cDKO mice injected with AAV-Venus when compared to the APPsα injected group. This altered neuronal excitability was only detectable when the stimulus intensity was correlated to the *f*EPSP slope (Figure 3.7C, p_{50}= 0.01, p_{75}= 0.02, p_{100}= 0.02, p_{125}= 0.01, p_{150}= 0.02, p_{175}= 0.02, p_{200}= 0.02, p_{225}= 0.03, p_{250}= 0.04, one-way ANOVA), while I observed no differences using the fiber volley amplitude between the groups (Figure 3.7D). Moreover, I studied short-term plasticity and presynaptic function using the PPF paradigm (Figure 3.7E). None of the viral injected animals yielded altered presynaptic functionality. Overall these findings were not like expected as the described electrophysiological phenotype of NexCre cDKOs could not be re-produced under control conditions (AAV-Venus injections). Furthermore disappointing was the observation that APPsα overexpression did not result in a rescue of the LTP deficit like expected from its neurotrophic characteristics and based on the positive findings using an acute treatment with recombinant APPsα (Hick et al., 2015).

Based on the study of Taylor and colleagues (2008) which showed a dose-dependent facilitation of APPsα on LTP with low (0.3 nM) or high concentrations (1000 nM) having no effect on *f*EPSP change, I asked the question if the viral titer for injection was rightly chosen. In that publication it was indicated that 11 nM APPsα significantly increased *f*EPSP responses, while 3300 nM significantly decreased the *f*EPSP size at PP-DG synapses *in vivo*. Moreover, surprising was the visual effect of the fluorescent Venus signal under normal light seen on the brain surface, hippocampus and cortex during preparation of acute hippocampal slices of AAV injected mice pointing towards a high amount of viral expression in the tissue (Figure 3.8A). I used only one hemisphere of each injected mouse for LTP recording and fixed the other one in Golgi solution to perform later on spine density analysis. By looking at the overview pictures taken with an Axioplan 2 imaging microscope (Zeiss) following staining of the sections, a dramatic loss of neurons especially in the CA1 region of the hippocampus for all injected viruses can be noticed (Figure 3.8B). These results led me to further investigate toxic effects which might be initiated by virus expression and to prove if moreover immune responses were induced. To this end, I performed

immunohistochemical stainings on slices that I fixed in 4% PFA in 0.1M PB when LTP recording was completed. Slicing of 400 µm thick acute slices into 30 µm thick sections allowed the staining for astrocytes using GFAP or to prove for the inflammatory factor Caspase 3 (Casp-3). As control I used a section without intense yellow coloring caused by high expression of the Venus protein (Figure 3.8C upper panel) and compared it to slices having a quite high virus load (Figure 3.8C middle and lower panel). Comparing the GFAP staining in slices with a strong Venus expression revealed a more intense GFAP signal when exposed for the same time like slices with a weaker Venus expression. Especially in hippocampal regions with a strong Venus signal GFAP staining is more pronounced and indicates astrogliosis. The results for activated Caspase 3 document the initiation of a protease cascade that amplifies the apoptotic signaling pathway and lead to rapid cell death in regions with high Venus expression (Elmore, 2007).

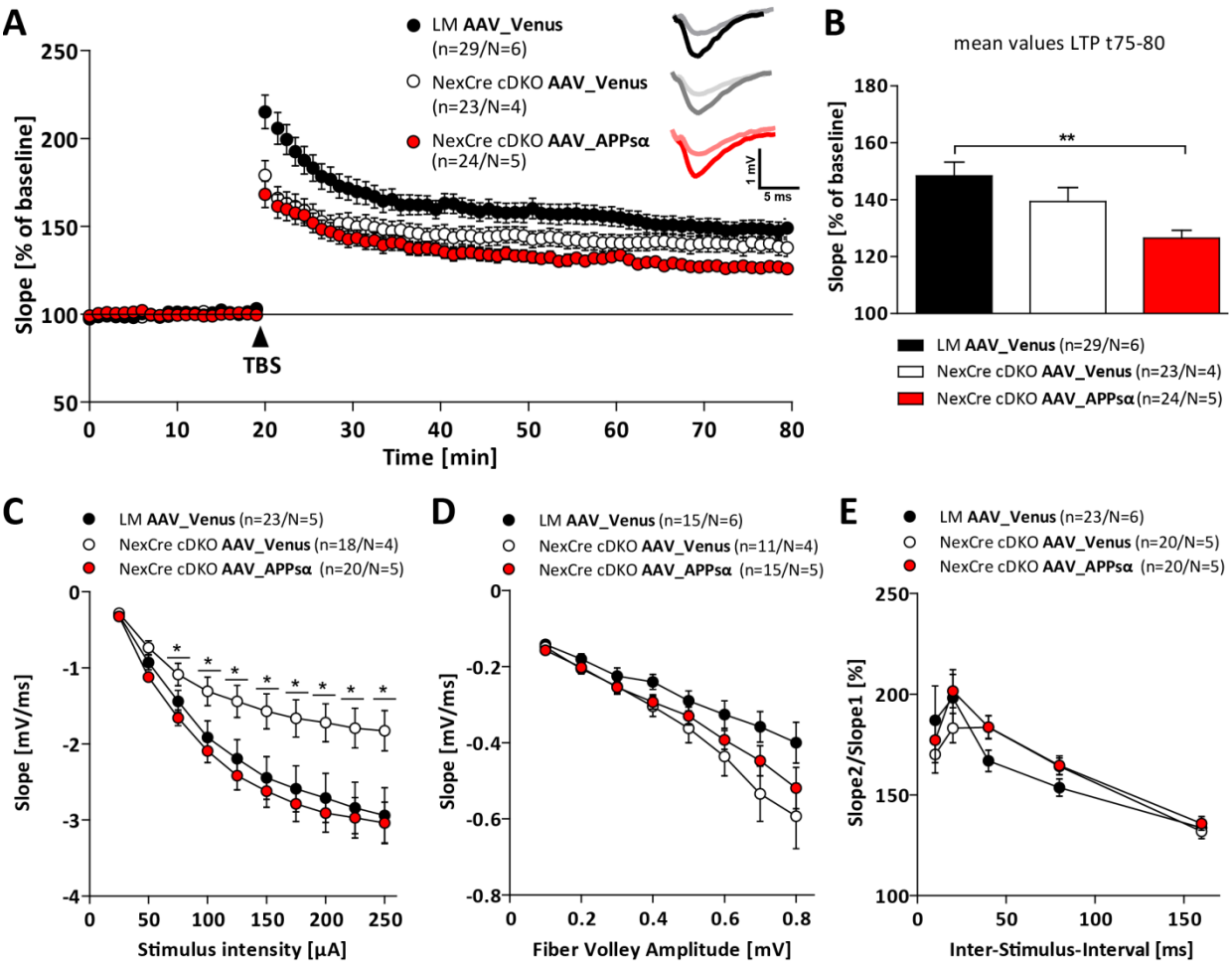

Figure 3.7: High amounts of APPsα or Venus negatively regulate synaptic plasticity in NexCre cDKO and littermate mice. *f*EPSPs were recorded in CA1 region by stimulating Schaffer collateral axons of area CA3 at a frequency of 0.1 Hz in acute hippocampal slices of littermate controls injected with AAV-Venus (APLP2-KO, black circles), NexCre cDKO mice with AAV-Venus (open circles) or NexCre cDKO that received AAV-APPsα (red circles) at an age of 3 to 4 months, 4 weeks following virus injection. The LTP induction rate is shown as percentage % of mean baseline slope. Data points were averaged over 6 time points and error bars indicate SEM, n= number of recorded slices/N= number of animals. Data were analyzed by one-way ANOVA. **(A)** Acute slices of both injected NexCre cDKO mice revealed significantly lower induction of LTP following TBS (arrowhead), while only the maintenance of NexCre cDKO APPsα injected mice resulted in impaired LTP maintenance.

Representative insets of original traces at baseline (light color) or following stimulation (dark color). **(B)** Averaged potentiation levels of the last 5 minutes of LTP (75 -80 minutes after TBS) were highly significant reduced in NexCre cDKO APPsα injected mice compared to that of LMs. **(C)** Neuronal excitability was significantly impaired in NexCre cDKOs overexpressing Venus at stimulus intensities ranging from 50 to 250 µA. **(D)** Analyzing the Input-Output (IO) strength indicated no difference between genotypes at any FV amplitude tested. **(E)** PPF revealed no alterations between groups.

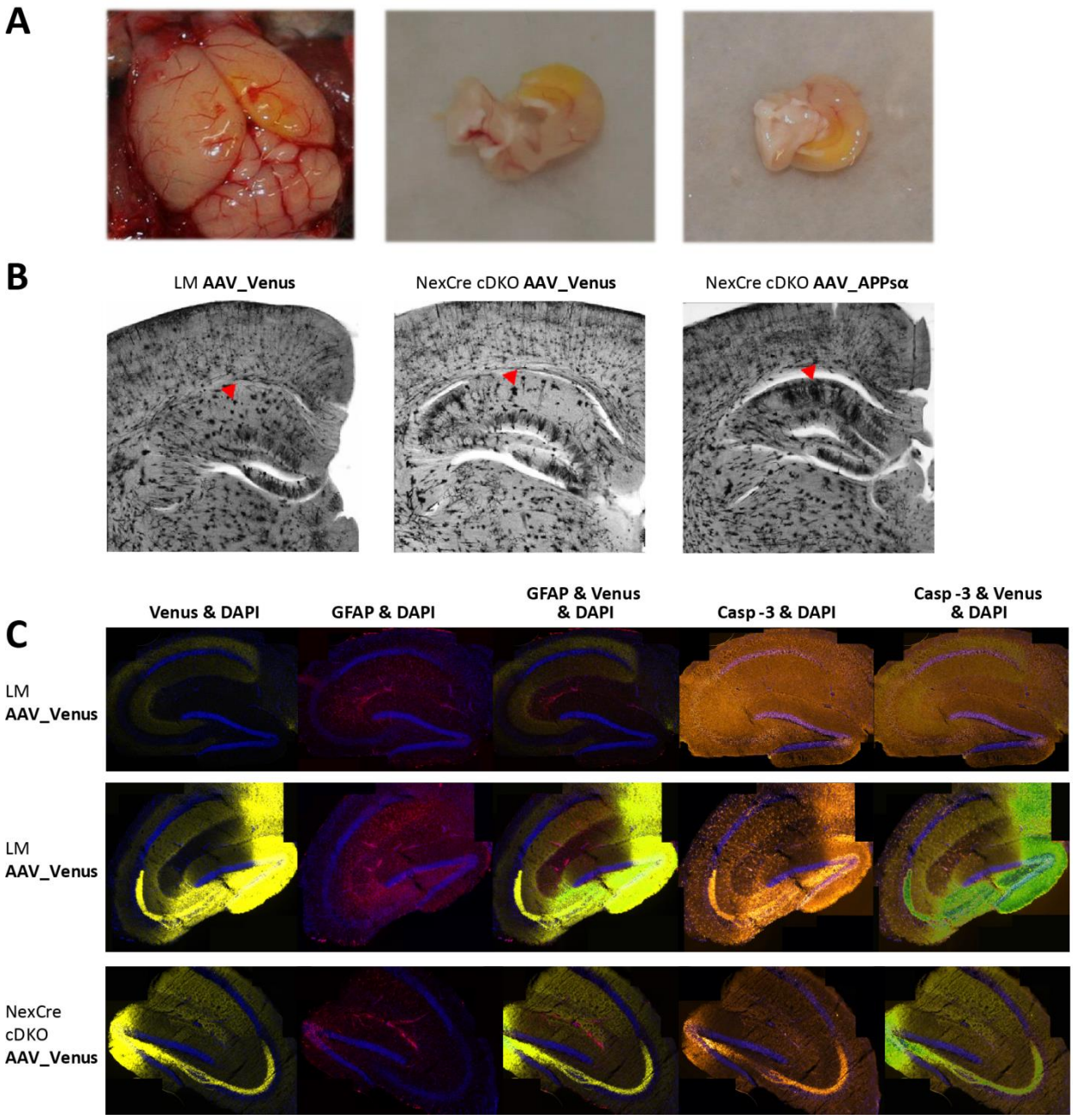

Figure 3.8: Neurotoxic effects following un-tolerated virus titer injections. (A) *Left:* mouse brain with injection wholes and yellow discoloring on the surface. *Middle and right panel*: unfolded hemisphere with yellow colored hippocampi and cortex. **(B)** Overview images of Golgi-Cox stained coronal sections of LM and NexCre cDKO mice injected with Venus and NexCre cDKO mice overexpressing APPsα. Red arrowheads indicate neuronal loss in the CA1 region of the hippocampus. **(C)** Coronal microtome sections of LM with well-tolerated Venus-titer (upper panel) and strong Venus signal (middle) and NexCre cDKO with extensive Venus signal. GFAP staining revealed slight upregulation of astrocytes, while staining for active Caspase-3 (Casp-3) showed high amounts in animals with high viral titer injections compared to tolerated virus amounts in the upper panel.

3.5.2 Viral Driven APPsα Expression Rescues LTP and Impaired PPF in NexCre cDKO Mice

I performed another round of experiments at which the viral titer was before proven to be non-toxic with regard to neuronal death and without prompting immunological responses in injected brain areas. Hence, I analyzed NexCre cDKO or littermate controls (LM) stereotactic injected with the respective virus (AAV-Venus or AAV-APPsα-Venus) with a titer of $1*10^9$ gc/hemisphere at least 4 weeks before recording activity-dependent synaptic plasticity at an age of three to four months.

To this end I recorded the enlargement of *f*EPSP slope for 60 minutes following TBS and observed a pronounced defect in induction and maintenance of LTP in NexCre cDKO mice overexpressing the control AAV_Venus virus when compared to LM controls similarly injected with AAV_Venus (Figure 3.9A). In contrast, NexCre cDKO mice overexpressing the APPsα fragment of APP showed a LTP curve progression that was not significantly different to that of LMs + AAV_Venus. The quantification of the potentiation levels of the last five minutes of LTP recording (75 -80 minutes after TBS) revealed a highly significant reduction in NexCre cDKO mice injected with AAV_Venus (128.12± 3.41%) in comparison to LM controls (156.69 ± 4.75%; $p< 0.001$, one-way ANOVA) similarly injected with the control virus. Viral overexpression of APPsα in cDKO animals resulted in a rescue of LTP as the averaged potentiation was not significantly different when compared to LM controls (150.34 ± 3.55% vs. 156.69 ± 4.75%, $p> 0.5$) injected with AAV_Venus ($p= 0.80$) and significantly higher than in cDKO mice that received AAV-Venus ($p< 0.001$, one-way ANOVA). Moreover, I investigated if the LTP deficit in NexCre cDKO mice injected with the AAV_Venus control virus might be accompanied by impaired presynaptic functionality as it was shown for un-injected mice (Hick et al., 2015) or if other basal synaptic properties might be altered and if they might be rescued following APPsα overexpression. Analyzing the input-output strength at different fiber volley amplitudes (Figure 3.9C) or stimulus intensities (Figure 3.9D) revealed unchanged neuronal excitability for all groups. In contrast, the investigation of short-term plasticity and presynaptic function using the PPF paradigm yielded significant alterations in NexCre cDKO AAV_Venus injected mice (Figure 3.9E). Acute slices showed altered PPF in comparison to LM controls expressing Venus at inter-stimulus-intervals (ISIs) of 10 ms ($p= 0.038$) and 20 ms ($p= 0.025$). Surprisingly, viral overexpression of APPsα rescued the PPF deficit and increased the PPF responses at every ISI when compared to AAV injected NexCre cDKO mice. Altogether the electrophysiological results indicated that with a well-tolerated viral titer, APPsα is able to rescue the pronounced LTP deficit in induction and maintenance in NexCre cDKO mice. Furthermore, these results pointed out that APPsα might exert its positive effect by improving the function of the presynapse.

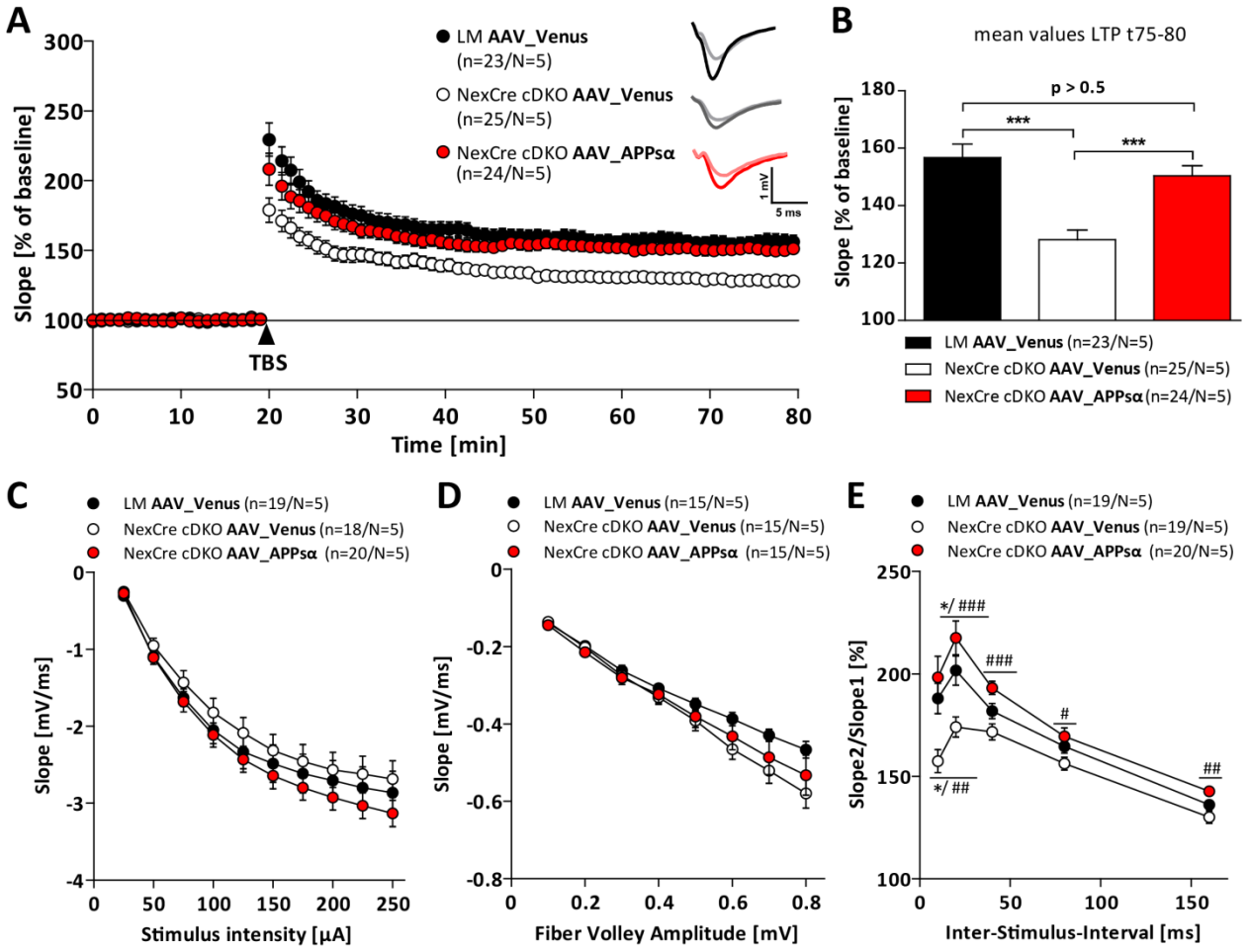

Figure 3.9: Viral overexpression of APPsα rescues the LTP deficit and impaired short-term synaptic plasticity in NexCre cDKO mice. *f*EPSPs of acute hippocampal slices of littermate control (LM) mice injected with AAV_Venus (black circles), NexCre cDKO animals similar injected with AAV_Venus (open circles) and NexCre cDKO mice that received AAV_APPsα (red circles) were recorded in CA1 region by stimulating Schaffer collateral axons of area CA3 at a frequency of 0.1 Hz. **(A)** LTP was induced by application of TBS after 20 min baseline stimulation (arrowhead). During sixty minutes of LTP recording acute slices of NexCre cDKO mice expressing Venus exhibited significant lower induction and maintenance of LTP compared to LM controls showing similar expression of Venus. The LTP curve of NexCre cDKO mice overexpressing APPsα is not significantly different to that of LM controls. The LTP induction rate is shown as percentage % of mean baseline slope. Data points were averaged over 6 time points and error bars indicate SEM, n= number of recorded slices/N= number of animals. Data were analyzed by one-way ANOVA followed by Bonferroni´s post-hoc test. Representative insets of original traces at baseline (light color) or following stimulation (dark color). **(B)** Averaged potentiation of the last 5 minutes of LTP recording (t75-80) indicated significantly reduced LTP in NexCre cDKO mice injected with AAV_Venus in comparison to LM controls. Viral overexpression of APPsα in cDKO animals resulted in a rescue of LTP. No alterations were detected analyzing the input-output strength of all viral injected mice at any FV amplitude **(C)** as well as stimulus intensity (25 – 250 µA) tested **(D)**. **(E)** PPF yielded significant alterations in the presynapse of NexCre cDKO mice injected with AAV_Venus at ISIs of 10 ms and 20 ms. Viral overexpression of APPsα rescues the PPF deficit and increased the PPF responses at every ISI when compared to AAV injected NexCre cDKO. Significant ($p < 0.05$, *) differences between littermates expressing Venus and NexCre cDKO animals injected with AAV_Venus are displayed by * and between NexCre injected with AAV-Venus and APPsα by #.

3.5.3 APPsβ Has No Modulatory Role on Synaptic Plasticity in NexCre cDKO Mice

Next I studied the relevance of the APPsβ APP fragment in activity-dependent synaptic plasticity. The physiological role of that APP cleavage product has been less attended so far. It was used only in a few studies as control to APPsα despite the fact that both extracellular peptides differ only in 16 amino acids. APPsβ is released upon cleavage of APP by the β-secretase BACE-1 and is thereby slightly shorter than

APPsα (see Figure 1.4). Only two studies addressed so far the role of APPsβ in synaptic plasticity using electrophysiological recordings *in vitro* (Hick et al., 2015) or *in vivo* (Taylor et al., 2008). Thereby APPsβ was administered both times acutely. Within the study of Hick and colleagues (2015) the bath application of 50 nM recAPPsβ on acute hippocampal slices of APP/APLP2 cDKO mice had no influence on LTP or basal synaptic transmission. I used the same conditional mouse model (NexCre cDKO) which is also the same model used in the experiments for the AAV-driven APPsα overexpression (see 3.5.1/3.5.2). In contrast to the study of Hick et al. (2015) and Taylor et al. (2008) I investigated mice not after an acute treatment with APPsβ, but following seven to eight weeks of stable viral driven overexpression upon stereotactical injection in the hippocampus with a titer of $1*10^9$ gc/hemisphere.

To this end I recorded *f*EPSPs at the Schaffer collateral CA1 pathway at a frequency of 0.1 Hz. Potentiation levels of acute slices of NexCre cDKO mice overexpressing APPsβ were indistinguishable in induction and maintenance from that of NexCre cDKO injected with the control AAV_Venus virus (Figure 3.10A). Finally, TBS induced strengthening of *f*EPSPs resulted in similar potentiation levels for the last 5 minutes of recording (t75-80: NexCre_AAV-Venus: 125.58± 2.69% vs. NexCre_AAV-APPsβ: 124.42± 1.96%, p= 0.68, Students t-test, Figure 3.10B). Analysis of basal synaptic transmission properties revealed no differences in the input-output characteristics upon variation of stimulus intensity (Figure 3.10C) or fiber volley amplitude (3.10D). Moreover, I assessed presynaptic function and in contrast to APPsα, APPsβ had no influence on short-term plasticity and was not able to improve presynaptic function (Figure 3.10E). Overall these findings suggested that APPsβ, maybe as a consequence of the missing last 16 amino acids compared to APPsα, lost the potential to promote activity-dependent synaptic plasticity and to positively modulate the function of the presynapse when injected with the same titer.

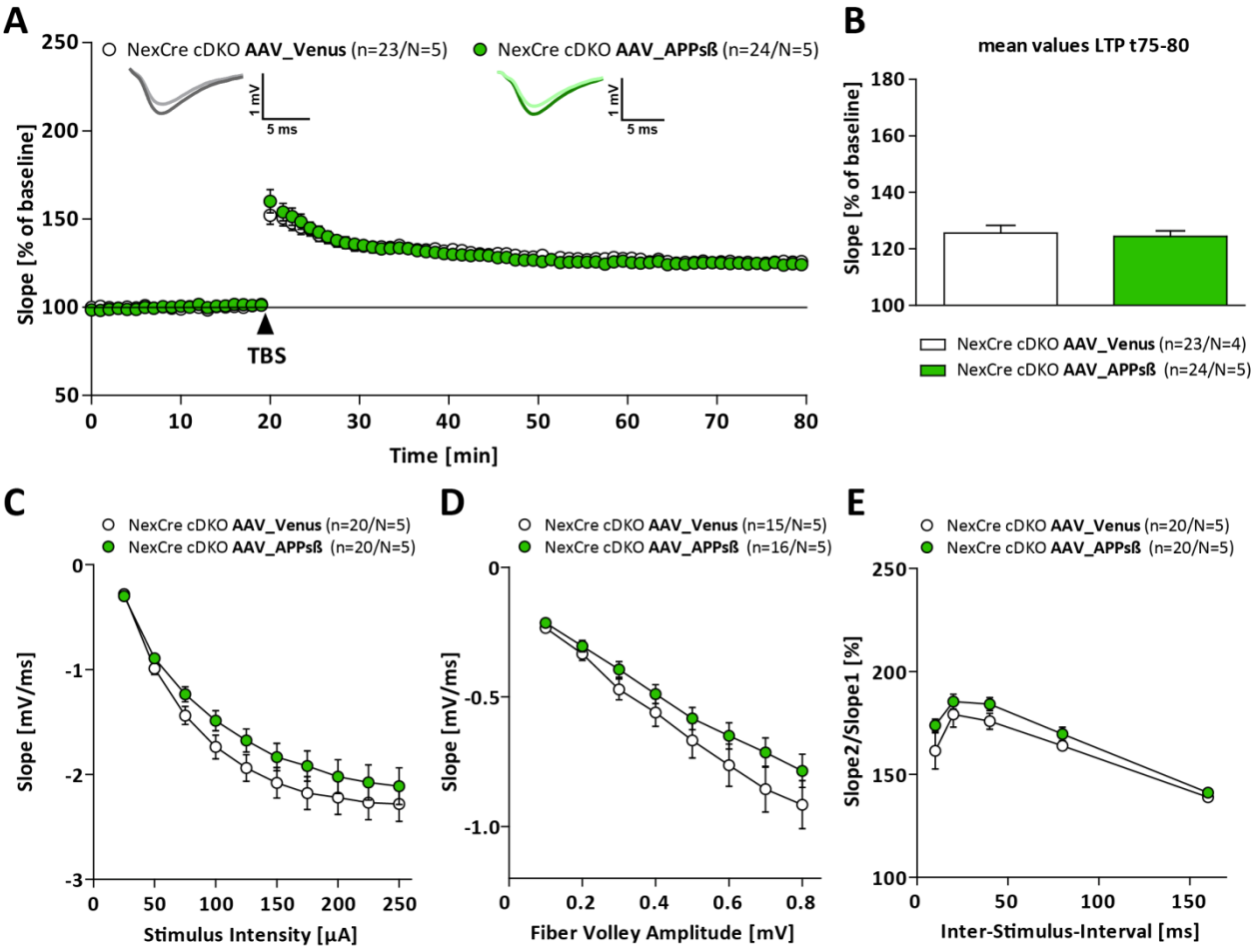

Figure 3.10: AAV-mediated overexpression of APPsβ failed to rescue the LTP defect of NexCre cDKO mice. (A, B) Activity dependent synaptic plasticity was investigated in 6,5 to 7 months old NexCre cDKO mice 7 to 8 weeks after stereotactical virus injection. LTP induction and maintenance of mice overexpressing APPsβ (green circles) was unaltered compared to NexCre cDKO injected with AAV-Venus control virus (open circles). TBS induced strengthening of *f*EPSPs resulted in similar potentiation levels for the last 5 minutes of recording. The LTP induction rate is shown as percentage % of mean baseline slope. Data points were averaged over 6 time points and error bars indicate SEM, n= number of recorded slices/N= number of animals. Data were analyzed by one-way ANOVA followed by Bonferroni´s post-hoc test. Representative insets of original traces at baseline (light color) or following stimulation (dark color). **(C, D)** Neither increasing stimulus intensity nor adjusting fiber volley amplitude revealed changes in basal synaptic transmission between both groups. **(E)** The PPF paradigm yielded no differences between viral injected NexCre cDKO mice.

3.6 AVV-driven Expression of APPsα and APPsβ in APP/PS1ΔE9 tg Mice and Their Effects on Synaptic Plasticity and Spine Density

Having confirmed the neurotrophic properties of APPsα, but not APPsβ upon stable overexpression in the hippocampus of APP deficient mice with a severe LTP deficit, I proved the potential of APPsα to rescue the LTP impairment in AD mice and included moreover a morphological analysis involving spine density assessment of hippocampal neurons.

3.6.1 AVV-driven Expression of APPsα Rescues Synaptic Plasticity and Spine density in APP/PS1ΔE9 tg mice

Based on the observed neurotrophic activity of APPsα during processes of activity-dependent synaptic plasticity in APP deficient mice (see 3.5.2), I next proved its relevance using the AD model mice:

APP/PS1ΔE9. I wanted to elucidate if APPsα might have the same effect like in APP/APLP2 cDKO mice to enhance or even to restore LTP, which is heavily impaired in AD models. APPsα might therefore be of therapeutic relevance for the disease. Consequently, APP/PS1ΔE9 tg mice were injected with either a control (AAV-Venus) or AAV-APPsα virus in the hippocampus (10^{10} vg/hippocampus) at an age of twelve to thirteen months, a time-point when spatial memory impairments and altered synaptic plasticity are well described (Savonenko et al., 2005b, Heneka et al., 2013).

Four to five months following injection, I recorded *f*EPSPs in the CA1 region by stimulating Schaffer collateral axons of CA3 at a frequency of 0.1 Hz on acute hippocampal slices of APP/PS1ΔE9 tg mice and wild-type littermates (LM) stereotactically injected with AAV_Venus control virus or AAV_APPsα. Induction of LTP occurred via TBS after 20 min baseline recording and was monitored for another 60 min (Figure 3.11A). During these sixty minutes of LTP recording acute slices of APP/PS1ΔE9 tg mice expressing Venus exhibited already at induction of LTP significant lower potentiation levels which lasted throughout the whole recording time compared to LMs. The averaged potentiation for the stable phase of LTP, ranging from minute 50 to 80 after TBS, was 178.01 ± 8.98% for LMs and thereby significant higher than that of APP/PS1ΔE9 tg mice expressing the same fluorescent protein with 148.47 ± 6.04% (p= 0.023, 1-way ANOVA). Acute slices of APP/PS1ΔE9 transgenics injected with AAV-APPsα showed nearly the same potentiation upon TBS in the phase of PTP and LTP like LM slices expressing Venus (Figure 3.11A) confirming the beneficial role of the α-secretase released APP fragment. This was moreover visible when comparing the averaged potentiation levels in the bar graph (Fig. 3.11B), where no significant alteration in the mean potentiation values for the last 30 minutes between LMs 178.01 ± 8.98% and APPsα overexpressing transgenics were detectable (167.31 ± 8.98%, p= 0.86, 1-way ANOVA). Next, I investigated if the LTP defect identified in acute slices of APP/PS1ΔE9 tg mice expressing the control virus was due to altered synaptic transmission. Therefore, the excitability of hippocampal neurons was tested by increasing the FV amplitude (Figure 3.11C) or stimulus intensity (Figure 3.11D) to defined values. Analyzing the input-output strength of APP/PS1ΔE9 tg animals injected with AAV_Venus using this two paradigms revealed no alterations in basal synaptic transmission in comparison to LM slices also expressing the fluorescence protein (EPSP: p≥ 0.74 at all stimulus intensities analyzed by 1-way ANOVA; FV: p≥ 0.20 at all fiber volley amplitudes analyzed by 1-way ANOVA). Furthermore, addressing the functional consequences of APPsα overexpression in transgenic mice indicated unchanged excitability of hippocampal CA3/CA1 neurons compared to the two other groups. Consistently these results yielded that none of the genotypes was impaired in its postsynaptic functionality, so that I furthermore assessed the function of the presynapse and short-term plasticity using the paired-pulse facilitation (PPF) paradigm (Figure 3.11E). The PPF yielded significant alterations in the presynapse of hippocampal slices of APP/PS1ΔE9 tg mice that received the control AAV_Venus virus compared to LMs similarly expressing Venus. There was nearly no facilitation within shorter inter-stimulus-intervals (ISI) in slices of APP/PS1ΔE9 tgs injected with AAV_Venus compared to LM+ AAV_Venus slices, reaching a significant impairment in presynaptic functionality at an ISI of 10 ms (p= 0.027 1-way ANOVA). Comparing the PPF development of APP/PS1dE9 tg mice overexpressing APPsα to LMs that received the AAV_Venus virus revealed similar behavior towards the second stimulus applied within that paradigm, only the shortest interval tested showed a smaller ratio for the rescue group without reaching significance (p= 0.48). These results additionally underline the beneficial role of APPsα as far as I was not able to detect a defect in presynaptic function in APP/PS1ΔE9 tg mice following APPsα overexpression. Taken together, investigating synaptic plasticity in the hippocampus *in vitro* revealed a LTP defect for APP/PS1ΔE9 tg

animals expressing Venus probably as a result of impaired presynaptic functionality while excitability of the postsynapse was unaltered. Moreover, I showed that APPsα restored LTP and the function of the presynapse without altering basal synaptic transmission in these AD model mice.

As far as defects in hippocampal function might be related to altered morphology of CA1 and/or CA3 pyramidal neurons I next examined spine density in this two areas where LTP recording took place. I determined if the mutation in *APP* and *PSN1* alters the spine number of basal and mid-apical dendritic segments of hippocampal CA1 and CA3 neurons that might contribute to the observed LTP defect in APP/PS1ΔE9 tg animals by using Golgi-Cox staining (Figure 3.11F). Previous studies already indicated reduced spine density in various AD mouse models (Spires-Jones and Knafo, 2012) and consistent with the literature, I found an overall reduction in spine density in APP/PS1ΔE9 tg mice at both dendritic compartments of CA1 and CA3 neurons in comparison to LMs similarly injected with AAV-Venus (Figure 3.11G,H). At CA1 neurons, the effect was even more pronounced in the basal (p= 0.002, 1-way ANOVA) than in the apical (p= 0.04) dendritic segment. The analysis of CA3 neurons revealed significantly fewer spines in both basal (p= 0.01) as well as apical (p= 0.014) dendritic branches when comparing AAV-Venus expressing APP/PS1ΔE9 tg mice and non-transgenic LMs. Importantly, AAV-APPsα overexpression partially restored spine density in apical compartments of CA1 and CA3 segments. A complete rescue of the spine density deficit was achieved in basal dendrites of CA1 (p= 0.019) and CA3 dendrites (p= 0.039) of APP/PS1ΔE9 tg mice. Collectively, these data indicated that viral driven APPsα expression substantially ameliorated both structural and functional synaptic impairments of aged AD model mice.

Figure 3.11 (next page): APP/PS1ΔE9 mice reveal structural and functional synaptic impairments that are ameliorated by APPsα expression. (A, B) LTP was induced by TBS at hippocampal CA3-CA1 synapses after 20 min baseline recordings (arrowhead). Acute slices of AAV-Venus injected APP/PS1ΔE9 animals (open circles) exhibited significant lower induction and maintenance of LTP compared to littermate controls (LM, black circles) showing similar expression of Venus (averaged potentiation minutes t50-80: 148.47 ± 6.04% vs. 178.01 ± 8.98%, p= 0.021). Viral expression of APPsα (red circles) restored potentiation after TBS (171.48 ± 6.29%) in transgenic animals and resulted in an LTP curve progression comparable to that of LM controls. The LTP induction rate is shown as percentage % of mean baseline slope, n = number of slices, N = number of mice. Representative insets of original traces at baseline (light color) or following stimulation (dark color). **(C, D)** Input-Output strength of all AAV-injected mice showed no alterations between genotypes at any fiber volley (FV) amplitude or stimulus intensity tested. **(E)** Altered PPF at the 10 ms ISI revealed a significant impairment in the presynapse of APP/PS1ΔE9 mice injected with AAV-Venus in comparison to LM controls (*p= 0.030) that was restored after AAV-APPsα injection (#p= 0.047). **(F)** Detailed segments of 2nd or 3rd order dendritic branches of apical and basal dendrites of CA1 and CA3 neurons after Golgi-Cox staining, scale bar 8 µm. **(G)** APP/PS1ΔE9 Venus injected mice had significantly less spines at apical (p= 0.043) and basal (p= 0.002) dendrites in comparison to their littermate controls. APPsα overexpression partially restored the spine density deficit at apical and completely at basal compartments (p= 0.019). **(H)** Reduced spine density at CA3 apical (p=0.014) and basal (p=0.011) dendritic segments of APP/PS1ΔE9 AAV-Venus injected mice that is partially rescued at apical and completely at basal dendrites (p= 0.039) by APPsα. N = number of animals, n = number of neurons. Data represent mean ± SEM and were analyzed by one-way ANOVA followed by Bonferroni´s post-hoc test.

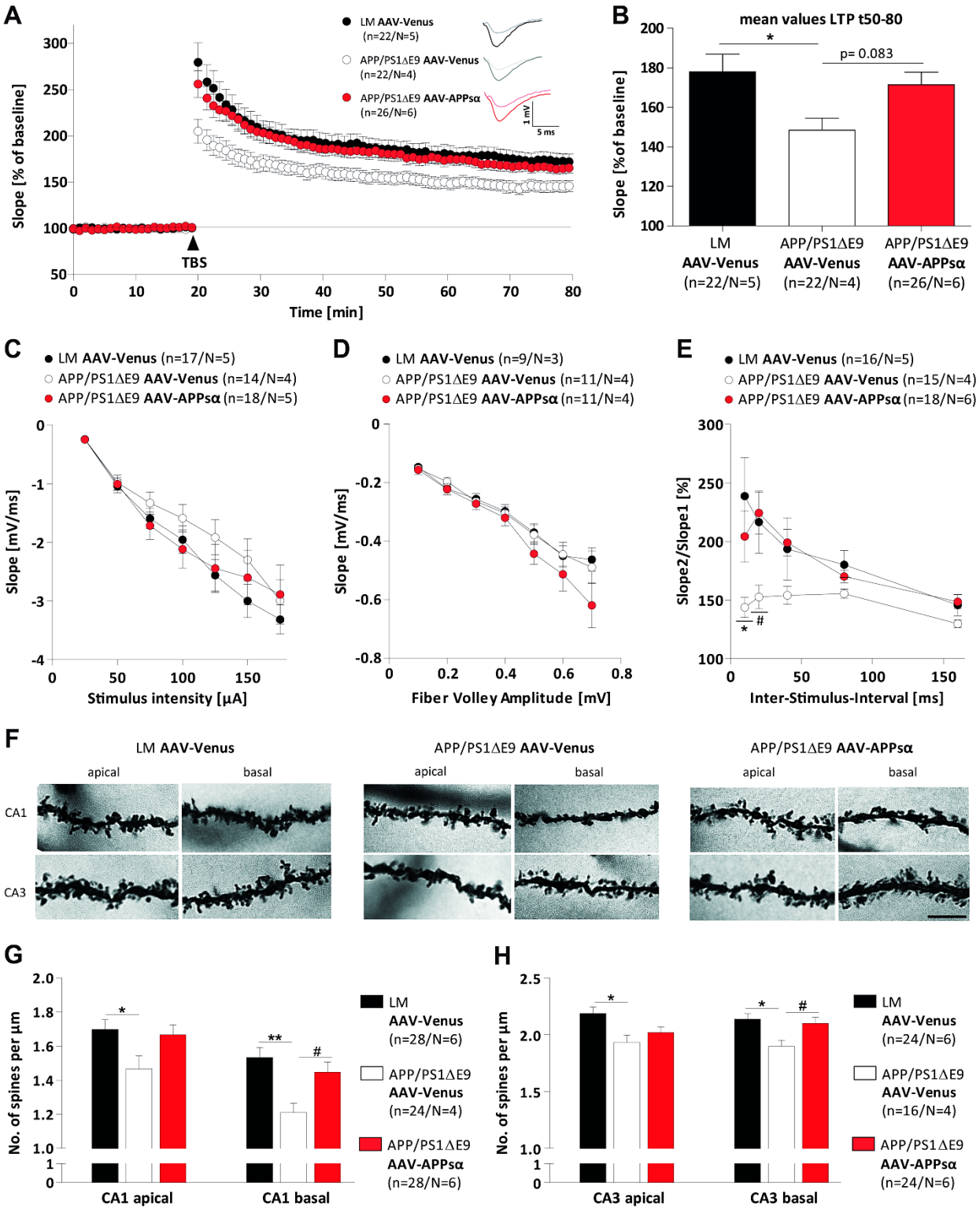
A
LM AAV-Venus (n=22/N=5)
APP/PS1ΔE9 AAV-Venus (n=22/N=4)
APP/PS1ΔE9 AAV-APPsα (n=26/N=6)
1 mV
5 ms
Slope [% of baseline]
TBS
Time [min]
B
mean values LTP t50-80
Slope [%of baseline]
p= 0.083
LM AAV-Venus (n=22/N=5)
APP/PS1ΔE9 AAV-Venus (n=22/N=4)
APP/PS1ΔE9 AAV-APPsα (n=26/N=6)
C
LM AAV-Venus (n=17/N=5)
APP/PS1ΔE9 AAV-Venus (n=14/N=4)
APP/PS1ΔE9 AAV-APPsα (n=18/N=5)
Slope [mV/ms]
Stimulus intensity [µA]
D
LM AAV-Venus (n=9/N=3)
APP/PS1ΔE9 AAV-Venus (n=11/N=4)
APP/PS1ΔE9 AAV-APPsα (n=11/N=4)
Slope [mV/ms]
Fiber Volley Amplitude [mV]
E
LM AAV-Venus (n=16/N=5)
APP/PS1ΔE9 AAV-Venus (n=15/N=4)
APP/PS1ΔE9 AAV-APPsα (n=18/N=6)
Slope2/Slope1 [%]
Inter-Stimulus-Interval [ms]
F
LM AAV-Venus
APP/PS1ΔE9 AAV-Venus
APP/PS1ΔE9 AAV-APPsα
apical
basal
CA1
CA3
G
No. of spines per µm
LM AAV-Venus (n=28/N=6)
APP/PS1ΔE9 AAV-Venus (n=24/N=4)
APP/PS1ΔE9 AAV-APPsα (n=28/N=6)
CA1 apical
CA1 basal
H
No. of spines per µm
LM AAV-Venus (n=24/N=6)
APP/PS1ΔE9 AAV-Venus (n=16/N=4)
APP/PS1ΔE9 AAV-APPsα (n=24/N=6)
CA3 apical
CA3 basal

3.6.2 APPsβ Has No Modulatory Role on Synaptic Plasticity and Spine Density in APP/PS1ΔE9 tg Mice

Next, I investigated if the β-secretase released APP fragment APPsβ had any influence on activity-dependent synaptic plasticity. Compared to APPsα, APPsβ lacks the last 16 amino acids present at the N-terminus of the Aβ peptide (Chasseigneaux et al., 2011). Using APP/APLP2 deficient mice (see 3.5.2) no modulatory role on synaptic plasticity was found when APPsβ was virally overexpressed for 2 months or acutely applied as recombinant peptide on acute hippocampal slices (Hick et al., 2015). Nevertheless, little is known about a possible involvement of APPsβ in the pathogenic process of AD and whether APPsβ might have a similar neuroprotective potential as APPsα, but to a lower extent (Furukawa et al., 1996).

To examine the effects of APPsβ in activity-dependent synaptic plasticity, I recorded the electrophysiological response of neurons four to five months after AAV injection (10^{10} vg/hippocampus) at an age of twelve to thirteen months in APP/PS1ΔE9 tg mice. I evaluated if the discrepancies of the soluble APP ectodomains seen in APP deficient mice are further mirrored at the functional network level of AD mice. Therefore, I induced after 20 minutes baseline recording LTP by TBS (Figure 3.12A). Acute slices of littermate control mice (LM) that solely overexpress Venus exhibited a robust LTP induction and maintenance, while consistently to the previous study (see 3.6.1) and results of non-injected APP/PS1ΔE9 animals (Corrigan et al., 2012, Jonsson et al., 2013), transgenic mice overexpressing Venus revealed a strong LTP deficit (Figure 3.11A). 60 minutes after TBS acute slices of APP/PS1ΔE9-AAV-Venus mice reached significantly reduced potentiation levels of 154.09 ± 7.55% when compared to AAV-Venus injected LMs 193.33 ± 5.97% ($p< 0.001$, one-way ANOVA, Figure 3.12B). Analog to my set of experiments reported in section 3.6.2, AAV-driven APPsα expression rescued LTP as shown by potentiation levels of 198.25±8.62% similar to that of littermate controls ($p= 0.99$, one-Way ANOVA, Figure 3.12B) and this time significantly higher than that of APP/PS1ΔE9-Venus transgenics ($p= 0.003$). AAV-APPsβ treatment in contrast failed to restore the impairment of *f*EPSP strengthening in response to tetanic stimulation reflected by only 156.08 ± 5.03% of potentiation, representing the LTP deficit of APP/PS1ΔE9-Venus mice ($p= 0.99$). As previously, I observed impaired presynaptic functionality in the AD mouse model (3.6.1), I addressed again basal synaptic transmission properties. I confirmed that there are no alterations in postsynaptic function by comparing *f*EPSP sizes at defined stimulus intensities (Figure 3.12C) or fiber volley amplitudes (Figure 3.12D) between genotypes after AAV-injection. The PPF paradigm revealed and confirmed altered presynaptic function of APP/PS1ΔE9-Venus mice, getting significant at an inter-stimulus interval of 20 ms ($p= 0.017$) compared to LM AAV-Venus injected controls (Figure 3.12E). While AAV-APPsα expression rescued the function of the presynapse at stimuli applied at 20 ms ($p= 0.009$) and with a strong tendency at 10 ms ($p= 0.06$), AAV-APPsβ treatment was again ineffective.

Next, I determined spine density at CA1 pyramidal neurons by Golgi-Cox staining in the mice used to analyze synaptic plasticity since functional changes in synaptic strength often correlate with morphological alterations (Figure 3.12H). Indeed, I observed a significant reduction in spine density at mid-apical dendrites of hippocampal CA1 neurons for APP/PS1ΔE9 tg mice ($p= 0.008$, one-way ANOVA) and a tendency at basal dendritic compartments ($p= 0.09$) compared to LMs similarly injected with AAV-Venus (Figure 3.12F, G). Strikingly and consistent to what I observed previously (see section 3.6.1), unaltered spine numbers were obtained after APPsα treatment for both compartments ($p> 0.8$), while AAV driven APPsβ expression didn´t elevate spine density in transgenic mice. Spine number was

significantly reduced in AAV-APPsβ injected APP/PS1ΔE9 tg mice at mid-apical dendrites compared to LMs ($p < 0.001$) or APPsα injected mice ($p < 0.001$). The reduction in spine density was further evident in the basal dendritic compartment ($p < 0.003$). Overall these data indicated that only APPsα expression improves functional and structural synaptic impairments in aged APP/PS1ΔE9 tg mice, while APPsβ is not capable.

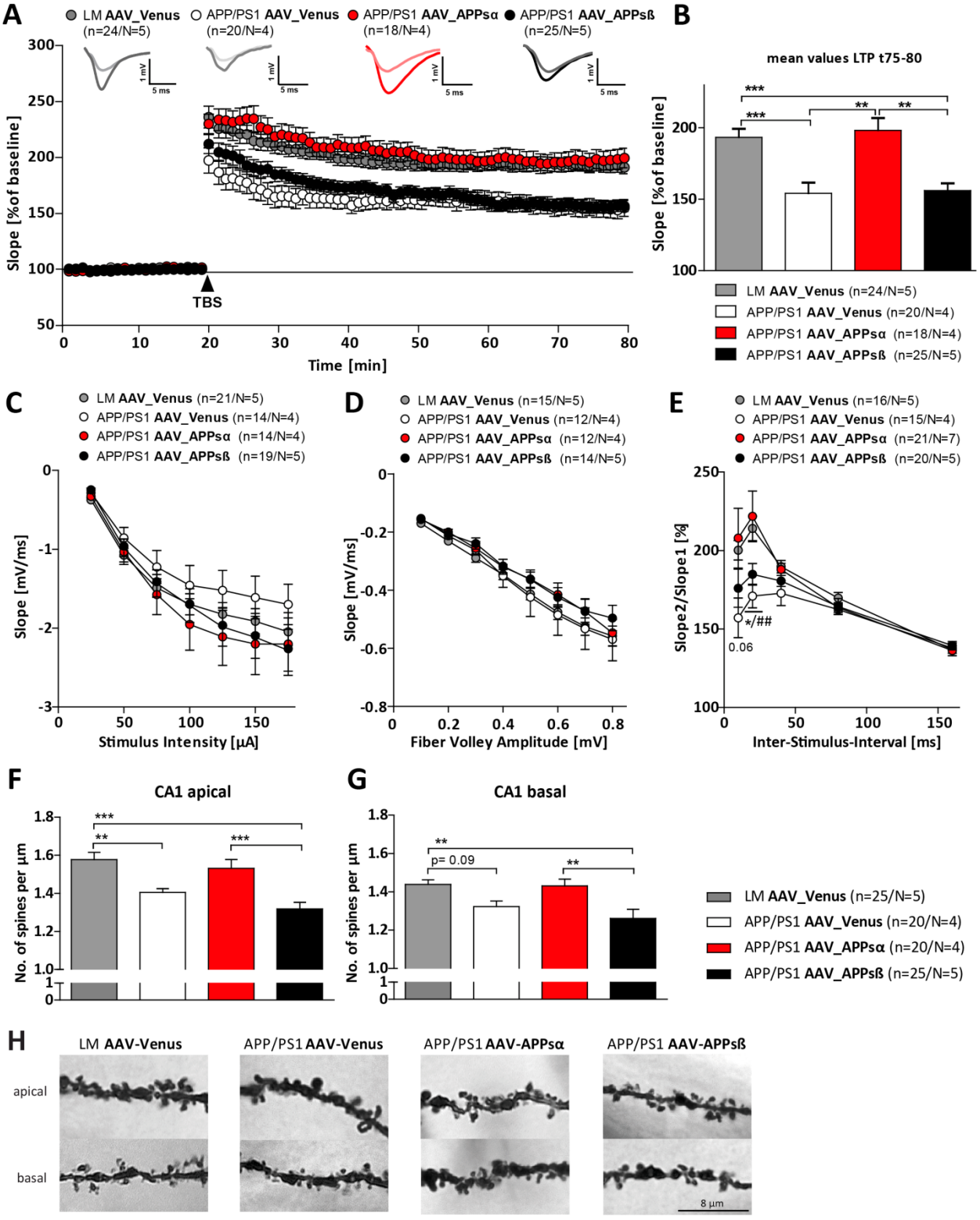

Figure 3.12 (previous page): Only APPsα, but not APPsβ overexpression rescues impaired synaptic plasticity and spine density in APP/PS1ΔE9 tg mice. (A, B) Activity-dependent synaptic plasticity induced by TBS (arrowhaed) at the hippocampal Schaffer collateral CA1 pathway after 20 min baseline recording is shown as percentage % of mean baseline slope (n= number of slices, N= number of animals, representative traces shown for each group before and after TBS). Only acute slices of APP/PS1ΔE9 transgenics overexpressing APPsα (red circles) showed significantly elevated LTP induction and maintenance like littermate controls (LM, grey circles), quantified for the last five minutes of LTP in (B) (LM-Venus: 193.33±5.97% vs. APP/PS1ΔE9-APPsα: 198.25±8.62% ; Tukey´s post-hoc test: p= 0.997). AAV driven APPsβ overexpression in transgenic mice (black circles) failed to increase LTP (156.08 ±5.03%) representing the LTP deficit of Venus expressing APP/PS1ΔE9 transgenics (open circles, 154.0908 ±7.55%) when compared to LM-Venus (p< 0.001) or APP/PS1ΔE9-APPsα (p= 0.003). **(C, D)** Input-Output characteristics assessed by increasing stimulus intensity or adjusting the fiber volley amplitude revealed no alterations between groups. **(E)** The PPF paradigm indicated significantly lowered facilitation towards the second stimulus applied for Venus overexpressing APP/PS1ΔE9 tg (*p= 0.02) when compared to LM controls. Instead of APPsβ, only APPsα overexpression was able to restore that presynaptic impairment ($^{\#\#}$p=0.009). **(F, G)** APP/PS1ΔE9 tg mice injected with Venus or APPsβ revealed a pronounced spine density deficit at CA1 apical (p= 0.008) and basal dendrites (p= 0.001) in comparison to LM controls that is restored by APPsα overexpression (p(basal)= 0.005). **(H)** Detailed segments of 2nd or 3rd order dendritic branches of apical and basal dendrites of CA1 neurons after Golgi–Cox staining scale bar 8 µm.

3.6.3 Effect of AAV-driven APPsβ Expression in Wild-type Littermates

I furthermore proved, if APPsβ overexpression itself may cause alterations in activity-dependent synaptic plasticity or basal synaptic properties in wild-type littermate mice (C57Bl/6JxC3H/HeJ, LM) as so far only the study of Taylor and colleagues 2008 addressed this question recording LTP *in vivo* in the dentate gyrus (DG) of anesthetized rats. However, that study found no evidence that APPsβ when infused into the DG facilitates LTP. Nevertheless, I investigated activity-dependent synaptic plasticity in twelve to thirteen months old littermate mice (LM) four to five months upon AAV injection (10^{10} vg/hippocampus).
To this end, I recorded *f*EPSPs at the Schaffer collateral CA1 pathway at a frequency of 0.1 Hz. Potentiation levels of acute slices of LMs overexpressing APPsβ were indistinguishable in induction and maintenance from that of LMs injected with the control AAV_Venus virus (Figure 3.13A). Finally, TBS induced strengthening of *f*EPSPs resulted in similar potentiation levels for the last 5 minutes of recording (t75-80: LM_AAV-Venus: 193.33 ± 5.96% vs. LM_AAV-APPsβ: 180.84 ± 5.18%, p= 0.13, Students t-test, Figure 3.13B). Analysis of basal synaptic transmission properties revealed no differences in the input-output characteristics upon variation of stimulus intensity (Figure 3.13C) or fiber volley amplitude (3.13D). Moreover, I assessed presynaptic function using the PPF paradigm which revealed that overexpression of APPsβ had no influence on short-term plasticity and didn´t alter presynaptic function (Figure 3.13E).
Additionally, I addressed the consequences of APPsβ overexpression on spine number and investigated mid-apical dendrites of CA1 pyramidal neurons following Golgi-Cox staining (Figure 3.13G). I found a mild reduction in spine density at CA1 apical (1.58 ± 0.04 vs. 1.48 ± 0.02 spines/µm, p= 0.014, Student´s t-test), but not at CA1 basal dendrites upon APPsβ overexpression (Figure 3.13F).
Overall these findings suggest that enhanced APPsβ expression didn´t alter activity-dependent synaptic plasticity at the CA1-CA3 pathway *in vitro*, but that higher amounts of APPsβ in the hippocampus reduced the spine number of CA1 midapical dendrites while basal compartments of pyramidal neurons were unaffected in wild-type mice.

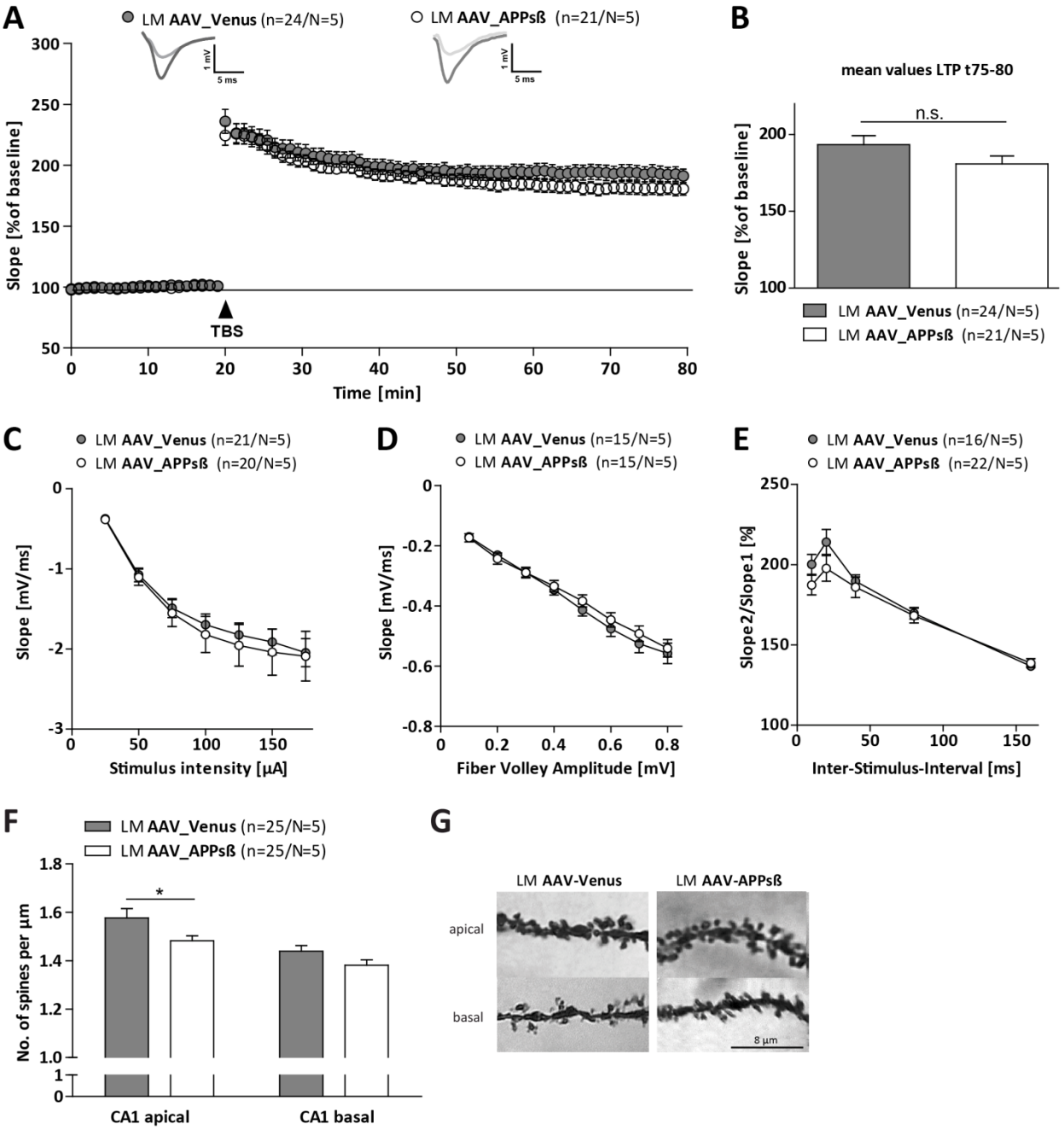

Figure 3.13: Unaltered synaptic plasticity and transmission by APPsβ overexpression in littermates, but slightly reduced spine density. (A, B) Extracellular field recordings at hippocampal CA1-CA3 synapses after TBS stimulation (arrowhead) indicated unaltered induction and maintenance of LTP between LMs overexpressing Venus (grey circles) or APPsβ (open circles). The LTP induction rate is shown as percentage % of mean baseline slope. Data points were averaged over 6 time points and error bars indicate SEM, n= number of recorded slices/N= number of animals. Data were analyzed by one-way ANOVA followed by Turkey´s post-hoc test. Representative insets of original traces at baseline (light color) or following stimulation (dark color**). (C, D)** Neither increased stimulus intensity nor adjusted fiber volley amplitude revealed differences in basal synaptic transmission. **(E)** PPF yielded normal presynaptic function for both groups. **(F)** APPsβ overexpressing LMs revealed significantly less spines at CA1 apical dendrites, while no decrease in spine number is observed for the basal compartment. **(G)** Detailed segments of 2nd or 3rd order dendritic branches of apical and basal dendrites of CA1 neurons after Golgi–Cox staining scale bar 8 µm.

3.7 Disturbed Ca^{2+} Homeostasis in Primary Dissociated Hippocampal Cultures of NexCre cDKO Mice

Neuronal calcium (Ca^{2+}) signaling is important for normal cell function and impairments in Ca^{2+} handling have been implicated in a variety of neurodegenerative disorders including Alzheimer's disease (AD). Alterations in Ca^{2+} homeostasis have been reported within several *in vitro* and *in vivo* studies of mice expressing AD associated transgenes, presenilins (PS) and amyloid precursor protein (APP) (Etcheberrigaray et al., 1998, Stutzmann et al., 2004, Stutzmann et al., 2006, Kuchibhotla et al., 2008). Ca^{2+} signaling activates a series of different intracellular cascades and genes like the calmodulin kinase II (CamKII) and MAP kinase. Moreover, it induces protein modifications that support synaptic function and transmission that are further essential for synaptic plasticity (see chapter 1.2.2). Learning and memory are based on functional synapses and intact synaptic transmission, something that is altered in AD. LTP and LTD are the electrophysiological correlates of learning and memory and have been shown to be impaired in several AD mouse models (Mattson and Chan, 2003, Kuchibhotla et al., 2008, Demuro et al., 2010, Sun et al., 2014, Zhang et al., 2015a) and APP deficient mice (Ring et al., 2007, Weyer et al., 2011, Hick et al., 2015). The APP/APLP2 deficient mouse model generated and characterized by Hick and colleagues (2015) has despite a pronounced LTP deficit strong alterations in short-term plasticity, indicating a possible presynaptic defect and thereby a conceivable Ca^{2+} handling deficit. To investigate if alterations in Ca^{2+} homeostasis might underlie the observed synaptic plasticity defect, I performed quantitative Ca^{2+} Imaging experiments and induced chemical LTP (cLTP) in primary dissociated hippocampal cultures of NexCre cDKO mice. As shown in this thesis that APPsα positively modulated LTP and STP, I performed my experiments following viral transduction of the cultures with either a control virus (AAV-Syn-Venus) or an APPsα overexpressing virus (AAV-syn-APPsα-Venus). To perform quantitative measurements of Ca^{2+} changes, I used the dual-wavelength indicator Fura-2AM and an experimental schedule that allowed me to perform cLTP experiments on a timescale that is comparable to the electrophysiologically induced LTP (eLTP).

To this end I recorded Ca^{2+} signals six days following virus transduction *in vitro* using dissociated hippocampal cultures of NexCre cDKO embryos prepared at embryonic stage 18.5. I examined Ca^{2+} dynamics at baseline activity (t-20 and t-10), representing the baseline of eLTP recordings, and following cLTP induction (t0, t10, t40), being comparable to the initial phase as well as the maintenance of eLTP. As the AAV-vectors contained the synapsin promotor, expression of the encoded fluorescent protein Venus or APPsα-Venus was restricted to neurons (Fol et al., 2016) and only cells that revealed expression of the fluorescent protein were included in the analysis. I depicted the Ca^{2+} imaging results obtained in the analysis in two different ways to facilitate reviewing of the data. The graph in Figure 3.14A illustrates the results of littermate controls (APLP2-KO+AAV-syn-Venus= black bars; APLP2-KO+AAV-syn-APPsα-Venus= black and white dotted) and NexCre cDKO cultures (APP/APLP2 cDKO+AAV-syn-Venus= red bars; APP/APLP2 cDKO+AAV-syn-APPsα-Venus) separately for the treatment, whereas the graph in Figure 3.14A' illustrates every time-point recorded during imaging while all genotypes were compared.

Littermate cultures that received the AAV-syn-Venus control virus (black bars) showed a significant and robust increase in cytosolic Ca^{2+} when cLTP was induced by glycine (gly) application, while endogenous glycine receptors were blocked with strychnine (str) ($p(t0)< 0.001$, $p(t10)< 0.01$, $p(t40)< 0.01$, one-way ANOVA). Nearly the same result was detected in littermates transduced with the AAV virus overexpressing APPsα beside that Ca^{2+} levels upon gly+str stimulation were not significantly elevated at

t40 when comparing Ca^{2+} concentrations at rest and upon cLTP induction (Figure 3.14A). However, NexCre cDKO cultures treated with the control virus showed a significant increase in cytosolic Ca^{2+}, indicating that they were able to induce and maintain cLTP but to a lower extent with regard to the amount of Ca^{2+} and which was only significantly elevated for time-points t0 and t10 following chemical stimulation (Figure 3.14A). AAV driven APPsα overexpression in NexCre cDKOs increased Ca^{2+} levels at rest, but resulted only in a significant increase upon cLTP induction at t0. The differences in cytosolic Ca^{2+} amount became more obvious when comparing the genotypes at the different imaging time-points (Figure 3.14A´). NexCre cDKO cultures with AAV-syn-Venus revealed significantly lower Ca^{2+} levels at baseline actvity (t-10, $p< 0.01$) when compared to LMs+AAV-syn-APPsα-Venus and upon induction of cLTP ($p(t0)< 0.01$ in comparison to LMs+AAV-syn-APPsα-Venus, $p(t0)< 0.05$ compared to NexCre cDKO+ AAV-syn-APPsα-Venus; $p(t10)< 0.05$ compared to LMs+AAV-syn-Venus; $p(t40)< 0.01$ compared to LMs+AAV-syn-Venus and LMs+AAV-syn-APPsα-Venus; one-way ANOVA). Depicting only the control situation (Figure 3.14B), meaning littermate and NexCre cDKO cultures that were transduced with the AAV-syn-Venus virus, identified a significant reduction in basal Ca^{2+} levels in NexCre cDKOs ($p(t-20)= 0.01$, $p(t-10)= 0.01$, Student´s t-test). The lowered Ca^{2+} levels at time-points of spontaneous activity were sustained upon glycine administration at t0 ($p= 0.086$) and significantly at t10 ($p= 0.0047$) and t40 ($p= 0.002$). Separately comparing Ca^{2+} levels of NexCre cDKO cultures that received either the AAV-syn-Venus or APPsα overexpressing virus (Figure 3.14B´), I could demonstrate that APPsα first of all restored Ca^{2+} levels at baseline activity ($p(t-20)= 0.0097$, $p(t-10)= 0.02$) and moreover that the induction of cLTP by gly+stry administration resulted in significantly increased Ca^{2+} responses at t0 ($p= 0.007$), t40 ($p= 0.007$) and by trend at t10 ($p= 0.069$). Based on these results two different alterations in Ca^{2+} handling were observed: impaired Ca^{2+} homeostasis in NexCre cDKO mice and impaired cLTP which was rescued after viral APPsα overexpression. As already impaired cytosolic Ca^{2+} levels without any stimulation might contribute to the observed cLTP defect, Ca^{2+} ratios obtained after cLTP induction were normalized to Ca^{2+} levels at baseline activity (Figure 3.14C, C´). Only LM+AAV-syn-Venus cultures revealed a stable and significant increase upon gly+stry stimulation while all other groups showed only significant increases in cytosolic Ca^{2+} at individual time-points following cLTP induction. However, interesting are the results in Figure 3.14C´when normalized Ca^{2+} ratios were compared at the different imaging time-points. These data indicated that the relative change in intracellular Ca^{2+} was almost the same independent of the genotype.

Altogether the results obtained with quantitative Ca^{2+} imaging revealed that NexCre cDKO mice had strongly altered Ca^{2+} homeostasis, while these cultures were able to respond to the same extent to gly+str stimulation with increases in cytosolic Ca^{2+} that were observed in littermates when cLTP responses were normalized to resting Ca^{2+} amounts. I could further underlie the neurotrophic action of APPsα that rescued the Ca^{2+} homeostasis deficit of NexCre cDKO mice and led to cLTP responses observed in control littermates.

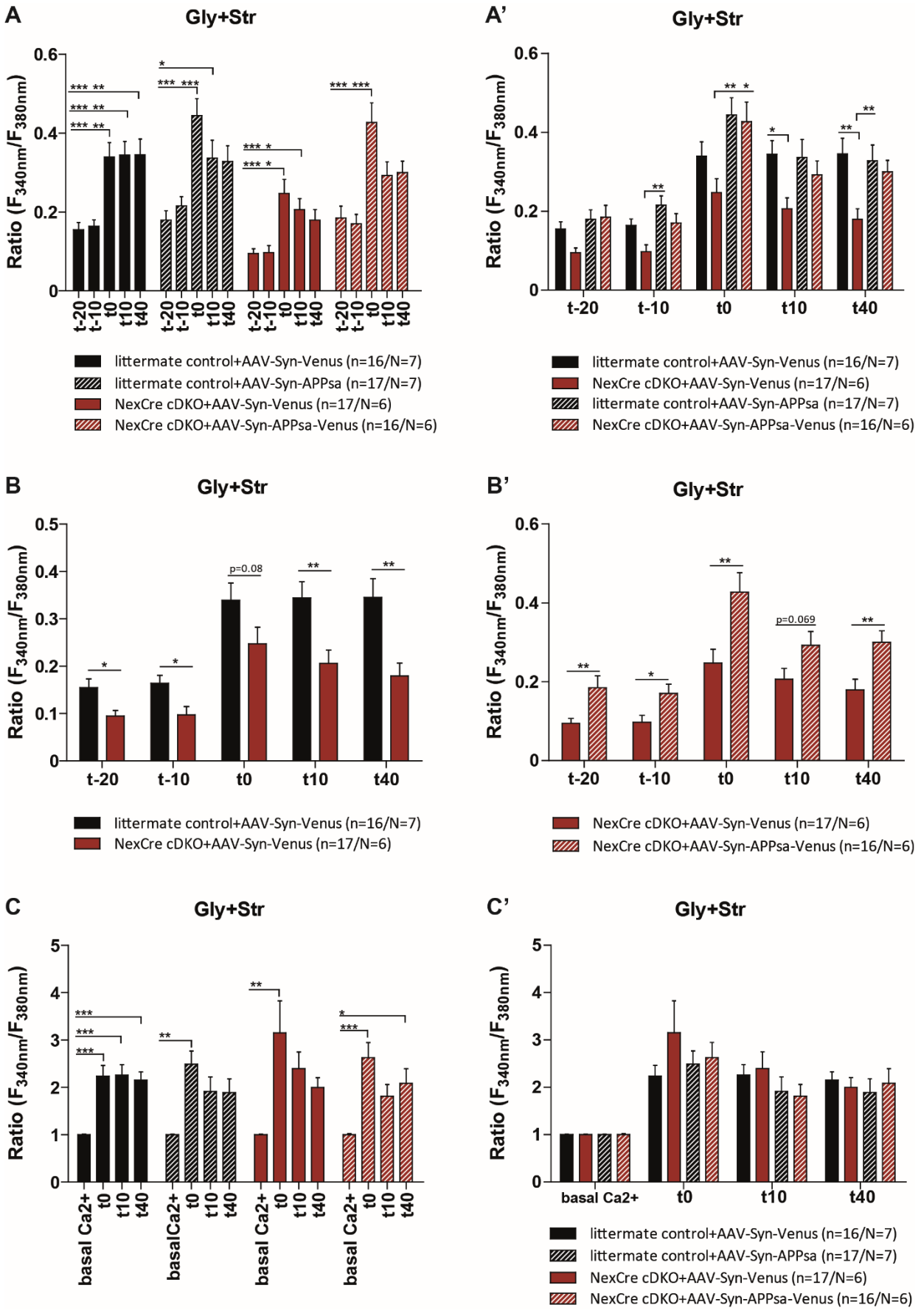
A
Gly+Str
Ratio (F340nm/F380nm)
t-20 t-10 t0 t10 t40
littermate control+AAV-Syn-Venus (n=16/N=7)
littermate control+AAV-Syn-APPsa (n=17/N=7)
NexCre cDKO+AAV-Syn-Venus (n=17/N=6)
NexCre cDKO+AAV-Syn-APPsa-Venus (n=16/N=6)
A'
Gly+Str
littermate control+AAV-Syn-Venus (n=16/N=7)
NexCre cDKO+AAV-Syn-Venus (n=17/N=6)
littermate control+AAV-Syn-APPsa (n=17/N=7)
NexCre cDKO+AAV-Syn-APPsa-Venus (n=16/N=6)
B
Gly+Str
p=0.08
littermate control+AAV-Syn-Venus (n=16/N=7)
NexCre cDKO+AAV-Syn-Venus (n=17/N=6)
B'
Gly+Str
p=0.069
NexCre cDKO+AAV-Syn-Venus (n=17/N=6)
NexCre cDKO+AAV-Syn-APPsa-Venus (n=16/N=6)
C
Gly+Str
basal Ca2+ t0 t10 t40
C'
Gly+Str
basal Ca2+ t0 t10 t40
littermate control+AAV-Syn-Venus (n=16/N=7)
littermate control+AAV-Syn-APPsa (n=17/N=7)
NexCre cDKO+AAV-Syn-Venus (n=17/N=6)
NexCre cDKO+AAV-Syn-APPsa-Venus (n=16/N=6)

Figure 3.14 (previous page): Quantitative Ca^{2+} Imaging uncovered a severe Ca^{2+} homeostasis deficit in NexCre cDKO mice resulting in impaired cLTP, but can be rescued following APPsα overexpression. Imaging time-points t-20 and t-10 mirror Ca^{2+} concentration at basal activity, while t0, t10 and t40 reflect the quantified cytosolic Ca^{2+} amount upon glycine (gly) and strychnine (str) application. **(A)** Upon glycine stimulation littermate controls transduced with AAV-syn-Venus showed a strong increase in cytosolic Ca^{2+} levels, while littermates overexpressing APPsα failed to reach a significant elevation in cytosolic Ca^{2+} at t40. NexCre cDKO cultures treated with the control virus yielded however a significant increase, but to a lower extent. Following APPsα overexpression Ca^{2+} levels were significantly higher. **(A´)** Differences in cytosolic Ca^{2+} became more obvious when comparing genotypes at different imaging time-points. NexCre cDKO cultures revealed significantly lower Ca^{2+} levels at basal activity (t-10) and upon induction of cLTP. **(B)** Depicting only the control situation, meaning both genotypes that were transduced with the AAV-syn-Venus virus, identified a significant reduction of basal Ca^{2+} levels in NexCre cDKOs. The lowered Ca^{2+} levels were sustained upon glycine administration by trend at t0 and significantly at t10 and t40. **(B´)** Illustration of the "rescue" situation (APPsα overexpression in NexCre cDKO cultures) compared to NexCre cDKOs treated with AAV-syn-Venus showed that cytosolic Ca^{2+} at basal conditions and upon cLTP induction were restored, beside a strong tendency at t10. **(C)** Normalized cytosolic Ca^{2+} levels to Ca^{2+} load at rest revealed only for LM+AAV-syn-Venus cultures a stable and significant increase upon gly+stry stimulation while all other groups showed only significant increases in cytosolic Ca^{2+} at individual time-points following cLTP induction. **(C´)** Comparing normalized Ca^{2+} levels between genotypes at single imaging time-points revealed no differences in Ca^{2+} increase following gly+stry stimulation. Significances were plotted as *p < 0.05, **p < 0.01 and ***p < 0.001. Error bars indicate ± SEM, n= number of experiments, N= number of culture preparations.

3.7.1 Disturbed ER Activity in NexCre cDKO Mice Contributes to Impaired cLTP

Neurons have several sources of Ca^{2+} and regulate Ca^{2+} entry by a variety of channels from the extracellular space or by the release of Ca^{2+} from internal stores. Ligand-gated (e.g. NMDA-R), voltage-gated Ca^{2+} (VGCCs or Ca_V) and store-operated Ca^{2+} channels (SOCCs) allow Ca^{2+} entry following depolarization of the membrane, while the main internal Ca^{2+} stores in neurons are located in the endoplasmatic reticulm (ER) (LaFerla, 2002). Cytosolic Ca^{2+} is pumped by the sarco-/endoplasmic reticulum calcium ATPase (SERCA) in the ER Ca^{2+} store. In contrast, the release of Ca^{2+} from the ER can take place by three different ways. First of all, active G-protein coupled receptors on the plasma membrane induce an inositol-1,4,5-trisphosphate (IP_3) dependent activation of IP_3-receptors or second the influx of extracellular Ca^{2+} into the cytosol triggers ryanodine receptors that in turn induce a Ca^{2+} induced Ca^{2+} release (CiCR) from the ER. Lastly, the ER contains leak channels composed of Sec61 core complexes enabling Ca^{2+} the efflux from the ER into the cytosol (Samtleben et al., 2013). Ca^{2+} levels are maintained and relatively low at basal conditions (50 to 300 nM), while upon electrical, synaptic or receptor-activation the amount of Ca^{2+} increases rapidly. Thereby the depletion of ER Ca^{2+} stores initiates the influx of extracellular Ca^{2+} into the cytosol via SOCCs located in the plasma membrane. Hence, accumulated cytosolic Ca^{2+} is replenished and taken up in the ER by the SERCA ATPase. This mechanism is called capacitive Ca^{2+} entry and known to be implicated in the pathogenesis of AD (Leissring et al., 2000, LaFerla, 2002). Knowing that ER Ca^{2+} is mainly implicated in cytosolic Ca^{2+} levels and was imaged within the quantitative approach to investigate if deficits in synaptic plasticity observed in NexCre cDKO mice might be the reason led me to the following experiments: to investigate which role plays the ER Ca^{2+} as source for cytosolic Ca^{2+} entry. Therefore, I blocked the re-uptake of Ca^{2+} via the SERCA ATPase back into the ER by a co-application of cyclopiazonic acid (CPA, 10 µM) during the stimulation of cultures with glycine and strychnine.

Blocking the SERCA-ATPase activity during cLTP induction heavily impaired the maintenance of cLTP in littermates with AAV-syn-Venus and AAV-syn-APPsα-Venus as well as NexCre cDKO transduced with AAV-syn-APPsα-Venus (Figure 3.15A). Following glycine, strychnine and CPA stimulation all three groups revealed only initially a significant increase in cytosolic Ca^{2+} levels at time-point t0 and a decline of the Ca^{2+} amount in the ongoing imaging procedure. In contrast, NexCre cDKO cultures overexpressing Venus showed a highly significant increase in cytosolic Ca^{2+} levels at t0 and t10 and only a decrease at t40, due

to the fact that the reversible CPA blocker was washed out. Even clearer was the picture when comparing the genotypes at the different time-points with each other (Figure 3.15A´). NexCre cDKO cultures transduced with AAV-syn-Venus revealed significant lower cytosolic Ca^{2+} levels at basal activity, but unaltered Ca^{2+} increase following gly+stry stimulation when the SERCA ATPase was blocked pointing towards altered function of the ER loading ATPase. I moreover normalized the Ca^{2+} amounts gained upon stimulation to the Ca^{2+} levels at baseline activity (Figure 3.15B, B´). Like in Figure 3.15A, only an initial increase at t0 was observable in cytosolic Ca^{2+} upon gly+str stimulation when CPA was co-applied in both littermate cultures as well as NexCre cDKOs transduced with APPsα. In contrast, an intense increase was observable in NexCre cDKO cultures overexpressing Venus at initial time-points after cLTP induction (t0 and t10), which was not maintained till t40. The comparison of normalized Ca^{2+} levels between genotypes at single imaging time-points demonstrated the powerful increase in cytosolic Ca^{2+} in NexCre cDKO+AAV-syn-Venus following gly+stry+CPA stimulation at t0, t10 and t40 in contrast to the other groups. Lastly, I illustrated the data obtained in NexCre cDKO mice following glycine and strychnine stimulation and of the APP/APLP2 deficient mice upon additional application of CPA (Figure 3.15C, C´). While cytosolic Ca^{2+} levels at baseline actvity were altered in NexCre cDKO mice transduced with AAV-syn-Venus and rescued upon APPsα overexpression, only the glycine and strychnine stimulation resulted in impaired cLTP in the Venus treated cDKO cultures while co-administration of CPA elevated cLTP responses to an extent observed in APPsα overexpressing cultures upon glycine and strychnine treatment.

Overall these data indicate that blocking the SERCA-ATPase resulted in highly significant elevated Ca^{2+} levels in NexCre cDKO cultures transduced with AAV-syn-Venus, while this effect was missing in cDKO cultures with APPsα overexpression. In conclusion, it could be assumed that in NexCre cDKO mice the activity of the SERCA-ATPase might be altered. Further, the read-outs on littermate cultures revealed that the SERCA-ATPase activity is essential to maintain cLTP as it was abolished upon CPA co-administration.

Figure 3.15 (next page): Blocking of the ER-SERCA-ATPase elevates cLTP in NexCre cDKO cultures. Imaging time-points t-20 and t-10 mirror Ca^{2+} concentration at rest, while t0, t10 and t40 reflect quantified cytosolic Ca^{2+} amount upon glycine (gly), strychnine (str) and cyclopiazonic acid (CPA) application. **(A)** Blocking the SERCA-ATPase activity during cLTP induction resulted only in a significant increase in cytosolic Ca^{2+} levels in littermates with AAV-syn-Venus and AAV-syn-APPsα-Venus as well as in NexCre cDKOs overexpressing APPsα at t0, while no maintenance of Ca^{2+} level elevation was observable. In contrast, NexCre cDKO mice transduced with AAV-syn-Venus showed a highly significant increase in cytosolic Ca^{2+} levels at t0 and t10 and only a decrease at t40. **(A´)** NexCre cDKO cultures overexpressing Venus revealed significant lower cytosolic Ca2+ levels at rest, but unaltered Ca2+ increase following gly+stry stimulation when the SERCA ATPase was blocked. **(B)** Normalized cytosolic Ca^{2+} levels to Ca^{2+} load at rest yielded only an initial increase (t0) in cytosolic Ca^{2+} upon gly+str stimulation when CPA was co-applied in both littermate cultures and NexCre cDKOs transduced with APPsα. In contrast, an intense increase was observable in NexCre cDKO cultures over-expressing Venus at t0 and t10, which was not maintained till t40. **(B´)** Comparing normalized Ca^{2+} levels between genotypes at single imaging time-points demonstrated the powerful Ca^{2+} increase in NexCre cDKO+AAV-syn-Venus following gly+stry+CPA stimulation at t0, t10 and t40. **(C, C´)** Ca^{2+} ratios obtained with gly+ str (red) and with gly+str+CPA (green) stimulation. While Ca^{2+} levels at rest were altered in NexCre cDKO mice transduced with AAV-syn-Venus and rescued upon APPsα overexpression, only the gly+stry stimulation resulted in impaired cLTP in the Venus treated cDKO cultures while CPA co-application elevated cLTP responses to an extent observed in APPsα overexpressing cultures. Significances were plotted as *p < 0.05, **p < 0.01 and ***p < 0.001. Error bars indicate ± SEM, n= number of experiments, N= number of culture preparations.

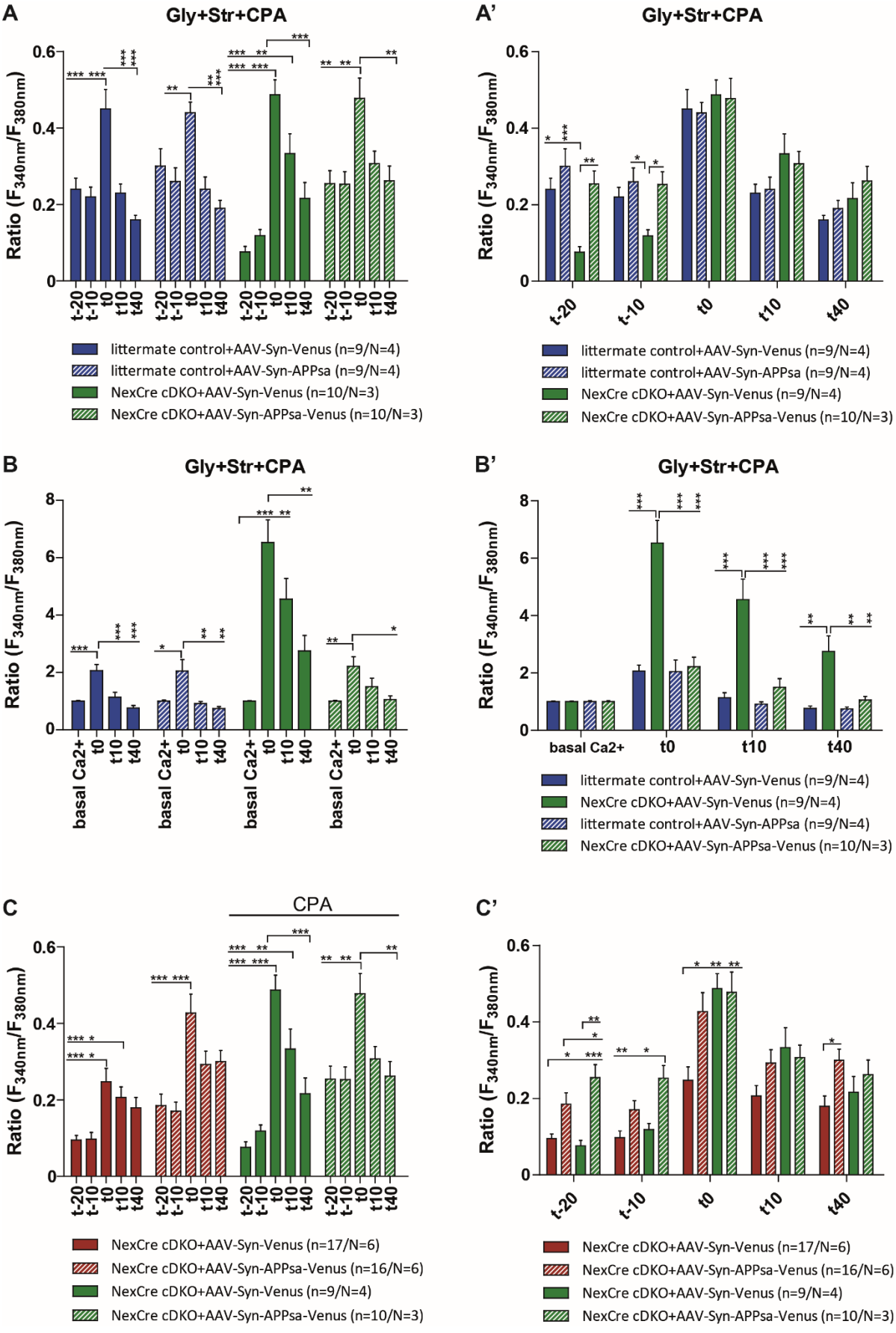
A
Gly+Str+CPA
Ratio (F340nm/F380nm)
littermate control+AAV-Syn-Venus (n=9/N=4)
littermate control+AAV-Syn-APPsa (n=9/N=4)
NexCre cDKO+AAV-Syn-Venus (n=10/N=3)
NexCre cDKO+AAV-Syn-APPsa-Venus (n=10/N=3)
A'
Gly+Str+CPA
littermate control+AAV-Syn-Venus (n=9/N=4)
littermate control+AAV-Syn-APPsa (n=9/N=4)
NexCre cDKO+AAV-Syn-Venus (n=9/N=4)
NexCre cDKO+AAV-Syn-APPsa-Venus (n=10/N=3)
B
Gly+Str+CPA
basal Ca2+
B'
Gly+Str+CPA
littermate control+AAV-Syn-Venus (n=9/N=4)
NexCre cDKO+AAV-Syn-Venus (n=9/N=4)
littermate control+AAV-Syn-APPsa (n=9/N=4)
NexCre cDKO+AAV-Syn-APPsa-Venus (n=10/N=3)
C
CPA
NexCre cDKO+AAV-Syn-Venus (n=17/N=6)
NexCre cDKO+AAV-Syn-APPsa-Venus (n=16/N=6)
NexCre cDKO+AAV-Syn-Venus (n=9/N=4)
NexCre cDKO+AAV-Syn-APPsa-Venus (n=10/N=3)
C'
NexCre cDKO+AAV-Syn-Venus (n=17/N=6)
NexCre cDKO+AAV-Syn-APPsa-Venus (n=16/N=6)
NexCre cDKO+AAV-Syn-Venus (n=9/N=4)
NexCre cDKO+AAV-Syn-APPsa-Venus (n=10/N=3)

3.7.2 Unaltered Ca^{2+} Signal Frequency in NexCre cDKO Mice

Beside the investigation of quantitative changes of cytosolic Ca^{2+} levels, the frequencies of the Ca^{2+} signals occurring at the individual time-points were proven to be altered. Therefore, I plotted the frequency of spontaneous activity per minute again separately for each genotype over time or the Ca^{2+} signals of each genotypes per imaging time-point upon glycine (gly), strychnine (str) stimulation only or additional CPA administration (Figure 3.16).

Upon gly+str stimulation all groups showed a significant reduction in Ca^{2+} frequency elevation when comparing the frequency of the spontaneous Ca^{2+} increase at rest (t-20, t-10) and following cLTP induction (t0, t10, t40, Figure 3.16A), indicating a synchronization of the network. Moreover, the Ca^{2+} signals quantified at the different imaging time-points were not different between analyzed groups (Figure 3.16A´), supporting that impaired Ca^{2+} homeostasis and cLTP in NexCre cDKO cultures transduced with AAV-syn-Venus were not caused by altered Ca^{2+} signal frequency. When I co-applied CPA with gly+str to induce cLTP while blocking the SERCA ATPase, I observed that the frequency of Ca^{2+} events was only initially (t0) reduced in both littermate cultures, while the frequency increased for t10 and t40, an effect which was also seen for NexCre cDKOs transduced with AAV-syn-APPsα-Venus (Figure 3.16B). In contrast, NexCre cDKO mice solely expressing Venus showed a significant reduction in Ca^{2+} signal frequency upon gly+str+CPA stimulation. When further comparing the Ca^{2+} signal frequency between genotypes at single imaging time-points no alterations between groups were detected (Figure 3.16B´). All in all, the results using gly+stry+CPA stimulation revealed that ER Ca^{2+} is necessary to maintain cLTP (Figure 3.15) and to synchronize the network (Figure 3.16), while blocking of the SERCA ATPase significantly enhanced Ca^{2+} responses upon stimulation (Figure 3.15) without affecting Ca^{2+} signal frequency (Figure 3.16).

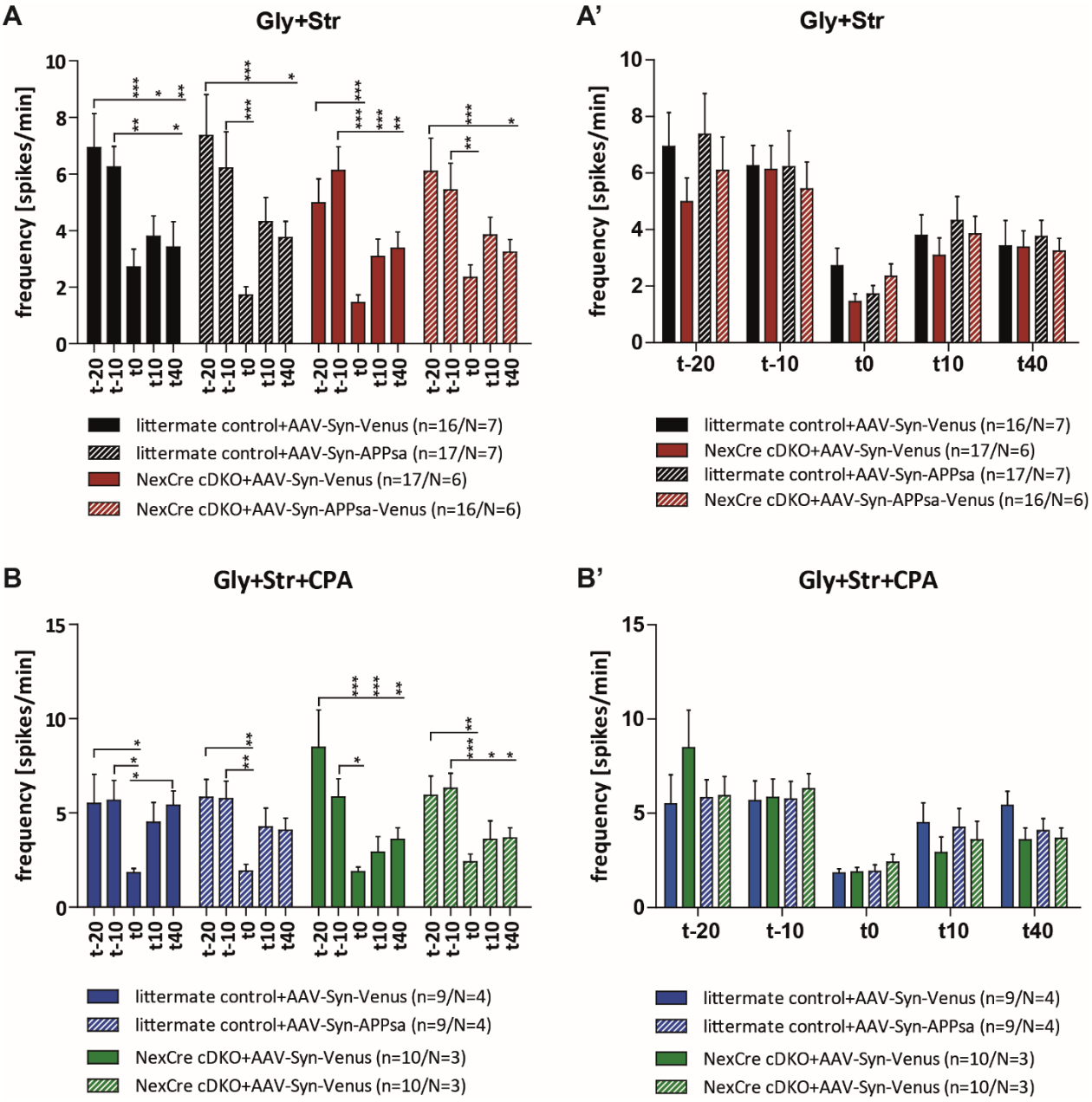

Figure 3.16: Unaltered Ca^{2+} signal frequency in NexCre cDKO mice upon cLTP induction with glycine and strychnine and when CPA is co-applied. Imaging time-points t-20 and t-10 reflect the frequency in number of spikes/min at basal Ca^{2+} concentration. t0, t10 and t40 depict the quantification of spikes/min upon glycine (gly), strychnine (str) stimulation only or additional CPA administration. **(A)** All groups showed a significant reduction in Ca^{2+} signal frequency upon gly+str stimulation. **(A´)** Comparing the Ca^{2+} signal frequency between genotypes at single imaging time-points revealed no alterations. **(B)** Upon co-administration of CPA to gly+stry the frequency of Ca^{2+} events was only initially (t0) reduced in littermates, while the frequency increased for t10 and t40 also for NexCre cDKO transduced with AAV-syn-APPsα-Venus. NexCre cDKO mice solely expressing Venus showed a significant reduction in Ca^{2+} signal frequency upon gly+str+CPA stimulation. **(B´)** The comparison of Ca^{2+} signal frequency between genotypes at single time-points revealed no alterations between groups. Significances were plotted as *p < 0.05, **p < 0.01 and ***p < 0.001. Error bars indicate ± SEM, n= number of experiments, N= number of culture preparations.

3.7.3 Spontaneous Ca^{2+} Dynamics in NexCre cDKO Cultures

As mentioned in chapter 3.7.1. the influx of Ca^{2+} is mediated by Ca^{2+}-permeable ion channels like voltage-gated Ca^{2+} channels (VGCCs) or ionotropic glutamate receptors upon neuronal activation (LaFerla, 2002). Moreover, the cytosolic Ca^{2+} concentration is regulated by the SERCA ATPase, pumping Ca^{2+} into the ER and thereby maintaining cytosolic Ca^{2+} levels. However, the ER contains also Ca^{2+} leakage channels (Sec61) leading to a passive efflux of Ca^{2+} from the ER into the cytosol (Lang et al., 2011, Schäuble et al., 2012). The depletion of ER Ca^{2+} stores initiates the influx of extracellular Ca^{2+} into the cytosol via SOCCs located in the plasma membrane. The study of Samtleben et al., (2015) showed that leaking Ca^{2+} from the ER is not taken up by the ER again but instead leaves the cell across the plasma membrane. The resulting loss of ER Ca^{2+} was shown to be compensated by a continuous Ca^{2+} influx at rest by activation of receptors with SOCC-like properties (Samtleben et al., 2015) like the ones activated upon ER store depletion. As the mechanism of capacitive Ca^{2+} entry is implicated in the pathogenesis of AD (Leissring et al., 2000, LaFerla, 2002) and has an important role at basal Ca^{2+} conditions I designed an experimental setup to investigate spontaneous Ca^{2+} activity without stimulation and to get insights into the function of SOCC channels (see Figure 3.17A). Therefore, I adapted the experimental time periods of my setup according to the publication of Samtleben et al., 2015.

Following twenty minutes of adaptation of the cultures to the chamber conditions, I took one image of spontaneous Ca^{2+} activity of the cells, where NexCre cDKO cultures transduced with AAV-syn-Venus revealed lower basal Ca^{2+} levels in comparison to APP/APLP2 deficient ones overexpressing APPsα (Figure 3.17B´). Afterwards I reduced the external Ca^{2+} amount in the perfusion media from 3.8 to 1.3 mM and acquired images after ten minutes (Figure 3.17A). While only a small decline in the alterations of cytoplasmic Ca^{2+} levels at spontaneous activity was observable in NexCre cDKOs treated with AAV-Venus, a clearer effect was seen in cultures with AAV-syn-APPsα-Venus (Figure 3.17B). When moreover comparing both groups following reduction of external Ca^{2+}, NexCre cDKO+AAV-syn-APPsα-Venus revealed by trend a higher change in cytosolic Ca^{2+} levels at spontaneous activity (Figure 3.17B´). Next, I switched the perfusion media back to 3.8 mM Ca^{2+} and observed the recovery of cytosolic Ca^{2+} five minutes later (Figure 3.17A). The re-addition of external Ca^{2+} led only to a small increase in the change of cytosolic Ca^{2+} levels at spontaneous activity in NexCre+AAV-syn-Venus cultures, but to a significant elevation in cDKOs transduced with AAV-syn-APPsα-Venus (Figure 3.17B, B´). Interestingly, the ratios obtained for NexCre cDKO+AAV-syn-Venus cultures were 0.17 before and 0.12 after the re-addition of Ca^{2+}, while in NexCre cDKO+AAV-syn-APPsα-Venus the ratios were 0.20 before and 0.23 after Ca^{2+} re-addition. These data indicate that under control conditions alterations in cytosolic Ca^{2+} levels at spontaneous activity were not completely restored in NexCre cDKOs, while upon APPsα overexpression cells got more sensitive to external Ca^{2+} and yielded higher changes in Ca^{2+} levels when cells were spontaneous active. To examine then the contribution of ER Ca^{2+} stores in the cultures, ER stores were depleted by co-administration of the SERCA-ATPase blocker CPA (10 µM) while cells were perfused with HBSS containing low Ca^{2+} (1.3 mM) (Figure 3.17A). Monitoring spontaneous Ca^{2+} signals at these conditions revealed reduced alterations in cytosolic Ca^{2+} levels in both groups at spontaneous cell activity with slightly higher ratios in NexCre cDKOs overexpressing APPsα (Figure 3.17B, B´). Afterwards, I monitored the SOCC dependent Ca^{2+} entry by looking at spontaneous Ca^{2+} signals evoked by restoration of external Ca^{2+} when the SERCA ATPase of the ER is moreover blocked (Figure 3.17A) (Parekh and Putney, 2005, Linde et al., 2011). The observation of the SOCC dependent Ca^{2+} entry revealed only an elevation of cytosolic Ca^{2+} levels in NexCre cDKOs transduced with AAV-syn-APPsα-Venus cultures at

times of spontaneous activity, while cDKOs treated with the control virus failed to show a change in Ca^{2+} levels when cells were spontaneous active (Figure 3.17B,B´). In contrast, NexCre+AAV-syn-Venus cultures exhibited even a small decline in Ca^{2+} levels detected at spontaneous activity indicating that the SOCC-dependent Ca^{2+} entry might be impaired in NexCre cDKO cultures (Figure 3.17B).

As under basal conditions, where no stimulation of cells occurred, also voltage-gated Ca^{2+} channels (VGCCs) contribute to the influx of external Ca^{2+} across the plasma membrane, I performed the same set of experiments while blocking these Ca^{2+} channels using 10 µM Nifedipine (Figure 3.17C). First of all, NexCre cDKOs transduced with the control or APPsα overexpressing virus revealed a decrease in the alterations of cytosolic Ca^{2+} levels at spontaneous activity after lowering the amount of external Ca^{2+} from 3.8 to 1.3 mM (Figure 3.17D, D´). In contrast to the series performed without the VGCCs blocker, now also NexCre cDKOs treated with AAV-syn-APPsα-Venus showed only a partial elevation in the change of cytosolic Ca^{2+} levels at spontaneous activity, when external Ca^{2+} was re-added, indicating that APPsα might rescue basal Ca^{2+} levels by enhancing VGCCs function. Next of all, I monitored the contribution of SOCCs to basal Ca^{2+} amounts after depleting ER Ca^{2+} stores with the SERCA ATPase blocker CPA (Figure 3.17C). I observed impaired uptake of external Ca^{2+} for both groups when cells were spontaneously active and when VGCCs and ER Ca^{2+} stores were blocked, but external Ca^{2+} in the perfusion media was re-stored.

Overall these data indicate that NexCre cDKOs cultures might have impairments in SOCC-dependent Ca^{2+} entry and that APPsα seems to exert its trophic action at rest by enhancing the influx of external Ca^{2+} via VGCCs.

Figure 3.17 (next page): Altered Ca^{2+} dynamic in NexCre cDKO cultures at basal conditions. (A) Experimental setup to quantify spontaneous Ca^{2+} activity (t1) and following reduction of the external Ca^{2+} amount to 1.3 mM (t2). Next Ca^{2+} was re-added and the recovery of Ca^{2+} signals observed (t3). Then, external Ca^{2+} was lowered to 1.3 mM and additionally ER Ca^{2+} depleted by CPA administration (t4). The subsequent restoration of external Ca^{2+} to 3.8 mM, while the SERCA-ATPase was blocked, monitored then the SOCC mediated Ca^{2+} influx into the cytosol (t5). **(B)** Small decline in the change of cytosolic Ca^{2+} levels at spontaneous activity in NexCre cDKOs+AAV-syn-Venus upon reduction of external Ca^{2+} that was only partial restored when external Ca^{2+} was increased to 3.8 mM. SOCC-dependent Ca^{2+} entry was not observable in NexCre cDKOs transduced with the control virus. APPsα treated cDKO cultures revealed a decrease in the alterations of cytosolic Ca^{2+} levels at spontaneous activity following reduction of external Ca^{2+} and full recovery of relative Ca^{2+} amounts when external Ca^{2+} was re-stored. Small, but detectable SOCC-dependent Ca^{2+} entry in NexCre cDKOs+AAV-syn-APPsα-Venus cultures at spontaneous cell activity. **(B´)** Significantly lower basal Ca^{2+} levels in NexCre cDKOs transduced with AAV-Venus at spontaneous cell activity and by trend upon lowering of external Ca^{2+} to 1.3 mM. Significant smaller change in cytosolic Ca^{2+} levels in NexCre cDKOs+AAV-Venus cultures at spontaneous activity after external Ca^{2+} re-storation and when the SOCC-dependent Ca^{2+} entry was monitored. **(C)** Same experimental setup like shown in (A) beside that additional VGCCs were blocked for the whole imaging time by application of 10 µM Nifedipine. **(D)** Significant reduction in the alteration of cytosolic Ca^{2+} levels at spontaneous activity upon reduction of external Ca^{2+} to 1.3 mM and only partial recovery when the external Ca^{2+} amount was restored in both groups. No SOCC-dependent Ca^{2+} entry when VGCCs are blocked in both cultures. **(D´)** Unaltered Fura2-AM/Ca^{2+} ratios at spontaneous cell activity between groups when VGCCs were blocked additionally. Significances were plotted as *$p < 0.05$, **$p < 0.01$ and ***$p < 0.001$. Error bars indicate ± SEM, n= number of experiments, N= number of culture preparations.

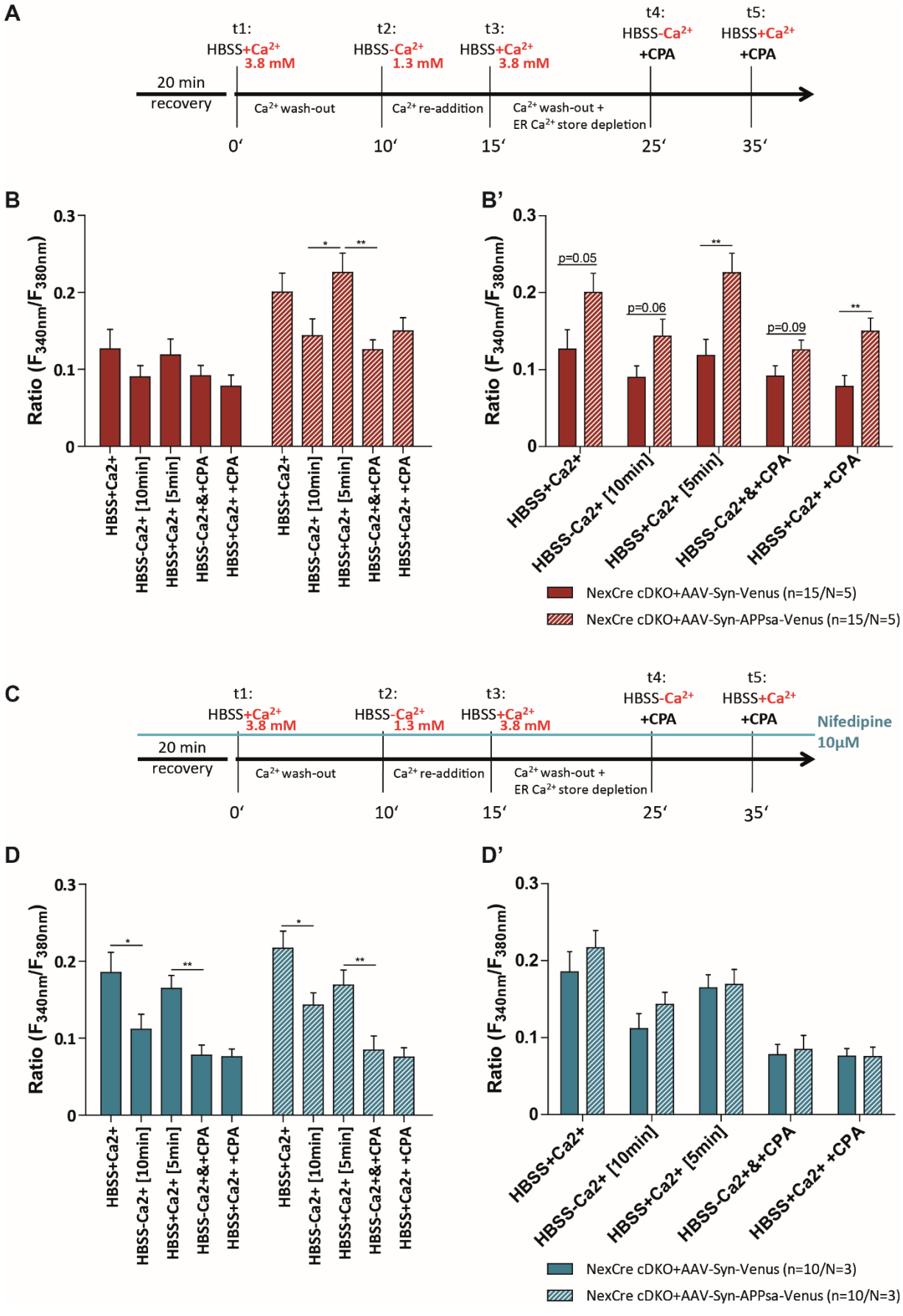
A
t1:
HBSS+Ca2+
3.8 mM
t2:
HBSS-Ca2+
1.3 mM
t3:
HBSS+Ca2+
3.8 mM
t4:
HBSS-Ca2+
+CPA
t5:
HBSS+Ca2+
+CPA
20 min
recovery
Ca2+ wash-out
Ca2+ re-addition
Ca2+ wash-out +
ER Ca2+ store depletion
0'
10'
15'
25'
35'
B
B'
Ratio (F340nm/F380nm)
HBSS+Ca2+
HBSS-Ca2+ [10min]
HBSS+Ca2+ [5min]
HBSS-Ca2+&+CPA
HBSS+Ca2+ +CPA
p=0.05
p=0.06
p=0.09
NexCre cDKO+AAV-Syn-Venus (n=15/N=5)
NexCre cDKO+AAV-Syn-APPsa-Venus (n=15/N=5)
C
Nifedipine
10µM
D
D'
NexCre cDKO+AAV-Syn-Venus (n=10/N=3)
NexCre cDKO+AAV-Syn-APPsa-Venus (n=10/N=3)

3.7.4 External Ca^{2+} Modulates Spontaneous Ca^{2+} Frequency

The experimental set-up used to investigate Ca^{2+} handling at basal activity, where no stimulation occurred, and to examine SOCC function in NexCre cDKOs provided me further the possibility to analyze the number of spontaneous Ca^{2+} spikes which occurred at the different experimental conditions as well as between groups at the different imaging time-points.

The reduction of external Ca^{2+} from 3.8 mM to 1.3 mM significantly elevates the frequency of spontaneous Ca^{2+} spikes within the constant kept imaging duration per time-point (Figure 3.18A, B). This increase in spontaneous Ca^{2+} spikes per minute detected for both NexCre cDKOs cultures was independent of the transduced virus and decreased to the same spike number when external Ca^{2+} was re-stored (Figure 3.18B, B´). The same effect was observed when ER Ca^{2+} stores were emptied at low external Ca^{2+} conditions and after the re-addition of Ca^{2+} amounts from 1.3 to 3.8 mM (Figure 3.18A, B, B´).

When I moreover applied during the imaging session the VGCC blocker Nifedipine (10 µM), I noticed the same behavior of NexCre cDKO cultures, that showed increased spontaneous Ca^{2+} frequencies at imaging time-points with low external Ca^{2+} (1.3 mM) in contrast to conditions with normal, 3.8 mM, Ca^{2+} (Figure 3.18D, D´). There was only one time-point during the experimental setup where NexCre cDKOs transduced with AAV-syn-APPsα-Venus revealed a significantly higher spontaneous Ca^{2+} signal frequency when compared to cultures that received the control virus (p= 0.03), while at all other imaging time-points no significant differences were found between both groups. Maybe the increased spontaneous Ca^{2+} signal frequency affected the SOCC dependent Ca^{2+} entry when VGCCS were blocked as no alterations in number of spontaneous spikes per minute were detected without Nifedipine application between groups (Figure 3.18B´, D´).

Taken together, these results indicated that beside the one alteration found at the imaging time-point to monitor SOCC-dependent Ca^{2+} entry when VGCCS were blocked, the number of spontaneous Ca^{2+} spikes per minute was not altered between genotypes and did thus not influence the amplitude of spontaneous cytosolic Ca^{2+} levels at rest.

Figure 3.18 (next page): External Ca^{2+} modulates spontaneous Ca^{2+} frequency without stimulation in NexCre cDKOs. (A) Experimental setup to quantify spontaneous Ca^{2+} activity (t1) and following lowering the external Ca^{2+} amount to 1.3 mM (t2). Next, Ca^{2+} was re-added and the recovery of Ca^{2+} signals observed (t3). Afterwards, external Ca^{2+} was lowered to 1.3 mM and additional ER Ca^{2+} was depleted by CPA administration (t4). The subsequent restoration of external Ca^{2+} to 3.8 mM while the SERCA-ATPase was blocked monitored then the SOCC mediated Ca^{2+} influx into the cytosol (t5). **(B)** Reducing external Ca^{2+} from 3.8 mM to 1.3 mM significantly elevates the frequency of spontaneous Ca^{2+} spikes within constant kept imaging duration per time-point independently of SERCA ATPase blocking. **(B´)** Unaltered spontaneous Ca^{2+} signal frequency between groups at individual imaging time-points. **(C)** Same experimental setup like shown in (A) beside that additional VGCCs were blocked for the whole imaging time by application of 10 µM Nifedipine. **(D)** Significant elevation in spontaneous Ca^{2+} signal frequency upon reduction of external Ca^{2+} to 1.3 mM that is reduced to basal conditions when the Ca^{2+} amount was restored. **(D´)** Significant increased spontaneous Ca^{2+} signal frequency in NexCre cDKO+AAV-syn-APPsα-Venus when monitoring SOCC-dependent Ca^{2+} entry while at all other imaging time-point the number of spikes per minute were not different between groups. Significances were plotted as *$p < 0.05$, **$p < 0.01$ and ***$p < 0.001$. Error bars indicate ± SEM, n= number of experiments, N= number of culture preparations.

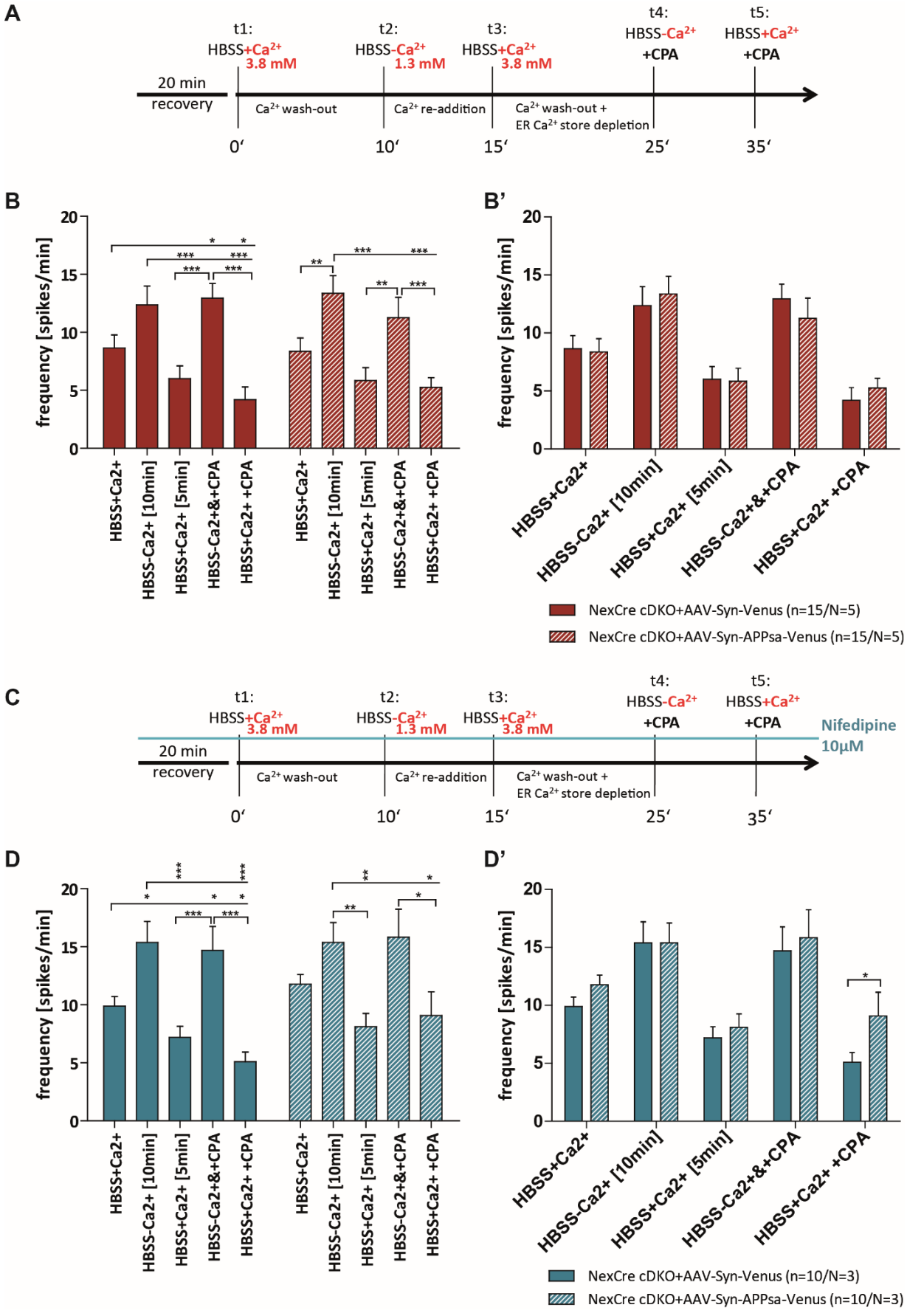
A
t1:
HBSS+Ca2+
3.8 mM
t2:
HBSS-Ca2+
1.3 mM
t3:
HBSS+Ca2+
3.8 mM
t4:
HBSS-Ca2+
+CPA
t5:
HBSS+Ca2+
+CPA
20 min
recovery
Ca2+ wash-out
Ca2+ re-addition
Ca2+ wash-out +
ER Ca2+ store depletion
0'
10'
15'
25'
35'
B
B'
frequency [spikes/min]
HBSS+Ca2+
HBSS-Ca2+ [10min]
HBSS+Ca2+ [5min]
HBSS-Ca2+&+CPA
HBSS+Ca2+ +CPA
NexCre cDKO+AAV-Syn-Venus (n=15/N=5)
NexCre cDKO+AAV-Syn-APPsa-Venus (n=15/N=5)
C
Nifedipine
10µM
D
D'
NexCre cDKO+AAV-Syn-Venus (n=10/N=3)
NexCre cDKO+AAV-Syn-APPsa-Venus (n=10/N=3)

3.7.5 APPsα Expression Rescues Spine Density in NexCre cDKO Cultures

Spines build the active postsynaptic part of the synapse changing in number and shape during synaptic plasticity as they are single compartmentalized units (Engert and Bonhoeffer, 1999, Holtmaat and Svoboda, 2009, Ho et al., 2011). Thus fewer and less functional spines might cause reductions in synaptic activity as the neuronal network is kept in a more immature state which might further be visible in altered Ca^{2+} responses. Importantly Hick and colleagues (2015) described reduced spine numbers with a shift from mature mushroom spines towards immature stubby ones in NexCre cDKO hippocampal CA1 neurons. Impaired spine density might therefore be linked to altered Ca^{2+} handling upon conditional APP and APLP2 deletion, while APPsα was shown to ameliorate spine numbers in APP/PS1ΔE9 tg mice (chapter 3.6). To this end I examined spine numbers in dissociated hippocampal cultures of littermate and NexCre cDKO mice transduced with the control AAV-syn-Venus or AAV-syn-APPsα-Venus virus after transfection of single cells with the fluorescent protein mApple.

Consistently to the report of Hick and colleagues, hippocampal dendrites of NexCre cDKO cultures revealed significantly fewer spines per µm dendrite when compared to littermate controls overexpressing APPsα (p= 0.03, one-way ANOVA followed by Bonferroni´s post-hoc test) and by trend to littermate controls transduced with AAV-syn-Venus (p= 0.053, Figure 3.19B). Strikingly, viral transduction of APPsα rescued spine density in NexCre cDKO cultures (p= 0.024).

Altogether the results indicate that beside a functional modulation of APPsα regarding Ca^{2+} channel function and ER Ca^{2+} stores, also a morphological rescue of spine density might contribute to restored Ca^{2+} handling and synaptic plasticity in NexCre cDKO mice and cultures.

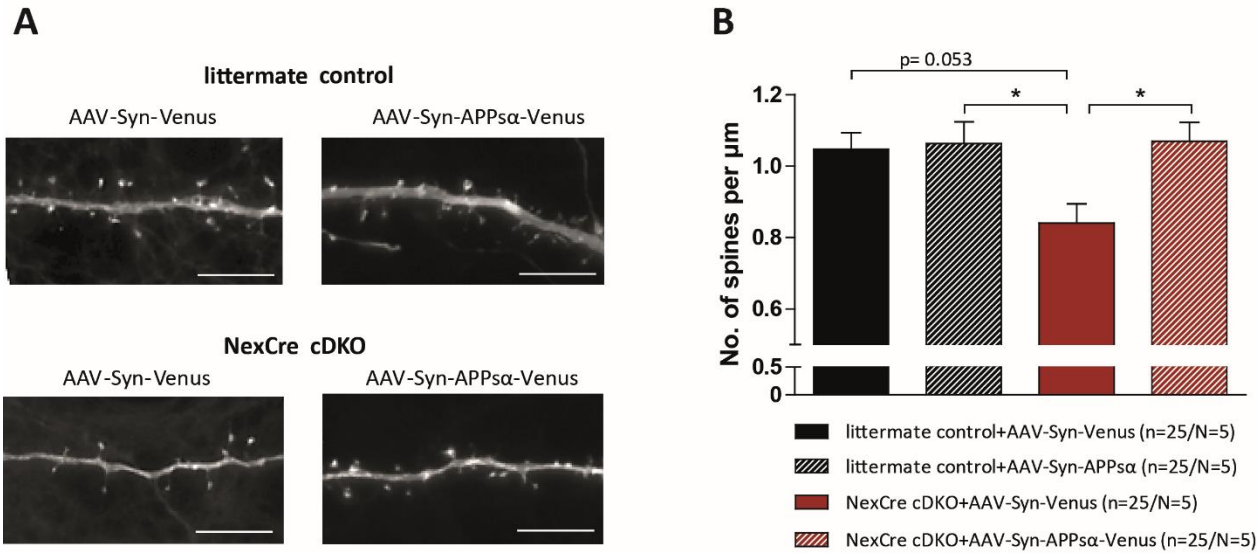

Figure 3.19: APPsα rescues spine density in dissociated hippocampal neurons of NexCre cDKOs. (A) Representative images of 2nd or 3rd order dendritic branches of hippocampal dendrites of CA1 and CA3 neurons transfected with mApple, scale bar 10 µm. **(B)** NexCre cDKO cultures transduced with AAV-syn-Venus had significantly less spines at dendrites in comparison to littermate controls overexpressing APPsα (p= 0.03) and by trend to littermate controls that received AAV-syn-Venus. APPsα overexpression rescued spine density in NexCre cDKO cultures (p= 0.024). N = number of embryonal cultures, n = number of neurons. Data represent mean ± SEM and were analyzed by one-way ANOVA followed by Bonferroni´s post-hoc test.

3.8 The 16 Amino Acid Difference Between APPsα and APPsβ and Its Effect on Synaptic Plasticity

The previous results of this thesis showed that APPsα but not APPsβ was able to rescue severe LTP deficits and short-term plasticity in APP deficient mice (see 3.5) as well as in AD model mice (see 3.6). Moreover, APPsα restored the cLTP defect as well as altered Ca^{2+} homeostasis in NexCre cDKO cultures (see 3.7). This led me to further investigate if the 16 amino acids (Aβ1-16) building the difference between both extracellular released APP peptides, may represent the active neurotrophic domain of APPsα. To investigate the function of Aβ1-16 on activity-dependent synaptic plasticity, the murine peptide was synthesized and acutely applied on hippocampal slices of APP/APLP2 cDKO mice (NexCre cDKO) used already in the AAV overexpression (see 3.5) and Ca^{2+} imaging experiments (see 3.7). The experimental design for the *ex vivo* application of the recombinant peptide was similar to the one Hick and colleagues (2015) used in their study to examine the role of recAPPsα and recAPPsβ on synaptic plasticity. Therefore, I pre-incubated acute hippocampal slices of NexCre cDKO for one hour and applied the peptide or its scrambled control (Aβ1-16 scr) during the whole *f*EPSP recording. The peptide concentration of 10 nM was based on the effective dose of APPsα used in the experiments of Hick and co-workers (2015).

The exogenous application of recAβ1-16 was sufficient to restore the pronounced deficit in induction and maintenance of LTP in NexCre cDKO mice (Figure 3.20A,B) as acute slices of cDKO mice treated with the scrambled inactive version of the peptide revealed a LTP curve progression that was significantly lower starting directly after TBS. The quantification of the initial potentiation levels during the phase of post-tetanic potentiation (PTP) yielded significantly higher potentiation levels for acute slices treated with the active Aβ1-16 peptide with 191.49 ± 8.82% when compared to the values reached with the inactive peptide (165.12 ± 8.82%, p= 0.041, Student´s t-test, Figure 3.20B). Furthermore, maintained potentiation levels following Aβ1-16 application were significant higher than that upon treatment with the scrambled peptide (148.08 ± 3.65% vs. 132.18 ± 4.26%, p= 0.0099, Student´s t-test). Moreover, I investigated basal synaptic transmission properties upon application of the respective peptide as NexCre cDKO mice itself revealed impaired presynaptic function (see 3.5 and (Hick et al., 2015)). The analysis of the input-output strength showed that recAβ1-16 nor its scrambled version had any significant effect on *f*EPSP slopes correlated to defined stimulus intensities (Figure 3.20C) or fiber volley amplitudes (Figure 3.19D), observations that were in line with the results obtained before (see 3.5 and (Hick et al., 2015)). Strikingly and consistent with the results I gained with the viral driven overexpression of Venus or APPsα, the function of the presynapse was significantly rescued following Aβ1-16 treatment, as the curve of the PPF paradigm was at all inter-stimulus-intervals (ISI) applied higher than that of acute slices which received Aβ1-16 scr (Figure 3.20E). Significant alterations were observed at ISI of 160 (p= 0.003), 80 (p= 0.02) and 40 ms (p= 0.002). Altogether, Aβ1-16 might be the neurotrophic domain of APPsα as it rescued the LTP deficit as well as short-term synaptic plasticity of NexCre cDKO mice without altering the function of the postsynapse.

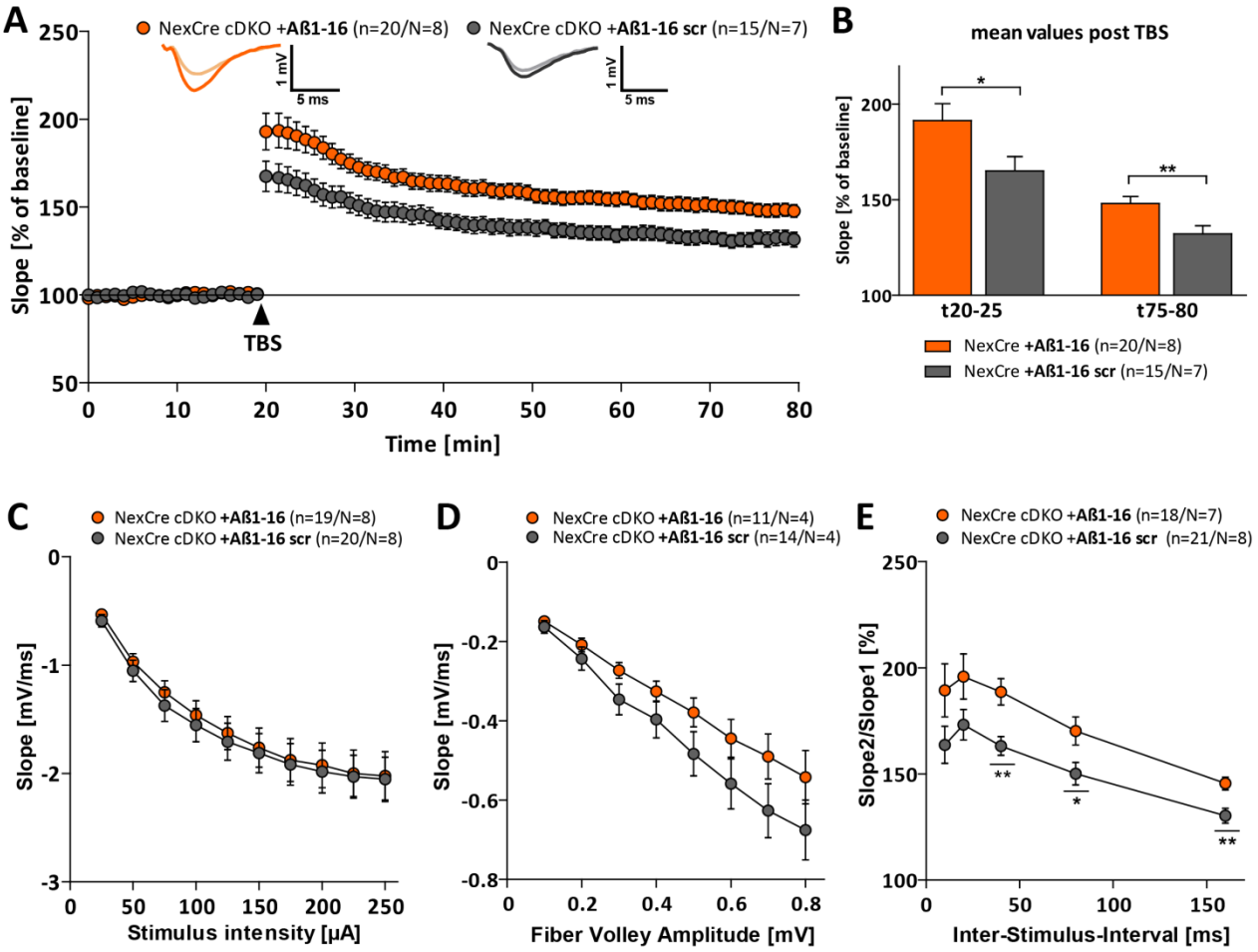

Figure 3.20: Aβ1-16 enhances long and short-term synaptic plasticity in NexCre cDKO mice. Field excitatory postsynaptic potentials (*f*EPSPs) of acute hippocampal slices of NexCre cDKO animals were recorded in CA1 region by stimulating Schaffer collateral axons of area CA3 at a frequency of 0.1 Hz after 1 hour pre-incubation with 10 nM Aβ1-16 or Aβ1-16 scrambled. **(A)** LTP was induced by application of TBS after 20 min baseline stimulation (arrowhead). During sixty minutes of LTP recording acute slices of NexCre cDKO mice pre-incubated with scrambled Aβ1-16 peptide exhibited significant lower induction and maintenance of LTP. The LTP induction rate is shown as percentage % of mean baseline slope. Data points were averaged over 6 time-points and error bars indicate SEM, n= number of recorded slices/N= number of animals. Data were analyzed by unpaired Students t-test. **(B)** Averaged potentiation levels at LTP induction (t20-25) revealed a significantly enhancement by Aβ1-16 (191.49±8.82% vs. 165.12±8.82%, p=0.041) that was present over the whole recoding time. Maintained potentiation levels (t75-80) were significantly increased in the presence of Aβ1-16 (148.08±3.65% vs. 132.18±4.26%, p= 0.0099). **(C)** No alterations were detected analyzing the Input-Output (IO) strength at any FV amplitude or stimulus intensity by Aβ-16 peptide application. **(E)** Aβ1-16 significantly enhanced short-term synaptic plasticity at inter-stimulus intervals of 160, 80 and 40 ms.

3.8.1 Influence of the α7-nAChR in Aβ1-16 Mediated Signaling in Synaptic Plasticity

As the results following APPsα and Aβ1-16 administration revealed that LTP as well as short-term plasticity and thereby presynaptic function were positively modulated, I proved which receptor might be involved in that mechanism. While for APPsα a putative receptor still remains elusive, two presynaptic receptors have been proved to be activated at pico- to nanomolar concentrations by the Aβ peptide, which contains like APPsα the 16 amino acids of Aβ1-16. Aβ was shown to directly activate the α7-nicotinic acetylcholine receptor (α7-nAChR) and to thus regulate synaptic plasticity (Puzzo et al., 2008, Mehta et al., 2009, Khan et al., 2010) or to associate with metabotropic glutamate receptors (Chin et al.,

2007). The study of Lawrence and colleagues (2014) further revealed that the N-terminal, hydrophilic part of Aβ (Aβ1-15), augments TBS-induced post-tetanic potentiation (PTP) and LTP in mouse hippocampal slice and that it moreover rescues the reduced LTP upon high levels of full-length Aβ. Within that study it was moreover shown that following bilateral injection of Aβ1-15 contextual fear conditioning was enhanced, but attenuated when the nicotinic antagonist methyllycaconitine (MLA) was co-applied. Besides MLA also α-Bungarotoxin (α-BTX) is a highly selective antagonist for the α7-nAChR and often administered during acute hippocampal slice recordings (Chen et al., 2006b, Puzzo et al., 2008, Criscuolo et al., 2015), so that I decided to use it to investigate if the action of Aβ1-16 at the presynapse might be mediated by the α7-nAChR. Hence, I pre-incubated acute hippocampal slices of NexCre cDKO for 1 h with recombinant Aβ1-16 (Aβ1-16) and provided the peptide further during the whole *f*EPSP recording, while inhibiting the α7-nAChR following administration of 10 nM α-BTX 10 minutes before the PPF paradigm was performed or before baseline recording of LTP started. To evaluate the effect of 10 nM α-BTX itself, I further included a littermate (LM) control group that received no α-BTX or where 10 nM α-BTX was administered in the same way like in NexCre cDKOs.

First of all, the *f*EPSP recordings depicted in Figure 3.21A and B confirmed the potential of Aβ1-16 to rescue impaired LTP in induction and maintenance. The LTP curve of NexCre cDKO+Aβ1-16 was indistinguishable from that of LMs which is further represented by the quantified LTP values gained for the initial phase of LTP as well as during maintenance. To identify the effect of the α-BTX administration in LMs or NexCre cDKO mice, I plotted these two groups separately. Blocking of the α7-nAChR interfered only slightly with Aβ1-16 action as the initial curve and the quantified *f*EPSP slopes during PTP were only marginally reduced (180.39± 8.33% vs. 169.38± 7.01%, p= 0.34, Student´s t-test, Figure 3.21A´, B´). However, the maintenance of LTP was completely unaffected following α-BTX administration in NexCre cDKOs (145.88± 4.89% vs. 140.97± 4.43%, p=0.48, Student´s t-test). Contrary were the results I obtained upon α7-nAChR blocking in LMs (Figure 3.21A´´, B´´) with significantly reductions during the phase of PTP (184.01± 5.59% vs. 158.04± 8.35%, p= 0.026, Student´s t-test) and maintenance of LTP (147.25± 3.87% vs. 131.24± 4.99%, p=0.028, Student´s t-test), confirming that the α7-nAChR is involved in mechanisms of synaptic plasticity. Moreover, I assessed short-term synaptic plasticity using the PPF paradigm to investigate a potential presynaptic action of Aβ1-16 which might be blocked after α-BTX administration. Figure 3.21C illustrates that blocking of the α7-nAChR doesn´t alter presynaptic function, neither in the presence of Aβ1-16 nor in LMs. Based on this set of experiments I could not exclude that the α7-nAChR might be involved in Aβ1-16 mediated signaling as following α-BTX treatment the LTP curve of acute slices of NexCre cDKO mice with Aβ1-16 was slightly lower when compared to BTX untreated controls. This might be due to the fact that the α7-nAChR is also expressed at postsynapses which might have an additional influence besides the presynaptic action of Aβ1-16. Moreover, I found no hints of alterations in the functionality of the presynapse upon α-BTX administration in any group which might further underline a potential postsynaptic effect following α-BTX treatment.

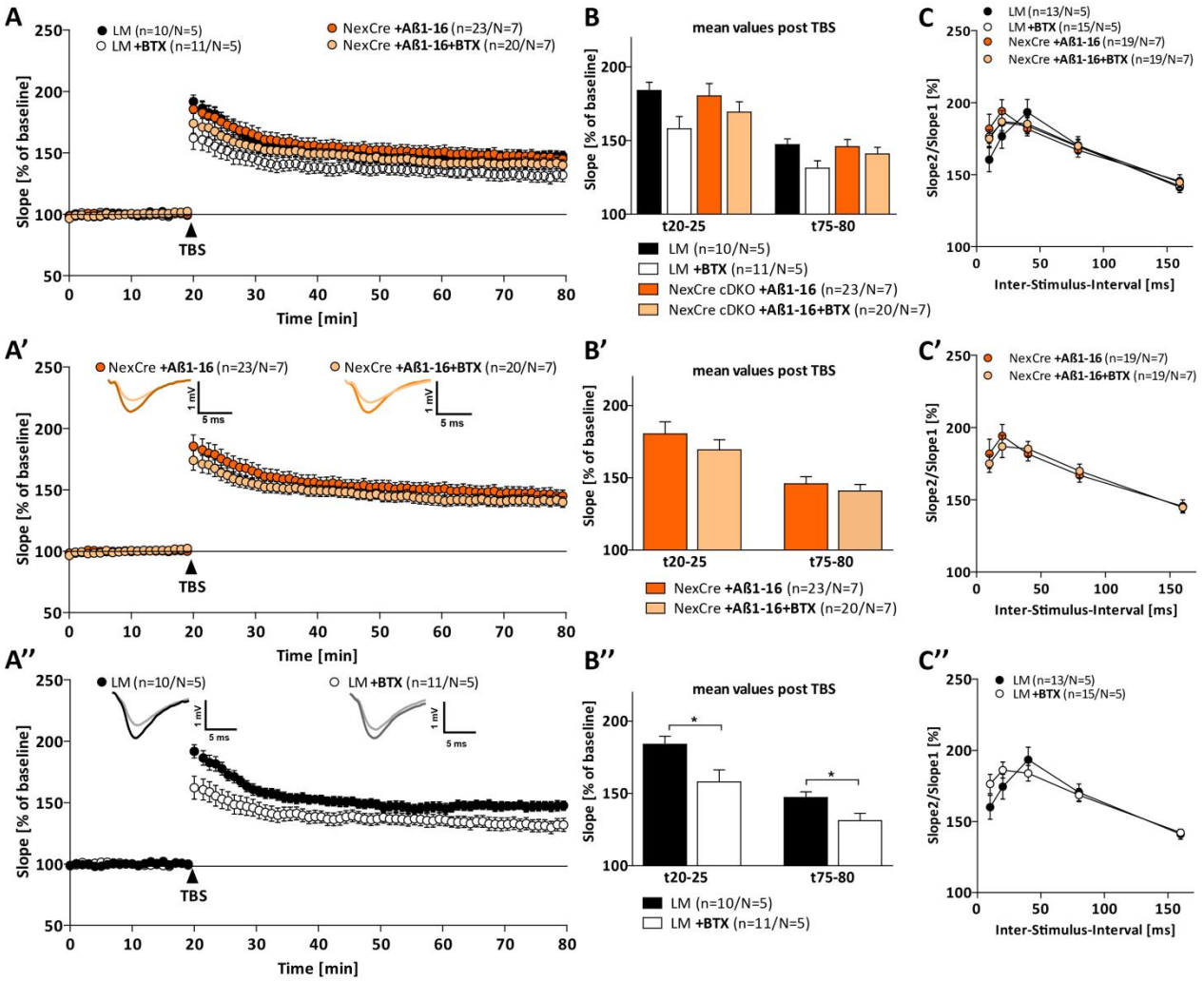

Figure 3.21: α-Bungarotoxin significantly affects PTP and LTP in littermates and slightly interferes with Aβ1-16 at the phase of LTP induction in NexCre cDKO mice. After 1 hour pre-incubation with 10 nM Aβ1-16 acute slices were transferred to submerged recording chamber and *f*EPSP recorded at the CA3-CA1 pathway. 10 nM α-Bungarotoxin was washed-in 10 min before the PPF paradigm and was present throughout whole LTP recording. **(A, B)** 10 nM α-BTX significantly reduced LTP induction and maintenance in littermates (LM, open circles, **B''**: t20-25: p= 0.026 and t75-80: p =0.028 with Students t-test, but not significant when plotting all groups and analyzing differences by 1-way ANOVA in **(B)**. **(A´, B')** NexCre cDKO treated slices with the α7-nAChR blocker showed only mildly interference with Aβ1-16 at initial stages of LTP. Maintained potentiation levels were not significantly different following α-BTX administration in the presence of Aβ1-16 in NexCre cDKO mice. **(C)** PPF yielded no significant differences after α-Bungarotoxin treatment in littermates or NexCre cDKO mice.

3.8.2 Co-application of Aβ1-16 and α-Bungarotoxin During Recordings of Synaptic Plasticity in NexCre cDKO Mice

The acute inhibition of the α7-nAChR using 10 nM α-BTX did not confirm that the Aβ1-16 peptide might modulate synaptic plasticity by activating the receptor. As the enhancement of synaptic transmission by Aβ1-16 could not be reasoned without fail, I started another set of experiments. Thereby, I simultaneously pre-incubated the α7-nAChR blocker α-BTX with Aβ1-16 to prevent a possible interaction of Aβ1-16 with the nicotinic receptor already during the one hour of pre-incubation with the peptide alone.

The administration of Aβ1-16 and α-BTX at the same time resulted in impaired induction and maintenance of LTP following TBS when compared to acute hippocampal slices of NexCre cDKO mice

that were treated with the Aβ1-16 peptide alone (Figure 3.22A). Quantification of the average potentiation levels during the initial phase of LTP, directly after stimulation revealed significantly lower levels for NexCre cDKO mice which received Aβ1-16 and BTX simultaneously (t20-25: 176.23 ± 4.69% vs. 153.75 ± 5.05%, p= 0.01, Student´s t-test, Figure 3.22B). The same held true for the maintenance phase of LTP at the end of recordings where slices in which the α7-nAChR was blocked reached only potentiation levels of 129.24± 3.40% which were significantly reduced when compared to NexCre cDKOs treated with Aβ1-16 reaching 144.37± 2.34% (t75-80: p= 0.002, Student´s t-test, Figure 3.22B). I assessed moreover if following α-BTX administration basal synaptic transmission was altered. The comparison of *f*EPSP slopes at defined stimulus intensities revealed no differences in the input-output behavior between groups (Figure 3.22C). I further assessed short-term plasticity using the PPF paradigm and found no evidence for altered presynaptic function. Altogether these results indicated that the simultaneous application of Aβ1-16 and the α7-nAChR blocker α-BTX impaired activity dependent synaptic plasticity without affecting baseline synaptic transmission.

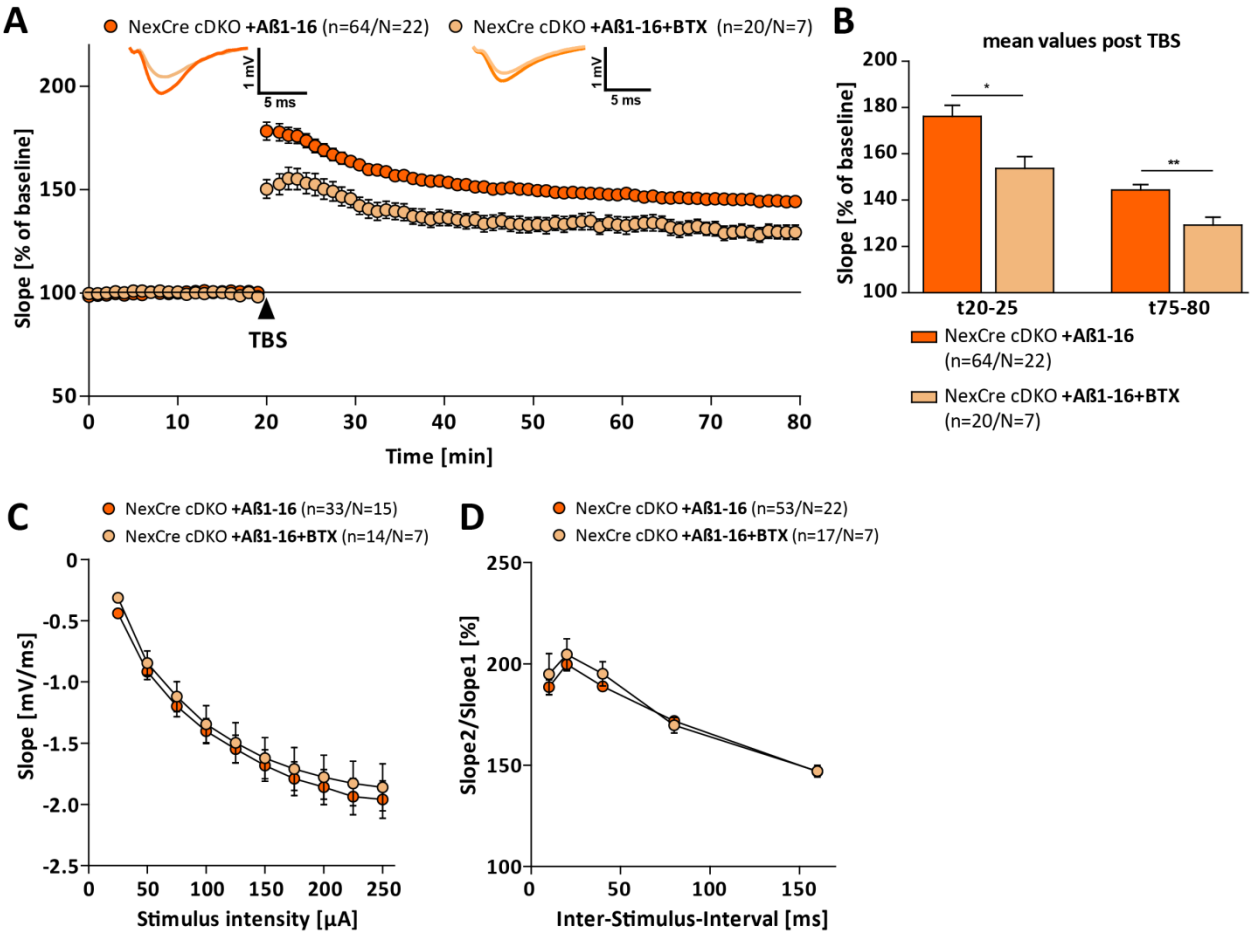

Figure 3.22: Co-application of α-Bungarotoxin and Aβ1-16 alters synaptic plasticity in NexCre cDKO mice. After 1 hour pre-incubation with 10 nM Aβ1-16 or 10 nM Aβ1-16 and 10 nM α-BTX acute slices of NexCre cDKO mice were transferred to a submerged recording chamber and *f*EPSPs were recorded at the CA3-CA1 pathway. Peptide and inhibitor used for pre-incubation circulated throughout whole LTP recording. **(A, B)** Hippocampal acute slices treated with 10 nM α-BTX and Aβ1-16 revealed significantly impaired induction and maintenance of LTP in comparison to slices of cDKO mice recorded in the presence of Aβ1-16 alone. **(B)** Averaged potentiation levels at the phase of post-tetanic potentiation (t20-25: 176.23±4.69% vs. 153.75±5.05%, p= 0.01) and at the end of recording (t75-80: 144.37±2.34 vs. 129.24±3.40) were significantly reduced in the presence of 10 nM α-BTX. **(C, D)** Neither pre- nor postsynaptic basal transmission was affected by the applied compounds.

3.8.3 Efficacy of Aβ1-16 in Comparison to APPsα to Rescue Impaired LTP in NexCre cDKO Mice

I showed already with several electrophysiological recordings that the acute application of Aβ1-16 was able to restore impaired synaptic plasticity in APP/APLP2 deficient (NexCre cDKO) mice *in vitro* (see 3.8 – 3.8.2). Lastly, I wanted to see if the neurotrophic activity of Aβ1-16 and APPsα is similar in processes of activity-dependent synaptic plasticity. To this end, I applied both recombinant peptides in the same way, meaning one hour of pre-incubation and circulation during *f*EPSP recording, on acute hippocampal slices of NexCre cDKO mice.

The *f*EPSP recordings depicted in Figure 3.23A and B show that the LTP curves following recombinant Aβ1-16 or recombinant APPsα administration were indistinguishable in induction and maintenance as seen comparing LTP values gained for the initial phase of LTP as well as during maintenance. During the phase of post-tetanic potentiation (PTP, t20-25) both groups revealed comparable potentiation levels with 198.53 ± 8.35% for NexCre cDKO+ APPsα and 191.49 ± 8.82% for NexCre cDKO+ Aβ1-16. The quantification of the last five minutes of LTP recording confirmed no differences in activity-dependent synaptic plasticity upon APPsα or Aβ1-16 application (146.15 ± 4.21% vs. 148.08 ± 3.65%). Analyzing the input-output strength at different stimulus intensities yielded that both peptides had no significant effect on the function of the postsynapse (Figure 3.23C). I further investigated the functionality of the presynapse and assessed if both peptides were able to enhance short-term plasticity to the same extent (Figure 3.23D). The curves generated applying the PPF paradigm revealed that APPsα and Aβ1-16 modulate the function of the presynapse equally. Overall these data indicated that Aβ1-16 might be the functional domain of APPsα as I observed no differences in activity-dependent synaptic plasticity and basal synaptic transmission in NexCre cDKO mice upon treatment with any of the recombinant peptides.

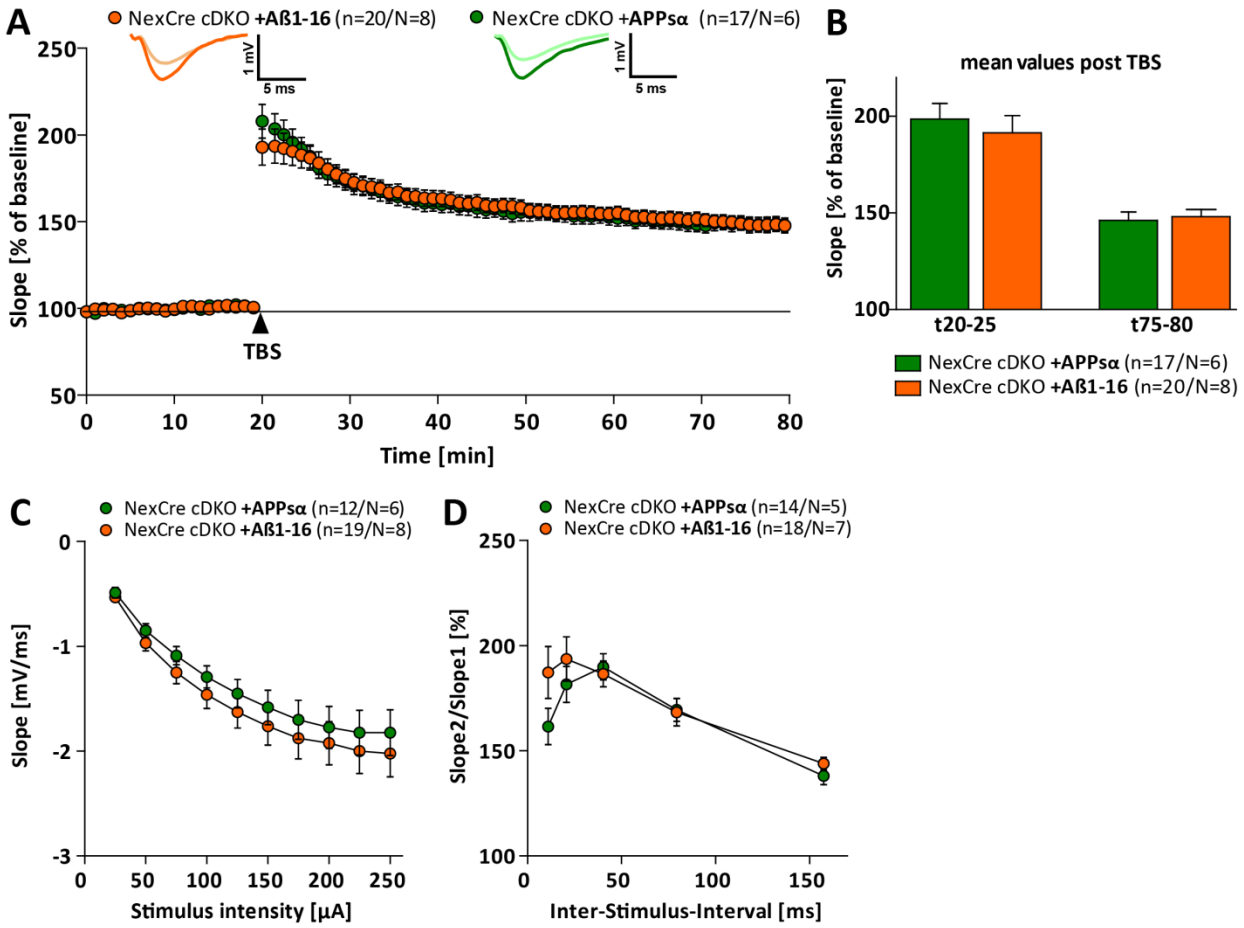

Figure 3.23: Acute application of recombinant Aβ1-16 and APPsα elevates LTP in NexCre cDKO slices to same extent. After 1 hour pre-incubation with 10 nM Aβ1-16 or APPsα acute slices of NexCre cDKO mice were transferred to a submerged recording chamber and *f*EPSPs recorded at the CA3-CA1 pathway. **(A, B)** Induction of LTP by TBS resulted in unaltered strengthening of *f*EPSP signals initially and throughout 60 minutes of recording (t20-25: 198.53±8.35% vs. 191.49±8.82% and t75-80: 146.15±4.21% vs. 148.08±3.65%). **(C)** The Input-Output curve revealed no alterations between applied peptides at different stimulus intensities tested. **(D)** Aβ1-16 and APPsα modulate presynaptic function of NexCre cDKO mice in the same manner.

4 Discussion

Alzheimer´s disease (AD) is a neurodegenerative disorder with aging as the most significant risk factor. AD is the most common form of dementia, being responsible for 60 to 80% of the cases. The number of diagnosed patients per year is growing rapidly and intense research focuses on the development of effective therapeutics as well as on ways to prevent the disease. While it is well known that accumulation of the neurotoxic amyloid β (Aβ) peptide, a cleavage product of the amyloid precursor protein (APP), is the key event in the disease, the physiological role of the APP protein family is still not fully understood. To develop potential therapeutic approaches it is essential to understand first of all the physiological role of the APP protein family and their secreted peptides and as well how they modulate synaptic function. Another possibility for AD might be that decreased levels of APP proteolytic products generated in the healthy organism lead to synaptic dysfunction. Thus, I analyzed different gene-targeted mice in this thesis to elucidate the role of APP/APLPs and their functional domains in processes of activity-dependent synaptic plasticity in the hippocampus, a brain region severely affected by AD.

First of all I could show that the so far less attended APP homolog APLP1 exerts an age-dependent role in supporting basal synaptic transmission at the hippocampal CA3-CA1 synapse (chapter 3.1). Moreover, the generation of a conditional APP triple KO mouse model allowed me to study synaptic plasticity in surviving adult mice and revealed an important role for all three family members during development (chapter 3.2). Besides investigating the APP proteins in full-length, I examined the role of their functional domains. Elucidating the role of the Fe65 protein family as downstream actors of APP confirmed an essential link between the adapter family and APP modulating synaptic function by intracellular signaling (chapter 3.3).

In more detail I assessed the role of the α-secretase cleavage product APPsα and its claimed neurotrophic properties. While I found no impairments on hippocampal LTP following acute inhibition of the α-secretase ADAM-10 in wild-type mice (chapter 3.4), I show that stable, viral driven expression of APPsα in APP/APLP2 deficient mice as well as in a mouse model of AD (APP/PS1ΔE9 tg) restored LTP deficits presumably by acting at presynaptic terminals (chapter 3.5, 3.6). In contrast, the 16 amino acid shorter APP fragment APPsβ seems not to be involved in processes of synaptic plasticity. The analysis of dendritic spine density revealed a pivotal role for APPsα ameliorating spine density in AD mice and APP/APLP2 deficient cultures, while APPsβ was again ineffective (chapter 3.6.1, 3.6.2, 3.7.5).

Moreover, I could show that chemically induced LTP is impaired in primary hippocampal cultures of APP/APLP2 deficient mice in Ca^{2+} imaging experiments. I observed a defect in Ca^{2+} homeostasis, which was rescued upon viral transduction of cultures with APPsα. Within these experiments a dysregulation of ER Ca^{2+} handling and SOCC channel activity was observed for APP/APLP2 deficient cultures consistent with results found in the literature for AD mice (chapter 3.7).

Lastly, I studied the role of the 16 amino acids differentiating the two APP extracellular domains, APPsα and APPsβ. The administration of recAβ1-16 revealed that this domain mediates the functional neuroprotective properties of APPsα. Pharmacological experiments performed to provide a potential targeted receptor yielded that the α7-nAChR receptor might be involved in synaptic signaling during processes of synaptic plasticity (chapter 3.8).

4.1 APLP1 Deficiency Causes Age-Dependent Impairments in Basal Synaptic Transmission

APLP1 exhibits like the other APP homolog APLP2 an overlapping sequence to APP and thereby also partial covering functions. In contrast to the two other family proteins, APLP1 shows restricted expression to the brain (Lorent et al., 1995) and is present only in one isoform (Wasco et al., 1992, Paliga et al., 1997). The highest presence at the plasma membrane has been observed for APLP1 suggesting that it might be the family member with the upmost potential to mediate cell contacts (Kaden et al., 2009) being crucial to build and maintain synaptic contacts. Thereby enhanced trans or cis interaction of APLP1 proteins is accompanied by a reduction of ectodomain shedding (Stahl et al., 2014, Mayer et al., 2016) and might therefore interfere with the ability to modulate synaptic function. While it was recently shown that APP and APLP2 exhibit basal adhesive properties, APLP1 mediated neuronal adhesion is dynamic and regulated by zinc (Mayer et al., 2016). Nevertheless, despite the generation and first characterization of the conventional APLP1-KO mouse in 2000 by Heber and colleagues, the in vivo function of this homolog has been less attended. Heber et al. (2000) described only minor (if any) distinct phenotypes of APLP1-KOs. The ablation of the APLP1 gene function caused a 10 % reduction in body weight, but did not result in impaired cognitive behavioral performance in the Morris-Water-Maze (MWM) task. The only read-out regarding synaptic plasticity was done in vivo at the perforant path-granule cell synapse (PP-DG) in young adult mice (16–20 weeks old) and revealed unaltered short-term plasticity (STP) and LTP, but was associated with enhanced excitatory transmission (Vnencak et al., 2015). Opposite to the APP/APLP2 DKO mice dying shortly after birth (Heber et al., 2000), the combined KO of APP and APLP1 caused no lethality. This underlines the redundant functions within the APP family but also unique properties of each member. Interestingly, aged APP-KO mice reveal age-dependent impairments in spatial learning (Ring et al., 2007), LTP (Seabrook et al., 1999, Ring et al., 2007) and neuronal morphology (Tyan et al., 2012, Weyer et al., 2014), while no age-dependent impairments were recognized for APLP2-KO mice (Weyer et al., 2011, Midthune et al., 2012, Weyer et al., 2014). In this thesis I addressed the age-dependent characteristics of APLP1-KO mice regarding activity-dependent synaptic plasticity. The analysis included young (4 – 6 months, chapter 3.1.1) and aged (11-13 months old, chapter 3.1.2) APLP1-KO mice versus their age-matched littermate controls. Following 20 minutes of stable baseline recording neither young nor aged APLP1-KO mice displayed alterations in LTP induction and maintenance (Figure 3.1A, B and 3.2A, B) in line with intact spatial memory performance in the MWM task reported by Heber and colleagues (2000). However, the analysis of basal synaptic transmission expressed as the strength of fEPSP responses to excitatory synaptic stimulation revealed impaired input-output behavior in aged, but not young APLP1-KO mice (Figure 3.1C, D and 3.2C, D). The amplitude of the fiber volley is representative for the number of axons firing an action potential and serves as an estimate of the strength of an afferent input. While the amplitude remained the same (like the stimulus intensity applied) in controls and APLP1-KOs, but evoked smaller fEPSP responses in aged APLP1-KO mice, the defect seems either to be related to postsynaptic alterations or could be due to a lower number of synapses at apical dendrites of CA1 neurons of the hippocampus. The latter can be proven by spine density analysis as the number of spines represents the amount of excitatory synapses and should be done in future experiments. Overall, the electrophysiological results indicate that APLP1 might have an individual role at the synapse within the APP family, supporting postsynaptic transmission, as aged APP and APLP2-KO showed unaltered behavior within these paradigms (Ring et al., 2007, Weyer

et al., 2011, Midthune et al., 2012, Tyan et al., 2012). However, I additionally proofed for putative presynaptic changes using the paired-pulse-facilitation (PPF) paradigm that further provides information about STP in APLP1-KO mice. Analyzing the ratio of the second *f*EPSP slope versus the first revealed unchanged PPF characteristics in young (Figure 3.1E) as well as aged APLP1-KO mice (Figure 3.2E) and implied normal presynaptic function in APLP1 deficient mice when compared to littermate controls. These results are in line with the presynaptic characteristics described for young and aged APP-KO and APLP2-KO mice (Ring et al., 2007, Weyer et al., 2011, Midthune et al., 2012, Tyan et al., 2012) and the observations of Vnencak and colleagues (2015) reporting intact STP at PP-DG cell synapses *in vivo* for APLP1 deficient animals. Furthermore consistent with the results of Vnencak and coworkers (2015) I found no alterations in LTP in young APLP1-KO mice as observed for other single APP mutants. However, as for aged APLP2-KO mice displaying intact LTP (Seabrook et al., 1999, Ring et al., 2007) APLP1-KOs showed no age-dependent LTP deficit like the one observed for aged APP-KO (Ring et al., 2007). This in conclusion indicates that APP and APLP1 have distinct functions at the synapse. Age-related impairments in synaptic plasticity in APP-KO mice have been attributed to the loss of APPsα as the Knock-In of APPsα was sufficient to rescue LTP in aged APP-KO mice (Ring et al., 2007, Weyer et al., 2011). While all APP family members were shown to interact with NMDA-Rs, possibly by their extracellular domain (Cousins et al., 2015), the binding of APLP1sα might initiate different functions at the synapse when compared to APPsα.

The strengthening of *f*EPSP response to excitatory stimulation (input–output curve) was significantly decreased in aged APLP1-KO mice, strongly suggesting that APLP1 is essential for normal postsynaptic signal transmission. To prove if aging itself might have an influence on the EPSP or FV read-outs performed, I plotted the input-output curves for littermate controls and APLP1-KO separately by age (Figure 3.3). While littermate controls showed unaltered neuronal excitability with age, older APLP1-KOs were impaired when compared to young mice. Here, altered basal synaptic transmission at the postsynapse suggests a loss of synapses, either anatomical or functional (Landfield et al., 1986, Barnes et al., 1992, Deupree et al., 1993). While I provide a functional read-out, anatomical alterations need to be examined e.g. by spine density and spine morphology analysis. However, while aged APLP1-KO mice have a postsynaptic signal transmission deficit, they didn´t show altered LTP meaning that they were able to compensate for their impairment upon high frequent stimulation. This might be due to the fact that APP is expressed in aged APLP1-KOs and APPsα release, known to facilitate NMDA-R function, is enhanced upon tetanic stimulation (Taylor et al., 2008, Moreno et al., 2015) and might thus compensate for the loss of APLP1 during LTP recordings.

4.2 The APP Protein Family Is Essential During Brain Development and Adult Brain Function

As mentioned in the previous chapter, the embryonic lethality caused by the co-deletion of APLP2 with one of the other family member indicates the essential role of the gene family in the mammalian organism. The only viable DKO is the APP/APLP1 mutant mouse displaying normal brain morphology, but reduced body weight (Heber et al., 2000). The differences in embryonic lethality upon APLP2 deletion with one of the other APP family member might arise from their overlapping expression patterns throughout the body. In contrast to APP and APLP2, APLP1 expression is restricted to the brain (Lorent et al., 1995) and thereby not able to overtake functions in the peripheral system, particularly at the neuromuscular junction (NMJ), where severe alterations in diaphragm morphology are seen when APP

and APLP2 are co-deleted resulting in breathing impairments directly after birth. Additionally the expression of APP and APLP2 in proliferative zones of the developing cortex and of APLP1 in the cortical plate are indicative for a role of the APP protein family during brain development (Lopez-Sanchez et al., 2005). In conclusion, the triple KO (TKO) of APP, APLP1 and 2 results in a severe morphological brain phenotype which is associated with cranial abnormalities so that TKO mice die shortly after birth. Neuronal cells thereby migrate beyond their normal positions building ectopic clusters in dorsal regions of the frontoparietal cortex. This focal cortical dysplasia resembles type II lissencephaly of humans. Moreover, APP-TKO mice have a reduced number of Cajal Retzius cells which might induce less reelin secretion and thus result in neuronal over-migration (Herms et al., 2004). In order to investigate APP family protein functions in the adult brain, conditional DKO or TKO mice needed to be engendered. First of all, the generation of a conditional DKO for APP and APLP2 provided the possibility to study the function of these two proteins in the adult organism (Hick et al., 2015), especially their function in excitatory neurons of the forebrain as Cre-mediated deletion of APP was induced under control of the NEX promoter (Goebbels et al., 2006). Using a novel conditional approach developed by the laboratory of Ulrike Müller at the IPMB, Heidelberg, I was able to investigate adult APP cTKOs ($NexCre^{+/T}APP^{flox/flox}APLP2^{flox/flox}APLP1^{-/-}$). In these mice, on an APLP1 deficient background the ablation of APP and APLP2 is initiated at embryonic day 11.5 (E11.5) under the control of the NEX promoter. While already the conditional double KO of APP and APLP2 resulted in defective hippocampus-dependent memory and impaired activity dependent synaptic plasticity possibly caused by altered presynaptic function (Hick et al., 2015), APP cTKO mice revealed an even more severe synaptic phenotype. Beside a highly pronounced deficit in induction and maintenance of LTP, APP cTKO mice showed heavily impaired basal synaptic transmission at the postsynapse additional to already altered presynaptic function (Figure 3.4). These results support that APP, APLP1 and APLP2 have an essential synaptic role during early development and adult brain function and that the co-deletion of APLP1 causes additional impairments in synaptic function. The additional postsynaptic transmission deficit is further in line with the observation gained for APLP1-KO mice (chapter 3.1, 4.1) revealing an essential role for APLP1 at this synaptic compartment. Moreover, during hippocampal slice preparation I recognized alterations in the shape of the hippocampus and a massively altered CA1-CA3 cell body layer suggesting atrophy that might contribute to the functional impairments in synaptic plasticity. Finally, both a morphological analysis by Nissl staining as well as a behavioral characterization and detailed analysis of dendritic and spine morphology needs to be done before further functional investigations can be performed and final conclusions can be made.

4.3 The Fe65 Protein Family Interaction with APP/APLPs Is Essential for Synaptic Plasticity

The Fe65 gene family is well-known to associate as adapter molecules by their phosphotyrosine binding domain with the intracellular domains of APP and APLPs (Borg et al., 1996, Bressler et al., 1996). The Fe65 proteins control the shuttling of a multimeric complex containing the APP intracellular domain (AICD), Fe65 and Tip60 into the nucleus where it was shown to regulate gene transcription (Cao and Sudhof, 2001), an essential feature regarding long-term modulation of synaptic transmission being dependent on new protein synthesis. In addition, Fe65 gene members co-localize with APP in the endoplasmatic reticulum (ER) and golgi apparatus and facilitate the translocation of the precursor proteins to the cell surface (Sabo et al., 1999). This process might be coupled to activity-dependent

synaptic plasticity as under resting conditions APP family members are enriched in intracellular compartments (Thinakaran and Koo, 2008) and thus be essential for synaptic function. Most intriguing is the fact that Fe65/Fe65L1 double deficient mice show a similar phenotype of cortical dysplasia as observed for the APP triple KO animals (Guenette et al., 2006) and have so far not been investigated regarding synaptic plasticity. By now only the isoform specific p97 Fe65-KO was shown to have deficits in non-spatial learning tasks like the temporal dissociative passive avoidance (Wang et al., 2004, Wang et al., 2009) and classical fear conditioning (Wang et al., 2009) independently of age. On the other hand, only aged (> than 14 months) p97 Fe65-KO mice revealed altered performance in the hippocampus-dependent MWM task which is in line with the deficits seen in E-LTP at Schaffer collateral-CA1 synapses that was induced by a 100 Hz high-frequent stimulus *in vivo* (Wang et al., 2009). Hence the results of Wang and coworkers already indicated that Fe65 might also be involved in protein-synthesis independent forms of plasticity. The age-dependent impairments resemble those of APP-KO mice where the APP homologs compensate for the loss of APP at young ages, but fail to do so in older mice (Seabrook et al., 1999, Ring et al., 2007). In p97 Fe65-KO mice either a compensation of Fe65L1 or Fe65L2 might mask defects in young single KOs or the reported upregulation of the p60 Fe65 isoform upon p97 Fe65 deletion. The p60 Fe65 isoform lacks a binding domain being crucial to induce gene transcription, but should therefore not cause alterations in E-LTP recordings which is the form of plasticity being independent of new protein synthesis (Wang et al., 2009). To get a clearer picture of the role of the Fe65 protein family in activity-dependent synaptic plasticity I investigated a Fe65-KO mouse in which the p79 as well as p60 isoform were deleted as well as Fe65L1-KO and Fe65/Fe65L1 dKO animals. These mice were generated and partially characterized by Guenette and colleagues (2006). Fe65 KO mice reveal deficits in the hanging wire task while no overt abnormalities regarding brain morphology were noticed. The impairment was moreover seen in Fe65L1-KO mice while only Fe65/Fe65L1-dKOs exhibit deficits in neuronal positioning and axon outgrowth in the developing cortex (phenotype of cortical dysplasia mentioned above) (Guenette et al., 2006, Suh et al., 2015). The detailed investigation of Fe65-KO, Fe65L1-KO and Fe65/Fe65L1-dKO mice regarding motor and cognitive function was performed in cooperation with P. Strecker and S. Kins from the University of Kaiserslautern and already published (Strecker et al., 2016). First of all we were able to show that Fe65-KO mice, also lacking the p60 isoform, yielded impaired spatial memory already at young ages. Moreover, impairments within the MWM task were noticed for the Fe65L1-KO, while Fe65/Fe65L1-dKO mice showed very strong deficits during the task due to altered anxiety, motor activity and impaired vision. Analysis of activity-dependent synaptic plasticity (Figure 3.5) revealed consistently pronounced deficits in induction and maintenance of LTP in dKO mice, while only the initial induction phase of LTP was affected in Fe65-KOs and no impairments were observed for Fe65-L1-KO mice. Interestingly, Fe65-L1-KOs were the only ones displaying impairments in presynaptic function (Figure 3.5E) while for Fe65/Fe65L1-dKO an indication towards altered postsynaptic function was gained by correlating *f*EPSP strength to defined stimulus intensities (Figure 3.5D). Overall these data led to the assumption that Fe65 proteins are crucial at synapses in order to trigger processes of synaptic plasticity, while comparably to the APP protein family, each member might have individual roles at synapses. However, the electrophysiological results did not fully represent the observations of the MWM task maybe due to slightly alterations in motor function upon Fe65 deletion which influenced the behavioral paradigm. Another important fact one needs to consider is the upregulation of another Fe65 isoform following the deletion of Fe65 alone or together with Fe65L1 (Guenette et al., 2006). The p58 protein band found in western blot analysis has a so far unknown

identity and it´s increase of around 50 % upon deletion of Fe65 or Fe65L1 might mask deficits as for p90 Fe65-KO mice. Nevertheless, the electrophysiological data revealed that Fe65 and Fe65L1 are important for presynaptic function. Support for the involvement of both Fe65 proteins at the presynapse originates from observations made in mature cortical neurons whereupon the lack of the three Mint/X11 proteins, which are critically involved in presynaptic vesicle release, increased amounts of Fe65 and Fe65L1 proteins were noticed (Ho et al., 2006). Another possible important molecule mediating the interaction between Fe65 and APP and thereby presynaptic function is the small GTPase ARF6. ARF6 influences endocytic and membrane trafficking in neurons and may form a tripartite complex with APP and Fe65 (Sannerud et al., 2011, Cheung et al., 2014, Tang et al., 2015). Fe65 was shown to stimulate the activation of ARF6. ARF6 in turn is involved in processes of activity-dependent synaptic plasticity via the regulation of AMPA-R trafficking (Oku and Huganir, 2013) and the cycling of readily releasable synaptic vesicles at presynapses (Tagliatti et al., 2016).

Impaired locomotor activity, synaptic plasticity and deficits at the neuromuscular junction have been observed both for Fe65/Fe65L1-dKO and APP mice that lack the Fe65/Fe65L1 interacting site or carry a mutation within the binding motif on an APLP2 deficient background (Barbagallo et al., 2011, Weyer et al., 2011, Klevanski et al., 2015) confirming an interaction between the two protein families. In conclusion, Fe65 and Fe65L1 might mediate downstream signaling of APP/APLPs at the synapse, especially by nuclear signaling (Cao and Sudhof, 2001), via the regulation of the actin cytoskeleton (Lambrechts et al., 2000, Kimberly et al., 2001), the Ca^{2+} homeostasis (Nensa et al., 2014) and the proteosomal degradation of APP (Chow et al., 2015). Nevertheless, for a complete and clear picture it would be necessary to study additional combined DKOs of APP and Fe65 family members to underscore the role of both in the central nervous system.

4.4 Acute Inhibition of α-Secretase Activity Does Not Influence Synaptic Plasticity

Following α-secretase cleavage of APP family proteins mainly by ADAM-10, APPsα, APLP1sα or APLP2sα are released in the extracellular space (Lammich et al., 1999). Evidence from several studies in animals as well as in humans suggest that reduced APPsα levels aggravate AD symptoms. It was shown that a mutation within the α-secretase cleavage site of the human APP gene caused early onset of dementia (Kaden et al., 2012). Lowered production of APPsα lead at the same time to increased levels of toxic Aβ species. Moreover, supporting are observations that the complex of ADAM10/SAP97, which is mandatory for synaptic ADAM-10 localization, is reduced in AD patients (Epis et al., 2010). Additionally, forebrain-specific ADAM-10 conditional KO mice reveal increased Aβ levels and impaired short- as well as long-term synaptic plasticity (Prox et al., 2013). The α-secretase cleavage of APP family proteins was shown to be activity dependent so that neuronal depolarization, high frequency stimulation as well as the activity of metabotropic glutamate and acetylcholine receptors facilitates the production of extracellular peptides like APPsα (Nitsch et al., 1992, Nitsch et al., 1993, Fazeli et al., 1994, Gakhar-Koppole et al., 2008). I addressed the question of whether the acute inhibition of the α-secretase ADAM-10 in acute hippocampal slices of wildtype mice might interfere with the ability to show intact STP and LTP (chapter 3.4). Ten minute inhibition of ADAM-10 activity with the GI254023X compound (Weyer et al., 2011) resulted only in slightly lowered induction and maintenance of LTP (Figure 3.6A, B) which was not significantly different to vehicle treated controls. A possible explanation for this is that the inhibitor was not able to penetrate throughout the hippocampal slice during the application time, reaching the intact neuronal layers at around 150 µm depth where *f*EPSP recordings occurred. Another problem might

be that not only ADAM-10, but also ADAM9 and ADAM17 are located at the cell surface and are able to cleave APP at the α-secretase site (Lichtenthaler, 2012, Saftig and Lichtenthaler, 2015). While it has been reported that the acute application of recombinant APPsα rescues LTP, it needs to be considered that the application of the peptide was done for up to one hour before recordings (Hick et al., 2015) and thus represent a different "acute" timescale. Nevertheless, consistent to the acute application of recombinant APPsα, the acute inhibition of APPsα production does not alter basal synaptic transmission nor presynaptic function or STP. Using the GI254023X ADAM-10 inhibitor so far only one study reported significant changes in synaptic plasticity *in vitro* upon the treatment of APLP2 deficient OHCs for five consecutive days (Weyer et al., 2011). This further indicates that by the activity of other ADAM secretases enough APPsα, APLP1sα or APLP2sα might be produced to exhibit normal LTP when the GI254023X ADAM-10 inhibitor is applied acutely. Experiments performed with another ADAM-10 inhibitor combined with *in vivo* recordings yielded reduced tetanically evoked NMDA-R currents (Taylor et al., 2008) assuming different target specificity and local diffusion problems on inhibitors that cause differences in the experimental read-outs.

4.5 APPsα But Not APPsβ Is the Functional Domain Supporting Synaptic Plasticity

The APPsα peptide liberated from α-secretase APP processing is a 612 amino acid long protein shown to promote the survival and growth of cultured neurons under physiological as well as non-physiological conditions including hypoglycemia and glutamate toxicity (Mattson et al., 1993, Furukawa et al., 1996) and quite interestingly, against Aβ toxicity (Barger and Mattson, 1996, Guo et al., 1998). Moreover, supportive for the neuroprotective function of APPsα are the observations where APPsα attenuates the effects of disease-associated insults like excessive NMDA-R activation (Ryan et al., 2013) or impaired proteosomal function (Copanaki et al., 2010, Kundu et al., 2016). Neuroprotective functions of APPsα are thereby regulated by the binding of APPsα to cell surface expressed APP which in turns initiates the G_o protein triggered pro-survival Akt kinase pathway by its intracellular domain (Milosch et al., 2014). Another possibility might be that APPsα promotes its further production by blocking β-secretase activity in a positive feedback cycle (Peters-Libeu et al., 2015). A crucial role of APPsα in synaptogenesis and in modulation of spine density has been reported in several animal studies. The Knock-In of APPsα rescued the spine density deficit and spine type alterations described for APP-KO mice *in vivo* (Weyer et al., 2014) while only partial restoration was achieved by APPsα in cultured APP-KO neurons *in vitro* (Tyan et al., 2012). These reports further depicted that APPsα mediates spine formation and maintenance by coupling to a so far unknown receptor distinct from APP as full-length APP is absent in the investigated mice and cultures. A recent study of Zou and colleagues revealed decreased cortical spine turnover rates in APP-KO mice *in vivo*, indicating that altered spine dynamics might contribute to impairments in synaptic plasticity and memory. Interestingly, APP-KO mice have decreased levels of D-Serine, a co-agonist for NMDA-Rs (Zou et al., 2016), while recombinant APPsα infusion was shown to enhance NMDA-R function, but not recombinant APPsβ (Taylor et al., 2008). Especially the role of APPsα in processes of synaptic plasticity implies it to counteract the effects of Aβ. In the late 90´s Ishida and colleagues already showed the facilitation of LTP expression induced by 100 Hz stimulation by APPsα possibly mediated by a protein kinase G dependent mechanism (Ishida et al., 1997). Recently the acute synaptic function of APPsα was demonstrated by the incubation of hippocampal slices of APP/APLP2 conditional KO mice using 10 nM of the recombinant peptide resulting in a rescue of the severe LTP deficit, while again in this context recAPPsβ was ineffective (Hick et al., 2015). Another recent study

reported that recAPPsα is able to rescue age-dependent LTP deficits *in vitro* (Moreno et al., 2015). These results were in line with previous findings of Taylor et al. (2008) reporting that intrahippocampal infusion of recAPPsα in the dentate gyrus (DG) of anesthetized rats enhances LTP recorded at the PP-DG pathway *in vivo*. Interestingly, that study showed that APPsα exerted an inverted U-shaped dose-dependent facilitation of LTP. High amounts of recAPPsα decreased *f*EPSP responses in the DG, consistent to what I´ve seen following the stable viral driven overexpression of APPsα in APP/APLP2 cDKO mice (Figure 3.7). Too high levels of APPsα caused toxicity, resulted in severe astrogliosis and increased the inflammatory factor Caspase 3 (Casp-3) (Figure 3.8C). Activated Casp-3 is considered as commitment to cell death (Elmore, 2007), while astroglios is indicative for cytotoxicity both resulting in a drastic loss of hippocampal neurons shown by Golgi-Cox staining of hippocampal sections of injected mice (Figure 3.8B). Adenoviruses used to drive the transgene expression are immunogenic and used for vaccination of humans against infections (Puntel et al., 2010). Indeed, AAV vectors can also elicit dose-dependent inflammatory and cytotoxic effects (Thomas et al., 2001, Zirger et al., 2006). In this regard, Ciesielska et al. have shown that cell transduction in rodents by an AAV-based vector expressing the green fluorescent protein (GFP) increased immunological neurotoxicity when compared to similar vectors expressing endogenous proteins, observations that were supported by Samaranch et al. (Ciesielska et al., 2013, Samaranch et al., 2014) and consistent to what I have observed upon expression of the fluorescent protein Venus. Both studies used the same AAV serotype 9 that has been chosen as vector backbone for this thesis and induced immune responses when a foreign marker protein (GFP or in this thesis Venus) was expressed. It has in fact been shown that the expression of an endogenous protein in heterogeneous sites or at levels well beyond normal expression was sufficient to prime systemic immune responses (Chenuaud et al., 2004, Gao et al., 2004) and thus explains the unexpected results gained in the first series of recordings, where I was not able to reproduce the described LTP phenotype of NexCre cDKO mice. Following determination of a viral titer that was proven to be non-toxic with regard to neuronal cell death and did not prompt immunological responses in injected brain areas a next set of electrophysiological recordings was performed (chapter 3.5.2). The results indicate that with a well-tolerated viral titer, APPsα is able to rescue the pronounced LTP deficit in induction and maintenance in NexCre cDKO (APP/APLP2 cDKO) mice paralleling enhanced LTP upon acute recAPPsα administration on hippocampal slices (Hick et al., 2015) or in the rat DG (Taylor et al., 2008). Furthermore, my results indicate that APPsα might exert its positive effects by improving the function of the presynapse something that has not been shown following recAPPsα application as PPF curves showed the same course for NexCre cDKO slices (Hick et al., 2015). On the contrary, the viral-driven overexpression of APPsβ yielded no potential to promote activity-dependent synaptic plasticity or to positively modulate the function of the presynapse when injected with the same titer in NexCre cDKO mice (Figure 3.10). These results were in line with the observations upon acute extracellular or *in vivo* application of APPsβ on rodent slices or in the rodent brain (Taylor et al., 2008, Hick et al., 2015). The results upon acute as well as viral-driven overexpression of endogenous APPsα highlight that the APP extracellular domain modulates synaptic function acutely as already established deficits could be rescued in APP deficient mice and age-dependent impairments in synaptic plasticity in wildtype rats were restored (Moreno et al., 2015). The fact, that APPsβ was completely ineffective might be a consequence of the absent last 16 amino acids compared to APPsα containing a neuroprotective domain (Furukawa et al., 1996). The shorter sequence might lead to different conformational structures of APPsβ that in turn might activate other types of receptors (Ludewig and Korte, 2017). Importantly, in contrast to APPsα the Knock-In of

APPsβ in mice was unable to rescue the perinatal lethality seen for APP and APLP2 DKO mice suggesting functional differences between these two large extracellular domains (Li et al., 2010, Weyer et al., 2011). Moreover, APPsβ was shown to be 50 to 100 times less protective against glucose deprivation and excitotoxicity (Furukawa et al., 1996, Barger and Harmon, 1997) and does not prevent against apoptosis mediated cell death (Copanaki et al., 2010). These reported APPsβ characteristics support the differences observed in the electrophysiological recordings, where only APPsα but not APPsβ was beneficial.

4.5.1 APPsα, But Not APPsβ, Rescues the Synaptic Failure in an Alzheimer´s Disease Mouse Model

Having confirmed the neurotrophic properties of APPsα also upon stable viral overexpression, I extended my research to the potential of APPsα as therapeutic agent. To this end I performed recordings on a APP/PS1ΔE9 tg mouse model of AD, upon the viral driven overexpression of APPsα in animals with already established plaque pathology and impairments in memory as well as synaptic plasticity. Thereby a single bilateral injection of AAV-APPsα particles was sufficient to mediate long-lasting expression of the APP extracellular domain over five months that was well tolerated without apparent adverse effects on brain morphology. These experiments were performed in cooperation with R. Fol, J. Bradeau and N. Cartier from the University Paris Sud and the INSERM U1169/MIRCen CEA in France and some results were already published (Fol et al., 2016) and shown in chapter 3.6. APP/PS1ΔE9 tg mice harbor a chimeric human/murine APP construct bearing the swedish double mutation as well as an exon-9-deleted mutation in the presinilin-1 gene. These mutations lead to a shift in APP cleavage at the γ-secretase site resulting in higher levels of the amyloidogenic $A\beta_{42}$ peptide which is prone to aggregate (Jankowsky et al., 2004). Transgenic mice exhibit increased levels of Aβ at six months of age and develop an accelerated plaque pathology correlating with age. These pathological characteristics are accompanied by spatial memory impairments in the Barnes maze and MWM starting to appear at seven to eight months of age (Cao et al., 2007, Reiserer et al., 2007). The cognitive deficits become more pronounced with age and correlate with increased plaque deposition (Savonenko et al., 2005a, Zhang et al., 2011). In line with the literature we observed impaired spatial memory in the MWM task, increased $A\beta_{42}$ levels and plaque load in aged APP/PS1ΔE9 tg mice that overexpressed the control virus AAV-Venus in comparison to littermate controls similarly expressing the fluorescent protein (Fol et al., 2016). The AAV-mediated APPsα expression was sufficient to rescue the impaired probe trial performance of mice in the spatial navigation task and reduced the levels of soluble Aβ species as well as the plaque load in the hippocampus and cortex. We moreover proved the modulatory potential of APPsβ in those readouts, but found beside a decrease in soluble Aβ levels no evidence for a modulatory role with respect to memory restoration or reduction in plaque load. The recognized reductions in Aβ levels by APPsα might thereby be mediated by the binding of the extracellular APP domain to the β-secretase BACE-1 leading to a reduction in Aβ production (Obregon et al., 2012). We further observed that following APPsα expression microglia were recruited and activated in the close vicinity to plaques, something that was absent upon APPsβ treatment. Moreover, the observation of an increased expression of TREM2, a receptor known to sustain the microglial response to Aβ and shown to function as a sensor for anionic lipids (Wang et al., 2015), suggested that microglia were active. The clearance of Aβ and plaques seems to be mediated by activated microglia as also the proteolytic enzyme IDE (insulin-degrading enzyme) which is produced by microglia (Leissring et al., 2003), was upregulated following APPsα overexpression. These results already indicate the pivotal neurotrophic role of APPsα so that I further tested whether the

improvements of spatial memory were also reflected on the functional network level. Therefore, I analyzed synaptic plasticity representing the cellular correlate of learning and memory as it reveals if synapses are able to increase their synaptic strength towards patterns of activity. Consistently to the results of non-injected APP/PS1ΔE9 animals (Spires-Jones and Knafo, 2012, Heneka et al., 2013), AAV-Venus injected transgenic mice exhibited significantly lower induction and maintenance of LTP when compared to AAV-Venus injected littermate controls (Figure 3.11, 3.12). AAV-mediated expression of APPsα largely ameliorated LTP deficits of APP/PS1ΔE9 tg mice as evidenced by a closely overlapping and statistically indistinguishable LTP curve to littermate controls. On the contrary, APPsβ overexpression failed to enhance LTP. The LTP deficit in APP/PS1ΔE9 tg mice was thereby accompanied by impaired short-term plasticity evaluated by the PPF paradigm, while basal synaptic transmission was unaltered. Notably, AAV-APPsα treatment completely rescued presynaptic functionality while again APPsβ administration was proven to be ineffective with acute slices displaying a similar PPF curve which was seen for APP/PS1ΔE9+AAV-Venus mice. This lead to the conclusion that APPsα positively modulates presynaptic function which might than in turn restore LTP. Evidence for that kind of APPsα action is based on studies showing that APP is localized at synaptic sites, especially the presynaptic active zone (Lassek et al., 2013, Wilhelm et al., 2014). Moreover, also in APP/APLP2 cDKOs APPsα positively modulated presynaptic function while viral overexpressed APPsβ showed no effect (Figure 3.9, 3.10). Further evidence for a presynaptic action of APP was described in the study of Weyer and colleagues (2011) where a reduction in the quantal content as well as in the ready releasable pool of synaptic vesicles has been observed at the NMJ for APP/APLP2 mutant mice. Moreover, it has been shown that the Knock-In of APPsα was sufficient to rescue impaired LTP in aged APP-KO mice (Ring et al., 2007) emphasizing the role of APPsα to positively modulate synaptic plasticity mechanisms.

As spine density can be seen as a correlate for the number of excitatory synapses, I evaluated if spine numbers were changed in the same set of mice used for electrophysiology. Previous studies had indicated reduced spine density correlating with cognitive deficits in various AD mouse models as well is in AD patients, presumably due to Aβ-mediated toxic effects (Scheff et al., 1990, Scheff et al., 2006, Spires-Jones and Knafo, 2012). Consistent with the literature I observed an overall reduction in spine density in APP/PS1ΔE9 tg mice at both dendritic compartments of CA1 and CA3 hippocampal neurons in comparison to littermate controls similarly injected with AAV-Venus (Figure 3.11, 3.12). Importantly, AAV-APPsα overexpression restored spine density in apical compartments of CA1 segments and CA3 neurons, while APPsβ showed also regarding neuronal morphology no modulatory role. Several reports already indicated that APPsα might have synaptotrophic properties under pathological conditions, too. Mucke and co-workers (1996) reported that moderate overexpression of human APP (huAPP) in transgenic mice leads to increased spine density. On the contrary, the expression of mutant huAPP in Tg2576 mice decreased spine density in aged animals, whereas an increase in spine density was observed in young mice prior to plaque deposition pointing towards a possibly trophic effect of APPsα (Lee et al., 2010). Moreover, indirect upregulation of APPsα by transgenic expression of the α-secretase ADAM10 (Berger et al., 2015), that is enriched at synaptic contacts (Marcello et al., 2007), increased synaptic density supporting the observations I have gained following the analysis of spine numbers in the hippocampus of APP/PS1ΔE9 tg mice.

Overall, we could therefore show that increases in spine counts upon viral APPsα expression were reflected by a rescue of synaptic plasticity as well as improved spatial memory in AD model mice which might not only be important with regard to AD, but also emphasizes the ability of APPsα to enhance

memory in normal WT mice or to rescue age-dependent impairments in healthy rats (Moreno et al., 2015, Xiong et al., 2017). While the receptor that might be activated by APPsα still remains elusive, APPsα was shown to facilitate tetanically evoked NMDA-R-mediated currents *in vitro* (Taylor et al., 2008) and might therefore compensate for the impaired expression of NMDA-Rs in AD model mice (Snyder et al., 2005). For transmembrane APP an interaction with GluN1/GluN2 NMDA-Rs has been shown in immunoprecipitation experiments leading to increased cell surface expression of receptors *in vitro* (Cousins et al., 2009, Cousins et al., 2013), while evidence for a role of APPsα within that mechanism is currently missing. Moreover supporting the role of APPsα in mechanisms of plasticity is the increase of synaptodendritic *de novo* protein synthesis upon recAPPsα administration (Claasen et al., 2009), which is inhibited in AD (Li et al., 2011). However, a recent study suggested that cell surface holo-APP is a receptor binding APPsα and conferring neuroprotection via a G protein-coupled activation of the Akt stress signaling pathway (Milosch et al., 2014). In the latter study holo-APP was assumed as a receptor mediating pro-survival and anti-apoptotic signaling, while the experiments of Hick and colleagues (2015) indicate that APPsα is able to mediate the rescue of LTP on an acute time-scale in the absence of APP and APLP2 using APP/APLP2 mutant mice. Despite the fact that the complete mechanism how APPsα might mediate its trophic properties is still not fully clarified, it provides evidence that synaptic repair might be an option to ameliorate pathophysiology and to improve the clinical outcome as an alternative to eliminate toxic factors as a recent concept (Lu et al., 2013). Synapses have a highly plastic nature so that synaptic dysfunction and loss of synapses are reversible processes and APPsα might be a potential therapeutic agent to rescue synaptic failures even in the presence of pathological symptoms. In this regard the review of Mockett *et.* al 2017 discusses the potential to either enhance α-secretase mediated APP processing or to upregulate APPsα expression by other means as an alternative to the promising results gained with anti-Aβ antibody treatments of AD patients (Sevigny et al., 2016). Besides in AD therapy, the administration of APPsα was also shown to protect against acute forms of brain injury *in vivo* like transient ischemia (Smith-Swintosky et al., 1994) or traumatic brain injury (Corrigan et al., 2012, Corrigan et al., 2014, Plummer et al., 2016) reinforcing the potency of APPsα as therapeutic tool.

Despite the fact that APPsβ lacks only 16 amino acids compared to APPsα, the physiological function of this extracellular APP domain has been less attended so far. Only a few studies took APPsβ as control condition when investigating the biological functions of APPsα. Importantly, the neuroprotective properties of APPsα in comparison to APPsβ are best demonstrated by the study of Li and colleagues (2010). While the knock-in of APPsα rescued the lethality of APP/APLP2-DKO mice, APPsβ was ineffective (Li et al., 2010). With regard to synaptic plasticity, APPsβ cannot restore the LTP defect of APP/APLP2 cDKO mice (Hick et al., 2015) and does not facilitate LTP recorded *in vivo* within the DG of rats (Taylor et al., 2008). APPsβ was further shown to have no influence on synaptic protein synthesis (Claasen et al., 2009). Consistent with the functional readout on synapses, Tyan et al. (2012) showed that only APPsα but not APPsβ partially rescued defects in dendritic spine number and morphology of primary hippocampal neurons from APP-KO mice. In this thesis I consistently observed that APPsβ does not influence synaptic transmission neither in APP-deficient mice (chapter 3.5.3), in AD model mice (chapter 3.6.2) nor in WTs (chapter 3.6.3). I further showed that APPsβ was ineffective to restore spine density in APP/PS1ΔE9 tg mice and moreover slightly reduced spine numbers in WT animals.

4.6 The APP Family is Essential for Intact Ca^{2+} Homeostasis

Neuronal calcium (Ca^{2+}) signaling is an important prerequisite for normal cell function and impairments in Ca^{2+} handling have been implicated in a variety of neurodegenerative disorders including AD. Alterations in Ca^{2+} homeostasis have therefore been reported within several *in vitro* and *in vivo* studies of mice expressing the AD associated transgenes, presenilins (PS) and APP. It was shown that mutations within the genes causing familial AD affect endoplasmatic reticulum (ER) Ca^{2+} signaling by overloading ER stores resulting in exaggerated Ca^{2+} release (Etcheberrigaray et al., 1998). In 3x transgenic AD mice, the PSEN1-M146V mutation augmented Ca^{2+} release from IP_3- and caffeine-gated stores in hippocampal and cortical neurons (Stutzmann et al., 2004, Stutzmann et al., 2006). Moreover, fibroblasts derived from AD patients carrying the Swedish APP-K670N/M671L double mutation, showed reduced bombesin-induced intracellular Ca^{2+} elevations compared to controls (Gibson et al., 1997) *in vitro*. *In vivo* Ca^{2+} imaging experiments performed on aged APP transgenics carrying the 2567 mutation and on APP/PS1ΔE9 mice revealed that neurons in close proximity to Aβ plaques were overloaded with Ca^{2+} when compared to controls (Kuchibhotla et al., 2008). The intracellular increase of Ca^{2+} results from pores in the cell membrane formed by Aβ and are further caused by an increase in the conductance of Ca^{2+} channels (Arispe et al., 1993, LaFerla, 2002). Under resting conditions, cytosolic Ca^{2+} is maintained at low nanomolar concentrations by a variety of pumps, buffers and transport mechanisms. Ca^{2+} entry into the cytosol is strictly regulated and originates from one of two major sources: the extracellular fluid by an entry across the plasma membrane through receptor-, voltage- and store-operated channels as well as Ca^{2+} exchangers and second from intracellular stores such as the ER and mitochondria (Berridge, 2010). Ca^{2+} signaling is essential to support synaptic function and transmission and as learning and memory are based on functional synapses and intact synaptic transmission which is impaired in AD and APP mutant mice, the APP gene family might indeed play an important role. The Ca^{2+}-Imaging experiments I performed in this thesis emphasize a role for APP/APLPs to support Ca^{2+} homeostasis. Thereby I chemically induced LTP using glycine, a NMDA-R agonist, on a timescale that was comparable to my electrophysiological recordings. Glycine stimulation resulted in a strong and maintained increase of Ca^{2+} signals recorded at t0, t10 and t40 when compared to ratios obtained from spontaneous activity at baseline time-points in littermate control cultures (Figure 3.14). Evidence and support for a long-lasting increase in synaptic strength following a brief application of high concentrations of glycine comes from studies that applied the NMDA-R agonist in acute hippocampal slices and observed increased synaptic potentiation upon glycine treatment when compared to tetanus-induced LTP (Shahi and Baudry, 1993, Shahi et al., 1993). The same group showed that the glycine protocol represents tetanically induced LTP in OHCs (Musleh et al., 1997) which I could reproduce in our lab (Michaelsen-Preusse et al., 2016) and transferred it finally to primary dissociated hippocampal cultures.

The analysis of NexCre cDKO primary hippocampal cultures revealed impairments in Ca^{2+} dynamics before and upon chemically induced LTP by glycine when they were transduced with the control AAV-Venus virus, but restored upon APPsα overexpression (Figure 3.14). These results are consistent with the electrophysiological readouts of APP/APLP2 cDKOs upon viral-vector injection and suggest that altered Ca^{2+} signaling might indeed contribute to impaired synaptic plasticity (Figure 3.9), while the frequency of spontaneous Ca^{2+} signals itself was not altered between genotypes (Figure 3.16). Furthermore, it needs to be considered, that NexCre cDKO neurons show reduced spine numbers with a shift from mature mushroom spines towards immature stubby ones which is further attended by reduced PSD95 levels

(Hick et al., 2015). Consistently, impaired spine density was observed in NexCre cDKO cultures transduced with the control virus, while APPsα overexpression rescued spine numbers to the level quantified in littermate controls (Figure 3.19B). Thus fewer and less functional spines might cause reductions in synaptic activity as the neuronal network is kept in a more immature state and is not as connected as in littermate cultures being in the end visible by decreased Ca^{2+} responses. Consistently, Ca^{2+} signaling in APP deficient astrocytes (Hamid et al., 2007, Linde et al., 2011) and fibroblasts (Leissring et al., 2002) was shown to be dysregulated. Further evidence comes from a mouse model of murine Down syndrome (Cardenas et al., 2002). In these mice the APP gene located on chromosome 16 is present in triplicate. Thus, a gene dosage effect caused higher intracellular Ca^{2+} concentrations paralleling the effects observed in the AD mouse model (Kuchibhotla et al., 2008). When APP expression was reduced to only 40% in the mouse model of Down syndrome a significant reduction in Ca^{2+} responses was observed already before cLTP induction (Rojas et al., 2008). This confirms reduced basal Ca^{2+} levels of NexCre cDKO mice at time points of spontaneous activity without any stimulation (Figure 3.14). In conclusion the results show that APP and APLP2 are essential to maintain intracellular Ca^{2+} concentrations at time-points of spontaneous activity. Interestingly, the cDKO cultures were able to respond to the same extent with an increase in Ca^{2+} responses as observed for littermate cultures when I normalized cLTP responses to resting Ca^{2+} amounts supporting that despite described morphological alterations, NexCre cDKO neurons were as functional as littermate cultures regarding the ability to be stimulated. Consistently to what I observed in the electrophysiological recordings, APPsα rescued the cLTP deficit and moreover the impaired Ca^{2+} homeostasis at time-points of spontaneous activity, possibly by stabilizing intracellular Ca^{2+} levels (Mattson et al., 1993, Ma et al., 2009). Recently, Hefter et al. (2016) reported altered Ca^{2+} homeostasis in APP deficient mice. A transient induction of hypoxia disrupted electrical activity at the cellular and network level. APP-KO slices exhibited an increased rise of intracellular Ca^{2+}, a faster loss of function as well as a higher incidence of spreading behavior so that the functional recovery upon re-oxygenation was significantly impaired. However, the selective expression of APPsα was able to rescue most of the alterations as well as the pharmacological inhibition of L-type Ca^{2+} channels (Hefter et al., 2016). Based on these results and the ones gained in this thesis, APPsα can indeed be seen as the neurotrophic functional domain of APP. Moreover, both studies highlight that not only morphological differences might contribute to disturbed Ca^{2+} handling in APP deficient mice, but that alterations within receptors regulating the entrance and efflux of Ca^{2+} as well as the function of internal Ca^{2+} stores might be regulated by APP family proteins.

4.6.1 Alterations in ER Ca^{2+} Stores Contribute to Impaired cLTP in NexCre cDKO Mice

In order to mechanistically address the question which receptors or internal stores might by affected upon APP and APLP2 deletion, I performed Ca^{2+}-Imaging experiments in the presence of the sarco-/endoplasmatic reticulum calcium ATPase (SERCA) blocker cyclopiazonic acid (CPA). The main internal Ca^{2+} stores in neurons are located in the ER and mitochondria. ER stores are refilled with cytosolic Ca^{2+} by the SERCA-ATPase, while the depletion of Ca^{2+} from stores is mediated by three different ways (LaFerla, 2002). Either active G-protein coupled receptors on the plasma membrane induce an inositol-1,4,5-trisphosphate (IP_3) dependent activation of IP_3-receptors or the influx of extracellular Ca^{2+} into the cytosol triggers ryanodine receptors that in turn induce a Ca^{2+} induced Ca^{2+} release (CiCR) from the ER. The third option is mediated by ER leak channels composed of Sec61 core complexes enabling Ca^{2+} the efflux from the ER into the cytosol (S. Samtleben et al., 2013). The depletion of ER Ca^{2+} stores initiates

the influx of extracellular Ca^{2+} into the cytosol via store-operated Ca^{2+} channels (SOCCs) located in the plasma membrane. Hence, accumulated cytosolic Ca^{2+} is replenished and taken up in the ER by the SERCA ATPase. This mechanism is called capacitive Ca^{2+} entry and known to be implicated in the pathogenesis of AD (LaFerla, 2002; Leissring et al., 2000). Blocking of SERCA-ATPase activity during cLTP induction significantly increased Ca^{2+} responses in NexCre cDKO cultures transduced with the control AAV-Venus virus (Figure 3.15), while it prevented a stable increase in Ca^{2+} responses in littermate or NexCre cDKOs that were treated with AAV-APPsα. Based on these observations, altered SERCA-ATPase activity in NexCre cDKO cultures can be assumed. A possible mechanism might be that the ATPase pumps quite efficiently cytosolic Ca^{2+} in the ER so that cytosolic Ca^{2+} amounts are significantly lower in NexCre cDKO cultures. What can be excluded are potential effects of altered Ca^{2+} buffer protein expression or function as these are mainly located in inhibitory neurons of the hippocampus that comprise only 5 to 10 % in the cultures and their expression would take too long upon cLTP induction to have any influence on the experimental readout. However, evidence for the need of internal stores to maintain enhanced Ca^{2+} responses and to synchronize the network are based on the observations gained for littermates upon cLTP induction in the presence of CPA. The maintenance of cLTP was abolished upon CPA co-administration as well as a stable reduction in spontaneous Ca^{2+} signal frequency indicating no synchronization of the neuronal network. The Ca^{2+} store depletion is a rapid process and free Ca^{2+} from the ER and cytosol was shown to be continuously lost across the plasma membrane (Samtleben et al., 2015). Thus Samtleben and colleagues propose that a prominent Ca^{2+} influx mechanism must be present to maintain ER Ca^{2+} levels at rest. This might be mediated by the already mentioned store-operated Ca^{2+} entry that is mediated by SOCCs. Continuous SOCC mediated Ca^{2+} entry does not need a stimulus and was shown to be present in neurons enabling them to balance cytosolic and ER Ca^{2+} levels and to maintain a moderate Ca^{2+} concentration in the ER which is essential to sustain Ca^{2+} oscillations (Pizzo et al., 2001, Samtleben et al., 2013). Interestingly, it was shown that presenilins (PSs) cause an ER Ca^{2+} leak function which is abundant in hippocampal neurons (Tu et al., 2006, Shilling et al., 2012). Defects in ER Ca^{2+} leakage were partially rescued by genetic removal of PSs causing a cell-autonomous compensatory upregulation of ryanodine receptors (Zhang et al., 2010). Further the study of Linde and colleagues using APP-KO astrocytes showed that the leakage of ER Ca^{2+} was significantly smaller in freshly plated astrocytes of APP-KOs or in WT cultures following the siRNA mediated Knock-down of APP. Moreover, SOCC mediated Ca^{2+} entry was significantly impaired in APP-KO astrocytes and further reflected by downregulated expression of TRPC1 (C-type transient receptor potential) and Orai1 proteins, essential components of SOCCs (Liou et al., 2007, Luik et al., 2008, Malarkey et al., 2008, Linde et al., 2011). Zeiger et al. (2013) showed a dramatic reduction in Aβ secretion using a mutant of the luminal EF-hand domain of stromal interaction molecule 1 (STIM1), STIM1D76A, which leads to the constitutive activation of Ca^{2+} influx even when ER stores were depleted (Liou et al., 2005). In conclusion, Ca^{2+} influx pathways might have multiple effects on APP maturation and processing and are thus essential for Ca^{2+} homeostasis. With regard to AD, the familial linked PS1 mutation increases Aβ production and was found to decrease SOCC activity (Yoo et al., 2000). Further it was shown that STIM2 regulates neuronal SOCCs in postsynaptic spines which is essential for the stability of mushroom-type spines by maintaining the activity of synaptically expressed CamKII. In a mouse model of AD that carries a PS mutation downregulated STIM2-SOCC-CamKII activity has been observed and resulted in a drastic loss of hippocampal spines (Sun et al., 2014). Additionally also the Knock-In of APP caused the loss of mushroom spine on hippocampal neurons as a result of accumulated extracellular $A\beta_{42}$ in the cell culture media

(Zhang et al., 2015b). Zhang and colleagues (2015) argue that Aβ over-activates mGluR5 receptors in APP-KI neurons that cause on the one hand an elevation of ER Ca^{2+} levels and on the other hand a compensatory downregulation of STIM2 that in turn impairs synaptic SOCC function and CamKII activity. Overall recent publications point toward an essential function of SOCC activity to support normal Ca^{2+} handling in neurons which might be regulated in different ways by APP family proteins and their proteolytic domains.

4.6.2 Evidence for Altered SOCC-Activity in NexCre cDKO Cultures

Several studies indicate that neuronal SOCC function is indispensable for Ca^{2+} homeostasis (Pizzo et al., 2001, Samtleben et al., 2013) and that APP family members might influence SOCC activity (Linde et al., 2011, Zhang et al., 2015b) as for a number of AD models impaired Ca^{2+} handling has been reported (Yoo et al., 2000, Sun et al., 2014, Zhang et al., 2015a). In order to investigate if SOCC activity might be altered upon APP and APLP2 conditional deletion, I performed Ca^{2+}-Imaging experiments in the presence of the sarco-/endoplasmic reticulum calcium ATPase (SERCA) blocker cyclopiazonic acid (CPA) and modified the extracellular Ca^{2+} concentration in the perfusion medium. The simple reduction of external Ca^{2+} from around 4 to 1 mM resulted in a decline of spontaneously occuring cytosolic Ca^{2+} elevations for NexCre cDKOs transduced with AAV-Venus and APPsα. Interestingly, while the re-addition of external Ca^{2+} revealed a full recovery of intracellular Ca^{2+} amounts in the presence of APPsα at time-points of spontaneous activity, only a partial recovery was observed in NexCre cDKOs treated with the control virus (Figure 3.17A-C). To examine then moreover the contribution of intracellular ER Ca^{2+} stores within that refilling process, ER stores were unloaded by co-administration of the SERCA-ATPase blocker CPA while cells were perfused with HBSS containing low Ca^{2+} (1.3 mM). The observation of spontaneous Ca^{2+} signals evoked by restoration of external Ca^{2+} when the SERCA ATPase of the ER was moreover blocked allowed the examination of the SOCC dependent Ca^{2+} entry (Parekh and Putney, 2005, Linde et al., 2011). Remarkably, I was only able to observe a SOCC dependent Ca^{2+} entry in NexCre cDKOs transduced with AAV-syn-APPsα-Venus, while cDKOs treated with the control virus failed to restore basal Ca^{2+} levels at time-points of spontaneous activity (Figure 3.17A-C). NexCre+AAV-syn-Venus cultures showed even a small decline in the change of intracellular Ca^{2+} levels during spontaneous activity indicating that the SOCC-dependent Ca^{2+} entry might be impaired upon APP and APLP2 deletion. However, it needs to be taken into account that changes in Ca^{2+} dynamics occur on a very rapid timescale in neurons and are regulated by a variety of channels so that important Ca^{2+} dynamic contributors might not be addressable with this method.

In another experimental set I moreover excluded the impact of voltage-gated Ca^{2+} channels (VGCCs) which are expressed in the cell membrane and are almost exclusively conductive for Ca^{2+} (Zuccotti et al., 2011). When VGCCs were blocked by co-application of Nifedipine no differences in the change of Ca^{2+} levels between cultures treated with control and APPsα virus was detectable when simply reducing and restoring extracellular Ca^{2+} amounts in the perfusion medium (Figure 3.17D-F). Quantification of Ca^{2+} concentrations revealed for both cultures only a partial restoration in the change of intracellular Ca^{2+} amounts at spontaneous activity. These results indicate that the additional increase observed for APPsα transduced cultures upon external Ca^{2+} reconstitution without VGCC blocker might be mediated by enhanced VGCC function and are maybe driven by the non-amyloidogenic APP extracellular domain. From the literature it is known that the expression of $Ca_v1.2$ L-type VGCC channels is driven by Aβ (Webster et al., 2006) and its blockage has been identified as a potential pharmacotherapeutical target

for AD (Anekonda and Quinn, 2011, Lovell et al., 2015). APPsα contains the sequence of Aβ which might alter $Ca_v1.2$ function while APP deficiency prevented the production of Aβ in NexCre cultures. Moreover, it was shown that APP directly regulates $Ca_v1.2$ channels in cultured GABAergic neurons of the hippocampus and striatum with APP deletion leading to aberrant activity of $Ca_v1.2$ that resulted in altered short-term plasticity (Yang et al., 2009). Further evidence for APP to modulate VGCC function is based on impaired Ca^{2+} oscillations upon human APP expression in rat primary cortical neurons (Santos et al., 2009) and by the neuroprotective role of APP to regulate VGCC activity in response to hypoxia (Hefter et al., 2016). Nevertheless, a balanced activity of Ca^{2+} channels to maintain Ca^{2+} homeostasis is the key role that might be regulated by APP/APLP2 and their proteolytic peptides in different ways. APPsα is in this regard the extracellular domain mediating neuroprotective and neurotrophic effects, whereas amyloidogenic cleavage products cause harmful events. This in turn implicates that a shift in APP cleavage disturbs the balance and causes a loss of neuroprotective functions driving disease development.

4.7 The 16 Amino Acid Difference between APPsα and APPsβ Mediates the Neurotrophic Peptide Functions

Compared to APPsα, APPsβ lacks the 16 amino acids present at the N-Terminus of the Aβ peptide (Chasseigneaux et al., 2011). Only a few studies in the literature focused on the physiological role of APPsβ and most of them could not show any effect when compared to APPsα (Copanaki et al., 2010, Hick et al., 2015). Nevertheless, trophic effects for APPsβ have been reported albeit overall less efficient than those exerted by APPsα. APPsβ seems to be more potent than APPsα to induce neuronal differentiation of pluripotent stem cells (Freude et al., 2011) and was demonstrated to stimulate the activation of microglia (Barger and Harmon, 1997) as well to promote neurite outgrowth *in vitro* (Chasseigneaux et al., 2011). Notably, APPsβ was shown to undergo further cleavage resulting in a 35 kDa APP peptide which binds to the death receptor 6 resulting in the activation of caspase-6 and thus mediating deleterious effects resulting in neurodegeneration (Nikolaev et al., 2009). Evidence pointing to a role of APP fragments in processes of synaptic plasticity arose from the observations that APP processing by α- and β-secretase is activity-dependent (Nitsch et al., 1993, Fazeli et al., 1994, Kamenetz et al., 2003, Gakhar-Koppole et al., 2008) and can thus be potentiated by neuronal depolarization or high frequency stimulation (HFS). APPsα was shown to facilitate LTP within several studies, while APPsβ had no influence (Ishida et al., 1997, Taylor et al., 2008, Hick et al., 2015, Moreno et al., 2015). Together with the findings I gained within that thesis, that viral driven overexpression of APPsα rescued LTP in APP/APLP2 deficient and AD model mice and restored moreover impairments in Ca^{2+} homeostasis, several evidence exists that APPsα is crucial for normal synaptic function. The 16 C-terminal amino acids present in APPsα but not in APPsβ could cause a shift in functionality or alter the conformation of the peptide in a critical way and thereby modify its signaling (Ludewig and Korte, 2017). To elucidate if the functional differences arise from the additional amino acids, I investigated the role of the synthetized 16 amino acid murine peptide (recAβ1-16) in processes of activity-dependent synaptic plasticity (chapter 3.8). The exogenous application of recAβ1-16 was sufficient to restore the pronounced deficit in induction and maintenance of LTP in NexCre cDKO mice (Figure 3.20A, B) that was still present in acute slices treated with the scrambled and therefore inactive version of the peptide. Moreover, recAβ1-16 enhanced like APPsα short-term plasticity without altering the function of the postsynapse indicating that Aβ1-16 might be

the neurotrophic domain of APPsα as also the direct functional comparison of APPsα and recAβ1-16 revealed no modulatory differences in electrophysiological recordings (Figure 3.23). In line with these observations are the reports concerning the short functional domain Aβ1-15 (or Aβ1-16) which was shown to be generated by successive α- and β-secretase activity (Portelius et al., 2011). Aβ1–15 significantly enhanced PTP and LTP without altering baseline synaptic transmission at femtomolar concentrations, while higher amounts had no effect on hippocampal LTP (Lawrence et al., 2014). A dose-dependent activity was also shown for APPsα, with low picomolar and very high nanomolar concentrations having no effect on *f*EPSP strengthening that is dependent on NMDA-R activity (Taylor et al., 2008, Ryan et al., 2013). Besides the facilitation of LTP by Aβ1-15 in WT mice, Lawrence and colleagues (2014) further showed that the short APP fragment is able to rescue LTP deficits that are caused by synthetically applied $A\beta_{42}$ or present in APP/PS1 tg AD model mice. The latter supports my results gained following the viral driven overexpression of APPsα in APP/PS1 tg mice which might be caused by the 16 amino acid sequence.

Interestingly, Lawrence *et al.* (2014) documented that Aβ-15 injection in the dorsal hippocampus augmented contextual fear conditioning in wildtype mice which was attenuated by the co-administration of the nicotinic antagonist methylcaconitine (MLA). While for APPsα a putative receptor still remains elusive two possible targets at the synapse have been proposed for the amyloidogenic Aβ peptide itself. Aβ contains like APPsα the 16 amino acids that are absent in APPsβ. Potential targets are the nicotinic acetylcholine receptor (nAChR; (Wang et al., 2000a, Liu et al., 2001, Pettit et al., 2001) and certain metabotropic glutamate receptors (Chin et al., 2007). The agonist-like action of Aβ regulating synaptic plasticity was suggested to happen at presynaptically expressed nAChRs (Dougherty et al., 2003, Mehta et al., 2009) especially via the alpha-7 subtype (Tong et al., 2011). Consistently, the acute and chronic administration of nicotine enhanced memory (Levin and Simon, 1998) and increased LTP (Fujii et al., 2000) not only in animal models of AD, but was moreover shown to improve cognition in AD patients (Newhouse et al., 1988). Interestingly, Aβ and the α7-nAChR are both present in neuritic plaques and were shown to co-localize in neurons of the cortex in pathological brain material of AD patients (Wang et al., 2000a, Wang et al., 2000b). The α7-nAChR is abundantly expressed in neurons of the basal forebrain which projects to the hippocampus and cortex, the brain areas exhibiting severe plaque pathology in AD (Wang et al., 2000b). Overall, there is strong evidence that α7-nAChR activity plays a critical role in the pathogenesis of AD: Aβ induced LTP deficits were shown to be caused by a deterioration of α7-nAChRs activity (Chen et al., 2006b), while functional α7-nAChRs augment memory formation in the hippocampus of AD mouse models through an acute influx of Ca^{2+} (Hunter et al., 1994, Wang et al., 2000b). In this regard the α7-nAChR might be a possible target also for APPsα and Aβ1-16. Beside MLA also α-Bungarotoxin (α-BTX) is a highly selective antagonist for the α7-nAChR and often administered during acute hippocampal slice recordings (L. Chen, Yamada, Nabeshima, & Sokabe, 2006; Criscuolo, Accorroni, Domenici, & Origlia, 2015; Puzzo et al., 2008). The application of 10 nM α-BTX significantly reduced LTP initially as well as its maintenance confirming that the α7-nAChR is involved in mechanisms of synaptic plasticity under control conditions (Figure 3.21A'', B'') consistently to what is observed in the literature (Chen et al., 2006b, Criscuolo et al., 2015). In contrast, the inhibition of the α7-nAChR interfered only slightly with Aβ1-16 action in APP/APLP2 cDKO mice (Figure 3.21A', B'). Further testing for a presynaptic action of Aβ1-16 by the PPF paradigm revealed that blocking of the α7-nAChR does not alter presynaptic function, neither in the presence of Aβ1-16 nor in LMs (Figure 3.21C',C''). This might be due to the fact that α-BTX treatment might have additional modulatory effects on postsynapses as α7-

nAChRs are also expressed at these synaptic compartments (Orr-Urtreger et al., 1997). Furthermore, the acute inhibition by α-BTX might just have been to short or at the wrong time, so that during the one hour Aβ1-16 pre-incubation already modulatory effects in the hippocampal slices could have happen and thus mask potential effects during the acute inhibition of the α7-nAChR. Conceivable effects could here be the activation of kinases which modulate α7-nAChRs or other receptors. To circumvent this problem, I simultaneously pre-incubated the α7-nAChR blocker α-BTX with Aβ1-16 preventing a possible interaction of Aβ1-16 with the nicotinic receptor already during the one hour pre-incubation period with the peptide alone. This experimental setup showed that the α7-nAChR is a potential target for Aβ1-16 as activity-dependent synaptic plasticity was impaired, while I could not observe any effects regarding baseline synaptic transmission or STP (Figure 3.21). Nevertheless, an important point that needs to be considered are dose-dependent effects that are not only mediated by the APP peptide (Wang et al., 2000a, Taylor et al., 2008, Lawrence et al., 2014), but also by the inhibitors applied (Chen et al., 2006b).

Overall the results obtained by recAPPsα and recAβ1-16 application on acute hippocampal slices of APP/APLP2 deficient mice provide evidence for a neurotrophic role of both peptides, positively modulating synaptic plasticity. With regard to therapeutic treatment of AD, the smaller Aβ1-16 peptide has several advantages. It would be easier to apply than APPsα as direct stereotactical injections needed to deliver the longer peptide into the brain could be circumvented as Aβ1-16 might directly cross the blood-brain-barrier. Thereby a more efficient sequence of action can be achieved. Nevertheless the detailed mode of action of APPsα and Aβ1-16 would need to be first of all to be clarified in detail as the inhibition of α7-nAChR function did not reveal any changes in presynaptic transmission that was clearly modulated by both peptides and so far hypothesized to be the basis for the LTP rescue in APP/APLP2 cDKO and AD mice.

4.8 Conclusion and Outlook

In this thesis I could show an indispensable role of the APP protein family in the rodent CNS during development as well as in the mature and aging brain. The so far less attended, but exclusively neuronal expressed APP homolog APLP1 was shown to have an age-dependent role in maintaining basal synaptic transmission at postsynapses in aged animals. These results highlight that each APP family member has individual roles at synaptic compartments and that impairments at young ages might be compensated by the two other gene members. It would be essential to test whether synaptic alterations are caused by impaired structural or functional plasticity upon APLP1 deletion. Analysis of spine density representing the number of excitatory synapses would indicate if aging decreases the number of active synapses in APLP1-KO mice. Moreover, interaction studies regarding APLP1 and postsynaptic surface receptors like the NMDA-Rs would provide insights about signaling cascades triggered which might be different to the ones by APP and APLP2.

I further successfully reproduced the previously described developmental role of APP and APLP2 in excitatory principle neurons regarding synaptic plasticity. I demonstrated that the additional conditional co-deletion of APLP1 caused an even more severe synaptic phenotype. Beside a highly pronounced deficit in induction and maintenance of LTP, APP cTKO mice yielded heavily impaired basal synaptic transmission at the postsynapse additionally to already altered presynaptic function observed in APP/APLP2 (NexCre) cDKO animals. As I noticed during hippocampal slice preparations alterations in the shape of the hippocampus and massive changes in the CA1-CA3 cell body layer suggesting atrophy, it is necessary to perform a detailed morphological characterization of APP cTKO brains. Impairments in neuronal architecture would influence functional synaptic plasticity and should thus be verified.

One more important finding of this thesis is the interaction of Fe65 family proteins downstream to APP/APLPs. Not only that Fe65/Fe65L1 double deficient mice show a similar phenotype of cortical dysplasia as APP triple KO animals, they also reveal impaired activity-dependent synaptic plasticity when Fe65 and FE65L1 (like APP and APLP2) are co-deleted. It could therefore be assumed that Fe65/Fe65Ls mediate downstream signaling of APP/APLPs at the synapse. Nevertheless, for a complete and clear picture it would be necessary to study additional combined DKOs of APP and Fe65 family members to underscore the role of both and their interaction in the central nervous system.

Another key finding gained within this thesis is the neurotrophic role of the APP extracellular domain APPsα. Exogenous application of recombinant APPsα consistently restored impaired LTP in NexCre cDKO acute hippocampal slices as already reported. Furthermore, the re-expression of APPsα by AAV viruses upon their stereotactic injection rescued activity-dependent synaptic plasticity and restored presynaptic function in the hippocampus of APP/APLP2 cDKO mice. These results indicate that APPsα might modulate the presynaptic transmitter release or increases the amount of vesicles in the ready releasable pool in the presynapse additional to the described facilitation of NMDA-R currents at postsynapses. Moreover, I demonstrated that viral driven expression of APPsα in aged AD model mice, with already established plaque pathology and cognitive impairments, rescued impaired LTP and restored the functionality of the presynapse. Additionally, I showed that APPsα ameliorated spine density in APP/PS1ΔE9 tg mice and NexCre cDKO primary hippocampal cultures. Overall these results emphasize that APPsα is essential for proper neuronal function and that decreased levels of the proteolytic APP peptide might contribute to impairments in activity-dependent synaptic plasticity in rodents. As APPsα re-expression is able to functionally restore synaptic plasticity and rescue spine density, it might be a

potential therapeutic target for AD and other neurodegenerative diseases. The investigations of the 16 amino-acid shorter APPsβ peptide which was comparably re-introduced in the hippocampus of NexCre cDKO mice and AD model mice revealed that it has no potential to rescue deficits in LTP or spine density, highlighting that the functional domain might be located within the short sequence difference of both extracellular APP domains.

Interestingly, I could indeed show that the application of the synthesized amino acid sequence, building the difference between APPsα and APPsβ, enhanced LTP to the same extent like recAPPsα when applied on acute hippocampal slices of NexCre cDKO mice and thus rescued activity-dependent synaptic plasticity in this gene-targeted APP mouse model. As moreover presynaptic function was improved by recAβ1-16 several evidence exists to assume that this amino acid sequence harbors the neurotrophic properties of APPsα and builds the functional difference to APPsβ. Still further work is needed to examine how these 16 amino acids cause the shift in functionality. A thinkable phenomenon might be a conformational change resulting from the C-terminal sequence elongation in APPsα modifying its signaling. To elucidate potential interaction partners of APP proteolytic and functional domains, pull-down assays could be performed with APPsα, APPsβ and Aβ1-16.

The experiments regarding neuronal Ca^{2+} signaling suggest that impairments in Ca^{2+} handling might contribute to a variety of neurodegenerative disorders including AD. I could show that APP and APLP2 deficiency causes severe alterations in Ca^{2+} homeostasis paralleling the impairments in activity-dependent synaptic plasticity. In this regard I demonstrated once again the neuroprotective role of APPsα restoring normal Ca^{2+} levels during time-points of spontaneous activity in NexCre cDKO primary hippocampal cultures. Virally expressed APPsα moreover prevented the deficit in induction and maintenance of chemical LTP in cultured neurons. Besides morphological differences, that are well-characterized for these APP/APLP2 cDKOs also receptors and internal stores balancing intracellular Ca^{2+} levels were shown to be regulated by APP family proteins. In detail, I could show that NexCre cDKO cultures reveal altered SERCA-ATPase activity of the endoplasmatic reticulm (ER). A thinkable mechanism might be that the ATPase pumps quite efficiently cytosolic Ca^{2+} in the ER, so that cytosolic Ca^{2+} amounts are significantly lower in NexCre cDKO cultures. While it seems unlikely that altered Ca^{2+} buffer protein expression contribute to reduced Ca^{2+} levels at rest, Western Blot analysis could reveal if protein expression of calbindin, calretinin, parvalbumin or calmodulin are different in NexCre cDKOs. However, the results gained for littermates upon cLTP induction in the presence of CPA evidence the need of internal stores to maintain enhanced Ca^{2+} responses and to synchronize neuronal networks. Moreover essential is the continuous SOCC mediated Ca^{2+} entry which doesn´t need a stimulus and was shown to be altered in APP/APLP2 deficient cultures. As the SOCC dependent Ca^{2+} influx was shown to be present in neurons enabling them to balance cytosolic and ER Ca^{2+} levels and to maintain a medium-high Ca^{2+} concentration in the ER, Ca^{2+} oscillations might be affected upon APP and APLP2 co-deletion by impaired SOCC function. I could further show that APPsα was able to partially restore SOCC-mediated Ca^{2+} entry and that it might modulate VGCC function *in vitro*. Overall my Ca^{2+} imaging results indicate that a balanced activity of Ca^{2+} channels to maintain Ca^{2+} homeostasis is the key role that might be regulated by APP and APLP2 and their proteolytic peptides in different ways. APPsα is in this regard the extracellular domain mediating neuroprotective and neurotrophic effects, whereas amyloidogenic cleavage products cause harmful events. This in turn implicates that a shift in APP cleavage disturbs the cellular homeostasis and causes a loss of neuroprotective functions driving disease development.

5 References

Abrahamsson T, Lalanne T, Watt AJ, Sjostrom PJ (2016) In Vitro Investigation of Synaptic Plasticity. Cold Spring Harbor protocols 2016:pdb.top087262.

Abramov E, Dolev I, Fogel H, Ciccotosto GD, Ruff E, Slutsky I (2009) Amyloid-beta as a positive endogenous regulator of release probability at hippocampal synapses. Nature neuroscience 12:1567-1576.

Agostini M, Fasolato C (2016) When, where and how? Focus on neuronal calcium dysfunctions in Alzheimer's Disease. Cell Calcium 60:289-298.

Almeida CG, Tampellini D, Takahashi RH, Greengard P, Lin MT, Snyder EM, Gouras GK (2005) Beta-amyloid accumulation in APP mutant neurons reduces PSD-95 and GluR1 in synapses. Neurobiol Dis 20:187-198.

Alzheimer's A (2016) 2016 Alzheimer's disease facts and figures. Alzheimer's & dementia : the journal of the Alzheimer's Association 12:459-509.

Andersen, Morris, Amaral, Bliss, O'Keefe (2006) The Hippocampus Book. Oxford Neuroscience Series.

Anekonda TS, Quinn JF (2011) Calcium channel blocking as a therapeutic strategy for Alzheimer's disease: the case for isradipine. Biochimica et biophysica acta 1812:1584-1590.

Araki Y, Tomita S, Yamaguchi H, Miyagi N, Sumioka A, Kirino Y, Suzuki T (2003) Novel cadherin-related membrane proteins, Alcadeins, enhance the X11-like protein-mediated stabilization of amyloid beta-protein precursor metabolism. The Journal of biological chemistry 278:49448-49458.

Arispe N, Rojas E, Pollard HB (1993) Alzheimer disease amyloid beta protein forms calcium channels in bilayer membranes: blockade by tromethamine and aluminum. Proceedings of the National Academy of Sciences of the United States of America 90:567-571.

Aurnhammer C, Haase M, Muether N, Hausl M, Rauschhuber C, Huber I, Nitschko H, Busch U, Sing A, Ehrhardt A, Baiker A (2012) Universal real-time PCR for the detection and quantification of adeno-associated virus serotype 2-derived inverted terminal repeat sequences. Human gene therapy methods 23:18-28.

Aydin D, Weyer SW, Muller UC (2012) Functions of the APP gene family in the nervous system: insights from mouse models. Exp Brain Res 217:423-434.

Barbagallo AP, Wang Z, Zheng H, D'Adamio L (2011) A single tyrosine residue in the amyloid precursor protein intracellular domain is essential for developmental function. The Journal of biological chemistry 286:8717-8721.

Barger SW, Harmon AD (1997) Microglial activation by Alzheimer amyloid precursor protein and modulation by apolipoprotein E. Nature 388:878-881.

Barger SW, Mattson MP (1996) Participation of gene expression in the protection against amyloid beta-peptide toxicity by the beta-amyloid precursor protein. Annals of the New York Academy of Sciences 777:303-309.

Barnes CA, Rao G, Foster TC, McNaughton BL (1992) Region-specific age effects on AMPA sensitivity: Electrophysiological evidence for loss of synaptic contacts in hippocampal field CA1. Hippocampus 2:457-468.

Barria A, Muller D, Derkach V, Griffith LC, Soderling TR (1997) Regulatory phosphorylation of AMPA-type glutamate receptors by CaM-KII during long-term potentiation. Science (New York, NY) 276:2042-2045.

Barthet G, Georgakopoulos A, Robakis NK (2012) Cellular mechanisms of gamma-secretase substrate selection, processing and toxicity. Progress in neurobiology 98.

Baumkotter F, Wagner K, Eggert S, Wild K, Kins S (2012) Structural aspects and physiological consequences of APP/APLP trans-dimerization. Exp Brain Res 217:389-395.

Berger A, Lorain S, Joséphine C, Desrosiers M, Peccate C, Voit T, Garcia L, Sahel J-A, Bemelmans A-P (2015) Repair of Rhodopsin mRNA by Spliceosome-Mediated RNA Trans-Splicing: A New Approach for Autosomal Dominant Retinitis Pigmentosa. Molecular Therapy 23:918-930.

Berridge MJ (2010) Calcium hypothesis of Alzheimer's disease. Pflugers Archiv : European journal of physiology 459:441-449.

Bliss TV, Collingridge GL (1993) A synaptic model of memory: long-term potentiation in the hippocampus. Nature 361:31-39.

Bliss TV, Lomo T (1973) Long-lasting potentiation of synaptic transmission in the dentate area of the anaesthetized rabbit following stimulation of the perforant path. The Journal of physiology 232:331-356.

Borchelt DR, Ratovitski T, van Lare J, Lee MK, Gonzales V, Jenkins NA, Copeland NG, Price DL, Sisodia SS (1997) Accelerated amyloid deposition in the brains of transgenic mice coexpressing mutant presenilin 1 and amyloid precursor proteins. Neuron 19:939-945.

Borg JP, Ooi J, Levy E, Margolis B (1996) The phosphotyrosine interaction domains of X11 and FE65 bind to distinct sites on the YENPTY motif of amyloid precursor protein. Molecular and cellular biology 16:6229-6241.

Brager DH, Cai X, Thompson SM (2003) Activity-dependent activation of presynaptic protein kinase C mediates post-tetanic potentiation. Nature neuroscience 6:551-552.

Bressler SL, Gray MD, Sopher BL, Hu Q, Hearn MG, Pham DG, Dinulos MB, Fukuchi K, Sisodia SS, Miller MA, Disteche CM, Martin GM (1996) cDNA cloning and chromosome mapping of the human Fe65 gene: interaction of the conserved cytoplasmic domains of the human beta-amyloid precursor protein and its homologues with the mouse Fe65 protein. Human molecular genetics 5:1589-1598.

Briggs CA, Chakroborty S, Stutzmann GE (2017) Emerging pathways driving early synaptic pathology in Alzheimer's disease. Biochemical and biophysical research communications 483:988-997.

Buzsaki G (2002) Theta oscillations in the hippocampus. Neuron 33:325-340.

Cao D, Lu H, Lewis TL, Li L (2007) Intake of sucrose-sweetened water induces insulin resistance and exacerbates memory deficits and amyloidosis in a transgenic mouse model of Alzheimer disease. The Journal of biological chemistry 282:36275-36282.

Cao X, Sudhof TC (2001) A transcriptionally [correction of transcriptively] active complex of APP with Fe65 and histone acetyltransferase Tip60. Science (New York, NY) 293:115-120.

Cardenas AM, Allen DD, Arriagada C, Olivares A, Bennett LB, Caviedes R, Dagnino-Subiabre A, Mendoza IE, Segura-Aguilar J, Rapoport SI, Caviedes P (2002) Establishment and characterization of immortalized neuronal cell lines derived from the spinal cord of normal and trisomy 16 fetal mice, an animal model of Down syndrome. Journal of neuroscience research 68:46-58.

Chasseigneaux S, Dinc L, Rose C, Chabret C, Coulpier F, Topilko P, Mauger G, Allinquant B (2011) Secreted amyloid precursor protein beta and secreted amyloid precursor protein alpha induce axon outgrowth in vitro through Egr1 signaling pathway. PloS one 6:e16301.

Chen CD, Oh SY, Hinman JD, Abraham CR (2006a) Visualization of APP dimerization and APP-Notch2 heterodimerization in living cells using bimolecular fluorescence complementation. Journal of neurochemistry 97:30-43.

Chen L, Yamada K, Nabeshima T, Sokabe M (2006b) alpha7 Nicotinic acetylcholine receptor as a target to rescue deficit in hippocampal LTP induction in beta-amyloid infused rats. Neuropharmacology 50:254-268.

Chen QS, Kagan BL, Hirakura Y, Xie CW (2000) Impairment of hippocampal long-term potentiation by Alzheimer amyloid beta-peptides. Journal of neuroscience research 60:65-72.

Chen QS, Wei WZ, Shimahara T, Xie CW (2002) Alzheimer amyloid beta-peptide inhibits the late phase of long-term potentiation through calcineurin-dependent mechanisms in the hippocampal dentate gyrus. Neurobiology of learning and memory 77:354-371.

Chenuaud P, Larcher T, Rabinowitz JE, Provost N, Cherel Y, Casadevall N, Samulski RJ, Moullier P (2004) Autoimmune anemia in macaques following erythropoietin gene therapy. Blood 103:3303-3304.

Cheung HN, Dunbar C, Morotz GM, Cheng WH, Chan HY, Miller CC, Lau KF (2014) FE65 interacts with ADP-ribosylation factor 6 to promote neurite outgrowth. FASEB journal : official publication of the Federation of American Societies for Experimental Biology 28:337-349.

Chin JH, Ma L, MacTavish D, Jhamandas JH (2007) Amyloid beta protein modulates glutamate-mediated neurotransmission in the rat basal forebrain: involvement of presynaptic neuronal nicotinic acetylcholine and metabotropic glutamate receptors. The Journal of neuroscience : the official journal of the Society for Neuroscience 27:9262-9269.

Chow WN, Cheung HN, Li W, Lau KF (2015) FE65: Roles beyond amyloid precursor protein processing. Cellular & molecular biology letters 20:66-87.

Ciesielska A, Hadaczek P, Mittermeyer G, Zhou S, Wright JF, Bankiewicz KS, Forsayeth J (2013) Cerebral infusion of AAV9 vector-encoding non-self proteins can elicit cell-mediated immune responses. Molecular therapy : the journal of the American Society of Gene Therapy 21:158-166.

Citri A, Malenka RC (2007) Synaptic Plasticity: Multiple Forms, Functions, and Mechanisms. Neuropsychopharmacology 33:18-41.

Claasen AM, Guevremont D, Mason-Parker SE, Bourne K, Tate WP, Abraham WC, Williams JM (2009) Secreted amyloid precursor protein-alpha upregulates synaptic protein synthesis by a protein kinase G-dependent mechanism. Neuroscience letters 460:92-96.

Copanaki E, Chang S, Vlachos A, Tschape JA, Muller UC, Kogel D, Deller T (2010) sAPPalpha antagonizes dendritic degeneration and neuron death triggered by proteasomal stress. Molecular and cellular neurosciences 44:386-393.

Corrigan F, Thornton E, Roisman LC, Leonard AV, Vink R, Blumbergs PC, van den Heuvel C, Cappai R (2014) The neuroprotective activity of the amyloid precursor protein against traumatic brain injury is mediated via the heparin binding site in residues 96-110. Journal of neurochemistry 128:196-204.

Corrigan F, Vink R, Blumbergs PC, Masters CL, Cappai R, van den Heuvel C (2012) sAPPα rescues deficits in amyloid precursor protein knockout mice following focal traumatic brain injury. Journal of neurochemistry 122:208-220.

Cousins SL, Dai W, Stephenson FA (2015) APLP1 and APLP2, members of the APP family of proteins, behave similarly to APP in that they associate with NMDA receptors and enhance NMDA receptor surface expression. Journal of neurochemistry 133:879-885.

Cousins SL, Hoey SE, Anne Stephenson F, Perkinton MS (2009) Amyloid precursor protein 695 associates with assembled NR2A- and NR2B-containing NMDA receptors to result in the enhancement of their cell surface delivery. Journal of neurochemistry 111:1501-1513.

Cousins SL, Innocent N, Stephenson FA (2013) Neto1 associates with the NMDA receptor/amyloid precursor protein complex. Journal of neurochemistry 126:554-564.

Criscuolo C, Accorroni A, Domenici L, Origlia N (2015) Impaired synaptic plasticity in the visual cortex of mice lacking alpha7-nicotinic receptor subunit. Neuroscience 294:166-171.

Dahms SO, Hoefgen S, Roeser D, Schlott B, Guhrs KH, Than ME (2010) Structure and biochemical analysis of the heparin-induced E1 dimer of the amyloid precursor protein. Proceedings of the National Academy of Sciences of the United States of America 107:5381-5386.

Dawkins E, Small DH (2014) Insights into the physiological function of the beta-amyloid precursor protein: beyond Alzheimer's disease. Journal of neurochemistry 129:756-769.

DeBoer SR, Dolios G, Wang R, Sisodia SS (2014) Differential release of beta-amyloid from dendrite- versus axon-targeted APP. The Journal of neuroscience : the official journal of the Society for Neuroscience 34:12313-12327.

Del Prete D, Lombino F, Liu X, D'Adamio L (2014) APP is cleaved by Bace1 in pre-synaptic vesicles and establishes a pre-synaptic interactome, via its intracellular domain, with molecular complexes that regulate pre-synaptic vesicles functions. PloS one 9:e108576.

Del Turco D, Paul MH, Schlaudraff J, Hick M, Endres K, Müller UC, Deller T (2016) Region-Specific Differences in Amyloid Precursor Protein Expression in the Mouse Hippocampus. Frontiers in Molecular Neuroscience 9.

Demuro A, Parker I, Stutzmann GE (2010) Calcium signaling and amyloid toxicity in Alzheimer disease. The Journal of biological chemistry 285:12463-12468.

Deupree DL, Bradley J, Turner DA (1993) Age-related alterations in potentiation in the CA1 region in F344 rats. Neurobiology of Aging 14:249-258.

Dobrunz LE, Huang EP, Stevens CF (1997) Very short-term plasticity in hippocampal synapses. Proceedings of the National Academy of Sciences of the United States of America 94:14843-14847.

Dobrunz LE, Stevens CF (1997) Heterogeneity of release probability, facilitation, and depletion at central synapses. Neuron 18:995-1008.

Dougherty JJ, Wu J, Nichols RA (2003) Beta-amyloid regulation of presynaptic nicotinic receptors in rat hippocampus and neocortex. The Journal of neuroscience : the official journal of the Society for Neuroscience 23:6740-6747.

Eggert S, Paliga K, Soba P, Evin G, Masters CL, Weidemann A, Beyreuther K (2004) The proteolytic processing of the amyloid precursor protein gene family members APLP-1 and APLP-2 involves alpha-, beta-, gamma-, and epsilon-like cleavages: modulation of APLP-1 processing by n-glycosylation. The Journal of biological chemistry 279:18146-18156.

Eichenbaum H (2004) Hippocampus: cognitive processes and neural representations that underlie declarative memory. Neuron 44:109-120.

El Haj M, Antoine P, Amouyel P, Lambert JC, Pasquier F, Kapogiannis D (2016) Apolipoprotein E (APOE) epsilon4 and episodic memory decline in Alzheimer's disease: A review. Ageing research reviews 27:15-22.

Elmore S (2007) Apoptosis: a review of programmed cell death. Toxicologic pathology 35:495-516.

Engert F, Bonhoeffer T (1999) Dendritic spine changes associated with hippocampal long-term synaptic plasticity. Nature 399:66-70.

Epis R, Marcello E, Gardoni F, Vastagh C, Malinverno M, Balducci C, Colombo A, Borroni B, Vara H, Dell'Agli M, Cattabeni F, Giustetto M, Borsello T, Forloni G, Padovani A, Di Luca M (2010) Blocking ADAM10 synaptic trafficking generates a model of sporadic Alzheimer's disease. Brain : a journal of neurology 133:3323-3335.

Etcheberrigaray R, Hirashima N, Nee L, Prince J, Govoni S, Racchi M, Tanzi RE, Alkon DL (1998) Calcium responses in fibroblasts from asymptomatic members of Alzheimer's disease families. Neurobiol Dis 5:37-45.

Fanutza T, Del Prete D, Ford MJ, Castillo PE, D'Adamio L (2015) APP and APLP2 interact with the synaptic release machinery and facilitate transmitter release at hippocampal synapses. eLife 4:e09743.

Farrer LA, Cupples LA, Haines JL, Hyman B, Kukull WA, Mayeux R, Myers RH, Pericak-Vance MA, Risch N, van Duijn CM (1997) Effects of age, sex, and ethnicity on the association between apolipoprotein E genotype and Alzheimer disease. A meta-analysis. APOE and Alzheimer Disease Meta Analysis Consortium. Jama 278:1349-1356.

Fazeli MS, Breen K, Errington ML, Bliss TV (1994) Increase in extracellular NCAM and amyloid precursor protein following induction of long-term potentiation in the dentate gyrus of anaesthetized rats. Neuroscience letters 169:77-80.

Fernandez MA, Klutkowski JA, Freret T, Wolfe MS (2014) Alzheimer presenilin-1 mutations dramatically reduce trimming of long amyloid beta-peptides (Abeta) by gamma-secretase to increase 42-to-40-residue Abeta. The Journal of biological chemistry 289:31043-31052.

Fol R, Braudeau J, Ludewig S, Abel T, Weyer SW, Roederer JP, Brod F, Audrain M, Bemelmans AP, Buchholz CJ, Korte M, Cartier N, Muller UC (2016) Viral gene transfer of APPsalpha rescues synaptic failure in an Alzheimer's disease mouse model. Acta neuropathologica 131:247-266.

Fratiglioni L, Ahlbom A, Viitanen M, Winblad B (1993) Risk factors for late-onset Alzheimer's disease: a population-based, case-control study. Annals of neurology 33:258-266.

Freude KK, Penjwini M, Davis JL, LaFerla FM, Blurton-Jones M (2011) Soluble amyloid precursor protein induces rapid neural differentiation of human embryonic stem cells. The Journal of biological chemistry 286:24264-24274.

Fujii S, Ji Z, Sumikawa K (2000) Inactivation of alpha7 ACh receptors and activation of non-alpha7 ACh receptors both contribute to long term potentiation induction in the hippocampal CA1 region. Neuroscience letters 286:134-138.

Fukunaga K, Muller D, Miyamoto E (1995) Increased phosphorylation of Ca2+/calmodulin-dependent protein kinase II and its endogenous substrates in the induction of long-term potentiation. The Journal of biological chemistry 270:6119-6124.

Furukawa K, Sopher BL, Rydel RE, Begley JG, Pham DG, Martin GM, Fox M, Mattson MP (1996) Increased activity-regulating and neuroprotective efficacy of alpha-secretase-derived secreted amyloid precursor protein conferred by a C-terminal heparin-binding domain. Journal of neurochemistry 67:1882-1896.

Gakhar-Koppole N, Hundeshagen P, Mandl C, Weyer SW, Allinquant B, Muller U, Ciccolini F (2008) Activity requires soluble amyloid precursor protein alpha to promote neurite outgrowth in neural stem cell-derived neurons via activation of the MAPK pathway. The European journal of neuroscience 28:871-882.

Gant JC, Sama MM, Landfield PW, Thibault O (2006) Early and simultaneous emergence of multiple hippocampal biomarkers of aging is mediated by Ca2+-induced Ca2+ release. The Journal of neuroscience : the official journal of the Society for Neuroscience 26:3482-3490.

Gao G, Lebherz C, Weiner DJ, Grant R, Calcedo R, McCullough B, Bagg A, Zhang Y, Wilson JM (2004) Erythropoietin gene therapy leads to autoimmune anemia in macaques. Blood 103:3300-3302.

Gibson GE, Vestling M, Zhang H, Szolosi S, Alkon D, Lannfelt L, Gandy S, Cowburn RF (1997) Abnormalities in Alzheimer's disease fibroblasts bearing the APP670/671 mutation. Neurobiol Aging 18:573-580.

Giese KP, Fedorov NB, Filipkowski RK, Silva AJ (1998) Autophosphorylation at Thr286 of the alpha calcium-calmodulin kinase II in LTP and learning. Science (New York, NY) 279:870-873.

Goebbels S, Bormuth I, Bode U, Hermanson O, Schwab MH, Nave KA (2006) Genetic targeting of principal neurons in neocortex and hippocampus of NEX-Cre mice. Genesis (New York, NY : 2000) 44:611-621.

Golgi C, Bentivoglio M, Swanson L (2001) On the fine structure of the pes Hippocampi major (with plates XIII-XXIII). 1886. Brain Res Bull 54:461-483.

Guenette S, Chang Y, Hiesberger T, Richardson JA, Eckman CB, Eckman EA, Hammer RE, Herz J (2006) Essential roles for the FE65 amyloid precursor protein-interacting proteins in brain development. Embo j 25:420-431.

Guo Q, Li H, Gaddam SS, Justice NJ, Robertson CS, Zheng H (2012a) Amyloid precursor protein revisited: neuron-specific expression and highly stable nature of soluble derivatives. The Journal of biological chemistry 287:2437-2445.

Guo Q, Robinson N, Mattson MP (1998) Secreted beta-amyloid precursor protein counteracts the proapoptotic action of mutant presenilin-1 by activation of NF-kappaB and stabilization of calcium homeostasis. The Journal of biological chemistry 273:12341-12351.

Guo Q, Wang Z, Li H, Wiese M, Zheng H (2012b) APP physiological and pathophysiological functions: insights from animal models. Cell research 22:78-89.

Haass C, Schlossmacher MG, Hung AY, Vigo-Pelfrey C, Mellon A, Ostaszewski BL (1992) Amyloid beta-peptide is produced by cultured cells during normal metabolism. Nature 359.

Hamid R, Kilger E, Willem M, Vassallo N, Kostka M, Bornhovd C, Reichert AS, Kretzschmar HA, Haass C, Herms J (2007) Amyloid precursor protein intracellular domain modulates cellular calcium homeostasis and ATP content. Journal of neurochemistry 102:1264-1275.

Heber S, Herms J, Gajic V, Hainfellner J, Aguzzi A, Rulicke T, von Kretzschmar H, von Koch C, Sisodia S, Tremml P, Lipp HP, Wolfer DP, Muller U (2000) Mice with combined gene knock-outs reveal essential and partially redundant functions of amyloid precursor protein family members. The Journal of neuroscience : the official journal of the Society for Neuroscience 20:7951-7963.

Hebert LE, Weuve J, Scherr PA, Evans DA (2013) Alzheimer disease in the United States (2010-2050) estimated using the 2010 census. Neurology 80:1778-1783.

Hefter D, Kaiser M, Weyer SW, Papageorgiou IE, Both M (2016) Amyloid Precursor Protein Protects Neuronal Network Function after Hypoxia via Control of Voltage-Gated Calcium Channels. 36:8356-8371.

Heneka MT, Kummer MP, Latz E (2014) Innate immune activation in neurodegenerative disease. Nature reviews Immunology 14:463-477.

Heneka MT, Kummer MP, Stutz A, Delekate A, Schwartz S, Vieira-Saecker A, Griep A, Axt D, Remus A, Tzeng TC, Gelpi E, Halle A, Korte M, Latz E, Golenbock DT (2013) NLRP3 is activated in Alzheimer's disease and contributes to pathology in APP/PS1 mice. Nature 493:674-678.

Heneka MT, O'Banion MK (2007) Inflammatory processes in Alzheimer's disease. Journal of neuroimmunology 184:69-91.

Henneberger C, Bard L, King C, Jennings A, Rusakov DA (2013) NMDA receptor activation: two targets for two co-agonists. Neurochemical research 38:1156-1162.

Herms J, Anliker B, Heber S, Ring S, Fuhrmann M, Kretzschmar H, Sisodia S, Muller U (2004) Cortical dysplasia resembling human type 2 lissencephaly in mice lacking all three APP family members. Embo j 23:4106-4115.

Herron CE, Lester RA, Coan EJ, Collingridge GL (1986) Frequency-dependent involvement of NMDA receptors in the hippocampus: a novel synaptic mechanism. Nature 322:265-268.

Hick M, Herrmann U, Weyer SW, Mallm JP, Tschape JA, Borgers M, Mercken M, Roth FC, Draguhn A, Slomianka L, Wolfer DP, Korte M, Muller UC (2015) Acute function of secreted amyloid precursor protein fragment APPsalpha in synaptic plasticity. Acta neuropathologica 129:21-37.

Ho A, Morishita W, Atasoy D, Liu X, Tabuchi K, Hammer RE, Malenka RC, Sudhof TC (2006) Genetic analysis of Mint/X11 proteins: essential presynaptic functions of a neuronal adaptor protein family. The Journal of neuroscience : the official journal of the Society for Neuroscience 26:13089-13101.

Ho A, Sudhof TC (2004) Binding of F-spondin to amyloid-beta precursor protein: a candidate amyloid-beta precursor protein ligand that modulates amyloid-beta precursor protein cleavage. Proceedings of the National Academy of Sciences of the United States of America 101:2548-2553.

Ho VM, Lee JA, Martin KC (2011) The cell biology of synaptic plasticity. Science (New York, NY) 334:623-628.

Hoe HS, Lee KJ, Carney RS, Lee J, Markova A, Lee JY, Howell BW, Hyman BT, Pak DT, Bu G, Rebeck GW (2009) Interaction of reelin with amyloid precursor protein promotes neurite outgrowth. The Journal of neuroscience : the official journal of the Society for Neuroscience 29:7459-7473.

Holtmaat A, Svoboda K (2009) Experience-dependent structural synaptic plasticity in the mammalian brain. Nature reviews Neuroscience 10:647-658.

Hsieh H, Boehm J, Sato C, Iwatsubo T, Tomita T, Sisodia S, Malinow R (2006) AMPAR removal underlies Abeta-induced synaptic depression and dendritic spine loss. Neuron 52:831-843.

Hunter BE, de Fiebre CM, Papke RL, Kem WR, Meyer EM (1994) A novel nicotinic agonist facilitates induction of long-term potentiation in the rat hippocampus. Neuroscience letters 168:130-134.

Ishida A, Furukawa K, Keller JN, Mattson MP (1997) Secreted form of beta-amyloid precursor protein shifts the frequency dependency for induction of LTD, and enhances LTP in hippocampal slices. Neuroreport 8:2133-2137.

Jacobsen KT, Iverfeldt K (2009) Amyloid precursor protein and its homologues: a family of proteolysis-dependent receptors. Cell Mol Life Sci 66.

Jankowsky JL, Fadale DJ, Anderson J, Xu GM, Gonzales V, Jenkins NA, Copeland NG, Lee MK, Younkin LH, Wagner SL, Younkin SG, Borchelt DR (2004) Mutant presenilins specifically elevate the levels of the 42 residue beta-amyloid peptide in vivo: evidence for augmentation of a 42-specific gamma secretase. Hum Mol Genet 13:159-170.

Jiang S, Li Y, Zhang X, Bu G, Xu H, Zhang YW (2014) Trafficking regulation of proteins in Alzheimer's disease. Molecular neurodegeneration 9:6.

Jonsson T, Stefansson H, Steinberg S, Jonsdottir I, Jonsson PV, Snaedal J, Bjornsson S, Huttenlocher J, Levey AI, Lah JJ, Rujescu D, Hampel H, Giegling I, Andreassen OA, Engedal K, Ulstein I, Djurovic S, Ibrahim-Verbaas C, Hofman A, Ikram MA, van Duijn CM, Thorsteinsdottir U, Kong A, Stefansson K (2013) Variant of TREM2 Associated with the Risk of Alzheimer's Disease. New England Journal of Medicine 368:107-116.

Kaden D, Harmeier A, Weise C, Munter LM, Althoff V, Rost BR, Hildebrand PW, Schmitz D, Schaefer M, Lurz R, Skodda S, Yamamoto R, Arlt S, Finckh U, Multhaup G (2012) Novel APP/Abeta mutation K16N produces highly toxic heteromeric Abeta oligomers. EMBO Mol Med 4:647-659.

Kaden D, Voigt P, Munter LM, Bobowski KD, Schaefer M, Multhaup G (2009) Subcellular localization and dimerization of APLP1 are strikingly different from APP and APLP2. J Cell Sci 122:368-377.

Kaeser PS, Regehr WG (2017) The readily releasable pool of synaptic vesicles. Curr Opin Neurobiol 43:63-70.

Kamenetz F, Tomita T, Hsieh H, Seabrook G, Borchelt D, Iwatsubo T, Sisodia S, Malinow R (2003) APP processing and synaptic function. Neuron 37:925-937.

Kandel ER (2001) The molecular biology of memory storage: a dialogue between genes and synapses. Science (New York, NY) 294:1030-1038.

Katz B, Miledi R (1968) The role of calcium in neuromuscular facilitation. The Journal of physiology 195:481-492.

Kelly BL, Ferreira A (2006) beta-Amyloid-induced dynamin 1 degradation is mediated by N-methyl-D-aspartate receptors in hippocampal neurons. The Journal of biological chemistry 281:28079-28089.

Kelly BL, Ferreira A (2007) Beta-amyloid disrupted synaptic vesicle endocytosis in cultured hippocampal neurons. Neuroscience 147:60-70.

Kelly BL, Vassar R, Ferreira A (2005) Beta-amyloid-induced dynamin 1 depletion in hippocampal neurons. A potential mechanism for early cognitive decline in Alzheimer disease. The Journal of biological chemistry 280:31746-31753.

Khan GM, Tong M, Jhun M, Arora K, Nichols RA (2010) beta-Amyloid activates presynaptic alpha7 nicotinic acetylcholine receptors reconstituted into a model nerve cell system: involvement of lipid rafts. The European journal of neuroscience 31:788-796.

Kim J, Onstead L, Randle S, Price R, Smithson L, Zwizinski C, Dickson DW, Golde T, McGowan E (2007) Abeta40 inhibits amyloid deposition in vivo. The Journal of neuroscience : the official journal of the Society for Neuroscience 27:627-633.

Kim JH, Anwyl R, Suh YH, Djamgoz MB, Rowan MJ (2001) Use-dependent effects of amyloidogenic fragments of (beta)-amyloid precursor protein on synaptic plasticity in rat hippocampus in vivo. The Journal of neuroscience : the official journal of the Society for Neuroscience 21:1327-1333.

Kimberly WT, Zheng JB, Guenette SY, Selkoe DJ (2001) The intracellular domain of the beta-amyloid precursor protein is stabilized by Fe65 and translocates to the nucleus in a notch-like manner. The Journal of biological chemistry 276:40288-40292.

Kirov SA, Harris KM (1999) Dendrites are more spiny on mature hippocampal neurons when synapses are inactivated. Nature neuroscience 2:878-883.

Klevanski M, Herrmann U, Weyer SW, Fol R, Cartier N, Wolfer DP, Caldwell JH, Korte M, Muller UC (2015) The APP Intracellular Domain Is Required for Normal Synaptic Morphology, Synaptic Plasticity, and Hippocampus-Dependent Behavior. The Journal of neuroscience : the official journal of the Society for Neuroscience 35:16018-16033.

Klevanski M, Saar M, Baumkotter F, Weyer SW, Kins S, Muller UC (2014) Differential role of APP and APLPs for neuromuscular synaptic morphology and function. Molecular and cellular neurosciences 61:201-210.

Kohara K, Pignatelli M, Rivest AJ, Jung HY, Kitamura T, Suh J, Frank D, Kajikawa K, Mise N, Obata Y, Wickersham IR, Tonegawa S (2014) Cell type-specific genetic and optogenetic tools reveal hippocampal CA2 circuits. Nature neuroscience 17:269-279.

Korte M, Herrmann U, Zhang X, Draguhn A (2012) The role of APP and APLP for synaptic transmission, plasticity, and network function: lessons from genetic mouse models. Exp Brain Res 217:435-440.

Korte M, Schmitz D (2016) Cellular and System Biology of Memory: Timing, Molecules, and Beyond. Physiological reviews 96:647-693.

Kuchibhotla KV, Goldman ST, Lattarulo CR, Wu HY, Hyman BT, Bacskai BJ (2008) Abeta plaques lead to aberrant regulation of calcium homeostasis in vivo resulting in structural and functional disruption of neuronal networks. Neuron 59:214-225.

Kuhn PH, Wang H, Dislich B, Colombo A, Zeitschel U, Ellwart JW, Kremmer E, Rossner S, Lichtenthaler SF (2010) ADAM10 is the physiologically relevant, constitutive alpha-secretase of the amyloid precursor protein in primary neurons. Embo j 29:3020-3032.

Kundu A, Milosch N, Antonietti P, Baumkotter F, Zymny A, Muller UC, Kins S, Hajieva P, Behl C, Kogel D (2016) Modulation of BAG3 Expression and Proteasomal Activity by sAPPalpha Does Not Require Membrane-Tethered Holo-APP. Mol Neurobiol 53:5985-5994.

Lacor PN, Buniel MC, Chang L, Fernandez SJ, Gong Y, Viola KL, Lambert MP, Velasco PT, Bigio EH, Finch CE, Krafft GA, Klein WL (2004) Synaptic targeting by Alzheimer's-related amyloid beta oligomers. The Journal of neuroscience : the official journal of the Society for Neuroscience 24:10191-10200.

LaFerla FM (2002) Calcium dyshomeostasis and intracellular signalling in Alzheimer's disease. Nature reviews Neuroscience 3:862-872.

Lambrechts A, Kwiatkowski AV, Lanier LM, Bear JE, Vandekerckhove J, Ampe C, Gertler FB (2000) cAMP-dependent protein kinase phosphorylation of EVL, a Mena/VASP relative, regulates its interaction with actin and SH3 domains. The Journal of biological chemistry 275:36143-36151.

Lammich S, Kojro E, Postina R, Gilbert S, Pfeiffer R, Jasionowski M, Haass C, Fahrenholz F (1999) Constitutive and regulated alpha-secretase cleavage of Alzheimer's amyloid precursor protein by a disintegrin metalloprotease. Proceedings of the National Academy of Sciences of the United States of America 96:3922-3927.

Landfield PW, Pitler TA, Applegate MD (1986) The effects of high Mg2+-to-Ca2+ ratios on frequency potentiation in hippocampal slices of young and aged rats. Journal of neurophysiology 56:797-811.

Lang S, Erdmann F, Jung M, Wagner R, Cavalie A, Zimmermann R (2011) Sec61 complexes form ubiquitous ER Ca2+ leak channels. Channels 5:228-235.

Lassek M, Weingarten J, Einsfelder U, Brendel P, Muller U, Volknandt W (2013) Amyloid precursor proteins are constituents of the presynaptic active zone. Journal of neurochemistry 127:48-56.

Lautenschlager NT, Cupples LA, Rao VS, Auerbach SA, Becker R, Burke J, Chui H, Duara R, Foley EJ, Glatt SL, Green RC, Jones R, Karlinsky H, Kukull WA, Kurz A, Larson EB, Martelli K, Sadovnick AD, Volicer L, Waring SC, Growdon JH, Farrer LA (1996) Risk of dementia among relatives of Alzheimer's disease patients in the MIRAGE study: What is in store for the oldest old? Neurology 46:641-650.

Lawrence JL, Tong M, Alfulaij N, Sherrin T, Contarino M, White MM, Bellinger FP, Todorovic C, Nichols RA (2014) Regulation of presynaptic Ca2+, synaptic plasticity and contextual fear conditioning by a N-terminal beta-amyloid fragment. The Journal of neuroscience : the official journal of the Society for Neuroscience 34:14210-14218.

LeBlanc AC, Papadopoulos M, Belair C, Chu W, Crosato M, Powell J, Goodyer CG (1997) Processing of amyloid precursor protein in human primary neuron and astrocyte cultures. Journal of neurochemistry 68:1183-1190.

Lee KJ, Moussa CE, Lee Y, Sung Y, Howell BW, Turner RS, Pak DT, Hoe HS (2010) Beta amyloid-independent role of amyloid precursor protein in generation and maintenance of dendritic spines. Neuroscience 169:344-356.

Leissring MA, Akbari Y, Fanger CM, Cahalan MD, Mattson MP, LaFerla FM (2000) Capacitative calcium entry deficits and elevated luminal calcium content in mutant presenilin-1 knockin mice. The Journal of cell biology 149:793-798.

Leissring MA, Farris W, Chang AY, Walsh DM, Wu X, Sun X, Frosch MP, Selkoe DJ (2003) Enhanced proteolysis of beta-amyloid in APP transgenic mice prevents plaque formation, secondary pathology, and premature death. Neuron 40:1087-1093.

Leissring MA, Murphy MP, Mead TR, Akbari Y, Sugarman MC, Jannatipour M, Anliker B, Muller U, Saftig P, De Strooper B, Wolfe MS, Golde TE, LaFerla FM (2002) A physiologic signaling role for the gamma -secretase-derived intracellular fragment of APP. Proceedings of the National Academy of Sciences of the United States of America 99:4697-4702.

Levin ED, Simon BB (1998) Nicotinic acetylcholine involvement in cognitive function in animals. Psychopharmacology 138:217-230.

Li H, Wang B, Wang Z, Guo Q, Tabuchi K, Hammer RE, Sudhof TC, Zheng H (2010) Soluble amyloid precursor protein (APP) regulates transthyretin and Klotho gene expression without rescuing the essential function of APP. Proceedings of the National Academy of Sciences of the United States of America 107:17362-17367.

Li S, Jin M, Koeglsperger T, Shepardson NE, Shankar GM, Selkoe DJ (2011) Soluble Abeta oligomers inhibit long-term potentiation through a mechanism involving excessive activation of extrasynaptic NR2B-containing NMDA receptors. The Journal of neuroscience : the official journal of the Society for Neuroscience 31:6627-6638.

Lichtenthaler SF (2012) Alpha-secretase cleavage of the amyloid precursor protein: proteolysis regulated by signaling pathways and protein trafficking. Current Alzheimer research 9:165-177.

Linde CI, Baryshnikov SG, Mazzocco-Spezzia A, Golovina VA (2011) Dysregulation of Ca2+ signaling in astrocytes from mice lacking amyloid precursor protein. American journal of physiology Cell physiology 300:C1502-1512.

Liou J, Fivaz M, Inoue T, Meyer T (2007) Live-cell imaging reveals sequential oligomerization and local plasma membrane targeting of stromal interaction molecule 1 after Ca2+ store depletion. Proceedings of the National Academy of Sciences of the United States of America 104:9301-9306.

Liou J, Kim ML, Heo WD, Jones JT, Myers JW, Ferrell JE, Jr., Meyer T (2005) STIM is a Ca2+ sensor essential for Ca2+-store-depletion-triggered Ca2+ influx. Current biology : CB 15:1235-1241.

Liu Q, Kawai H, Berg DK (2001) beta -Amyloid peptide blocks the response of alpha 7-containing nicotinic receptors on hippocampal neurons. Proceedings of the National Academy of Sciences of the United States of America 98:4734-4739.

Liu X, Yu X, Zack DJ, Zhu H, Qian J (2008) TiGER: a database for tissue-specific gene expression and regulation. BMC bioinformatics 9:271.

Lopez-Sanchez N, Muller U, Frade JM (2005) Lengthening of G2/mitosis in cortical precursors from mice lacking beta-amyloid precursor protein. Neuroscience 130:51-60.

Lorent K, Overbergh L, Moechars D, De Strooper B, Van Leuven F, Van den Berghe H (1995) Expression in mouse embryos and in adult mouse brain of three members of the amyloid precursor protein family, of the alpha-2-macroglobulin receptor/low density lipoprotein receptor-related protein and of its ligands apolipoprotein E, lipoprotein lipase, alpha-2-macroglobulin and the 40,000 molecular weight receptor-associated protein. Neuroscience 65:1009-1025.

Lovell MA, Abner E, Kryscio R, Xu L, Fister SX, Lynn BC (2015) Calcium Channel Blockers, Progression to Dementia, and Effects on Amyloid Beta Peptide Production. Oxidative medicine and cellular longevity 2015:787805.

Lu B, Nagappan G, Guan X, Nathan PJ, Wren P (2013) BDNF-based synaptic repair as a disease-modifying strategy for neurodegenerative diseases. Nature reviews Neuroscience 14:401-416.

Ludewig S, Korte M (2017) Novel Insights into the Physiological Function of the APP (Gene) Family and Its Proteolytic Fragments in Synaptic Plasticity. Frontiers in Molecular Neuroscience 9.

Luik RM, Wang B, Prakriya M, Wu MM, Lewis RS (2008) Oligomerization of STIM1 couples ER calcium depletion to CRAC channel activation. Nature 454:538-542.

Luscher C, Malenka RC (2012) NMDA receptor-dependent long-term potentiation and long-term depression (LTP/LTD). Cold Spring Harbor perspectives in biology 4.

Lynch MA (2004) Long-Term Potentiation and Memory. Physiological reviews 84:87-136.

Ma T, Zhao Y, Kwak YD, Yang Z, Thompson R, Luo Z, Xu H, Liao FF (2009) Statin's excitoprotection is mediated by sAPP and the subsequent attenuation of calpain-induced truncation events, likely via rho-ROCK signaling. The Journal of neuroscience : the official journal of the Society for Neuroscience 29:11226-11236.

Malarkey EB, Ni Y, Parpura V (2008) Ca2+ entry through TRPC1 channels contributes to intracellular Ca2+ dynamics and consequent glutamate release from rat astrocytes. Glia 56:821-835.

Mallm JP, Tschape JA, Hick M, Filippov MA, Muller UC (2010) Generation of conditional null alleles for APP and APLP2. Genesis (New York, NY : 2000) 48:200-206.

Manahan-Vaughan D, Kulla A, Frey JU (2000) Requirement of translation but not transcription for the maintenance of long-term depression in the CA1 region of freely moving rats. The Journal of neuroscience : the official journal of the Society for Neuroscience 20:8572-8576.

Marcello E, Gardoni F, Mauceri D, Romorini S, Jeromin A, Epis R, Borroni B, Cattabeni F, Sala C, Padovani A, Di Luca M (2007) Synapse-associated protein-97 mediates alpha-secretase ADAM10 trafficking and promotes its activity. The Journal of neuroscience : the official journal of the Society for Neuroscience 27:1682-1691.

Mathis DM, Furman JL, Norris CM (2011) Preparation of acute hippocampal slices from rats and transgenic mice for the study of synaptic alterations during aging and amyloid pathology. Journal of visualized experiments : JoVE.

Mattson MP (2004) Pathways towards and away from Alzheimer's disease. Nature 430:631-639.

Mattson MP, Chan SL (2003) Neuronal and glial calcium signaling in Alzheimer’s disease. Cell Calcium 34:385-397.

Mattson MP, Cheng B, Culwell AR, Esch FS, Lieberburg I, Rydel RE (1993) Evidence for excitoprotective and intraneuronal calcium-regulating roles for secreted forms of the beta-amyloid precursor protein. Neuron 10:243-254.

Mayer MC, Schauenburg L, Thompson-Steckel G, Dunsing V, Kaden D, Voigt P, Schaefer M, Chiantia S, Kennedy TE, Multhaup G (2016) Amyloid precursor-like protein 1 (APLP1) exhibits stronger zinc-dependent neuronal adhesion than amyloid precursor protein and APLP2. Journal of neurochemistry 137:266-276.

Mayford M, Siegelbaum SA, Kandel ER (2012) Synapses and memory storage. Cold Spring Harbor perspectives in biology 4.

Mehta TK, Dougherty JJ, Wu J, Choi CH, Khan GM, Nichols RA (2009) Defining pre-synaptic nicotinic receptors regulated by beta amyloid in mouse cortex and hippocampus with receptor null mutants. Journal of neurochemistry 109:1452-1458.

Meziane H, Dodart JC, Mathis C, Little S, Clemens J, Paul SM, Ungerer A (1998) Memory-enhancing effects of secreted forms of the beta-amyloid precursor protein in normal and amnestic mice. Proceedings of the National Academy of Sciences of the United States of America 95:12683-12688.

Michaelsen-Preusse K, Zessin S, Grigoryan G, Scharkowski F, Feuge J, Remus A, Korte M (2016) Neuronal profilins in health and disease: Relevance for spine plasticity and Fragile X syndrome. Proceedings of the National Academy of Sciences of the United States of America 113:3365-3370.

Midthune B, Tyan SH, Walsh JJ, Sarsoza F, Eggert S, Hof PR, Dickstein DL, Koo EH (2012) Deletion of the amyloid precursor-like protein 2 (APLP2) does not affect hippocampal neuron morphology or function. Molecular and cellular neurosciences 49:448-455.

Mileusnic R, Lancashire CL, Johnston AN, Rose SP (2000) APP is required during an early phase of memory formation. The European journal of neuroscience 12:4487-4495.

Mileusnic R, Lancashire CL, Rose SP (2004) The peptide sequence Arg-Glu-Arg, present in the amyloid precursor protein, protects against memory loss caused by A beta and acts as a cognitive enhancer. The European journal of neuroscience 19:1933-1938.

Milosch N, Tanriover G, Kundu A, Rami A, Francois JC, Baumkotter F, Weyer SW, Samanta A, Jaschke A, Brod F, Buchholz CJ, Kins S, Behl C, Muller UC, Kogel D (2014) Holo-APP and G-protein-mediated signaling are required for sAPPalpha-induced activation of the Akt survival pathway. Cell death & disease 5:e1391.

Minano-Molina AJ, Espana J, Martin E, Barneda-Zahonero B, Fado R, Sole M, Trullas R, Saura CA, Rodriguez-Alvarez J (2011) Soluble oligomers of amyloid-beta peptide disrupt membrane trafficking of alpha-amino-3-hydroxy-5-methylisoxazole-4-propionic acid receptor contributing to early synapse dysfunction. The Journal of biological chemistry 286:27311-27321.

Morales-Corraliza J, Mazzella MJ, Berger JD, Diaz NS, Choi JHK, Levy E, Matsuoka Y, Planel E, Mathews PM (2009) <italic>In Vivo</italic> Turnover of Tau and APP Metabolites in the Brains of Wild-Type and Tg2576 Mice: Greater Stability of sAPP in the β-Amyloid Depositing Mice. PloS one 4:e7134.

Moreno L, Rose C, Mohanraj A, Allinquant B, Billard JM, Dutar P (2015) sAbetaPPalpha Improves Hippocampal NMDA-Dependent Functional Alterations Linked to Healthy Aging. Journal of Alzheimer's disease : JAD 48:927-935.

Morris RG (1999) D.O. Hebb: The Organization of Behavior, Wiley: New York; 1949. Brain Res Bull 50:437.

Mumby DG, Astur RS, Weisend MP, Sutherland RJ (1999) Retrograde amnesia and selective damage to the hippocampal formation: memory for places and object discriminations. Behavioural brain research 106:97-107.

Musleh W, Bi X, Tocco G, Yaghoubi S, Baudry M (1997) Glycine-induced long-term potentiation is associated with structural and functional modifications of alpha-amino-3-hydroxyl-5-methyl-4-isoxazolepropionic acid receptors. Proceedings of the National Academy of Sciences of the United States of America 94:9451-9456.

Nensa FM, Neumann MH, Schrotter A, Przyborski A, Mastalski T, Susdalzew S, Loobetae C, Helling S, El Magraoui F, Erdmann R, Meyer HE, Uszkoreit J, Eisenacher M, Suh J, Guenette SY, Rohner N, Kogel D, Theiss C, Marcus K, Muller T (2014) Amyloid beta a4 precursor protein-binding family B member 1 (FE65) interactomics revealed synaptic vesicle glycoprotein 2A (SV2A) and

sarcoplasmic/endoplasmic reticulum calcium ATPase 2 (SERCA2) as new binding proteins in the human brain. Molecular & cellular proteomics : MCP 13:475-488.

Newhouse PA, Sunderland T, Tariot PN, Blumhardt CL, Weingartner H, Mellow A, Murphy DL (1988) Intravenous nicotine in Alzheimer's disease: a pilot study. Psychopharmacology 95:171-175.

Nhan HS, Chiang K, Koo EH (2015) The multifaceted nature of amyloid precursor protein and its proteolytic fragments: friends and foes. Acta neuropathologica 129:1-19.

Nikolaev A, McLaughlin T, O'Leary DD, Tessier-Lavigne M (2009) APP binds DR6 to trigger axon pruning and neuron death via distinct caspases. Nature 457:981-989.

Nimmrich V, Grimm C, Draguhn A, Barghorn S, Lehmann A, Schoemaker H, Hillen H, Gross G, Ebert U, Bruehl C (2008) Amyloid beta oligomers (A beta(1-42) globulomer) suppress spontaneous synaptic activity by inhibition of P/Q-type calcium currents. The Journal of neuroscience : the official journal of the Society for Neuroscience 28:788-797.

Ninomiya H, Roch JM, Sundsmo MP, Otero DA, Saitoh T (1993) Amino acid sequence RERMS represents the active domain of amyloid beta/A4 protein precursor that promotes fibroblast growth. The Journal of cell biology 121:879-886.

Nitsch RM, Farber SA, Growdon JH, Wurtman RJ (1993) Release of amyloid beta-protein precursor derivatives by electrical depolarization of rat hippocampal slices. Proceedings of the National Academy of Sciences of the United States of America 90:5191-5193.

Nitsch RM, Slack BE, Wurtman RJ, Growdon JH (1992) Release of Alzheimer amyloid precursor derivatives stimulated by activation of muscarinic acetylcholine receptors. Science (New York, NY) 258:304-307.

O'Keefe, Nadel (1978) The Hippocampus as a Cognitive Map. Oxford: Clarendon.

Obregon D, Hou H, Deng J, Giunta B, Tian J, Darlington D, Shahaduzzaman M, Zhu Y, Mori T, Mattson MP, Tan J (2012) Soluble amyloid precursor protein-alpha modulates beta-secretase activity and amyloid-beta generation. Nature communications 3:777.

Okochi M, Tagami S, Yanagida K, Takami M, Kodama TS, Mori K, Nakayama T, Ihara Y, Takeda M (2013) gamma-secretase modulators and presenilin 1 mutants act differently on presenilin/gamma-secretase function to cleave Abeta42 and Abeta43. Cell reports 3:42-51.

Oku Y, Huganir RL (2013) AGAP3 and Arf6 regulate trafficking of AMPA receptors and synaptic plasticity. The Journal of neuroscience : the official journal of the Society for Neuroscience 33:12586-12598.

Orr-Urtreger A, Goldner FM, Saeki M, Lorenzo I, Goldberg L, De Biasi M, Dani JA, Patrick JW, Beaudet AL (1997) Mice deficient in the alpha7 neuronal nicotinic acetylcholine receptor lack alpha-bungarotoxin binding sites and hippocampal fast nicotinic currents. The Journal of neuroscience : the official journal of the Society for Neuroscience 17:9165-9171.

Paliga K, Peraus G, Kreger S, Durrwang U, Hesse L, Multhaup G, Masters CL, Beyreuther K, Weidemann A (1997) Human amyloid precursor-like protein 1--cDNA cloning, ectopic expression in COS-7 cells and identification of soluble forms in the cerebrospinal fluid. European journal of biochemistry 250:354-363.

Parekh AB, Putney JW, Jr. (2005) Store-operated calcium channels. Physiological reviews 85:757-810.

Parihar MS, Brewer GJ (2010) Amyloid-beta as a modulator of synaptic plasticity. Journal of Alzheimer's disease : JAD 22:741-763.

Park JH, Gimbel DA, GrandPre T, Lee JK, Kim JE, Li W, Lee DH, Strittmatter SM (2006) Alzheimer precursor protein interaction with the Nogo-66 receptor reduces amyloid-beta plaque deposition. The Journal of neuroscience : the official journal of the Society for Neuroscience 26:1386-1395.

Peters-Libeu C, Campagna J, Mitsumori M, Poksay KS, Spilman P, Sabogal A, Bredesen DE, John V (2015) sAbetaPPalpha is a Potent Endogenous Inhibitor of BACE1. Journal of Alzheimer's disease : JAD 47:545-555.

Pettit DL, Shao Z, Yakel JL (2001) beta-Amyloid(1-42) peptide directly modulates nicotinic receptors in the rat hippocampal slice. The Journal of neuroscience : the official journal of the Society for Neuroscience 21:Rc120.

Pietrzik CU, Yoon IS, Jaeger S, Busse T, Weggen S, Koo EH (2004) FE65 constitutes the functional link between the low-density lipoprotein receptor-related protein and the amyloid precursor protein. The Journal of neuroscience : the official journal of the Society for Neuroscience 24:4259-4265.

Pizzo P, Burgo A, Pozzan T, Fasolato C (2001) Role of capacitative calcium entry on glutamate-induced calcium influx in type-I rat cortical astrocytes. Journal of neurochemistry 79:98-109.

Plummer S, Van den Heuvel C, Thornton E, Corrigan F, Cappai R (2016) The Neuroprotective Properties of the Amyloid Precursor Protein Following Traumatic Brain Injury. Aging and disease 7:163-179.

Portelius E, Price E, Brinkmalm G, Stiteler M, Olsson M, Persson R, Westman-Brinkmalm A, Zetterberg H, Simon AJ, Blennow K (2011) A novel pathway for amyloid precursor protein processing. Neurobiol Aging 32:1090-1098.

Povova J, Ambroz P, Bar M, Pavukova V, Sery O, Tomaskova H, Janout V (2012) Epidemiological of and risk factors for Alzheimer's disease: a review. Biomedical papers of the Medical Faculty of the University Palacky, Olomouc, Czechoslovakia 156:108-114.

Prox J, Bernreuther C, Altmeppen H, Grendel J, Glatzel M, D'Hooge R, Stroobants S, Ahmed T, Balschun D, Willem M, Lammich S, Isbrandt D, Schweizer M, Horre K, De Strooper B, Saftig P (2013) Postnatal disruption of the disintegrin/metalloproteinase ADAM10 in brain causes epileptic seizures, learning deficits, altered spine morphology, and defective synaptic functions. The Journal of neuroscience : the official journal of the Society for Neuroscience 33:12915-12928, 12928a.

Puntel M, Kroeger KM, Sanderson NS, Thomas CE, Castro MG, Lowenstein PR (2010) Gene transfer into rat brain using adenoviral vectors. Current protocols in neuroscience Chapter 4:Unit 4.24.

Purves, Augustine, Fitzpatrick (2001) Neuroglial Cells. Neuroscience 2nd edition.

Puzzo D, Privitera L, Leznik E, Fa M, Staniszewski A, Palmeri A, Arancio O (2008) Picomolar amyloid-beta positively modulates synaptic plasticity and memory in hippocampus. The Journal of neuroscience : the official journal of the Society for Neuroscience 28:14537-14545.

Regehr WG (2012) Short-term presynaptic plasticity. Cold Spring Harbor perspectives in biology 4:a005702.

Reiserer RS, Harrison FE, Syverud DC, McDonald MP (2007) Impaired spatial learning in the APPSwe + PSEN1DeltaE9 bigenic mouse model of Alzheimer's disease. Genes, brain, and behavior 6:54-65.

Reymann KG, Frey JU (2007) The late maintenance of hippocampal LTP: requirements, phases, 'synaptic tagging', 'late-associativity' and implications. Neuropharmacology 52:24-40.

Ring S, Weyer SW, Kilian SB, Waldron E, Pietrzik CU, Filippov MA, Herms J, Buchholz C, Eckman CB, Korte M, Wolfer DP, Muller UC (2007) The secreted beta-amyloid precursor protein ectodomain APPs alpha is sufficient to rescue the anatomical, behavioral, and electrophysiological abnormalities of APP-deficient mice. The Journal of neuroscience : the official journal of the Society for Neuroscience 27:7817-7826.

Robakis NK, Ramakrishna N, Wolfe G, Wisniewski HM (1987) Molecular cloning and characterization of a cDNA encoding the cerebrovascular and the neuritic plaque amyloid peptides. Proceedings of the National Academy of Sciences of the United States of America 84:4190-4194.

Roch JM, Jin LW, Ninomiya H, Schubert D, Saitoh T (1993) Biologically active domain of the secreted form of the amyloid beta/A4 protein precursor. Annals of the New York Academy of Sciences 695:149-157.

Rohan de Silva HA, Jen A, Wickenden C, Jen LS, Wilkinson SL, Patel AJ (1997) Cell-specific expression of beta-amyloid precursor protein isoform mRNAs and proteins in neurons and astrocytes. Brain research Molecular brain research 47:147-156.

Rojas G, Cardenas AM, Fernandez-Olivares P, Shimahara T, Segura-Aguilar J, Caviedes R, Caviedes P (2008) Effect of the knockdown of amyloid precursor protein on intracellular calcium increases in

a neuronal cell line derived from the cerebral cortex of a trisomy 16 mouse. Experimental neurology 209:234-242.

Rossjohn J, Cappai R, Feil SC, Henry A, McKinstry WJ, Galatis D, Hesse L, Multhaup G, Beyreuther K, Masters CL, Parker MW (1999) Crystal structure of the N-terminal, growth factor-like domain of Alzheimer amyloid precursor protein. Nature structural biology 6:327-331.

Ryan MM, Morris GP, Mockett BG, Bourne K, Abraham WC, Tate WP, Williams JM (2013) Time-dependent changes in gene expression induced by secreted amyloid precursor protein-alpha in the rat hippocampus. BMC genomics 14:376.

Sabo SL, Lanier LM, Ikin AF, Khorkova O, Sahasrabudhe S, Greengard P, Buxbaum JD (1999) Regulation of beta-amyloid secretion by FE65, an amyloid protein precursor-binding protein. The Journal of biological chemistry 274:7952-7957.

Saftig P, Lichtenthaler SF (2015) The alpha secretase ADAM10: A metalloprotease with multiple functions in the brain. Progress in neurobiology 135:1-20.

Sajikumar S, Navakkode S, Frey JU (2005) Protein synthesis-dependent long-term functional plasticity: methods and techniques. Curr Opin Neurobiol 15:607-613.

Samaranch L, San Sebastian W, Kells AP, Salegio EA, Heller G, Bringas JR, Pivirotto P, DeArmond S, Forsayeth J, Bankiewicz KS (2014) AAV9-mediated expression of a non-self protein in nonhuman primate central nervous system triggers widespread neuroinflammation driven by antigen-presenting cell transduction. Molecular therapy : the journal of the American Society of Gene Therapy 22:329-337.

Samtleben S, Jaepel J, Fecher C, Andreska T, Rehberg M, Blum R (2013) Direct imaging of ER calcium with targeted-esterase induced dye loading (TED). Journal of visualized experiments : JoVE e50317.

Samtleben S, Wachter B, Blum R (2015) Store-operated calcium entry compensates fast ER calcium loss in resting hippocampal neurons. Cell Calcium 58:147-159.

Sannerud R, Declerck I, Peric A, Raemaekers T, Menendez G, Zhou L, Veerle B, Coen K, Munck S, De Strooper B, Schiavo G, Annaert W (2011) ADP ribosylation factor 6 (ARF6) controls amyloid precursor protein (APP) processing by mediating the endosomal sorting of BACE1. Proceedings of the National Academy of Sciences of the United States of America 108:E559-568.

Santos SF, Pierrot N, Morel N, Gailly P, Sindic C, Octave JN (2009) Expression of human amyloid precursor protein in rat cortical neurons inhibits calcium oscillations. The Journal of neuroscience : the official journal of the Society for Neuroscience 29:4708-4718.

Sarkar A, Irwin M, Singh A, Riccetti M, Singh A (2016) Alzheimer's disease: the silver tsunami of the 21(st) century. Neural Regeneration Research 11:693-697.

Savonenko A, Xu GM, Melnikova T, Morton JL, Gonzales V, Wong MP, Price DL, Tang F, Markowska AL, Borchelt DR (2005a) Episodic-like memory deficits in the APPswe/PS1dE9 mouse model of Alzheimer's disease: relationships to beta-amyloid deposition and neurotransmitter abnormalities. Neurobiol Dis 18:602-617.

Savonenko A, Xu GM, Melnikova T, Morton JL, Gonzales V, Wong MPF, Price DL, Tang F, Markowska AL, Borchelt DR (2005b) Episodic-like memory deficits in the APPswe/PS1dE9 mouse model of Alzheimer's disease: Relationships to β-amyloid deposition and neurotransmitter abnormalities. Neurobiology of Disease 18:602-617.

Schäuble N, Lang S, Jung M, Cappel S, Schorr S, Ulucan Ö, Linxweiler J, Dudek J, Blum R, Helms V, Paton AW, Paton JC, Cavalié A, Zimmermann R (2012) BiP-mediated closing of the Sec61 channel limits Ca²⁺ leakage from the ER. The EMBO Journal 31:3282-3296.

Scheff SW, DeKosky ST, Price DA (1990) Quantitative assessment of cortical synaptic density in Alzheimer's disease. Neurobiol Aging 11:29-37.

Scheff SW, Price DA, Schmitt FA, Mufson EJ (2006) Hippocampal synaptic loss in early Alzheimer's disease and mild cognitive impairment. Neurobiol Aging 27:1372-1384.

Schmidt V, Sporbert A, Rohe M, Reimer T, Rehm A, Andersen OM, Willnow TE (2007) SorLA/LR11 regulates processing of amyloid precursor protein via interaction with adaptors GGA and PACS-1. The Journal of biological chemistry 282:32956-32964.

Scoville WB, Milner B (1957) Loss of recent memory after bilateral hippocampal lesions. Journal of neurology, neurosurgery, and psychiatry 20:11-21.

Seabrook GR, Smith DW, Bowery BJ, Easter A, Reynolds T, Fitzjohn SM, Morton RA, Zheng H, Dawson GR, Sirinathsinghji DJ, Davies CH, Collingridge GL, Hill RG (1999) Mechanisms contributing to the deficits in hippocampal synaptic plasticity in mice lacking amyloid precursor protein. Neuropharmacology 38:349-359.

Selkoe DJ (2002) Alzheimer's disease is a synaptic failure. Science (New York, NY) 298:789-791.

Selkoe DJ (2008) Soluble oligomers of the amyloid beta-protein impair synaptic plasticity and behavior. Behavioural brain research 192:106-113.

Selkoe DJ, Hardy J (2016) The amyloid hypothesis of Alzheimer's disease at 25 years. EMBO Mol Med 8:595-608.

Seshadri S, Beiser A, Kelly-Hayes M, Kase CS, Au R, Kannel WB, Wolf PA (2006) The lifetime risk of stroke: estimates from the Framingham Study. Stroke 37:345-350.

Sevigny J, Chiao P, Bussiere T, Weinreb PH, Williams L, Maier M, Dunstan R, Salloway S, Chen T, Ling Y, O'Gorman J, Qian F, Arastu M, Li M, Chollate S, Brennan MS, Quintero-Monzon O, Scannevin RH, Arnold HM, Engber T, Rhodes K, Ferrero J, Hang Y, Mikulskis A, Grimm J, Hock C, Nitsch RM, Sandrock A (2016) The antibody aducanumab reduces Abeta plaques in Alzheimer's disease. Nature 537:50-56.

Shahi K, Baudry M (1993) Glycine-induced changes in synaptic efficacy in hippocampal slices involve changes in AMPA receptors. Brain Res 627:261-266.

Shahi K, Marvizon JC, Baudry M (1993) High concentrations of glycine induce long-lasting changes in synaptic efficacy in rat hippocampal slices. Neuroscience letters 149:185-188.

Shilling D, Mak DO, Kang DE, Foskett JK (2012) Lack of evidence for presenilins as endoplasmic reticulum Ca2+ leak channels. The Journal of biological chemistry 287:10933-10944.

Silva AJ, Paylor R, Wehner JM, Tonegawa S (1992) Impaired spatial learning in alpha-calcium-calmodulin kinase II mutant mice. Science (New York, NY) 257:206-211.

Smith-Swintosky VL, Pettigrew LC, Craddock SD, Culwell AR, Rydel RE, Mattson MP (1994) Secreted forms of beta-amyloid precursor protein protect against ischemic brain injury. Journal of neurochemistry 63:781-784.

Snyder EM, Nong Y, Almeida CG, Paul S, Moran T, Choi EY, Nairn AC, Salter MW, Lombroso PJ, Gouras GK, Greengard P (2005) Regulation of NMDA receptor trafficking by amyloid-beta. Nature neuroscience 8:1051-1058.

Soba P, Eggert S, Wagner K, Zentgraf H, Siehl K, Kreger S, Lower A, Langer A, Merdes G, Paro R, Masters CL, Muller U, Kins S, Beyreuther K (2005) Homo- and heterodimerization of APP family members promotes intercellular adhesion. Embo j 24:3624-3634.

Spires-Jones T, Knafo S (2012) Spines, plasticity, and cognition in Alzheimer's model mice. Neural plasticity 2012:319836.

Stahl R, Schilling S, Soba P, Rupp C, Hartmann T, Wagner K, Merdes G, Eggert S, Kins S (2014) Shedding of APP limits its synaptogenic activity and cell adhesion properties. Frontiers in cellular neuroscience 8:410.

Steinbach JP, Muller U, Leist M, Li ZW, Nicotera P, Aguzzi A (1998) Hypersensitivity to seizures in beta-amyloid precursor protein deficient mice. Cell death and differentiation 5:858-866.

Strecker P, Ludewig S, Rust M, Mundinger TA, Gorlich A, Krachan EG, Mehrfeld C, Herz J, Korte M, Guenette SY, Kins S (2016) FE65 and FE65L1 share common synaptic functions and genetically interact with the APP family in neuromuscular junction formation. Scientific reports 6:25652.

Stutzmann GE, Caccamo A, LaFerla FM, Parker I (2004) Dysregulated IP3 signaling in cortical neurons of knock-in mice expressing an Alzheimer's-linked mutation in presenilin1 results in exaggerated Ca2+ signals and altered membrane excitability. The Journal of neuroscience : the official journal of the Society for Neuroscience 24:508-513.

Stutzmann GE, Smith I, Caccamo A, Oddo S, Laferla FM, Parker I (2006) Enhanced ryanodine receptor recruitment contributes to Ca2+ disruptions in young, adult, and aged Alzheimer's disease mice. The Journal of neuroscience : the official journal of the Society for Neuroscience 26:5180-5189.

Suh J, Moncaster JA, Wang L, Hafeez I, Herz J, Tanzi RE, Goldstein LE, Guenette SY (2015) FE65 and FE65L1 amyloid precursor protein-binding protein compound null mice display adult-onset cataract and muscle weakness. FASEB journal : official publication of the Federation of American Societies for Experimental Biology 29:2628-2639.

Sun S, Zhang H, Liu J, Popugaeva E, Xu NJ, Feske S, White CL, 3rd, Bezprozvanny I (2014) Reduced synaptic STIM2 expression and impaired store-operated calcium entry cause destabilization of mature spines in mutant presenilin mice. Neuron 82:79-93.

Tagliatti E, Fadda M, Falace A, Benfenati F, Fassio A (2016) Arf6 regulates the cycling and the readily releasable pool of synaptic vesicles at hippocampal synapse. eLife 5.

Tang W, Ehrlich I, Wolff SBE, Michalski A-M, Wölfl S, Hasan MT, Lüthi A, Sprengel R (2009) Faithful Expression of Multiple Proteins via 2A-Peptide Self-Processing: A Versatile and Reliable Method for Manipulating Brain Circuits. The Journal of Neuroscience 29:8621-8629.

Tang W, Tam JH, Seah C, Chiu J, Tyrer A, Cregan SP, Meakin SO, Pasternak SH (2015) Arf6 controls beta-amyloid production by regulating macropinocytosis of the Amyloid Precursor Protein to lysosomes. Molecular brain 8:41.

Taylor CJ, Ireland DR, Ballagh I, Bourne K, Marechal NM, Turner PR, Bilkey DK, Tate WP, Abraham WC (2008) Endogenous secreted amyloid precursor protein-alpha regulates hippocampal NMDA receptor function, long-term potentiation and spatial memory. Neurobiol Dis 31:250-260.

Thinakaran G, Koo EH (2008) Amyloid precursor protein trafficking, processing, and function. The Journal of biological chemistry 283:29615-29619.

Thomas CE, Birkett D, Anozie I, Castro MG, Lowenstein PR (2001) Acute direct adenoviral vector cytotoxicity and chronic, but not acute, inflammatory responses correlate with decreased vector-mediated transgene expression in the brain. Molecular therapy : the journal of the American Society of Gene Therapy 3:36-46.

Tomita T (2014) Molecular mechanism of intramembrane proteolysis by gamma-secretase. Journal of biochemistry 156:195-201.

Tong M, Arora K, White MM, Nichols RA (2011) Role of key aromatic residues in the ligand-binding domain of alpha7 nicotinic receptors in the agonist action of beta-amyloid. The Journal of biological chemistry 286:34373-34381.

Tu H, Nelson O, Bezprozvanny A, Wang Z, Lee SF, Hao YH, Serneels L, De Strooper B, Yu G, Bezprozvanny I (2006) Presenilins form ER Ca2+ leak channels, a function disrupted by familial Alzheimer's disease-linked mutations. Cell 126:981-993.

Tyan SH, Shih AY, Walsh JJ, Maruyama H, Sarsoza F, Ku L, Eggert S, Hof PR, Koo EH, Dickstein DL (2012) Amyloid precursor protein (APP) regulates synaptic structure and function. Molecular and cellular neurosciences 51:43-52.

van der Kant R, Goldstein LS (2015) Cellular functions of the amyloid precursor protein from development to dementia. Developmental cell 32:502-515.

Vassar R, Bennett BD, Babu-Khan S, Kahn S, Mendiaz EA, Denis P (1999) Beta-secretase cleavage of Alzheimer's amyloid precursor protein by the transmembrane aspartic protease BACE. Science (New York, NY) 286.

Vertes RP (2005) Hippocampal theta rhythm: a tag for short-term memory. Hippocampus 15:923-935.

Vnencak M, Paul MH, Hick M, Schwarzacher SW, Del Turco D, Muller UC, Deller T, Jedlicka P (2015) Deletion of the amyloid precursor-like protein 1 (APLP1) enhances excitatory synaptic transmission, reduces network inhibition but does not impair synaptic plasticity in the mouse dentate gyrus. The Journal of comparative neurology 523:1717-1729.

Volianskis A, France G, Jensen MS, Bortolotto ZA, Jane DE, Collingridge GL (2015) Long-term potentiation and the role of N-methyl-d-aspartate receptors. Brain Research 1621:5-16.

von Koch CS, Zheng H, Chen H, Trumbauer M, Thinakaran G, van der Ploeg LH, Price DL, Sisodia SS (1997) Generation of APLP2 KO mice and early postnatal lethality in APLP2/APP double KO mice. Neurobiol Aging 18:661-669.

Walsh DM, Klyubin I, Fadeeva JV, Cullen WK, Anwyl R, Wolfe MS, Rowan MJ, Selkoe DJ (2002) Naturally secreted oligomers of amyloid beta protein potently inhibit hippocampal long-term potentiation in vivo. Nature 416:535-539.

Walsh DM, Minogue AM, Sala Frigerio C, Fadeeva JV, Wasco W, Selkoe DJ (2007) The APP family of proteins: similarities and differences. Biochemical Society transactions 35:416-420.

Wang B, Hu Q, Hearn MG, Shimizu K, Ware CB, Liggitt DH, Jin LW, Cool BH, Storm DR, Martin GM (2004) Isoform-specific knockout of FE65 leads to impaired learning and memory. Journal of neuroscience research 75:12-24.

Wang B, Wang Z, Sun L, Yang L, Li H, Cole AL, Rodriguez-Rivera J, Lu HC, Zheng H (2014) The amyloid precursor protein controls adult hippocampal neurogenesis through GABAergic interneurons. The Journal of neuroscience : the official journal of the Society for Neuroscience 34:13314-13325.

Wang H, Megill A, He K, Kirkwood A, Lee HK (2012) Consequences of inhibiting amyloid precursor protein processing enzymes on synaptic function and plasticity. Neural plasticity 2012:272374.

Wang H, Sang N, Zhang C, Raghupathi R, Tanzi RE, Saunders A (2015) Cathepsin L Mediates the Degradation of Novel APP C-Terminal Fragments. Biochemistry 54:2806-2816.

Wang HY, Lee DH, D'Andrea MR, Peterson PA, Shank RP, Reitz AB (2000a) beta-Amyloid(1-42) binds to alpha7 nicotinic acetylcholine receptor with high affinity. Implications for Alzheimer's disease pathology. The Journal of biological chemistry 275:5626-5632.

Wang HY, Lee DH, Davis CB, Shank RP (2000b) Amyloid peptide Abeta(1-42) binds selectively and with picomolar affinity to alpha7 nicotinic acetylcholine receptors. Journal of neurochemistry 75:1155-1161.

Wang P, Yang G, Mosier DR, Chang P, Zaidi T, Gong YD, Zhao NM, Dominguez B, Lee KF, Gan WB, Zheng H (2005) Defective neuromuscular synapses in mice lacking amyloid precursor protein (APP) and APP-Like protein 2. The Journal of neuroscience : the official journal of the Society for Neuroscience 25:1219-1225.

Wang Y, Zhang M, Moon C, Hu Q, Wang B, Martin G, Sun Z, Wang H (2009) The APP-interacting protein FE65 is required for hippocampus-dependent learning and long-term potentiation. Learning & memory 16:537-544.

Wasco W, Bupp K, Magendantz M, Gusella JF, Tanzi RE, Solomon F (1992) Identification of a mouse brain cDNA that encodes a protein related to the Alzheimer disease-associated amyloid beta protein precursor. Proceedings of the National Academy of Sciences of the United States of America 89:10758-10762.

Wasco W, Gurubhagavatula S, Paradis MD, Romano DM, Sisodia SS, Hyman BT, Neve RL, Tanzi RE (1993) Isolation and characterization of APLP2 encoding a homologue of the Alzheimer's associated amyloid beta protein precursor. Nature genetics 5:95-100.

Webster NJ, Ramsden M, Boyle JP, Pearson HA, Peers C (2006) Amyloid peptides mediate hypoxic increase of L-type Ca2+ channels in central neurones. Neurobiol Aging 27:439-445.

Weyer SW, Klevanski M, Delekate A, Voikar V, Aydin D, Hick M, Filippov M, Drost N, Schaller KL, Saar M, Vogt MA, Gass P, Samanta A, Jaschke A, Korte M, Wolfer DP, Caldwell JH, Muller UC (2011) APP

and APLP2 are essential at PNS and CNS synapses for transmission, spatial learning and LTP. Embo j 30:2266-2280.

Weyer SW, Zagrebelsky M, Herrmann U, Hick M, Ganss L, Gobbert J, Gruber M, Altmann C, Korte M, Deller T, Muller UC (2014) Comparative analysis of single and combined APP/APLP knockouts reveals reduced spine density in APP-KO mice that is prevented by APPsalpha expression. Acta neuropathologica communications 2:36.

Wilhelm BG, Mandad S, Truckenbrodt S, Krohnert K, Schafer C, Rammner B, Koo SJ, Classen GA, Krauss M, Haucke V, Urlaub H, Rizzoli SO (2014) Composition of isolated synaptic boutons reveals the amounts of vesicle trafficking proteins. Science (New York, NY) 344:1023-1028.

Willem M, Tahirovic S, Busche MA, Ovsepian SV, Chafai M, Kootar S, Hornburg D, Evans LD, Moore S, Daria A, Hampel H, Muller V, Giudici C, Nuscher B, Wenninger-Weinzierl A, Kremmer E, Heneka MT, Thal DR, Giedraitis V, Lannfelt L, Muller U, Livesey FJ, Meissner F, Herms J, Konnerth A, Marie H, Haass C (2015) eta-Secretase processing of APP inhibits neuronal activity in the hippocampus. Nature 526:443-447.

Wu J, Anwyl R, Rowan MJ (1995) beta-Amyloid selectively augments NMDA receptor-mediated synaptic transmission in rat hippocampus. Neuroreport 6:2409-2413.

Xiong M, Jones OD, Peppercorn K, Ohline SM, Tate WP, Abraham WC (2017) Secreted amyloid precursor protein-alpha can restore novel object location memory and hippocampal LTP in aged rats. Neurobiology of learning and memory 138:291-299.

Yang L, Wang Z, Wang B, Justice NJ, Zheng H (2009) Amyloid precursor protein regulates Cav1.2 L-type calcium channel levels and function to influence GABAergic short-term plasticity. The Journal of neuroscience : the official journal of the Society for Neuroscience 29:15660-15668.

Yoo AS, Cheng I, Chung S, Grenfell TZ, Lee H, Pack-Chung E, Handler M, Shen J, Xia W, Tesco G, Saunders AJ, Ding K, Frosch MP, Tanzi RE, Kim TW (2000) Presenilin-mediated modulation of capacitative calcium entry. Neuron 27:561-572.

Zengel JE, Magleby KL (1982) Augmentation and facilitation of transmitter release. A quantitative description at the frog neuromuscular junction. The Journal of general physiology 80:583-611.

Zhang H, Liu J, Sun S, Pchitskaya E, Popugaeva E, Bezprozvanny I (2015a) Calcium signaling, excitability and synaptic plasticity defects in mouse model of Alzheimer's disease. Journal of Alzheimer's disease : JAD 45:561-580.

Zhang H, Sun S, Herreman A, De Strooper B, Bezprozvanny I (2010) Role of presenilins in neuronal calcium homeostasis. The Journal of neuroscience : the official journal of the Society for Neuroscience 30:8566-8580.

Zhang H, Wu L, Pchitskaya E, Zakharova O (2015b) Neuronal Store-Operated Calcium Entry and Mushroom Spine Loss in Amyloid Precursor Protein Knock-In Mouse Model of Alzheimer's Disease. 35:13275-13286.

Zhang W, Hao J, Liu R, Zhang Z, Lei G, Su C, Miao J, Li Z (2011) Soluble Abeta levels correlate with cognitive deficits in the 12-month-old APPswe/PS1dE9 mouse model of Alzheimer's disease. Behavioural brain research 222:342-350.

Zhao D, Watson JB, Xie CW (2004) Amyloid beta prevents activation of calcium/calmodulin-dependent protein kinase II and AMPA receptor phosphorylation during hippocampal long-term potentiation. Journal of neurophysiology 92:2853-2858.

Zirger JM, Barcia C, Liu C, Puntel M, Mitchell N, Campbell I, Castro M, Lowenstein PR (2006) Rapid upregulation of interferon-regulated and chemokine mRNAs upon injection of 108 international units, but not lower doses, of adenoviral vectors into the brain. Journal of virology 80:5655-5659.

Zou C, Crux S, Marinesco S, Montagna E, Sgobio C, Shi Y, Shi S, Zhu K, Dorostkar MM, Muller UC, Herms J (2016) Amyloid precursor protein maintains constitutive and adaptive plasticity of dendritic spines in adult brain by regulating D-serine homeostasis. EMBO J 35:2213-2222.

Zuccotti A, Clementi S, Reinbothe T, Torrente A, Vandael DH, Pirone A (2011) Structural and functional differences between L-type calcium channels: crucial issues for future selective targeting. Trends in pharmacological sciences 32:366-375.

Zucker RS, Regehr WG (2002) Short-term synaptic plasticity. Annual review of physiology 64:355-405.

6 List of Abbreviations

AAV	Adeno-associated virus
AC	Adenylyl cyclase
ACFS	Artificial cerebrospinal fluid
AD	Alzheimer's disease
ADAM	A disintegrin and metalloproteinase
AICD	APP intracellular domain
AM	Acetoxymethyl
AMPA-R	α-amino-3-hydroxy-5-methyl-4-isoxazole-propionic receptor
APLP	Amyloid precursor protein-like protein
APP	Amyloid precursor protein
APPsα or **sAPPα**	secreted Amyloid precursor protein ectodomain after α-secretase cleavage
APPsβ or **sAPPβ**	secreted Amyloid precursor protein ectodomain after β-secretase cleavage
APV	2-amino-5-phosphonopentanoic acid
Aβ	amyloid ß
Aβ1-16	C-terminal 16 amino acid sequence of APPsα
BACE	β-site APP cleaving enzyme
BDNF	Brain-derived nerve neurotrophic
CA	*cornu ammonis* (hippocampal subfields)
CaMKII	Calcium / calmodulin-dependent kinase II
cDKO	Conditional double knock-out
cKO	Conditional knock-out
cLTP	chemically induced long-term potentiation
cTKO	Conditional triple knock-out
CNS	Central nervous system
CPA	Cyclo piazoic acid
DG	Dentate gyrus
DIV	Days *in vitro*
DKO	Double knock-out
DM	Double mutant
DMSO	Dimethyl sulfoxide
EC	Entorhinal cortex
(f)EPSP	(Field) excitatory postsynaptic potential
ER	endoplasmatic reticulum
FV	Fiber volley
GABA	γ-aminobutyric acid
IP3R	Inositol-1, 4, 5-tris-phosphate receptor
ISI	Inter-stimulus interval

KI	Knock-in
KO	Knock-out
LFS	Low-frequency stimulation
L-LTP	Late-long-term potentiation
LM	littermate
LTD	Long-term depression
LTP	Long-term potentiation
mEPSC	miniature excitatory postsynaptic potential
Nex	neuronal helix-loop-helix protein 1
NFT	Neurofibrillary tangles
NGF	Nerve growth factor
NMDA-R	N-methyl-D-aspartate receptor
NO	Nitric oxide
n.s.	Not significant
OHC	Organotypic hippocampal culture
p75NTR	Pan neurotrophin receptor 75
P	postnatal day
PPD	Paired pulse depression
PPF	Paired pulse facilitation
PSD	Postsynaptic density
PSEN	Presenilin
PTP	Post-tetanic potentiation
PKA	Protein kinase A
rec	recombinant
ROI	Region of interest
RRP	Readily releasable pool
RT	Room temperature
RyR	Ryanodine receptor
SEM	Standard error of the mean
SERCA	sarco / endoplasmic reticulum calcium-ATPase
SOCC	store-operated Ca^{2+} channel
TBS	Theta-burst stimulation
TrkA	Tropomyosin receptor kinase A
VGCC	Voltage gated calcium channel
wt	Wildtype

Danksagung

An dieser Stelle möchte ich die Möglichkeit nutzen, um mich bei allen Menschen zu bedanken, die direkt oder indirekt zum Gelingen dieser Dissertation beigetragen haben:

Als erstes geht ein besonderer Dank an meinem Doktorvater Prof. Dr. Martin Korte für die vertrauensvolle und erfolgreiche Zusammenarbeit, die es mir ermöglichte, die Promotion in seiner Arbeitsgruppe anzufertigen.

Prof. Dr. Reinhard Köster danke ich für die Übernahme des Koreferates, sowie Prof Dr. Karsten Hiller für die Leitung der Promotionskommission.

Ich danke Prof. Dr. Ulrike Müller und ihrer Arbeitsgruppe für die gute wissenschaftliche Zusammenarbeit sowie fachlich hilfreichen Diskussionen in diesem Projekt, die die Kooperation mit weiteren tollen Wissenschaftlern wie Dr. Simone Eggert, Prof. Dr. Stefan Kins, Dr. Tobias Abel, Dr. Romain Fol, Dr. Jerome Bradeau und Prof. Dr. Nathalie Cartier ermöglichte.

Ein großer Dank gilt Dr. Kristin Michaelsen-Preusse für ihre wunderbare Unterstützung bei den Experimenten des quantitativen Calcium Imagings. In diesem Zug möchte ich ebenso PD Dr. Robert Blum für die wertvolle Diskussion der gewonnen Daten danken.

Ebenso möchte ich mich bei Dr. Marta Zagrebelsky, Dr. Kristin Michaelsen-Preusse, Dr. Martin Rothkegel, Dr. Andreas Holz und Dr. Ulrike Herrmann für wertvolle Ratschläge und sachkundige Diskussionen bedanken.

Zusätzlich besonders und herzlichen danken möchte ich Dr. Marta Marta Zagrebelsky, Dr. Kristin Michaelsen-Preusse und Dr. Ulrike Herrmann für das geduldige und intensive Korrekturlesen dieser Arbeit.

Ein besonderes Dankeschön geht an Diane Mundil für die wertvolle Unterstützung bei der Anfertigung der Primärkulturen und an Reinhard Huwe für sein technisches Knowhow in der Elektrophysiologie.

Tania Messerschmidt, Carmen Wucherpfennig, Heike Kessler danke ich für die Übernahme aller Bestellungen und Genotypisierungen.

Besonders möchte ich meiner liebgewonnen Bürokolleginnen Dr. Ulrike Herrmann danken, die mir ihr Fachwissen der Elektrophysiologie weitergegeben und mit Rat und Tat zur Seite gestanden hat. Danke für die tolle und freundschaftliche gemeinsame Zeit!

Für den fachlichen Austausch und die schöne Zeit miteinander danke ich Dr. Anita Remus, Dr. Stefanie Schweinhuber, Dr. Nina Gödecke, Dr. Marinna Weller, Dr. Franziska Scharkowski, Jan Kleveman, Dr. Qin Li, Dr. Cristina Iobbi, Shirin Hosseini, Niklas Lonnemann, Steffen Fricke, Leonie Salzburger und Kristin Metzdorf.

Meinen Magdeburger Unimädels danke ich für den tollen Zusammenhalt auch nach Ende unseres Studiums und die schönen Momente während unserer Treffen.

Jens und meine liebe Mama haben mich in all der Zeit begleitet, bestärkt und in jeglicher Hinsicht unterstützt. Danke! Ich liebe euch!